PB91-191346

Factors Controlling Minimum Soil Liner Thickness

Brown (K.W.) and Associates, Inc., College Station, TX

Prepared for:

Environmental Protection Agency, Cincinnati, OH

May 91

U.S. Department of Commerce
National Technical Information Service
NTIS

TECHNICAL REPORT DATA

(Please read Instructions on the reverse before complet

1. REPORT NO. EPA/600/2-91/008
2.
3. PB91-191346

4. TITLE AND SUBTITLE
FACTORS CONTROLLING MINIMUM SOIL LINER THICKNESS

5. REPORT DATE
May 1991

6. PERFORMING ORGANIZATION CODE
EPA/ORD

7. AUTHOR(S)
D.C. ANDERSON, M.J. LUPO, J.A. REHAGE, J.O. SAI, R.L. SHIVER, R.C. SPEAKE, K.W. BROWN AND D. DANIEL

8. PERFORMING ORGANIZATION REPORT NO.

9. PERFORMING ORGANIZATION NAME AND ADDRESS
K.W. BROWN & ASSOCIATES, COLLEGE STATION, TEXAS 77845
TEXAS AGRICULTURAL EXPERIMENT STATION, COLLEGE STATION, TEXAS 77843
UNIVERSITY OF TEXAS, AUSTIN, TEXAS

10. PROGRAM ELEMENT NO.

11. CONTRACT/GRANT NO.

12. SPONSORING AGENCY NAME AND ADDRESS
RISK REDUCTION ENGINEERING LABORATORY
OFFICE OF RESEARCH AND DEVELOPMENT
U.S. ENVIRONMENTAL PROTECTION AGENCY
CINCINNATI, OHIO 45268

13. TYPE OF REPORT AND PERIOD COVERED

14. SPONSORING AGENCY CODE
EPA/600/14

15. SUPPLEMENTARY NOTES
Project Officer: G. Kenneth Dotson Comml - (513) 569-7646. FTS - 684-7646

16. ABSTRACT

This report describes a three-part study to gather information on liquid flow through soil liners in hazardous waste disposal facilities.

In the first part of the study a model was developed to simulate flow occurring through discreet channels in lifts (a layer of compacted soil) and in the horizontal layer between lifts. The model indicated that high overall field hydraulic conductivity values may result from horizontal flow between lifts.

In the second part of the study, laboratory tests using large 60-cm-diameter permeameters showed that the conductivity to water typically increased by one order of magnitude with depth in a 23-cm-thick lift of compacted clay. Clod sizes ranging from 2.5 to 7.5-cm had little influence on the hydraulic conductivity. Exposure of the compacted soil to the atmosphere for as little as 24 hr resulted in severe cracking and associated high conductivities resulting from flow through the desiccation cracks. Bulk density was a poor predictor of the conductivity of a compacted soil. Dye patterns in the permeameters also indicated flow through preferential channels and inter-clod spaces.

In the third part, field studies of a 3-lift liner revealed that horizontal flow does indeed occur at the interface between the lifts when channels penetrate the overlying lift.

17. KEY WORDS AND DOCUMENT ANALYSIS

a. DESCRIPTORS	b. IDENTIFIERS/OPEN ENDED TERMS	c. COSATI Field/Group

18. DISTRIBUTION STATEMENT
Release to Public

19. SECURITY CLASS *(This Report)*
Unclassified

20. SECURITY CLASS *(This page)*
Unclassified

21. NO. OF PAGES

22. PRICE

EPA Form 2220-1 (Rev. 4-77) PREVIOUS EDITION IS OBSOLETE

PB91-191346

EPA/600/2-91/008
MAY 1991

FACTORS CONTROLLING MINIMUM SOIL LINER THICKNESS

by

David C. Anderson, Mark J. Lupo,
James A. Rehage, Joseph O. Sai,
Ronald L. Shiver and Robert C. Speake
K. W. Brown and Associates, Inc.
College Station, Texas 77840

K. W. Brown
Texas A&M University
Soil and Crop Sciences Department
College Station, Texas 77843

and

D. Daniel
University of Texas
Civil Engineering Department
Austin, Texas

Contract No. 68031816
Cooperative Agreement CR 813444-01-0

Project Officer
G. Kenneth Dotson
Waste Minimization, Destruction and Disposal Research Divsopm
Risk Reduction Engineering Laboratory
Cincinnati, Ohio 45268

RISK REDUCTION ENGINEERING LABORATORY
OFFICE OF RESEARCH AND DEVELOPMENT
U. S. ENVIRONMENTAL PROTECTION AGENCY
CINCINNATI, OHIO 45268

REPRODUCED BY
U.S. DEPARTMENT OF COMMERCE
NATIONAL TECHNICAL
INFORMATION SERVICE
SPRINGFIELD, VA 22161

DISCLAIMER

The information in this document has been funded wholly or in part by the United States Environmental Protection Agency under Contract No. 68-03-1816 to K. W. Brown and Associates and under Cooperative Agreement CR 813444 to Texas A&M University. It has been subject to the Agency's peer review and has been approved for publication as an EPA document. Mention of trade names or commercial products does not constitute endorsement or recommendation for use.

FOREWORD

Today's rapidly developing and changing technologies and industrial products and practices frequently carry with them the increased generation of materials that, if improperly dealt with, can threaten both public health and the environment. The U.S. Environmental Protection Agency is charged by Congress with protecting the Nation's land, air, and water resources. Under a mandate of national environmental laws, the agency strives to formulate and implement actions leading to a compatible balance between human activities and the ability of natural systems to support and nurture life. These laws direct the EPA to perform research to define our environmental problems, measure the impacts, and search for solutions.

The Risk Reduction Engineering Laboratory is responsible for planning, implementing, and managing research, development, and demonstration programs to provide an authoritative, defensible engineering basis in support of the policies, programs, and regulations of the EPA with respect to drinking water, wastewater, pesticides, toxic substances, solid and hazardous wastes, and Superfund-related activities. This publication is one of the products of that research and provides a vital communication link between the researcher and the user community.

This report describes factors which affect the necessary thickness of compacted soil liners. This information should be of assistance to those involved in research, design or policy development for soil liners. The goal is to provide insight into how the basic performance criteria of hydraulic conductivity and strength influence the minimum soil liner thickness needed to protect human health and the environment.

E. Timothy Oppelt, Director
Risk Reduction Engineering Laboratory

ABSTRACT

There are three main performance criteria which apply to soil liners:

1. Maintenance of a hydraulic conductivity less than 1×10^{-7} cm sec^{-1},

2. Retention of the strength needed to support all loads; and

3. The soil component in a secondary soil liner must prevent the breakthrough of any contaminant prior to the end of the post-closure care period.

Information is needed to allow determination of the minimum soil liner thickness necessary to meet these performance objectives. To develop this information, a literature review was conducted followed by the development of a model for flow through soil liners. Preliminary laboratory and field studies evaluated the validity of the model.

The model simulated flow occurring both through discreet channels in lifts and in the horizontal layer between lifts. The model indicated that very high overall field hydraulic conductivity values may result from excessive horizontal flow between lifts. In contrast, the model showed that even high hydraulic conductivity lifts can be used to construct low conductivity soil liners if horizontal flow between lifts can be sufficiently reduced.

Laboratory tests using large 60-cm-diameter permeameters showed that the conductivity to water typically increased by one order of magnitude with depth in a 23-cm thick lift of compacted clay. Clod sizes ranging from 2.5- to 7.5-cm had little influence on the hydraulic conductivity. In addition, it was shown that exposure of the compacted soil to the atmosphere for as little as 24-48 hr resulted in severe cracking and associated high conductivities resulting from flow through the desiccation cracks. The data showed that bulk density was a poor predictor of the conductivity of a compacted soil. Dye patterns in the permeameters also indicated flow through preferential channels and inter-clod spaces.

Field studies confirmed that flow through a compacted soil liner may be very rapid due to greater hydraulic conductivity in the lower portion of the lifts resulting in increased horizontal flow at the lift interfaces. Additional field and laboratory studies are recommended to characterize pore size distribution and effective porosity of compacted

soil liners. In addition, studies are needed to further characterize the factors influencing horizontal flow and the spatial distribution of channels within lifts of various thickness and density.

This report was submitted in fulfillment of Contract #68-03-1816, Work Assignment No. 2-10, by K. W. Brown and Associates, Inc., and Cooperative Agreement CR813444010 with Texas A&M University and University of Texas under the sponsorship of the U.S. Environmental Protection Agency. This report covers a period from April 1, 1986 to April 1, 1989 and work was completed as of December 31, 1988.

TABLE OF CONTENTS

Page

DISCLAIMER. ii
FOREWORD. iii
ABSTRACT. iv
LIST OF FIGURES viii
LIST OF TABLES. xiv

1. INTRODUCTION 1
2. CONCLUSIONS AND RECOMMENDATIONS. 3
    Conclusions 3
    Recommendations 4
3. LITERATURE REVIEW. 8
    Strength. 8
    Hydraulic Conductivity. 13
4. CHANNEL FLOW COMPUTER MODELS 34
    Hydraulic Conductivity of a Lift. 34
    Channel Density 42
    Multilift Soil Liners 46
    Models for Interlift Flow 50
    Channel-Centered Model. 52
    The Pocket Model. 58
    Comparison of Channel-Centered and Pocket Models 60
    Physical Explanation of Channel-Centered Model. 61
    The Unifying Model. 62
5. LABORATORY STUDY 77
    Materials and Methods 77
    Results and Discussion 80
6. FIELD STUDY. 115
    Materials and Methods 115
    Results 121
    Discussion. 129
7. STOCHASTIC ANALYSIS 134
    Introduction. 134
    Variability of the Hydraulic Properties of Soil 135
    The Convolution Model 135
    The Macropore Model 152
    Conclusions 175
8. REFERENCES 176

APPENDIX A 185
APPENDIX B 190
APPENDIX C 194
APPENDIX D 199
APPENDIX E 200
APPENDIX F 204

LIST OF FIGURES

Number Page

1. A multilift liner with limited interlift flow. 5

2. A multilift liner with extensive interlift flow. 6

3. Strength gain due to freeze-thaw (from Alkire and Jashimuddin, 1984) 12

4. Relationship between interclod porosity, intraclod porosity, and unit soil weight (from Speake, 1986) 17

5. Spacing versus channel radius for $K = 10^{-5}$, 10^{-6}, 10^{-7}, and 10^{-8} cm sec^{-1}. 41

6. Channel density versus channel size. 44

7. Number of channels versus channel radius 47

8. The channel-centered model for interlift flow. 51

9. The pocket model for interlift flow. 51

10. The difference between the number of effective flow paths and the number of active channels in the last lift 53

11. The difference between the number of effective flow paths and the fewest number of active channels in a lift 54

12. Interlift flow radius vs. average number of flow paths for two to eight lifts 57

13. Pocket radius vs. average number of flow paths for two to eight lifts 59

14. Liner thickness vs. breakthrough time for various interlift hydraulic conductivity values. 76

LIST OF FIGURES (continued)

Number Page

15. Schematic diagram of a permeameter for use in the containerized test section study 80

16. Water retention as a function of matric potential for the two soils used in this study 82

17. X-ray diffraction pattern of the clay fraction of Beaumont clay soil 84

18. X-ray diffraction pattern of the coarse clay fraction of Beaumont clay soil. 85

19. X-ray diffraction pattern of the fine clay fraction of Beaumont clay soil. 86

20. X-ray diffraction pattern of the clay fraction of Kosse soil 87

21. X-ray diffraction pattern of the coarse clay fraction of Kosse soil. 89

22. X-ray diffraction pattern of the fine clay fraction of Kosse soil. 90

23. Cumulative water inflow and outflow from a permeameter containing a complete lift of Kosse soil compacted with 2.5 cm clods. 94

24. Cumulative water inflow and outflow from a permeameter containing a complete lift of Kosse soil compacted with 5.0 cm clods. 95

25. Laboratory measured moisture-density curve for Kosse soil 98

26. Hydraulic conductivity of Kosse soil measured in the laboratory and using large permeameters, as a function of moisture content. 99

27. Measured hydraulic conductivity of compacted Kosse soil versus that predicted from the conductivity versus moisture content curve in Figure 26. 100

LIST OF FIGURES (continued)

Number Page

28. Hydraulic conductivity, as measured both in the laboratory and using large permeameters, of compacted Kosse soil as a function of the compacted soil bulk density. 101

29. Breakthrough time as a function of saturated hydraulic conductivity for a single lift of Beaumont clay soil 103

30. Breakthrough time as a function of saturated hydraulic conductivity for a single lift of Kosse soil 104

31. Schematic diagram of dyed soil at three depths in a permeameter of compacted Kosse soil using a 2.5 cm clod size (Replication 1). 108

32. Schematic diagram of dyed soil at three depths in a permeameter of compacted Kosse soil using a 2.5 cm clod size (Replication 2). 109

33. Schematic diagram of dyed soil at three depths in a permeameter of compacted Kosse soil using a 2.5 cm clod size (Replication 3). 110

34. Schematic diagram of dyed soil at three depths in a permeameter of compacted Kosse soil using a 2.5 cm clod size (Replication 4). 114

35. Schematic diagram of dyed soil at three depths in a permeameter of compacted Kosse soil using a 5.0 cm clod size (Replication 1). 112

36. Schematic diagram of dyed soil at three depths in a permeameter of compacted Kosse soil using a 5.0 cm clod size (Replication 2). 113

37. Schematic diagram of dyed soil at three depths in a permeameter of compacted Kosse soil using a 5.0 cm clod size (Replication 3). 114

38. Field infiltrometer configuration. 116

39. Schematic of a tracer infiltration apparatus 118

40. Schematic of excavated borehole and infiltrated area 119

41. Schematic of idealized wetting front 120

LIST OF FIGURES (continued)

Number Page

42. Histogram of crack depth determined from field study 122

43. Histogram of crack width determined from field study 123

44. Moisture/density curve for borrow material used to construct the compacted soil cover 124

45. Moisture content profile in interlift zone at T = 10 days for borehole #1 126

46. Bromide concentration gradient in interlift zone at T = 10 days for borehole #1. 127

47. Schematic showing the spatial relationship of infiltration standpipes 128

48. Schematic diagram of the dye-stained soil in the area near borehole #1 130

49. Schematic diagram of the dye-stained soil in the area near borehole #5 131

50. Configuration of the soil liner which is modeled by the convolution model. 136

51a. Vertical pathways through a soil liner 138

51b. Realizations of the first-passage times through a soil liner . 138

52. Seepage in one-dimension and multi-dimensions. 139

53a. A probability density function of the first-passage time . . . 140

53b. A reliability function of the first-passage-time distribution. 140

54. Effect of the mean hydraulic conductivity on the 95th, 50th, and 5th percentiles of first-passage-time. 143

55a. The reliability function for log-variances of 0.75 and 1.50. . 144

55b. The 95th percentile first-passage-time as a function of log-variance 144

56. Density functions of the (a) equivalent conductivity, (b) Equivalent resistivity, (b) and first-passage-time log-variances of 0.75 and 1.50 145

LIST OF FIGURES (continued)

Number Page

57. Reliability functions for several values of effective porosity 146

58. Influence of variance of hydraulic conductivity an flux presented (a) as a cumulative distribution function, and (b) a probability density function 149

59. Probability density functions for hydraulic conductivity . . . 150

60. Normalized 50th and 95th percentile fluxes versus log variance of hydraulic conductivity 150

61. Effect of number of lifts on probability density function and cumulative density functions for flux 151

62. Normalized flux and hydraulic gradient versus thickness of liner 152

63. Seepage in macropores in liners with good and poor interlift bonding 154

64. Macropores, spatial averaging, and hydraulic conductivity . . 155

65. A schematic of the hydraulic behavior of the interlift zone . 157

66. A schematic of the liner approximated with the macropore model 161

67. The effect of the number of channels on the 95th percentile and variance of the first-passage-time and the reliability function 165

68. Effect of the mean hydraulic conductivity of a partition, (a) the mean number of channels, and (b) the transmissivity of the interlift zone on the 95th percentile first-passage-time 167

69. Effect of the log-variance of the hydraulic conductivity of a partition on the reliability function, the 95th percentile first-passage-time and the density function of hydraulic conductivity 168

70. Effects of number of flow channels per partition on flux . . . 169

71. Effect of mean hydraulic conductivity upon flux 171

LIST OF FIGURES (continued)

Number Page

72. Effect of log-variance of hydraulic conductivity upon flux. . 172

73. Effect of number of lifts on mean flux and mean first-passage time. 174

74. Effect of thickness on mean equivalent hydraulic conductivity 174

LIST OF TABLES

Table Page

1. Physical Properties of Three Compacted Soils 20

2. Reported Uses of Dyes to Study Movement of Water Through Soils. 23

3. Spacing Versus Channel Radius For a Hydraulic Conductivity of 1 x 10^{-5} cm sec^{-1} 37

4. Spacing Versus Channel Radius For a Hydraulic Conductivity of 1 x 10^{-6} cm sec^{-1} 38

5. Spacing Versus Channel Radius For a Hydraulic Conductivity of 1 x 10^{-7} cm sec^{-1} 39

6. Spacing Versus Channel Radius For a Hydraulic Conductivity of 1 x 10^{-8} cm sec^{-1} 40

7. Number Of Through-Going Channels Expected With Different Instruments Where Actual Conductivity is 1 x 10^{-5} cm sec^{-1} . 43

8. Number Of Through-Going Channels Expected With Different Instruments Where Actual Conductivity is 1 x 10^{-6} cm sec^{-1} . 45

9. Number Of Through-Going Channels Expected With Different Instruments Where Actual Conductivity is 1 x 10^{-7} cm sec^{-1} . 46

10. Number Of Through-Going Channels Expected With Different Instruments Where Actual Conductivity is 1 x 10^{-8} cm sec^{-1} . 48

11. The Number of Channels in 2.32 m^2 Versus Channel Radius 49

12. The Number of Through-Going Channels in a Soil Liner With Two Lifts for the Channel-Centered Model 56

13. The Number of Through-Going Channels in a Soil Liner With Three Lifts for the Channel-Centered Model 58

14. The Number of Through-Going Channels in a Soil Liner With Four Lifts for the Channel-Centered Model. 60

LIST OF TABLES (continued)

Table | Page

15. The Number of Through-Going Channels in a Soil Liner With Five Lifts for the Channel-Centered Model. 61

16. The Number of Through-Going Channels in a Soil Liner With Six Lifts for the Channel-Centered Model 62

17. The Number of Through-Going Channels in a Soil Liner With Seven Lifts for the Channel-Centered Model 63

18. The Number of Through-Going Channels in a Soil Liner With Eight Lifts for the Channel-Centered Model 64

19. The Number of Through-Going Channels in a Soil Liner With Two Lifts For The Pocket Model 65

20. The Number of Through-Going Channels in a Soil Liner With Three Lifts For The Pocket Model 66

21. The Number of Through-Going Channels in a Soil Liner With Four Lifts For The Pocket Model. 67

22. The Number of Through-Going Channels in a Soil Liner With Five Lifts For The Pocket Model. 68

23. The Number of Through-Going Channels in a Soil Liner With Six Lifts For The Pocket Model 69

24. The Number of Through-Going Channels in a Soil Liner With Seven Lifts For The Pocket Model 70

25. The Number of Through-Going Channels in a Soil Liner With Eight Lifts For The Pocket Model 71

26. Interlift Flow Radius in Centimeters for Soil Liners With Various Horizontal Hydraulic Conductivities and Under 30 cm of Water 72

27. Average Breakthrough Time in Weeks When the Horizontal Hydraulic Conductivity is 1 x 10^{-5} cm sec^{-1}. 74

28. Average Breakthrough Time in Months When the Horizontal Hydraulic Conductivity is 1 x 10^{-6} cm sec^{-1}. 74

29. Average Breakthrough Time in Years When the Horizontal Hydraulic Conductivity is 1 x 10^{-7} cm sec^{-1}. 75

LIST OF TABLES (continued)

Number Page

30. Average Breakthrough Time in Years When the Horizontal Hydraulic Conductivity is 1 x 10^{-8} cm sec^{-1} 75

31. Physical Properties of the Two Soils Used in This Study . . 81

32. Hydraulic Conductivity (cm sec^{-1}) of Beaumont Clay for Complete Lift 88

33. Hydraulic Conductivity (cm sec^{-1}) of Beaumont Clay After 7.5 cm of Top Soil was Removed 91

34. Hydraulic Conductivity (cm sec^{-1}) of Beaumont Clay After 15 cm of Top Soil was Removed 92

35. Measured Bulk Density (g cm^3) of Beaumont Clay After Compaction 92

36. Measured Moisture Content (Percent by Weight) of Beaumont Clay at the Time of Compaction 92

37. Hydraulic Conductivity (cm sec^{-1}) of Kosse Soil for Complete Lift 93

38. Hydraulic conductivity (cm sec^{-1}) of Kosse Soil after 7.5 cm of Soil had been Removed 93

39. Hydraulic conductivity (cm sec^{-1}) of Kosse Soil after 15 cm of Soil had been Removed 96

40. Measured Bulk Density (g cm^3) of Kosse Soil after Compaction 96

41. Measured Moisture Content (Percent by Weight) of Kosse Clay at the Time of Compaction 97

42. Changes in Volumetric Moisture Content in Compacted Soils as a Result of Drying 102

43. Hydraulic Conductivity (cm sec^{-1}) of Beaumont Clay after Drying 105

44. Hydraulic Conductivity (cm sec^{-1}) of Kosse Clay after Drying 106

45. Laboratory Determined Soil Data 125

SECTION 1

INTRODUCTION

A compacted soil liner is a component of the required double liner system in hazardous waste disposal facilities. The compacted soil can be incorporated into double liner designs in either of the following two ways:

1. As the sole component of a secondary soil liner; or
2. As the lower component beneath a synthetic membrane in a composite liner.

Three minimum performance criteria apply to the soil component in either liner design:

1. Maintenance of an in-place hydraulic conductivity of less than or equal to 1×10^{-7} cm $\sec^{-1}$;
2. Retention of sufficient strength to support all potential overlying loads; and,
3. The soil component in a secondary soil liner must prevent the breakthrough of any contaminant prior to the end of the post-closure care period.

The primary purpose of this research was to initiate the data base required to determine the minimum thickness necessary for a soil liner to meet the performance objectives stated above. The majority of the information presented relates to these criteria (hydraulic conductivity and strength), which are applicable to the soil component of both secondary liner designs. The performance standard (preventing constituent breakthrough in secondary soil liners) is not a major focus of this document and is briefly addressed in Sections 3 and 4.

To begin the development of the data base discussed above, a literature review concentrating on the factors which influence hydraulic conductivity and strength in compacted soils was conducted (Section 3). A computer model was developed which examines the influence of channels or defects which completely penetrate a lift and horizontal flow between lifts (Section 4). A laboratory study (Section 5) was conducted to evaluate the effects of clod size on the hydraulic conductivity of compacted soils and the uniformity of conductivity with depth within a lift of compacted soil. A field study was undertaken to examine liquid flow patterns and characteristics in a compacted soil (Section 6). The study was designed to allow examination of both vertical and horizontal flow paths through the soil. A stochastic model (Section 7) was developed by researchers at the University of Texas. The model supports the data and conclusions from the laboratory and field studies. Based upon the observations and investigations described herein, further research and development of the soil liner data base has been recommended (Section 2).

SECTION 2

CONCLUSIONS AND RECOMMENDATIONS

CONCLUSIONS

The required thickness of a soil liner was investigated with respect to two basic properties: hydraulic conductivity and strength. Minimum thickness was found to be primarily dependent on hydraulic conductivity. Strength was not found to be greatly influenced by thickness. The following conclusions and observations were made:

1. Strength attained in the soil liner is not directly dependent upon thickness and will primarily be governed by control of moisture content and compaction. Adequate strength will generally be obtained with standard compaction practices. An important consideration is the stability of the native foundation soil and its ability to support the overlying load;

2. Hydraulic conductivity is the most important property in determining the thickness required in a soil liner. Conductivity achieved in the liner is affected by several factors including liner thickness, soil matrix permeability, lift thickness, horizontal flow between lifts, and the presence of channels or defects;

3. Hydraulic conductivity of the soil liner is also the most important factor affecting the time it takes for hazardous constituents to break through the liner;

4. Bulk density is a poor indicator of the hydraulic conductivity of a compacted clay soil;

5. Flow through a compacted clay liner is primarily through a small number of preferential channels;

6. Within a single 23-cm-thick lift of compacted clay, the hydraulic conductivity generally increased by one order of magnitude with depth.

The channel flow computer model presented in this report simulates flow occurring through discrete channels (defects) in each lift and describes how these channels affect the overall conductivity of the liner. The channels can be interconnected by horizontal flow between lifts to form a continuous flow route through the liner. Test runs using the model indicate that field procedures which would be effective in bonding lifts together and reducing horizontal flow should also reduce the conductivity of the overall liner by reducing the number of interconnected channels. To illustrate these points, consider the following two figures. Figure 1 depicts a scenario where horizontal flow between lifts is minimized. This restricts the downward migration of leachate by minimizing the number of interconnected channels which transect the entire liner thickness. In this instance, the hydraulic conductivity of the liner would be much lower than that of an individual lift. The scenario in Figure 2, on the other hand, shows the migration of leachate through channels connected by excessive horizontal flow between lifts. In this case the large number of interconnected channels results in a much higher hydraulic conductivity. When the horizontal flow of liquids is greater just above the lift interface, the conductivity of the liner is controlled by the least conductive lift. The computer model can also be used to simulate the effects of different horizontal hydraulic conductivities between lifts on breakthrough of leachate. Breakthrough time was found to be primarily a function of horizontal conductivity.

The stochastic model presented in this report shows that use of more than 4 to 6 15-cm lifts will result in little change in equivalent conductivity. The modeling showed that achieving good bonding between lifts to minimize interlift flow was most effective in minimizing hydraulic conductivity and maximizing contaminant breakthrough time.

RECOMMENDATIONS

The following studies should aid in expanding the data base necessary to determine the required thickness for a soil liner.

1. Field and laboratory studies to characterize the pore size distribution and effective porosity of compacted soil liners. The distribution of macropores is especially important. The occurrence of these features is widely variable spatially;

2. Field and laboratory studies to investigate the horizontal flow of liquids between lifts. Results will aid in determining factors which affect the rate and extent of interlift flow;

3. Studies of the depth functions for density, effective porosity, tracer movement, strength, and hydraulic conductivity within individual compacted lifts of varying

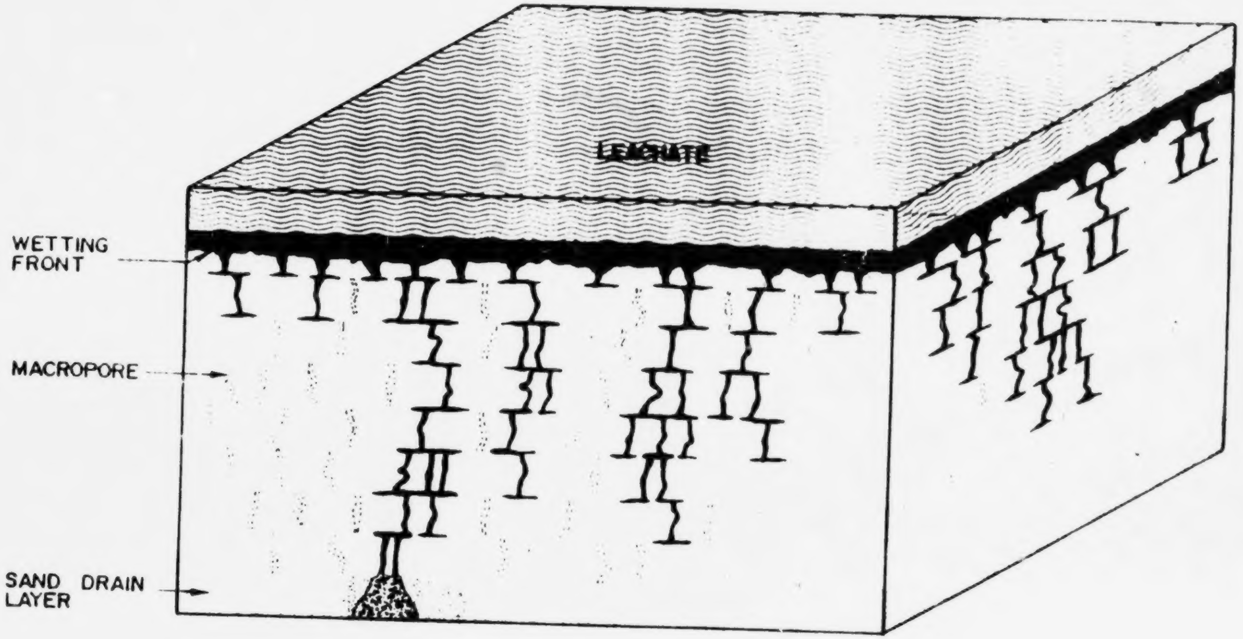
LEACHATE
WETTING FRONT
MACROPORE
SAND DRAIN LAYER

Figure 1. A multilift liner with limited interlift flow.

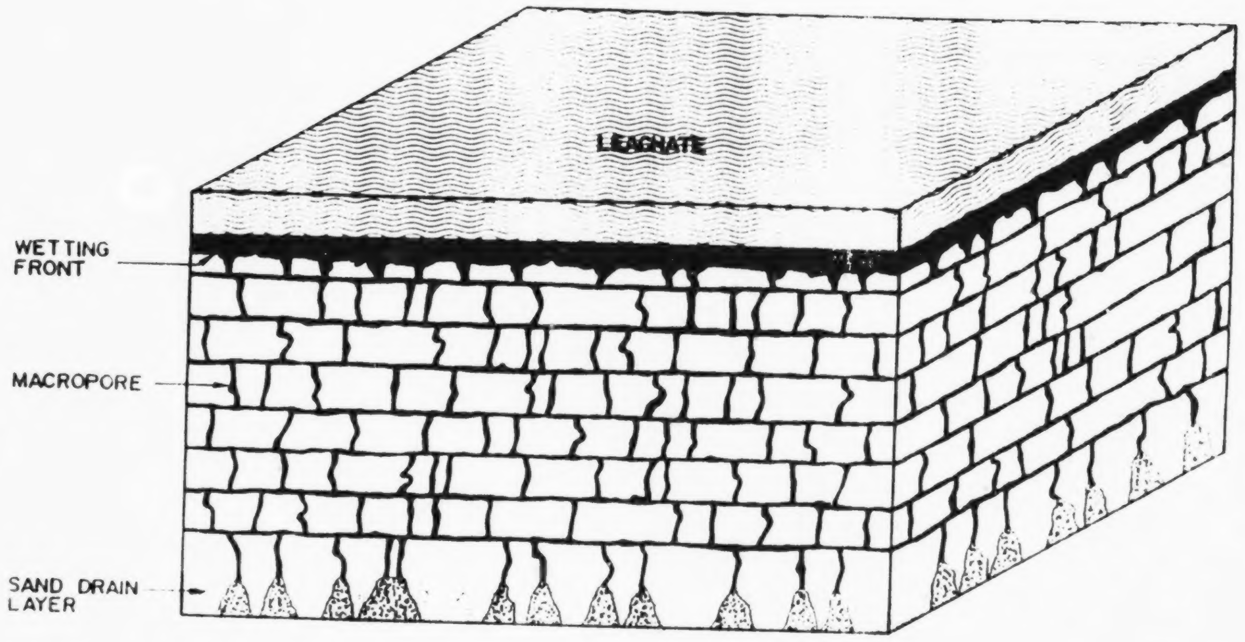
LEACHATE
WETTING FRONT
MACROPORE
SAND DRAIN LAYER

Figure 2. A multilift liner with extensive interlift flow.

thickness;

4. Evaluation of the effect of ponding on liner swelling and strength;

5. Investigation into whether constructing soil liners with a greater number of thinner lifts effectively reduces flow between lifts; and

6. Field morphological studies of dye tracer movement through a liner or individual lifts. Studies should develop relationships between dye-filled porosity and liner performance variables including hydraulic conductivity and strength.

Ideally, studies such as these would be conducted on a variety of soils compacted over a range of moisture contents and using a selection of commonly available equipment.

Results of Studies 1 and 2 can serve as inputs into numerical models which estimate transit times of solutes through compacted soil materials. Necessary thickness of a soil liner needed to prevent pollutant breakthrough during the active life and post-closure care period of a hazardous waste disposal facility could then be determined. This could be accomplished through the use of either of the computer models presented in the text or the model of Horton et al. (1985).

Studies 3, 4, and 5 are needed to evaluate current state-of-the-art liner construction criteria and to determine whether alternative construction practices are necessary and feasible. Study 6 is needed to select threshold values of easily determined parameters which can be used to predict performance of soil liners at full-scale hazardous waste facilities.

Studies conducted during this project suggest that flow through soil liners is controlled by a combination of vertical conductivity within lifts and horizontal conductivity at the interface between lifts. Consequently, the construction quality assurance program for a hazardous waste disposal facility should determine if such preferential flow paths exist in a given liner by conducting dye tracer studies on the soil liner of the test fill. It is suggested that dye be placed in the field infiltrometers used on the test fill so that subsequent dissection will reveal the extent and routes of preferential liquid flow.

SECTION 3

LITERATURE REVIEW

This section presents a review of published work on factors which affect the minimum thickness required in soil liners, in particular strength and hydraulic conductivity. The review was carried out to aid in establishing the main factors to consider in constructing a soil liner with sufficient thickness to maintain the required strength to support anticipated loads and an effective field hydraulic conductivity of 1×10^{-7} cm sec^{-1} or less.

STRENGTH

Minimum thickness of a soil liner must provide sufficient strength to withstand both the expected overburden, and the anticipated settlement. While many factors affect strength, no quantitative determinations of thickness requirement can be made based on the information assembled from existing studies. An effort was therefore made to contact technical experts in the area of soil strength. One conclusion drawn from these discussions was that the stability of the foundation soil has a much greater influence on long-term soil liner integrity than does the strength of the soil liner. When compacted to 90% modified or 95% standard proctor density, a soil liner would nearly always exhibit adequate initial strength to support the normally anticipated overburden pressures associated with a landfill liner. Strength with respect to overburden pressures was said to be much more dependant on foundation stability than liner thickness.

Strength of a soil can change with time due to either the formation of soil structure or swelling of the liner. Formation of soil structure can be caused by weathering cycles, concentrated organics or salts in leachate, and a tendency for compacted soil to gradually return to a more flocculated state. Swelling may occur where a soil liner containing expandable lattice clay minerals is flooded with water. Since flooding is likely in the leachate collection system overlying a liner, this factor should be considered for liners containing expandable clay minerals.

Again, no quantitative analysis of the necessary soil liner thickness can be made based on existing studies. However, 91-cm is the minimum suggested based on the potential for portions of the liner to be weakened as follows:

1. The lowermost portion of a liner may be weakened due to blending with unspecified materials present in the foundation soil; and

2. The uppermost portion of a liner may be weakened due to either of the following:

   a. exposure to weathering effects such as freeze-thaw or wet-dry cycles; and

   b. swelling due to flooding.

The following subsections cover soil properties and weathering conditions which may influence soil strength.

Structure

The influence of structure on the strength of undrained clay soils depends on the deformation criterion adopted as a basis for strength determination (Seed and Chan, 1959). In pavement design tests, the strength index of a soil is determined at strains of about 5%. In earth dam design tests, strengths are determined at strains of about 20%. Pavement design engineers would tend to conclude that soil structure has a pronounced influence on the strength of compacted soils. Earth dam designers would, however, conclude that structure has little or no influence on soil strength. Seed and Chan (1959) stated that this apparent conflicting conclusion can be reconciled by a consideration of the influence of structure on the entire stress-strain relationship for a compacted clay.

Seed and Chan (1959) also showed data which indicated that as long as structure remains unchanged, strength will increase with density. When a more dispersed structure is introduced, however, the strength at low strains may be markedly reduced in spite of density increases. This results from the higher pore-water pressures associated with the dispersed structure. Strengths determined at high strains showed the soil samples to exhibit approximately equal strengths irrespective of the structure.

Particle Size Distribution

Particle size distribution has been found to affect the strength of a compacted soil. Yoder and Woods (1946) conducted compaction and strength tests on four particle size mixtures to determine their compaction and wet strength characteristics with variations in soil particle size (material finer than 200 mesh sieve). The data indicated that, for a given gradation of particles, there is an optimum content of soil fines at which maximum densities are obtained. The optimum content of soil fines for maximum strength was less than that indicated for obtaining maximum density. Maximum densities do not necessarily mean maximum strengths. Yoder and Woods (1946) concluded that insofar as densities and strengths are concerned, a small quantity of soil fines mixed with granular material is desirable, but large quantities of these fines may have a negative effect on strength.

Drying and Wetting

Drying and wetting of the soil can affect the strength and potential for swell in the liner. Aisenstein et al. (1961) found that after ponding water over a 90-cm-thick liner constructed of highly plastic clay, the upper portion of the liner underwent swelling. This resulted in a decrease in strength and an increase in hydraulic conductivity. McDowell (1946) found that if soils are compacted at optimum moisture and maximum density for lower compactive efforts, subsequent swelling and strength will be low. One of the objectives during compaction should be to minimize swelling potential while obtaining as high a strength as possible. For swelling clays, the control of moisture content is equally as important as the control of density to obtain a high-strength soil liner with low swelling potential. McDowell (1946) showed that high strength and low-swelling potential can usually be obtained at moisture contents between 5% below and 1% above optimum. He suggested the use of strength and swell tests to assist in the selection of a desired density.

Soils containing expansive clay minerals develop cracks when desiccated. Often these cracks appear to be closed but still remain as planes of weakness and paths of seepage. The strength of such clays is dependent on orientation of the cracks, effect of changes in stress, and extent of seepage along the cracks.

Shear strength tends to decrease with increases in moisture content, and density tends to decrease as clays expand through saturation (Holtz and Gibbs, 1956). Extreme loss of strength may occur in both undisturbed and compacted expansive clays. Although density changes may be small, strength can be substantially reduced by wetting expansive clays.

Dubose (1956) pointed out the importance of selecting a combination of moisture content and compactive effort to produce a desired strength in compacted fills. Increases in strength and density were obtained with increases in compactive effort. Curves were presented which could be used to select a moisture content and compactive effort that would minimize volume change and maximize strength.

Freeze- Thaw

Soil strength and bearing capacity are reduced by freeze-thaw cycles. The reason is a modification of soil structure. Upon cooling, free water in larger pores freezes first. Hygroscopic water held by the soil matrix remains liquid longer and migrates to the ice crystals forming in the larger pores (Spangler and Handy, 1982). In the liner matrix, dehydrating clay particles are drawn more tightly to other grains and each other, while water in the larger pores is freezing and expanding, thereby forcing grains apart. The end result of several freeze-thaw cycles may be a loose collection of soil aggregates, much to the detriment of the strength of the liner. Soils containing even a small amount of fine-grained material were observed by Broms (1963) to be subjected to frost action.

In some cases, ice lenses of variable thickness are formed within a frozen, frost-susceptible soil material and cause expansion of the soil. When the ice lenses melt, the soil consolidates under the overlying soil weight. Static compression developed by waste loading is not, however, sufficient to recompact the clay material to its original compacted density. The important factors influencing strength of soils and bearing capacity during freeze-thaw cycles are the location of the ground-water table, particle size distribution, and density of the soil material.

Alkire and Jashimuddin (1984) conducted tests to determine the effect of water content on strength of a Manchester silt subjected to freeze-thaw. Samples were prepared at 10 and 20% moisture with densities of 90 and 100 pcf. Results indicated that strength is closely related to moisture content for both unfrozen soil and soil thawed following a freeze (Figure 3). Freeze-thaw was also found to cause an increase in strength of samples held at a constant water content while the strength decreased as water content increased. The effect of freeze-thaw on shear strength is greatest at higher unit weight (Figure 3). The main reason for the loss of strength of a soil subjected to freeze-thaw is the accompanying change in water content. A relationship was suggested involving water content, dry density, and the expected water content to predict the soil strength at a given time.

Soil properties such as hydraulic conductivity and deformation characteristics are also affected by freezing and thawing of the soil. The volume changes due to freeze-thaw can be determined by measuring the amount of heave that occurs as the soil freezes. Internal redistribution of water content within the soil is the primary cause of volume changes. An increase in volume and a decrease in density occurs when free water in a soil freezes. Another cause for volume change is movement of water from the ground-water table to the freezing front in the soil. The net results of the above changes are a decrease in the density and shear strength of the soil. Soil volume changes caused by heave can also cause a decrease of the slope stability for earth dams, dikes, embankments and cuts.

Broms and Yao (1964) investigated the shear strength and deformation characteristics of a silty clay subjected to freezing and thawing. Freezing rate, the surcharge, and drainage conditions greatly

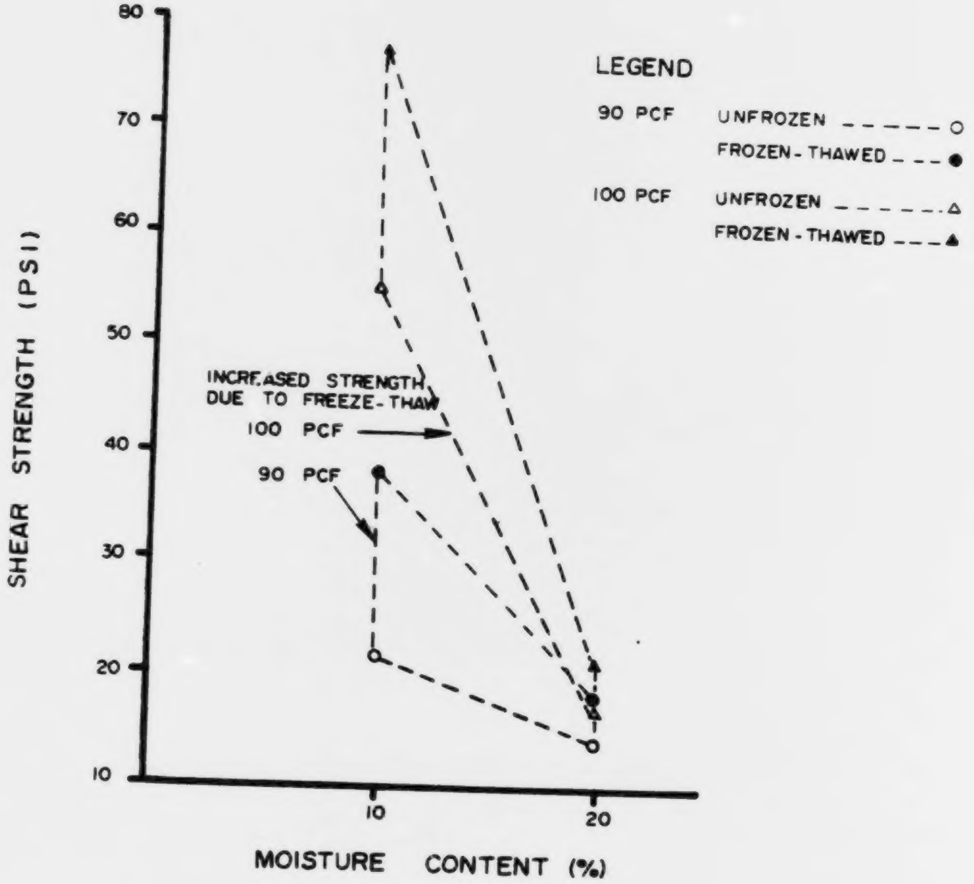

Figure 3. Strength gain due to Freeze-Thaw. (From Alkire and Jashimuddin, 1984).

affect the ultimate strength of the soil. Soils frozen at low freezing rates or subjected to alternating freezing and thawing became saturated during thawing.

In general, the post-thaw strength of a soil is below the pre-freeze strength (Wood, 1976; Broms and Yao, 1964; and Jessberger and Carbee, 1970). However, Alkire (1980) observed that a single freeze-thaw cycle increased the shear strength of an unsaturated silty soil and concluded that a change in basic soil structure occurred during freeze-thaw to account for the change in strength. Results from these studies seem to indicate a loss of strength due to freeze-thaw for saturated soil and an increased strength for partly saturated soils.

The bearing capacity of a frost-susceptible soil is greatly reduced during the spring breakup period (Yao and Broms, 1965). This reduction in strength is caused by an increase in water content and a decrease in density during freezing, followed by incomplete dissipation of the excess pore pressures during thawing.

Jessberger and Carbee (1970) also found the bearing capacity of frost-susceptible subgrade soils to be reduced during frost melting periods. The magnitude of this reduction in bearing capacity was determined by performing California Bearing Ratio (CBR) tests on soil samples subjected to several freeze-thaw cycles.

As mentioned earlier, several causal factors must act in concert for liner heave to occur. The major factors include ground freezing, readily available water, low soil moisture potential (capillarity), soil permeability, and time. Little or no frost heave will occur if the liner does not freeze, if the liner and foundation have low permeability, or if the foundation soils are dry and far above a water table.

HYDRAULIC CONDUCTIVITY

Hydraulic conductivity is the most important consideration in determining the minimum thickness necessary in a soil liner. The liner must have an effective field hydraulic conductivity of less than or equal to 1×10^{-7} cm sec^{-1}. The following sections provide a discussion on factors which affect the hydraulic conductivity of a soil liner including soil fabric, porosity, bulk density, lift thickness, and the spatial variability of soil properties.

Hydraulic conductivity consists of water movement through both channels (macropores) and capillaries (micropores). Pores make up approximately 25 to 40% of the total bulk volume of a compacted soil sample. After compaction is complete, it is possible for channels (cracks) to develop in the liner. Channels can occur as a result of post-construction subsidence or by shrinkage due to evaporation of soil moisture (Murphy and Gilbert, 1985). Channels also form between soil structural units which vary in size from small peds to large clods. Such channels in consolidated materials typically comprise 1 to 3% of the bulk volume of a sample (Duguid and Lee, 1977). The coefficient of permeability for a channel in a liner is many times higher than that for the unfractured matrix (Currie, 1974). Therefore, a thicker liner with more lifts and good scarification between lifts is not as likely to form a continuous channel through the entire thickness of a liner. These features do not provide a flow path through adjacent lifts unless they are hydraulically interconnected.

Clay Soil Fabric

The organization of solid particles and pores within soil liners, commonly called soil fabric, has considerable influence on liner hydraulic behavior. For example, two soil liners of approximately the same particle size distribution may differ widely in permeability simply because of differences in arrangement of pores or in packing of individual skeleton grains (Brewer, 1976). The fabric of soil liners is concerned not only with the spatial arrangement of discrete grains and the associated pores but also with that of particle aggregates (clods) and the pores between these aggregates.

The smallest scale of liner fabric organization concerns the composition, arrangement, and behavior of soil particles, especially clay-size particles. Patrick (1975) defines clay fabric as "the geometrical relationship between individual clay platelets and the manner in which they are associated." The state of clay soils can be further categorized into flocculated (edge-to-face), dispersed (face-to-face), flocculated groups (face-to-face aggregates having edge-to-face contact), and dispersed groups (face-to-face aggregates having face-to-face orientation).

The more commonly occurring clay minerals are kaolinite, illite, montmorillonite, and chlorite (McCarthy, 1982). The basic crystal unit of these minerals has been described as plate-shaped, irregular flake-shaped, or fibrous. Thus, clay particles are much smaller in one dimension than in the other two (Krauskopf, 1979). It has been noted from empirical studies that the edges of clay minerals (the shorter dimension) possess positive charges while the faces are negatively-charged. This allows for a preferred orientation of clay particles in response to atomic attraction. Since positive and negative charges have an electrochemical affinity for each other, it follows that the edges of clay particles are attracted to the faces of other clay particles. This type of fabric has been termed edge-to-face. The complement to this structure is called face-to-face fabric (Patrick, 1975).

Effect of Water Content --

Wood et al. (1983) claim that "the most important variable controlling the fabric of compacted clays is the water content at time of compaction." In a scanning electron microscope evaluation of samples of compacted kaolin, Patrick (1975) found a "distinct loss of air-filled voids" as well as good orientation of the clay platelets normal to the direction of compaction (dispersed fabric) for samples compacted at a water content 1% wet of optimum when compared to specimens compacted 5% dry of optimum. This suggests that the interstitial fluids are acting as lubricating agents. The water serves as a buffer in that it tends to decrease the attraction between negatively-charged edges and positively-charged faces of the clay particles, thereby allowing a dispersed orientation of platelets.

Kneading and vibratory compaction modes are preferable to static compaction since they induce a greater soil bulk density (McCarthy, 1982; Garcia-Bengochea, 1978) which may, under certain conditions, lower hydraulic conductivity. For soils having water contents wet of optimum, this implies that kneading and vibratory compactors are more effective at taking advantage of the decreased interparticle attraction. In a study of pore size distribution measurements of samples compacted by various methods in the field (static and kneading), Wood et al. (1983) reported that the fabrics of the field-compacted samples were found to be statistically different.

Effect of Compactive Effort --

Intuitively, compactive effort would seem to be the dominant variable in reorienting clay platelets into a dispersed (face-to-face) fabric. In fact, Patrick (1975) found that for Georgia kaolin samples "no increase in dispersed orientation is produced by increasing the compaction effort at a constant water content." However, because these specimens were compacted in the laboratory, extrapolation to field conditions should be considered with caution. Dynamic compaction does, however, produce a dispersed orientation of kaolinite platelets.

Patrick (1975) investigated the effect of compaction on fabric of kaolinitic soils. Samples of dry-processed Georgia kaolin, having the Unified Soil Classification designation of silt (MH), were compacted at low (3.6×10^4 kg M/M^3); medium (2.1×10^5 kg M/M^3); and high (3.8×10^5 kg M/M^3) compaction energies for various water contents. A section from each sample was then removed, freeze-dried, and mounted for SEM evaluation. Results of the experimentation confirmed the hypothesis that compaction produces some degree of dispersed (face-to-face) platelet orientation normal to the direction of compaction. Increased compaction energies resulted in greater unit weights, reorientation of particles, and close packing of individual particles. For samples compacted at water contents wet of optimum, dispersed structure was enhanced at the low compaction energy, but further enhancement at medium and high energies was not observed. This implies the existence of a limiting compactive effort for a given soil, and that the use of extremely heavy compaction equipment may not result in a more dispersed structure. While the use of heavy equipment may not increase the amount of dispersion, the added weight may serve to press the soil aggregates in the bottom of a lift closer together thus decreasing the interaggregate pore diameters and lowering the hydraulic conductivity.

Porosity

Porosity is an index of the relative pore volume in the soil. In compacted soil liners, the porosity is highly variable as the soil alternately swells, shrinks, aggregates, disperses, compacts, and cracks. Total porosity is the total volume of pores (non-solids) in a soil sample divided by the bulk sample volume. The total porosity is easily measured, however it reveals nothing about the pore size distribution, an important characteristic needed for estimation of the travel times and velocities of pollutant solutes through the liner. This section discusses characteristics and methods to evaluate the pore size distribution of compacted soils, the concept of effective porosity (the volume of pores primarily responsible for the transmission of fluids through the soils), how properties of the soil material and construction practices influence effective porosity of liners, and field methods to document the occurrence of effective pores in individual lifts or complete soil liners.

Pore Size Distribution --

From the standpoint of factors governing the hydraulic conductivity of a soil liner, the most important factor is the size distribution of pores. Large voids occurring between partially unaccommodating clods (clods which are not completely molded together after compaction) are considered structural defects in the liner. These defects, if continuous through the liner thickness, short circuit the liner matrix and can cause unpredicted releases of water and solutes. Compacted soil materials are composed of deformed soil aggregates of various sizes, each of which is composed of smaller, primary aggregates. As a consequence, the pore size distribution is typically bimodal with modes corresponding with the inter- and intra-aggregate pore diameters of the compacted materials (Garcia-Bengochea, 1978). The theoretical, maximum interclod porosity for a soil medium composed of porous soil clods stacked in a cubic packing arrangement is 47.6%. Compacted liners have much lower interclod porosity values because the compaction process deforms and closely packs soil clods. Figure 4 shows the relationship between unit weight and interclod porosity for clods having porosities of 10, 20, and 30%.

In general, there are two ways to investigate soil porosity: behavorial measurements and morphological measurements (Horton and Thompson, 1986). Behavioral measurements rely on acceptance of the

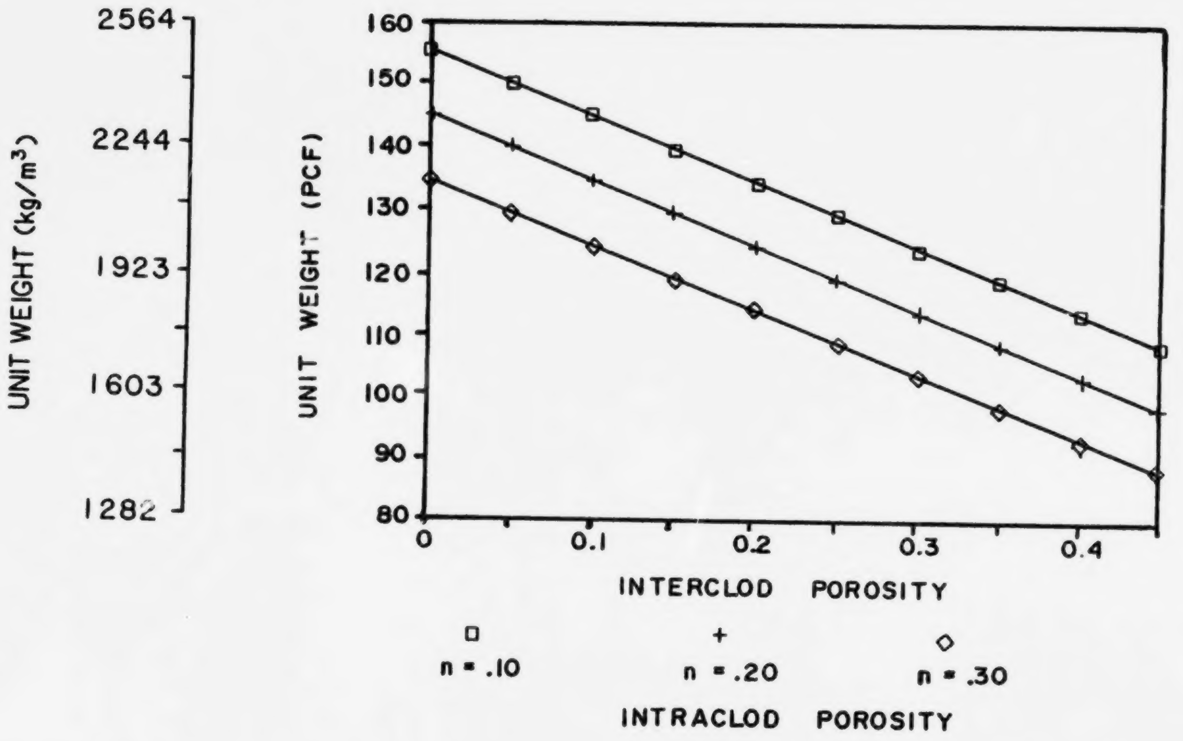

Figure 4. Relationship between interclod porosity, intraclod porosity, and unit soil weight (From Speake, 1986).

capillary model of soil pore space. This model allows estimation of effective pore diameters based on the suction or capillary pressure versus sorption or desorption of liquids. The two most common techniques are water retention measurements and mercury intrusion porosimetry. In water retention measurements, water is gradually pulled out of a saturated soil sample by equilibrating it at different pressures. In mercury porosimetry, mercury is gradually pushed into the soil sample with increasing pressure. In both instances, the volume of fluid sorbed or desorbed at known pressures gives information about pore sizes and can allow a continuous distribution of effective pore diameters to be obtained. Since behavioral measurements are based on the assumption that soil pores act as continuous, cylindrical, discrete capillary tubes, they are more appropriate for certain coarse-grained materials (Hillel, 1971). Mercury intrusion porosimetry has the additional disadvantages that (1) all water must be removed from the sample prior to testing, either through oven drying, freeze drying, or acetone replacement. This usually leads to alteration of the soil pore size distribution; and (2) the sample size is restricted to about 1 cm^3, thus widely spaced liner defects can not be statistically evaluated by this method.

Morphological measurements of soil porosity use visual images of the pores in a soil sample. Since the image is a simplified model of the porosity, it allows study of pore sizes as well as other characteristics, such as pore shapes, patterns, and the continuity of pores between serial-section images of the soil. Horton and Thompson (1986) discuss theoretical and practical considerations for three techniques of obtaining morphological images of soil porosity: (1) impregnation with plastic resin containing a UV sensitive dye and photographing polished slabs under ultraviolet light; (2) preparing soil thin sections approximately 30-um in thickness and photographing under circularly polarized light; and (3) viewing polished 2.5 x 2.5-cm slabs with a scanning electron microscope. The main difficulties with these techniques were problems in getting the resin to fill all micropores in the samples, the need for many replicate measurements due to the small scale of observation, high degree of variability in pore distributions and the inability to resolve a wide range of pore diameters.

A comprehensive study of the relationship between pore size distribution and hydraulic conductivity was conducted by Garcia-Bengochea (1978) using mercury intrusion porosimetry (MIP). The ultimate goal of this effort was to develop predictive equations for hydraulic conductivity using models that used parameters derived from the pore size distribution (PSD) as input. The MIP method basically consists of acquiring a small sample of clay. Soils employed in the study were mixtures of 90% silt/10% kaolin, 70% silt/30% kaolin, and 50% silt/50% kaolin. These materials were used to represent natural, silty clays frequently employed in earthwork construction. The samples were compacted using standard and modified Proctor compaction methods. Measured hydraulic conductivities ranged from 10^{-4} to 10^{-9} cm sec^{-1}.

The pore size distribution of most samples was found to be bi-modal with modes occurring at 0.2-um and 1- to 10-um. In addition, all of the specimens showed little or no volume of pores having diameters greater than 10-um. It is likely that larger pores would have a larger natural spatial separation and would be less likely to be detected in the small samples used in the study.

Results of the study showed that hydraulic conductivity of the soil decreases as the large pore mode (LPM) decreases. Since the compacted soils contained a binary system of pores, the position and frequency of the LPM was found to be the best indicator of the degree of soil fabric homogenization. The diameter of the pore corresponding to the small pore mode (SPM) remained relatively fixed for soils compacted at various moisture contents and compactive efforts. It is believed that the SPM is related to the particle size of the kaolinite platelets, and the frequency of the SPM is probably dependent on the percentage of clay minerals in a sample. The diameter of the LPM was generally dependent on compaction water content.

Effective Porosity --

Effective porosity has been described as that portion of the total liner porosity that contributes significantly to liquid flow. Effective porosities are less than total porosities because some pores are discontinuous and some pores have narrow necks that essentially prevent liquid flow.

Peyton et al. (1986) suggested that the effective porosity of a porous medium might vary with the nature of the solute as well as the actual flow conditions. For example, organic molecules which behave as cations are more strongly adsorbed to soil particles and experience retarded flow compared to anionic or nonpolar molecules.

Horton et al. (1985) developed a method for estimating the effective porosity of compacted soils based on mercury intrusion porosimetry and used this technique to predict transit times of noninteracting solutes through samples of compacted materials. Table 1 shows a comparison of physical properties of subsurface materials from three soils developed in major Iowa parent materials which were compacted at mosture contents 1 to 2% higher than optimum. The estimated effective porosities based on mercury intrusion porosimetry were 15 to 20% of the total porosities of the compacted soil materials.

These effective porosity values are slightly higher than those reported by Green et al. (1985). Those authors reported that only about 10% of the total porosity was effective in transmitting organic liquids through compacted soils.

TABLE 1. PHYSICAL PROPERTIES OF THREE COMPACTED SOILS.*

Soil Material	USDA Texture	USCS Class	K $(m^3/m^{-2}\ sec^{-1})$	Total Porosity	Effective Porosity
Nicollet	Sandy clay loam	CL	5×10^{-10}	0.29	0.04
Fayette	Silty clay loam	CL	2×10^{-8}	0.40	0.08
Clarinda	Clay	CH	1×10^{-9}	0.46	0.08

*From Horton et al. 1985

Development of Macroporosity --

Stresses caused by internal loading and tension forces arising from desiccation of a soil are of major importance in explaining the physical formation of macrofeatures (Moore and Ali, 1982). In a study aimed at modelling subsidence of landfill covers, Murphy and Gilbert (1985) suggest two possible physical causes for the development of cracks or fractures in a liner: subsidence cracking and/or desiccation cracking. Either mechanism may enhance the efficiency of the other (i.e., subsidence may enhance shrinkage cracking and vice versa). Boynton and Daniel (1985) investigated the effect of cracks on the hydraulic conductivity of kaolinite and fire clay. As expected, it was found that (1) fractures or cracks will form in a clay if allowed to desiccate, (2) cracks tend to close upon rewetting of the soil, and (3) hydraulic conductivity of a soil containing cracks is much higher than for a soil devoid of fractures. The authors also found that increasing the confining pressure in the permeameter causes a corresponding decrease in hydraulic conductivity, which suggests that the cracks in the sample tend to close as the confining pressure is increased. Fickies et al. (1979) reported that desiccation-induced cracks closed after the addition of water in response to swelling of the clay matrix. They also demonstrated that the hydraulic conductivity of a rewetted, fractured sample was not as low as for an unfractured specimen. They speculated that deposition of runoff-suspended silt, clay, sand, and organic matter into cracks may partially account for the inability of the soil to return to its unfractured permeability.

Barst (1965) conducted a study aimed at determining whether clays are susceptible to shrinkage in the presence of saline solutions. In an investigation to determine which clays are the most likely to experience syneresis, Barst introduced an aqueous solution with a salinity approximately that of sea water to specimens of bentonite, kaolinite, and mixed clay assemblies. After two weeks of saline solution additions, desiccation cracks were observed in the Wyoming bentonite. The Georgia kaolinite was least susceptible to the formation of shrinkage cracks with no cracks observed in the pure sample. Mixtures of 5, 10, and 25% bentonite with the kaolinite showed definite shrinkage crack development. It is apparent that the bentonite was responsible for the cracking in the kaolinite. Clay mixtures containing 35% illite, 10% bentonite, 5% chlorite, and 50% mixed-layer clay mixture experienced no more shrinkage than a soil containing from 5 to 10% bentonite. It appears that soils containing even small amounts of swelling lattice clay have the ability to alter their water-retention capacities in response to changes in the salinity of a surrounding aqueous medium.

Morphological Studies --

Studies of the morphology of a compacted soil liner can yield information useful in the determination of the necessary soil liner thickness. Comparative morphological studies can be used to document the effective porosity of field compacted soil liners, to document the fate of clods compacted with various types of compaction equipment, and to trace continuous flow paths through lifts or entire liners. Ritchie et al. (1972) used a fluorescent dye to trace water movement in a clay soil possessing a binary system of pores. The authors found that the dye provided qualitative evidence that most of the water which flowed through the soil passed through the larger system of pores. In a similar investigation, Omoti and Wild (1979a; 1979b) employed fluorescent dyes and ultraviolet (UV) photography to mark the pathways of solute movement through soils. They discovered that under UV light, the dye gave a clear indication of conducting and nonconducting channels. An interesting finding of the study was that high dye concentrations were frequently noted that were not found to exist in association with any channels; they speculated that zones of loosely-packed aggregates could be responsible for the occurrence of this phenomenon.

Use of Chemical Tracers to Study Water Movement--

Typically, the rate of dye movement through a soil liner is extremely slow so that the depths where morphological measurements can be made are limited. To overcome this problem, dye can be introduced onto horizontal surfaces excavated at various depths within the liner. For example, a liner composed of 15-cm lifts can be studied by applying dye at the surface to trace flow through the upper portion of the lift, and at a 7.5-cm depth (via an excavated 30 x 30-cm section) to study the bottom portion of the lift. By utilizing excavated surfaces, effective pores can be traced at any depth within the liner (Rehage et al. 1986). Another approach which can be utilized is dye introduction via open boreholes installed in the completed liner. This allows dye to move radially from the borehole, most likely following zones of lower density and lift interfaces.

Techniques for documenting the paths through which soil water flows has been a topic which has intrigued researchers for many years. Early attempts to document the heterogeneity of soil moisture movement centered on the use of gravimetric soil moisture measurements (Specht, 1957), resistance units (Voigt, 1960), and tensiometers (Rutter, 1964). A different approach developed by Tamm and Troedsson (1957) involved spreading ammonium thiocyanate on the soil surface, allowing it to infiltrate with rainwater, digging a pit and spraying the face of the pit with ferric chloride to cause the appearance of a blue color. This procedure was limited both by the destructive nature of the procedure and the similarity of the resultant colors with the natural soil colors.

For a dye to be effective in tracing the movement of soil water, it should meet the following criteria as set forth by Reynolds (1966):

1. It should exist in solution as an anion to minimize its adsorption by soil and organic matter.
2. It should have a color that contrasts with that of the soil.
3. It should be freely soluble in water.
4. It should resist microbial degradation.
5. It should be equally colorful in the wet or dry state.
6. The color or fluorescence should be stable over a wide pH range.

Twelve fluorescent dyes were evaluated in laboratory conditions for the above parameters (Reynolds, 1966). He found that Tinopal 2BP was rapidly precipitated while Rhodamine and Eriosin Brilliant Orange were adsorbed by the organic matter, presumably due to their basic nature. Pyranine was selected as best with Kiton Yellow as second best (Table 2). For a field test, Reynolds (1966) applied 5- to 10-cm wide bands of pyranine and kiton yellow dyes to forest soils, waited 36 days during which 4.11-cm of rain were received and then observed dye movement. In general, the dyes penetrated 2- to 10-cm into the A horizon; however much deeper penetration, up to 23-cm, occurred in the vicinity of stakes, tree trunks, and rhizomes.

Another evaluation of the available dyes was conducted by Smart and Laidlaw (1977). They compared the performance of eight fluorescent dyes; amino G acid, photine CU, fluorescein, lissamine FF, pyranine, rhodamine B, rhodamine WT, and sulpho rhodamine B in an extensive series of laboratory tests. Among the parameters evaluated were sensitivity and minimum detectability, the effect of water chemistry on

TABLE 2. REPORTED USES OF DYES TO STUDY MOVEMENT OF WATER THROUGH SOILS

Dyes Used	Type of Dye	Type of Study	Dye Selected as Best (Most Useful)	Source
Sulpho-rhodamine B	Fluorescent	Laboratory	Lissamine Yellow FF	Smettem and Trudgill (1983)
Lissamine Yellow FF	Fluorescent	"	"	"
Chlorantine Fast Green	Non-Fluorescent	"	"	"
Sirius Red	Non-Fluorescent	"	"	"
Chicago Blue	Non-Fluorescent	"	"	"
Lissamine Yellow FF	Fluorescent	Field		Smettem and Trudgill (1983)
Rhodamime WT	Fluorescent	Field		Trudgill et al., 1983
Lissamine FF	Fluorescent	"		
Amino G Acid	Fluorescent	"		
Pyranine	Fluorescent	Laboratory	Pyrinine best	Omoti and Wild (1979a)
Fluorescine	Fluorescent	"	Fluoresine second	"
Rhodamime B	Fluorescent	"	"	
Erio Acid Red XB	Fluorescent	"	"	
Dehydro-thio-paratoluidne Sulfanic acid	Fluorescent	"	"	
Uvitex CF 200	Fluorescent	"	"	
Uvitex WG	Fluorescent	"	"	
Tinopol 2BP	Fluorescent	"	"	
Diphenyl Brilliant Flavine 7GFF	Fluorescent	"	"	
Pyranine	Fluorescent	Field	Fluorescein because could be photographed. Pyranine lost too much fluorescence in field.	Omoti and Wild (1979b)
Fluorescein	Fluorescent	"		

TABLE 2 CONTINUED.

Dyes Used	Type of Dye	Type of Study	Dye Selected as Best (Most Useful)	Source
Amino G Acid	Fluorescent			Smart and Laidlaw, 1977.
Photine CU	Fluorescent			"
Fluorescein	Fluorescent			"
Lissamine FF	Fluorescent			"
Pyranine	Fluorescent			"
Rhodamine B	Fluorescent			"
Rhodamine WT	Fluorescent			"
Sulpho Rhodanine B	Fluorescent			"
Pyranine	Fluorescent	Laboratory	Pyranine and Keton Yellow least affected by soil	Reynolds, 1966
Tinopal AN	Fluorescent	"		"
Tinopal 2BP	Fluorescent	"		"
Rhodamine 6 G_{500}	Fluorescent	"	"	"
Rhodamine B_{500}	Fluorescent	"	"	"
Eriosin Brilliant Orange	Fluorescent	"	"	"
R Salt	Fluorescent	"	"	"
Dehydro-thio-paratoluidine-Sulphanic acid	Fluorescent	"	"	"
Primuline	Fluorescent	"	"	"
Keton Rhodamine B_{400}	Fluorescent	"	"	"
Fluorescein Water Soluble	Fluorescent	"	"	"
Keton Yellow EFF	Fluorescent	"	"	"
Pyranine	Fluorescent	Field	Pyranine best	Reynolds, 1966
Keton Yellow EFF	Fluorescent	"	"	"

fluorescence, photochemical and biological decay rates, adsorption losses, toxicity, and cost. Limited field tests of dye recovery from surface streams were also conducted. The results showed that for surface water, i.e. streams, rhodamine WT was best. In underground water applications, lissamine FF and Rhodamine WT performed equally well. Of the three dye color spectrums; orange, green and blue rhodamine WT, lissamine FF and amino G acid were selected respectively as best able to mark the paths in the soil through which water flowed.

Omoti and Wild (1979a) screened nine dyes including pyranine, fluorescein, rhodamine B, erio acid red XB, dehydro-thio-paratoluidine sulfonic acid, Uvitex CF 200, Uvitex WG, Tinopol 2BP, and diphenyl brilliant flavine 7GFF for use in tracing water movement through laboratory soil columns. Laboratory tests using 10-cm-diameter, 30-cm-long columns packed with a loamy sand showed that pyranine was much more mobile than fluorescein. The breakthrough curve for pyrinine closely resembled that of chloride. Distribution of dye in the soil as a function of depth was often less than that of chloride and ^3H_2O. The data showed that solute movement through soils is not reproducible. This was substantiated by observations that the dye concentrations were non-uniform across horizontal cross sections of the columns. Thus, it appears that much flow occurred via preferential channels even though the soil was carefully recompacted. They found pyranine to be the most useful dye due to its high fluorescence and low adsorption, however, its use is limited to short studies (less than 24-hr) due to its low stability in soil. In a companion field study, Omoti and Wild (1979b) isolated plots 1-m x 1-m in a field of loamy sand. Applications of pyranine and ^{36}Cl; pyranine and ^3H_2O; and fluorescein were made by spraying onto the soil. Ten-cm-diameter cores were taken from the plots, photographed, and extracted for ^{36}Cl, ^3H_2O, and dye concentration. Pyranine could only be measured on soil extracts due to reduced fluorescence under field conditions. The study showed high dye concentrations in earthworm channels indicating that these channels conducted large amounts of solutes. High dye concentrations were also associated with areas of low bulk density which included fissures of 0.05- to 0.1-mm wide. In some cases, it was found that these fissures and the pores between loosely packed aggregates were primarily responsible for conducting solutes. While the technique of using fluorescent dye was not quantitative, Omoti and Wild (1979b) concluded that the technique is able to distinguish the channels that transmit solutions.

Smettem and Trudgill (1983) conducted a laboratory evaluation of sulpho-rhodamine B, lissamine yellow FF, chlorantine fast green, sirius red and Chicago blue dyes. Of these, they concluded that lissamine yellow FF would be potentially useful for tracing water movement if the residence time was short. Retardation of lissamine yellow FF from laboratory soil columns was 2 to 2.5 times greater than chloride. A field study was conducted using 300-cm^2 by 30-cm-deep PVC columns. Each column was treated with 500 ug dye on the surface which was allowed to be washed into the soil by natural rainfall. The soil columns were then removed and subsampled and analyzed for dye content. The results showed that dye penetration was well correlated with visible soil structure and that the dye penetrated much more deeply than predicted through theoretical considerations. It therefore appears that Lissamine FF is the best suited dye for field use due to its persistence, solubility, anionic nature and good fluorescence characteristics. For short-term laboratory experiments, pyranine may be a better choice.

Use of Chemical Tracers to Study Water Movement--

When the goal of a soil water tracer study is to accurately measure water velocities, it becomes desirable to make use of a chemical tracer since most colorimetric dyes exhibit some degree of adsorption. Todd (1959) has presented some guidelines for use in the selection of a chemical tracer: (1) the tracer must be susceptible to quantitative determination at very low concentrations, (2) it should be absent, or nearly so, from the natural water, (3) it must not react with the natural water to form a precipitate, (4) it must not be adsorbed onto the porous medium, and (5) it should be inexpensive and readily obtainable.

Natural occurrences of bromide are usually low (Smith and Davis, 1974; Adriano and Doner, 1982; Bowman, 1984). Also, bromide is considered to be mobile in soil environments (Smith and Davis, 1974; Adriano and Doner, 1982). This is because bromide is not significantly sorbed by mineral and organic matter (Smith and Davis, 1974; Bowman, 1984). In addition, Bowman (1984) asserts that bromide is, generally, the most suitable of the common water tracers.

Lift Thickness

While there have not been any studies reported in the literature on the effect of lift thickness on the hydraulic conductivity of soil liners, there are reports that the thickness of the soil before and after compaction affects some of the physical characteristics imparted to the soil including density, strength, and the degree of clod remolding. The optimum thickness of the lift depends upon the size and type of compaction equipment as well as the maximum grain size of the soil (Holtz and Kovacs, 1981). After the soil is spread in the desired loose thickness, it is densified by compactive effort supplied by repeated passes of the compaction equipment. The effectiveness of the compaction is diminished in thicker lifts due to decreasing compactive effort at the lower depths (Turnbull and Foster, 1958).

For lift thicknesses greater than the length of the roller feet, the compaction effort of the equipment is diminished (Hilf, 1975). When a footed roller (sheepsfoot, pad foot, or tamping foot) is used to compact a soil with an excessive lift thickness, the foot sinks completely into the soil. At that point, the weight of the equipment is supported on the larger surface area of the drum, thereby decreasing the effective weight applied per unit area. This reduces the ability of the roller to remold the clods at the bottom of the lift. Consequently, it is better to use thin lifts since they result in higher minimum compactive efforts exerted for a given compaction energy (Shiver and Anderson, 1985).

Mitchell et al. (1965) state that, in general, as density increases, strength increases while hydraulic conductivity decreases. Uniform density is critical to provide a uniformly low hydraulic conductivity and high strength. Turnbull and Foster (1958) present data for compaction of soil in lifts varying from 15- to 60-cm. They showed that as the thickness of the lift increased, the density at the bottom of the lift decreased, resulting in a layered fill. The densities near the compaction surface were all approximately the same regardless of the lift thickness.

The Bureau of Reclamation invariably refers to the use of lifts not more than 15-cm thick after compaction (U.S. Bureau of Reclamation, 1974). The Bureau of Reclamation has built over 100 earthen dams and, in most cases, has compacted the earthfill in 15-cm lifts (Hilf, 1975).

Interlift Flow

Brown (1986) examined the flow patterns exhibited by both laboratory- and field-compacted soil liner samples. Laboratory samples were compacted in fixed wall permeameters using ASTM Procedure 698-70. Field tests employed 7.5-cm-thick lifts compacted to 95% Proctor with a gasoline engine-powered compactor. By using dyes to trace liquid flow paths, he determined that most of the flow through the liner occurred vertically through the lifts and horizontally between the lifts. In both the lab- and field-compacted samples, only isolated stained pores were found going vertically through lifts. In contrast, almost the entire interlift areas were dye-stained on all laboratory and field samples.

Such preferential horizonal flow between lifts may partially offset the benefits of constructing a soil liner in multiple lifts. One advantage of multiple lifts is that off-specification materials or poorly compacted areas are not likely to be located directly over each other in adjacent lifts. A liner could have a very low conductivity even if all lifts had defects but no connected series of defects extended throughout the liner thickness. This hypothesis would not hold, however, if all the defects in one lift were connected to defects in adjacent lifts due to unrestricted interlift flow.

Boynton (1983) found that soil liner samples compacted near optimum water content had a conductivity that was slightly higher in the horizontal direction than in the vertical. The differences, however, were not attributed to preferential flow between lifts. He hypothesized that the cause for higher horizontal flow might be preferential orientation of clay particles with their long axis perpendicular to the direction of the applied compactive effort. He also speculated that the difference may be attributed to vertical conductivity being controlled by the lowest conductivity lift while horizontal conductivity would tend to be an average of the values obtained for all the lifts. No dye studies were conducted to document the actual flow paths.

Bulk Density

During the soil liner design process, a moisture/density curve is developed for each type of earth material that may be used in the construction of the liner. The ideal method of determining the in situ hydraulic conductivity of a soil, however, would be a direct measurement in the field (Harrop-Williams, 1985). One method used in estimating the field hydraulic conductivity of a compacted soil is through an assessment of the degree of compaction via the moisture/density curve and assuming the field conductivity would be the same as was found for a sample compacted in the laboratory to that density and water content. Construction quality control requires that a soil be compacted to a specified percentage of the maximum dry unit weight (Wang and Huang, 1984). Since water content is difficult to control in the field, the moisture/density/conductivity curve is used to estimate a range of suitable moisture contents which will yield a liner with an acceptable hydraulic conductivity. To date, the validity of extrapolating this relationship to field conditions has not been proven.

Harrop-Williams (1985) performed linear regression using the variables dry unit weight, moisture content, specific gravity of the solids, unit weight of water, and residual water saturation. Holding all of these variables constant except dry unit weight and moisture content, the author was able to show, with a good degree of correlation, that hydraulic conductivity can be predicted from field measurements of moisture content and dry unit weight. In a similar analysis, Puckett et al. (1985) attempted to correlate bulk density of a soil to hydraulic conductivity, and found that the correlation coefficient was less than 0.7. In addition, the hydraulic conductivity could go up dramatically with time, making any earlier measurements meaningless. The authors elected to discard the regression.

During investigations of the movement of fluorescein-tagged water through soil, Omoti and Wild (1979a) measured dry bulk density to determine the frequency of occurrence of fissures and zones of poor packing. Accumulations of fluorescein-tagged water which infiltrated through the soil surface were noted in these same areas. The authors found a negative correlation between bulk density and fluorescein concentration (measured in micrograms of dye per gram of soil).

According to McCarthy (1982), the particle shape of the more common clay minerals ranges from plate-shaped to fibrous. In contrast to spherical grains, this morphology allows for extremely nonuniform packing of the constituent particles. Since bulk density is, by definition, the mass of solids per unit volume, the arrangement of clay particles is probably the most significant factor determining bulk density; closer packing of the grains results in more particles per unit volume. However, mineralogy, interstitial water chemistry, and electrochemical state can greatly affect the arrangement of clay crystals.

Spatial Variability

Nielson et al. (1973) studied the spatial variability of field-measured soil properties and concluded that hydraulic conductivity and soil water diffusivity were log-normally distributed in both the horizontal and vertical planes. They concluded that seemingly uniform soil areas may manifest large variations in hydraulic conductivity values, especially when water contents were low. Variations in texture, bulk density, and water content were found to be much less. Russo and Bressler (1981a) evaluated the effects of field variability in soil hydraulic properties on unsaturated soil-water and salt flows. The governing water and salt flow equations were solved numerically using field data of soil hydraulic conductivity and specific water capacity. Simulated values of pressure head, water flux and wetting front positions were used to estimate distributions of normal or log-normal probability functions.

Russo and Bressler (1981b) used sorptivity determination and five parameters describing the hydraulic conductivity and soil water retentivity to analyze the spatial distribution of hydraulic properties in an experimental field. The parameters were saturated hydraulic conductivity, air entry value, saturated and residual water contents and a constant characterizing the pore size distribution of the soil.

Rogowski (1986) measured the spatial variability of hydraulic conductivity in a 9.1 x 22.9-m field-scale clay liner research facility. A grid of 250 - one-square-meter underdrained cells and 28-cm diameter infiltration rings was used to monitor inflow and outflow rates in the 30-cm diameter thick liner over a 14-month period. Infiltration and outflow rates increased consistently following ponding for several months, then began to decrease slightly and apparently reached steady- state conditions after 10 months. Hydraulic conductivity values ranged over three orders of magnitude from 10-5 to 10-8 cm sec-1. While conductivity values varied spatially, there appeared to be no correlation with the distribution of density, the amount of water required to saturate the liner, or the distribution of soil volume change.

The ultimate choice of a minimum liner thickness which will assure the long-term protection of human health and the environment must also compensate for liner defects which result in increased spatial variability in hydraulic properties. Unfortunately, there are no quick or simple methods for evaluating the field hydraulic performance of a completed soil liner. In most cases, testing of liner hydraulic properties will be accomplished on a test liner section and the results extrapolated to the facility-sized liner (Bogardi and Kelly, 1986).

Liner Defects --

Defects can occur in both horizontal and vertical dimensions of the liner due to imperfections in liner materials, construction practices, inadequate quality control programs, and exposure to weather. The upper lift of a soil liner is especially susceptible to the effects of weathering. The bottom lift may not be effective due to mixing with the underlying soil material. This may occur, for example, where a sheepsfoot roller is used to compact the bottom lift over a granular, higher permeability drainage layer. The kneading action of the sheepsfoot roller would tend to mix the lift with the granular material.

Lenses of gravel, sand, silt, organic material, and coarse debris frequently occur within borrow areas. These features create zones of high permeability and, if pockets of such permeable material are excavated at the borrow site, they may be transported to the liner construction site (Anderson, 1986). Inadequate homogenization of the soil prior to compaction can transfer these regions of high conductivity to the liner (Anderson et al., 1986).

The compaction control parameters, dry density and water content, are always variable to some extent. This is caused by imperfect soil homogenization, uneven wetting, evaporative advection effects, uneven compaction, etc. As a result, the spatial variability of hydraulic conductivity is high even with careful compaction (Rogowski, 1986).

Natural weathering processes may result in the formation of macrofeatures within in situ clay soil deposits and compacted clay soils (Anderson and Rehage, 1986). Examples of these macrofeatures include fillings (White, 1964), faults, fissures, bedding planes, joints, sheeting (Skempton et al., 1969), root holes, burrows (Folkes, 1982), slickensides, subsurface erosion pipes (Griffin et al., 1984), blocky or prismatic structure (Baver et al., 1972), dehydration cracks (Boynton, 1983), and freeze-thaw disturbed areas.

Desiccation cracks are common in clay soils and can cause large increases in hydraulic conductivity (Griffin et al., 1985). Daniel (1984) described several case histories involving desiccation of soil liners. Desiccation of liners resulted in cracking which appeared to contribute to high leakage rates through the liners. Boynton (1983) desiccated laboratory slabs of clay and then prepared hand-trimmed samples for permeability testing. Desiccated samples were 10 to 100 times more permeable than undisturbed samples. It appeared that cracks were only partially closed after the soil was rewetted and swelling took place.

Most soil liners are constructed through the compaction of soil clods. When the compaction process does not completely destroy clod structure, there may be a network of continuous macropores between the clod remnants (Anderson, 1986). The number and size of these macropores often varies spatially within a lift and between adjacent lifts. EPA is currently conducting research to determine the compaction equipment and water contents which are most effective at removing clod structure and associated continuous macropores.

Difficulties in Measuring Hydraulic Conductivity --

While hydraulic conductivity is the most important consideration for determinations of minimum liner thickness, it is not a trivial matter to determine actual conductivity values. There are many sources of error which can be the same order of magnitude as the quantity being measured. For instance, the volume of water held in a field infiltrometer may increase faster due to thermal expansion than it decreases due to infiltration. The engineering standard practice of measuring the conductivity of 76-cm shelby tube cores will nearly always result in values substantially lower than actual field values. This should be considered in light of the fact that a given soil liner can only be relied on to the extent that its hydraulic conductivity has been adequately characterized.

Several recent studies have indicated that field hydraulic conductivity of a compacted soil liner may be much greater than would be predicted from laboratory tests. Griffin et al. (1984) conducted both laboratory and field hydraulic conductivity tests on clayey soil used as a liner for a hazardous waste landfill. Laboratory derived hydraulic conductivity values were all 2 x 10^{-7} cm sec^{-1} or less. In contrast, hydraulic conductivity values obtained in the field were as much as three orders of magnitude greater than the laboratory values. Routine monitoring of the actual hazardous waste landfill site revealed that organic contaminants were migrating two to three orders of magnitude faster than had been predicted (Griffin et al., 1985).

Daniel (1984) compared laboratory and field hydraulic conductivity values with the acutal leakage rates of four clay liners. In all four cases, the laboratory values were much lower than those measured in the field. In the two cases where field hydraulic conductivity tests were performed on the actual liner, values obtained from these field tests accurately reflected the leakage rate of the entire liner.

Other studies have also found large differences between field-measured and laboratory-measured hydraulic conductivities (Herzog and Morse, 1984; Boutwell and Donald, 1982; Gordon and Huebner, 1983). One reason cited for the higher values obtained in field tests is that laboratory samples can be more readily prepared without the defects which can greatly increase hydraulic conductivity. Methods used to prepare soil liners in the field are difficult to simulate in the laboratory. One example is the method of compaction. Soil liners are often compacted in the field with a kneading action using sheepsfoot rollers. In contrast, impact compaction is usually used to prepare soil liner samples in the laboratory. Even though identical densities and water contents may be obtained with these different compaction methods, the resulting samples may have very different hydraulic conductivities (Mitchell, 1976).

Several other reasons have been cited for the large discrepancies between laboratory and field derived hydraulic conductivity values. Soil liner samples prepared in the laboratory are not subjected to the climatic conditions (such as desiccation and freezing) which can cause cracking and hydraulic conductivity increases in field-prepared soil liners (EPA, 1984). There may also be a tendency to run laboratory tests on samples of selected, finer textured soil materials (Olson and Daniel, 1981). Probably the most widely cited and most important cause of the observed differences is that field tests can evaluate much larger and hence more representative samples than are practical in laboratory tests.

The EPA has long stated a requirement for compacted soil liners to have hydraulic conductivities of 1×10^{-7} cm sec^{-1} or less. It has only recently become practical to verify this performance standard in the field. In the past several years, several field infiltrometers have been developed and field-tested which measure very low hydraulic conductivity values (Day, 1984; Day et al., 1985; Anderson et al., 1984).

It is difficult to exactly quantify field hydraulic conductivity values which are substantially less than 1×10^{-7} cm sec^{-1} (Anderson et al., 1984). It is much easier, however, to simply verify that the field hydraulic conductivity is 1×10^{-7} cm sec^{-1} or less (Day et al., 1985). Such a verification would indicate that a soil liner meets or exceeds the EPA performance standard.

Numerical Analysis

The capability of a soil liner to retard the flow of liquids has been analyzed using a deterministic approach and by statistical methods. Moore and Ali (1982) used a statistical approach to investigate the effect of cracks on the conductivity of a soil liner. They found that (1) cracks in a liner render it more permeable, and (2) cracks can negatively affect the containment capability of a liner.

Ali et al. (1982) developed a random-walk statistical technique for analyzing the effect of uncertainties in liner parameters on the flowrate through the system. Parameters of interest in the study were

(1) liner thickness, (2) length of crack, (3) probability of occurrence of a crack, (4) liner permeability, (5) crack permeability, and (6) the ratio of crack length to liner thickness. In the model, the flow paths for liquid are simulated by tracing the movements of many single water particles within the flow domain. Results showed that the ratio of crack length to liner thickness was the most significant parameter and caused more of an effect than the crack frequency.

The EPA (1986) recently developed SOILINER, a sophisticated computer model which simulates one-dimensional flow through a soil liner during infiltration. The model calculates breakthrough times of pollutant migration fronts at a number of nodes including the interface between the liner and the underlying soil or drainage blanket. A finite difference method is used to calculate unsaturated flow through the liner matrix. Inputs to the SOILINER model include saturated hydraulic conductivity, number and thicknesses of layers, and soil moisture potential. The output includes a profile of moisture potential, moisture content and hydraulic conductivity for various depths within the liner, and the location of the pollutant migration front. Simulations of flow through homogeneous, isotropic media using SOILINER have been verified by comparison with the analytical solution of Gardner (1958) but not by actual field studies.

The SOILINER model was developed for determining the minimum soil liner thickness needed to prevent pollutant release from a soil liner during the expected active and post-closure care period. The depth of the simulated pollutant front is considered to be minimum liner thickness needed to insure no release of contaminants occurs. A serious limitation of SOILINER is that only one-dimensional flow through homogeneous layers is simulated. In other words, the model only considers vertical flow through the liner matrix. Preferential flow through vertical macropores, lift interfaces, and other liner defects is not considered. Consequently, erroneously large estimates of pollutant breakthrough times may result if the liner contains any defects.

Horton et al., (1985) presented a numerical model which theoretically could be used to calculate liner thickness directly as a function of effective porosity and estimated breakthrough times of noninteracting solutes. Estimates of chloride breakthrough times calculated with the model agreed well with results of experiments using 2.5-cm columns of compacted soil materials. One disadvantage of the Horton model is that it does not account for the effect that vertical layers within a soil liner have on flow behavior. Therefore, it can only be used to estimate breakthrough times for individual lifts. As with the SOILINER model, the Horton model presumes that a soil liner contains no defects that would increase hydraulic conductivity.

SECTION 4

CHANNEL FLOW COMPUTER MODELS

Any model for the flow of liquids in a soil liner must account for the controlling soil physical properties. Prevailing soil liner construction practices usually result in the occurrence of a number of liner defects, such as cracks, clod remnants, channels, continuous macropores, and incomplete bonding between lifts in the completed liner fabric. Therefore, for a model to be useful, it must include two kinds of processes, flow within each lift and flow between lifts (interlift flow). In addition, flow within a lift must encompass both matrix flow and flow through channels which short-circuit the liner matrix. This section presents a numerical model which accounts for the two types of flow processes in soil liners. This model should aid both policy development on minimum liner thickness and understanding of the critical construction parameters affecting overall liner performance.

The strategy used to compose the model is as follows:

1. Quantification of the conductivity of one lift, and isolation of the parameters that are important in determining conductivity;
2. Selection of values for these parameters and explanation of why they were chosen;
3. Development of physical models for interlift flow; and
4. Integration of the results into a composite model.

HYDRAULIC CONDUCTIVITY OF A LIFT

Hydraulic conductivity is the movement of a liquid through a medium subject to a hydraulic gradient. It is defined in terms of Q, the volume of liquid flowing per unit time, A, the area through which it flows, and the hydraulic gradient dH/dz, which is the change in head H over length z. The relationship of these parameters is given in Darcy's law as follows:

$$\frac{Q}{A} = K \frac{dH}{dz} \tag{4.1}$$

where K is hydraulic conductivity expressed in units of velocity. Another quantity used in describing flow in a medium is the permeability, which is the ability for a medium to allow liquid to flow through. Permeability is expressed in units of area. The most often used unit is the Darcy. One Darcy is 9.8697 x 10^{-9} cm^2. The Darcy is defined as the permeability necessary to drive water through a medium under a gradient of one atmosphere per centimeter, at the rate of one cubic centimeter per square centimeter per second. Permeability k is proportional to conductivity K by the following relation (Hubbert, 1940).

$$K = \frac{k \rho g}{\mu} \tag{4.2}$$

where ρ is the density of the liquid, g is the acceleration due to gravity and μ is the viscosity of the liquid. Darcy's law can be rewritten in terms of pressure P and permeability as

$$\frac{Q}{A} = \frac{k}{\mu} \frac{dP}{dz} \tag{4.3}$$

The permeability of a lift results from flow of liquid through the pores between grains and through defects such as channels. The effects can be added to give a total permeability (Parsons, 1966). Ignoring defects, the total permeability of a lift can be modeled as that of a slab with a population of perpendicular cylindrical pores, all of which have the same radius and all of which are equally spaced.

Actually, the pores are not equally spaced, they do not have the same radius and they are not perfectly oriented in the vertical direction. In addition, they do not have the same radius throughout their length. This model is still a useful approximation to reality. One must bear in mind that the radius here is an effective radius. As used in this model, an effective radius would be smaller than the minimum throat radius of a pore because this model has no tortuosity and does not account for chemical interactions between the soil and electrolytes in the water. The pores are assumed to have constant radii in contrast to constrained throats. Also, as far as the spacing is concerned, only the number of pores per unit area is important, not their distribution, due to the additive nature of permeability. It is also important to point out that only through-going pores are contributing to the permeability in this model. Through-going pores are defined as those with outlets to both the top and bottom of a lift. Through-going pores whose radii are significantly larger than those of the bulk of the pores shall be referred to as channels or defects.

Based on these assumptions, the contribution to the permeability of a lift made by these channels would be

$$k = \frac{\pi \ R^4}{8D^2} \tag{4.4}$$

where R is the radius of the channels and D is the spacing. This equation is derived in Appendix A. If a slab has a matrix permeability, k_r, then the total permeability caused by a combination of the small pores in the matrix and the channels would be

$$k = k_r + \frac{\pi \ R^4}{8D^2} \tag{4.5}$$

We shall see that the right-hand term is vastly greater than the matrix term if the channels have radii significantly greater than that of the pores contributing to the matrix permeability. Consequently, the smaller pores can be ignored in a bi-modal distribution of grain sizes. Following is an illustration:

First, equations (4.2) and (4.4) will be combined to give equation (4.6) to allow working in terms of conductivity.

$$K = \frac{\pi R^4 \rho g}{8 \mu D^2} \tag{4.6}$$

where the density and viscosity are that of ordinary water, 1 gram/cc^{-1} and 0.0089 poise, respectively, and the acceleration of gravity is 980 cm sec^{-2}.

If hydraulic conductivity (K) is chosen to be 10^{-5} cm sec^{-1}, Table 3 gives the spacing as a function of channel radius R. These same data are plotted in Figure 5. If all of the conductivity of a lift is due to cylindrical channels five microns in radius, the channels would have to be an average of 1.64 x 10^{-2} cm apart to maintain the conductivity of 10^{-5} cm sec^{-1}. If all channels had a radius of 100 microns, they would be 6.56-cm apart to give the same permeability. If the radii were 750 microns, they would have to be 3.69-m apart. If the channels were 2.54-cm in radius, they would have to be 4.2-km apart. However, if the liquid is water under a hydraulic gradient of unity, equation 4.6 cannot be extrapolated beyond a radius of 890 microns, because beyond this the fluid becomes turbulent. Tables 4, 5, and 6 give results for 10^{-6}, 10^{-7}, and 10^{-8} cm sec^{-1}, respectively. These are also plotted in Figure 5. These tables and figures clearly demonstrate that very few channels or defects can lead to large conductivities in compacted soil lifts. It is interesting to note that if all of the conductivity in a liner was due

TABLE 3. SPACING VERSUS CHANNEL RADIUS FOR A HYDRAULIC CONDUCTIVITY OF 1 x 10^{-5} CM SEC^{-1}

Channel Radius (um)	Metric Spacing (cm)	English Spacing (ft)	Metric Area (cm^2)	English Area (ft^2)	P(3-1)%*	P(3-2)%
1	6.57 E-4	2.15 E-5	4.31 E-7	4.64 E-10	C	C
5	1.64 E-2	5.39 E-4	2.70 E-4	2.90 E-7	C	C
10	6.57 E-2	2.15 E-3	4.31 E-3	4.64 E-6	C	C
25	.410	1.35 E-2	.168	1.81 E-4	C	C
50	1.64	5.39 E-2	2.70	2.90 E-3	C	C
60	2.36	7.76 E-2	5.59	6.02 E-3	C	C
70	3.22	.106	10.35	1.11 E-2	C	C
80	4.20	.138	17.66	1.90 E-2	C	C
90	5.32	.174	28.29	3.05 E-2	C	C
100	6.57	.215	43.12	4.64 E-2	C	C
125	10.26	.337	105.3	.113	43.31	18.76
250	41.04	1.34	1685	1.81	2.71	7.33 E-2
500	164.2	5.39	26,953	29.01	.169	2.86 E-4
750	369.4	12.12	136,449	146.9	3.34 E-2	1.12 E-5
890†	520	17.07	270,600	291.2	1.69 E-2	2.84 E-6

* P(3-1)% signifies the probability of finding a through-going macropore with a 7.6-cm shelby tube. P(3-2) denotes the probability of finding one in each of two consecutive lifts. Thus, $P(3\text{-}1)^2 = P(3\text{-}2)$. C denotes that one or more channels are expected. Average distance between channels expressed in scientific notation where E separates the mantissa (left side) from the exponent (right side).

† At radii greater than 890, Equation 4.6 no longer holds for water under a hydraulic gradient of unity because the Reynolds number of 2200 is exceeded. In this case, the fluid is no longer laminar.

TABLE 4. SPACING VERSUS CHANNEL RADIUS FOR A HYDRAULIC CONDUCTIVITY OF 1 x 10^{-6} CM SEC^{-1}

Channel Radius (um)	Metric Spacing (cm)	English Spacing (ft)	Metric Area (cm^2)	English Area (ft^2)	P(3-1)%*	P(3-2)%
1	2.08 E-3	6.81 E-5	4.31 E-6	4.64 E-9	C	C
5	5.19 E-2	1.70 E-2	2.69 E-3	2.90 E-6	C	C
10	.208	6.81 E-3	4.31 E-2	4.64 E-5	C	C
25	1.30	4.26 E-2	1.68	1.81 E-3	C	C
50	5.19	.170	26.95	2.90 E-2	C	C
60	7.48	.245	55.89	6.016E-2	81.596	66.6
70	10.18	.334	103.54	.111	44.64	19.40
80	13.29	.436	176.64	.190	25.82	6.67
90	16.82	.552	282.94	.305	16.12	2.60
100	20.77	.681	431.2	.464	10.57	1.12
125	32.44	1.06	1.05E3	1.13	4.33	.188
250	129.8	4.26	1.68E4	18.13	.271	7.33E-4
500	519.0	17.03	2.70E5	290	1.69E-2	2.86E-6
750	1168.0	38.32	1.36E6	1469	3.34E-3	1.12E-7
890†	1645.0	53.97	2.71E6	2912	1.69E-3	2.84E-8

* P(3-1)% signifies the probability of finding a through-going macropore with a 7.6-cm shelby tube. P(3-2) denotes the probability of finding one in each of two consecutive lifts. Thus, $P(3\text{-}1)^2 = P(3\text{-}2)$. C denotes that one or more channels are expected. Average distance between channels expressed in scientific notation where E separates the mantissa (left side) from the exponent (right side).

† At channel radii greater than 890, Equation 4.6 no longer holds for water under a hydraulic gradient of unity because the Reynolds number of 2200 is exceeded. In this case, the fluid is no longer laminar.

TABLE 5. SPACING VERSUS CHANNEL RADIUS FOR A HYDRAULIC CONDUCTIVITY OF 1×10^{-7} CM SEC^{-1}

Channel Radius (um)	Metric Spacing (cm)	English Spacing (ft)	Metric Area (cm^2)	English Area (ft^2)	P(3-1)%*	P(3-2)%
1	6.57E-3	2.15E-4	4.31E-5	4.6E-8	C	C
5	.164	5.386E-3	2.695E-2	2.90E-5	C	C
10	.6567	.02155	.4312	4.642E-4	C	C
25	4.104	.1347	16.846	0.01813	C	C
50	16.417	.5386	269.53	.2901	16.92	2.86
60	23.64	.7756	558.90	.6016	8.16	.666
70	32.17	1.0557	1035.4	1.1145	4.40	.194
80	42.03	1.3789	1766.4	1.9013	2.58	.0666
90	53.19	1.745	2829.4	3.0456	1.611	260E-2
100	65.67	2.1545	4312.5	4.642	1.057	1.12E-2
125	102.6	3.3664	10,529	11.333	.433	1.88E-2
250	410.4	13.47	1.68E-5	181.32	2.71E-2	7.33E-6
500	1641	53.86	2.69E-6	2901	1.69E-3	2.86E-8
750	3694	121.2	1.36E-7	14,687	3.34E-4	1.12E-9
890†	5202	170.7	2.71E-7	29,124	1.69E-4	2.84E-10

* P(3-1)% signifies the probability of finding a through-going macropore with a 7.6-cm shelby tube. P(3-2) denotes the probability of finding one in each of two consecutive lifts. Thus, $P(3-1)^2 = P(3-2)$. C denotes that one or more channels are expected. Average distance between channels expressed in scientific notation where E separates the mantissa (left side) from the exponent (right side).

† At radii greater than 890, Equation 4.6 no longer holds for water under a hydraulic gradient of unity because the Reynolds number of 2200 is exceeded. In this case, the fluid is no longer laminar.

TABLE 6. SPACING VERSUS CHANNEL RADIUS FOR A HYDRAULIC CONDUCTIVITY OF 1×10^{-8} CM SEC^{-1}

Channel Radius (um)	Metric Spacing (cm)	English Spacing (ft)	Metric Area (cm^2)	English Area (ft^2)	P(3-1)%*	P(3-2)%
1	.0208	6.81E-4	4.31E-4	4.64E-7	C	C
5	.5192	1703E-2	.2695	2.901E-4	C	C
10	2.077	0.0681	4.312	4.642E-3	C	C
25	2.979	.4258	168.5	.1813	27.07	7.33
50	51.92	1.703	2695	2.901	1.69	2.86 E-2
60	74.59	2.453	5589	6.016	.816	6.66 E-3
70	101.81	3.338	10,354	11.15	.440	1.94 E-3
80	132.9	4.360	17,663	19.01	.258	6.67 E-4
90	168.2	5.519	28,294	30.46	.161	2.60 E-4
100	207.7	6.813	43,124	46.42	.106	1.12 E-4
125	324.5	10.65	1.05E-5	113.3	4.43E-2	1.88 E-5
250	1298	42.58	1.68E-6	1813	2.71E-3	7.33 E-8
500	5192	170.3	2.70E-7	29,012	1.69E-4	2.86 E-10
750	11680	383.2	1.36E-8	146,873	3.34E-5	1.12 E-11
890 †	16450	539.7	2.71E-8	291,244	1.69E-5	2.84 E-12

* P(3-1)% signifies the probability of finding a through-going macropore with a 7.6-cm shelby tube. P(3-2) denotes the probability of finding one in each of two consecutive lifts. Thus, $P(3\text{-}1)^2 = P(3\text{-}2)$. C denotes that one or more channels are expected. Average distance between channels expressed in scientific notation where E separates the mantissa (left side) from the exponent (right side).

† At radii greater than 890, Equation 4.6 no longer holds for water under a hydraulic gradient of unity because the Reynolds number of 2200 is exceeded. In this case, the fluid is no longer laminar.

to channels 850 microns in radius, the channels would have to be 47.5-m apart for the liner to meet the EPA standard of 10^{-7} cm sec^{-1}. This would correspond to less than one such flaw per half acre.

Thus, the two most important parameters in considering the conductivity of a lift are the effective radius of the through-going channels and the average spacing. The average spacing can also be expressed as the number of channels per unit area i.e., channel density.

THE CHANNEL DENSITY

Channel density is important in calculating the actual lift conductivity and in interpreting laboratory and field measurements. If the conductivity of a lift is controlled by a few large channels, it is likely that these channels would be missed by sampling too small an area, resulting in an underestimation of the actual conductivity.

Suppose a lift has two populations of through-going pores. One population has a diameter of one millimeter (500 microns in radius) spaced 1.64-m apart. The other population has a radius of one micron spaced 0.208-m apart. The first population will result in a conductivity of 1×10^{-5} cm sec^{-1} (Table 3), while the second population will result in a conductivity of 1×10^{-8} cm sec^{-1} (Table 6). The resulting actual conductivity would be 1.001×10^{-5} cm sec^{-1}. Suppose a sample of the soil was taken with a standard 3-inch diameter shelby tube for laboratory measurement. It would likely contain 106,000 through-going pores whose radius is one micron. But since there is only one channel of the millimeter population per 2.7 m^2, there is only a 0.17% chance of such a flaw being present in the 7.6-cm diameter sample. Thus, the analyst will measure a conductivity of 10^{-8} cm sec^{-1}, having totally missed the channels which contribute 99.9% of the conductivity. The chance of detecting one of the larger pores would not be greatly improved by taking several samples. In fact, hundreds of samples would be needed to find one such flaw, and that sample would likely be discarded as defective.

If a 15.2-cm diameter shelby tube was used to collect samples for laboratory conductivity testing, chances of finding a one millimeter channel improve to only 0.68%. With a 1.5-m x 1.5-m infiltrometer, however, there would be an 86% chance of finding one of the larger pores. With a 4.9-m x 4.9-m infiltrometer, about eight of these channels would be detected, which would give a correct estimate of the conductivity.

Thus, if the conductivity of a lift is the result of only closely spaced small pores, a small sample will suffice. If it is caused by a few large pores, however, a very large sample is needed. Consequently, it is easy to understand the orders of magnitude discrepancy often found between laboratory and field measurements of the hydraulic conductivity.

Figure 6 shows channel density versus channel size for four conductivities. Tables 7 through 10 show the number of channels expected to be found with five instruments for 10 channel sizes if the conductivity is 1 x 10^{-5} through 10^{-8} cm sec^{-1}. If the number of channels in the area of measurement is less than five, it is possible the measurement will differ from actual conductivity by 25% or more. If the number of channels is less than one, it is possible the population would be completely missed and the instrument is inappropriate for the measurement. Channels greater than 1,000 microns are not listed since at channel radii greater than 890 microns, the liquid flow would be in the turbulent regime. Besides, such channels should be visible to the naked eye and should not occur in a carefully made liner.

TABLE 7. NUMBER OF THROUGH-GOING CHANNELS EXPECTED WITH DIFFERENT INSTRUMENTS WHERE ACTUAL CONDUCTIVITY IS 1 x 10^{-5} CM SEC^{-1}

	Instrument				
Radius of Channel (microns)	7.6-cm Shelby tube	15.2-cm Shelby tube	1.5 x 1.5-m infiltrometer	4.9 x 4.9-m infiltrometer	.405-ha test fill
1	1.057E8[†]	4.230E8	5.386E10	5.515E11	9.384E13
5	169,197	676,789	8.617E7	8.824E8	1.502E11
10	10,574	42,299	5,385,716	5.515E7	9.384E9
25	270	1,082	137,874	1,422,833	2.402E8
50	16	67	8,617	88,239	1.502E7
100	1	4	538	5,514	938,440
125	43.31%[††]	1	220	2,258	384,385
250	2.71%	10.83%	13	141	24,024
500	0.17%	0.68%	86.17%	8	1,501
1000	0.01%	0.04%	5.39%	55.15%	93

[†] The expected number of channels expressed in scientific notation where E separates the mantissa (left side) from the exponent (right side).

[††] If the expected number of channels is less than one, then the probability of finding one channel is given as percent.

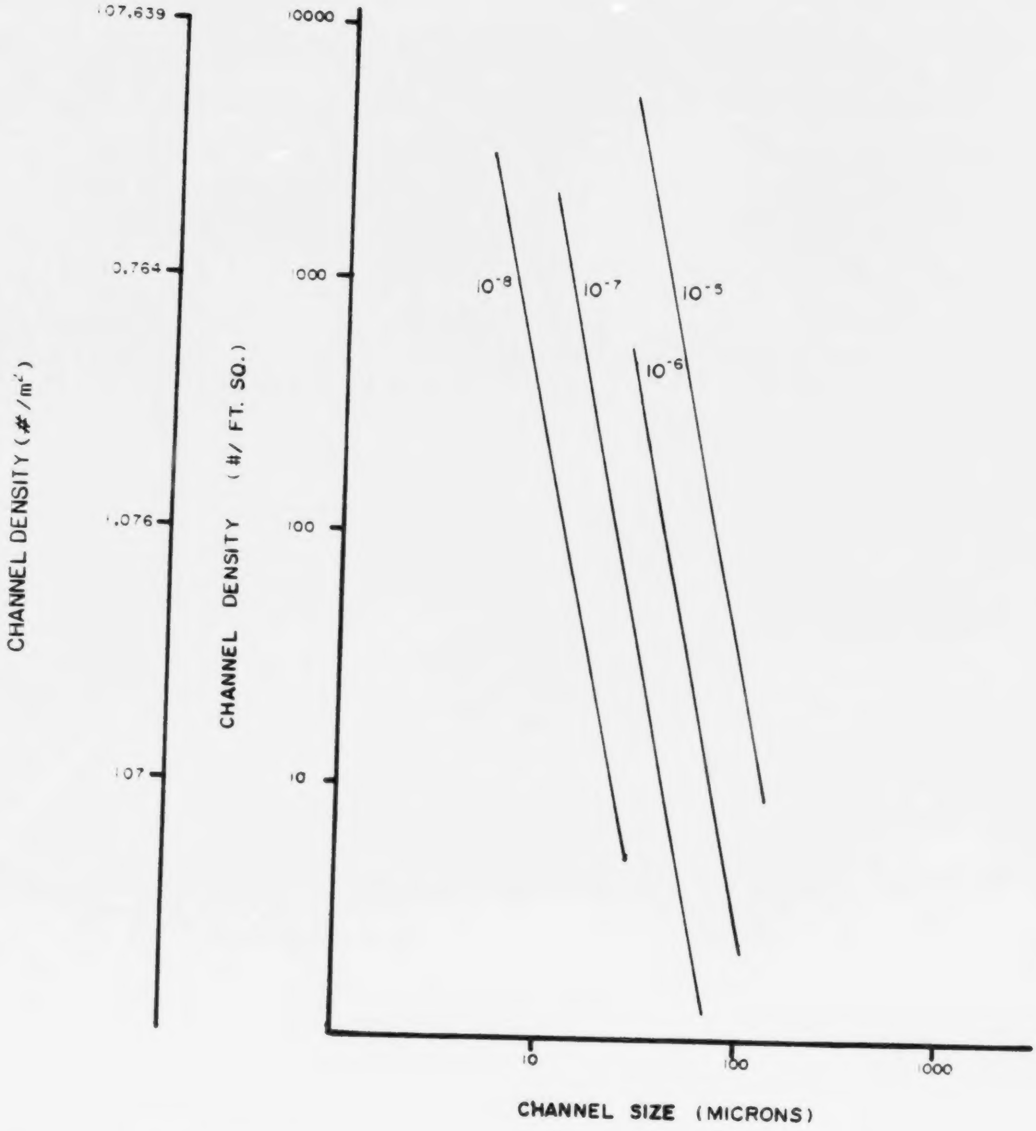

Figure 6. Channel density vs. channel size.

TABLE 8. NUMBER OF THROUGH-GOING CHANNELS EXPECTED WITH DIFFERENT INSTRUMENTS WHERE ACTUAL CONDUCTIVITY IS 1×10^{-6} CM SEC^{-1}

Radius of Channel (microns)	Instrument 7.6-cm Shelby tube	 15.2-cm Shelby tube	 1.5 x 1.5-m infiltrometer	 4.9 x 4.9-m infiltrometer	 .409-ha test fill
1	1.507E7†	4.230E7	5.386E9	5.515E10	9.384E12
5	16,919	67,678	8,617,146	8.824E7	1.502E10
10	1,057	4,229	538,571	5,514,974	9.384E8
25	27	108	13,787	141,183	2.402E8
50	1	6	861	8,823	1,501,505
100	10.57% ††	42.30%	53	551	93,844
125	4.33%	17.33%	22	225	38,438
250	0.27%	1.08%	1	14	2,402
500	0.02%	0.07%	8.62%	88.24%	150
1000			0.54%	5.51%	9

† The expected number of channels expressed in scientific notation where E separates the mantissa (left side) from the exponent (right side).

†† If the expected number of channels is less than one, then the probability of finding one channel is given as percent.

Assuming a lift conductivity of 1×10^{-5} cm sec^{-1}, Table 7 shows the limitation of small diameter shelby tube samples. These samples would only give the matrix conductivity, that is, the conductivity between the channels. Typical clay grains are one micron in diameter. In models presented later, 250 microns will be chosen as the size of a pore because anything significantly smaller would be detected by shelby tube samples. Larger pores would likely be missed by a 1.5 x 1.5-m infiltrometer.

TABLE 9. NUMBER OF THROUGH-GOING CHANNELS EXPECTED WITH DIFFERENT INSTRUMENTS WHERE ACTUAL CONDUCTIVITY IS 1×10^{-7} CM SEC^{-1}

Radius of Channel (microns)	Instrument				
	7.6-cm Shelby tube	15.2-cm Shelby tube	1.5 x 1.5-m infiltrometer	4.9 x 4.9-m infiltrometer	.405-ha test fill
1	1,057,483	4,229,933	5.386E8†	5.515E9	9.384E11
5	1,691	6,767	861,714	8,823,957	1.502E9
10	105	422	53,857	551,497	9.384E7
25	2	10	1,378	14,118	2,402,408
50	16.92% ††	67.68%	86	882	150,150
100	1.05%	4.23%	5	55	9,384
125	0.43%	1.73%	2	22	3,843
250	0.03%	0.11%	13.79%	1	240
500		0.01%	0.86%	8.82%	15
1000			0.05%	0.55%	93.84%

† The expected number of channels expressed in scientific notation where E separates the mantissa (left side) from the exponent (right side).

†† If the expected number of channels is less than one, then the probability of finding one channel is given as percent.

Channel radius and density will have to be evaluated before recommendations can be made on how to better construct compacted soil liners. When measurements are made, it should be borne in mind that the detectability of channels is a function of the size sample evaluated (Tables 7 through 10). If the distance between these channels is great, a very large sample is needed. Figure 7 and Table 11 give the number of channels expected versus channel radius for conductivities of 10^{-5}, 10^{-6}, 10^{-7}, and 10^{-8} cm sec^{-1}.

MULTILIFT SOIL LINERS

Compacted soil liners typically consist of several lifts. Since a lift is generally compacted to a 15.2-cm thickness, and since a liner is typically 0.6 to 1.2-m thick, there should be four to eight lifts. If most of the conductivity in each lift is caused by a few widely spaced

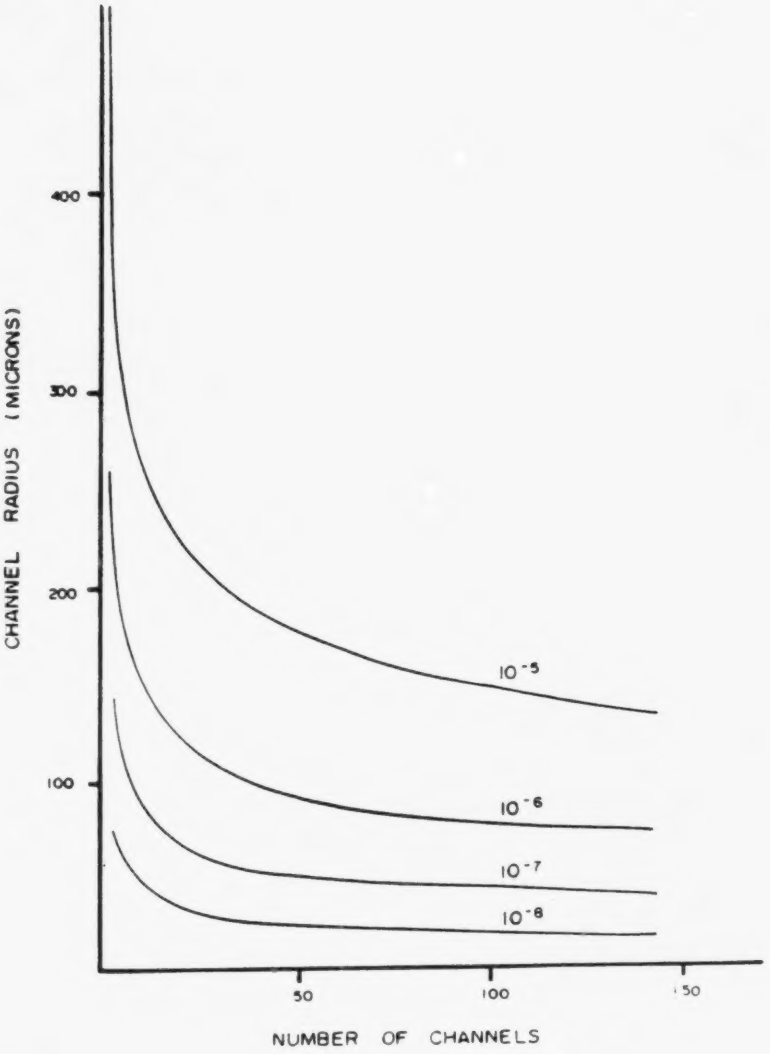

Figure 7. Number of channels vs. channel radius

TABLE 10. NUMBER OF THROUGH-GOING CHANNELS EXPECTED WITH DIFFERENT INSTRUMENTS WHERE ACTUAL CONDUCTIVITY IS 10^{-8} CM SEC^{-1}

	Instrument				
Radius of Channel (microns)	7.6-cm Shelby tube	15.2-cm Shelby tube	1.5 x 1.5-cm infiltrometer	4.9 x 4.9-m infiltrometer	.405-ha test fill
1	105,748	422,933	5.386E7 [†]	5.515E8	9.384E10
5	169	676	86,171	882,395	1.502E8
10	10	42	5,385	55,149	9,384,405
25	27.07%[††]	1	137	1,411	240,240
50	1.69%	6.77%	8	88	15,015
100	0.11%	0.42%	53.86%	5	938
125	0.04%	0.17%	22.06%	2	384
250		0.01%	1.38%	14.12%	24
500			0.09%	0.88%	1
1000			0.01%	0.06%	9.38%

[†] The expected number of channels expressed in scientific notation where E separates the mantissa (left side) from the exponent (right side).

[††] If the expected number of channels is less than one, then the probability of finding one channel is given as percent.

channels, then the interlift flow becomes important. Interlift flow is defined as the horizontal flow in the plane between two lifts. If interlift flow is unrestricted, then the hydraulic conductivity of the liner is equal to that of the tightest lift. In the models presented here, it is assumed that each lift has the same hydraulic conductivity, the same channel density and the same channel radius for the flow-controlling channels. Clearly, if interlift flow is restricted so that the continuous pores from one lift to another cannot communicate, the conductivity of a soil liner can be substantially less than that of the individual lifts. Such restriction of interlift flow will be dependent on the effectiveness of field compaction techniques in bonding the lifts.

TABLE 11. THE NUMBER OF CHANNELS IN 2.32 M^2 VERSUS CHANNEL RADIUS

	No. of Channels	Channel Radius Microns
a) At K = 10^{-5} cm sec^{-1}	1	481
	2	405
	3	366
	4	340
	5	322
	6	307
	10	270
	22	222
	30	205
	45	185
	82	160
	93	155
b) At K = 10^{-6} cm sec^{-1}	1	270
	2	227
	3	205
	4	191
	5	181
	6	173
	10	152
	22	125
	30	115
	44	105
	82	90
	103	85
c) At K = 10^{-7} cm sec^{-1}	2	128
	3	115
	4	107
	5	101
	6	95
	8	90
	10	85
	22	70
	41	60
	86	50
	210	40

(CONTINUED)

TABLE 11 CONTINUED

	No. of Channels	Channel Radius Microns
d) At $K = 10^{-8}$ cm sec^{-1}	1	85
	2	72
	3	65
	4	60
	5	57
	8	50
	21	40
	35	35
	66	30
	137	25

MODELS FOR INTERLIFT FLOW

Two models for interlift flow follow. The first model is the channel-centered model. In this model, it is assumed that there is a circular disk in the interlift plane at the bottom of every channel, centered on that channel. Inside the disk, flow is considered to be unrestricted. The lateral distance from a channel at the bottom of a lift that liquid can flow freely is designated the interlift flow radius (IR). This radius defines the disk. In this model, it is assumed that if any top of a channel in the lower lift is within the IR of a channel in the upper lift, liquid will flow from the channel in the upper lift into the channel in the lower lift. Further, if a channel in the lower lift is not within the IR of channel in the upper lift, then the channels will not constitute a flow path (through-going channel - Figure 8).

The second model is the pocket model. This model assumes an inhomogeneous interlift plane. The plane is divided into disks with radii of IR. In this case, the disks are not necessarily centered on channels, but are geometrically located, as in Figure 9. These disks are pockets of favorable horizontal flow. If any channels from an upper lift end in the same pocket that a channel begins in a lower lift, then liquid can flow from the upper channel into the lower one, resulting in a complete multi-lift flow path. The permeability of this path would be

$$\frac{R^2}{8} = k \qquad (4.7)$$

This result is derived in Appendix A. If m paths flow into a pocket from one lift and n connect with that pocket from another lift, the permeability of that flow system is

$$\frac{nR^2}{8} = k \tag{4.8}$$

if $n \leq m$, that is, if n is the lesser of the two numbers. If a channel does not have its opening in a pocket, or if it does not have its opening in a pocket with another channel from another lift, then that channel is not a flow path.

CHANNEL-CENTERED MODEL

A program was written to examine the effect of IR on flow through a soil liner (Appendix B). Variables for the model include (1) the desired effective hydraulic conductivity, (2) the channel radius, (3) the IR, and (4) the number of lifts. The program then computes the number of channels there would have to be in a 1.5 x 1.5-m section of each lift to attain the selected conductivity. The channels are assigned positions randomly. The program then measures the distance between defects in adjacent lifts. If a defect is within the interlift flow radius of an overlying channel, the match-up is printed as "CHANNEL (m,n) WITH (x,y)", where the first number in each ordered pair is the number of the lift, and the second is the number designating the defect. If a defect is not matched up with the interlift flow from a channel above it, it is considered "dead" and does not figure in computations in the next interlift plane.

In this way, a determination can be made of how many effective flow paths there are through a certain number of lifts as a function of IR. Each computation is a stochastic experiment, so the program must be run many times and the results tabulated. Furthermore, each run must be carefully examined in the form of a tree diagram. If the sixth lift has four channels that are "live" (i.e., connected through defects to the liquid above the liner), this does not necessarily mean that there are four effective through-going flow channels. It could be that on some higher lift (e.g., the fourth) all through-going flow is passing through one channel (see Figure 10). Neither can one simply find the lift with the fewest live channels and present that number as the total number of flow paths. Some of those might later dead end. Figure 11 is an example.

Let the hydraulic conductivity of each lift be approximately 1×10^{-5} cm sec^{-1} the radius of each channel be 250 um, and let the number of lifts be 2. The number of channels in a lift in this case

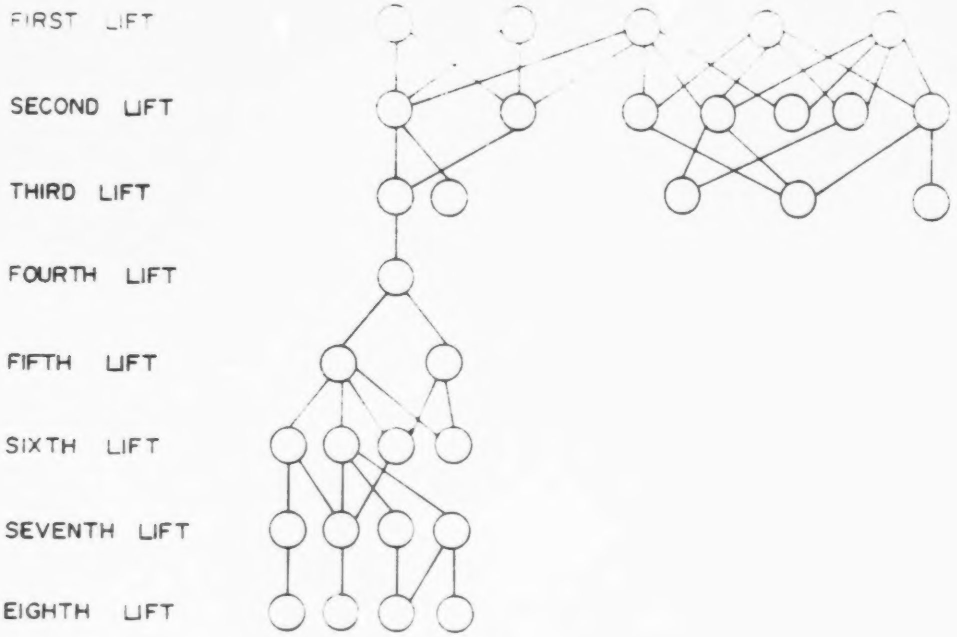
FIRST LIFT
SECOND LIFT
THIRD LIFT
FOURTH LIFT
FIFTH LIFT
SIXTH LIFT
SEVENTH LIFT
EIGHTH LIFT

CIRCLES REPRESENT CHANNELS AND LINES REPRESENT INTERCONNECTION. NOTICE THE CONSTRICTION AT THE FOURTH LIFT. ALTHOUGH THERE ARE FOUR ACTIVE DEFECTS IN THE LAST LIFT, THE NUMBER OF EFFECTIVE PASSAGE WAYS IS ONE.

Figure 10. The difference between the number of effective flow paths and the number of active channels in the last lift.

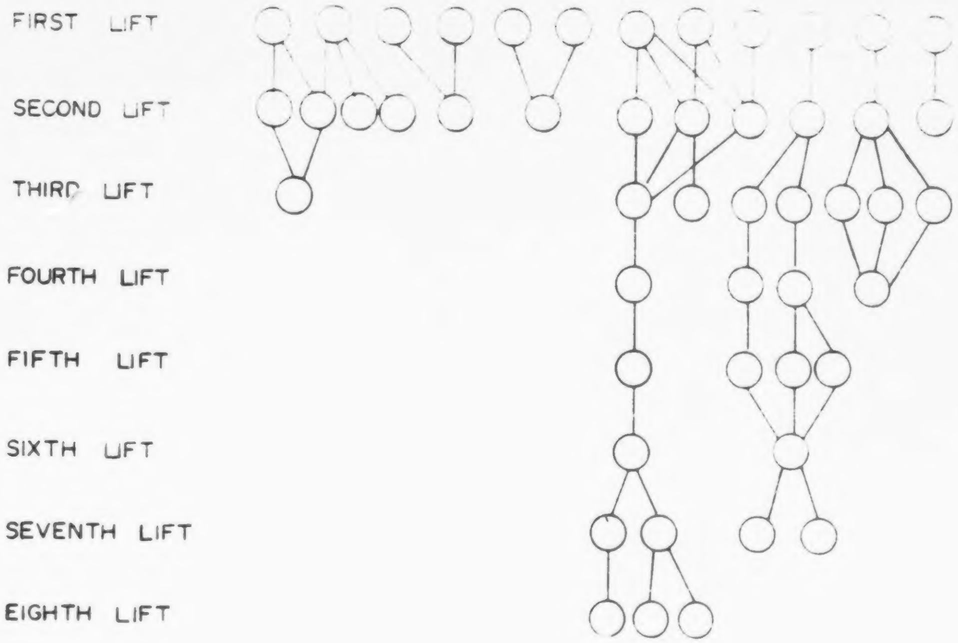
FIRST LIFT
SECOND LIFT
THIRD LIFT
FOURTH LIFT
FIFTH LIFT
SIXTH LIFT
SEVENTH LIFT
EIGHTH LIFT

THE FEWEST NUMBER OF INTERCONNECTIONS BETWEEN LIFTS IS THREE, YET THE NUMBER OF FLOW PATHS IS ONE.

Figure 11. The difference between the number of effective flow paths and the fewest number of active channels in a lift.

would be 13. If IR was 10-cm, then according to the results of the program, there was an average of 1.9 through-going channels. One such channel would result in a conductivity of 7.3 x 10^{-7} cm sec^{-1}. If all 13 of the channels were through-going, the effective conductivity would be 9.4 x 10^{-6}. Just 1.9 channels correspond to 1.4 x 10^{-6} cm sec^{-1}. Table 12 gives the results of 80 computer runs. In ten of the runs, no channels connected through. In two cases, for IR = 10-cm, there were five through-going channels (3.6 x 10^{-6} cm sec^{-1}). There were no cases of six paths.

When IR is 15-cm, there was a marked increase in through-flow. There was at least one through-going channel in each case, and a maximum of nine channels, for an average of 3.8 flow paths through the liner (K = 2.7 x 10^{-6} cm sec^{-1}). When IR = 20-cm, there is at least one channel in every case, and up to eight, for an average of 4.9 flow paths (K = 3.6 x 10^{-6} cm sec^{-1}). When IR = 25-cm, there were 6.9 flow paths (K = 5.0 x 10^{-6} cm sec^{-1}). When IR = 50-cm, there was an average of 10.7 paths (K = 7.8 x 10^{-6}). Clearly, interlift flow radius plays a large role in the conductivity of a liner with two lifts. The effect is even more important with more lifts. Table 13 shows results of runs of the program for three lifts. At 25-cm, there were through-going channels in all cases, yet with a 10-cm IR, there were through-going channels in only 25% of the cases. The number of flow paths with a 10-cm interlift flow radius averages at 0.3, for 15-cm it is 1.1, for 20-cm it is 2.5, and for 25-cm it is 4.4. Table 14 shows the four lift case. In this case, IR is very important. Only twice in 70 tries was there through-flow with an IR of 10-cm. There was an average of 0.03 paths in 2.3 m^2 K = 2.1 x 10^{-8} cm sec^{-1}. At 15-cm there were 0.4 flow paths (K = 3.1 x 10^{-7} cm sec^{-1}). But at 20-cm and 25-cm, there were 1.4 and 2.8 flow paths respectively.

Tables 15 through 18 show the cases of five through eight lifts, respectively. In all cases, there are no through-going channels when the IR is 10-cm. If IR is restricted to 15-cm, the average number of flow paths for six lifts was 0.08. This corresponds to K = 5.4 x 10^{-8} cm sec^{-1}, which is an acceptable conductivity (less than 1 x 10^{-7} cm sec^{-1}). With eight lifts, even IR = 20-cm gave an acceptable hydraulic conductivity, but with an IR of 25-cm conductivity was 5.26 x 10^{-7} cm sec^{-1}. The results in these seven tables are plotted in Figure 12. The results, of course, would be different if the assumptions were changed as to the average diameter of a channel. But the implications of this experiment are clear. Suppose that a lift with a matrix conductivity of 10^{-8} cm sec^{-1} contains 13 channels (with diameters of 1/2 millimeter), in each 2.3 m^2 area. The lift would have an effective hydraulic conductivity of 1 x 10^{-5} cm sec^{-1}. Even then, however, the EPA standards of 1 x 10^{-7} cm sec^{-1} would be satisfied with eight lifts if interlift flow could be limited to 20-cm. If it is limited to 10-cm, just four lifts will result in a conductivity of less than 1 x 10^{-7} cm sec^{-1}.

TABLE 12. THE NUMBER OF THROUGH-GOING CHANNELS IN A SOIL LINER WITH TWO LIFTS FOR THE CHANNEL-CENTERED MODEL †

IR		Number of Through-Going Channels												
		0	1	2	3	4	5	6	7	8	9	10	11	Avg.
IR = 30-cm	(a)	0	0	0	0	1	5	12	14	18	22	4	4	7.81
	(b)	0	0	0	0	1.25	6.25	15	17.5	22.5	27.5	5	5	
conductivity														56.73
IR = 25-cm	(a)	0	0	5	1	2	11	20	21	12	7	5	1	6.91
	(b)	0	0	0	1.25	2.5	13.75	25	26.25	15	8.75	6.25	1.25	
conductivity														50.12
IR = 20-cm	(a)	0	1	5	8	14	22	21	4	5	0	0	0	4.94
	(b)	0	1.25	6.25	10	17.5	27.5	26.25	5	6.25	0	0	0	
conductivity														35.83
IR = 15-cm	(a)	0	4	12	22	15	21	4	1	0	1	0	0	3.77
	(b)	0	5	15	27.5	18.75	26.25	5	1.25	0	1.25	0	0	
conductivity														27.34
IR = 10-cm	(a)	10	23	22	16	7	2	0	0	0	0	0	0	1.91
	(b)	12.5	28.75	27.5	20	8.75	2.5	0	0	0	0	0	0	
conductivity														13.85

---

† Conductivity is in 10^{-7} cm sec^{-1}.

(a) = Number of Incidence

(b) = Percentage of Incidence

TABLE 13. THE NUMBER OF THROUGH-GOING CHANNELS IN A SOIL LINER WITH THREE LIFTS FOR THE CHANNEL-CENTERED MODEL.†

IR	Number of Through-Going Channels										
	0	1	2	3	4	5	6	7	8	9	Avg.
IR = 30-cm (a)	0	0	2	10	12	22	18	13	2	1	5.20
(b)	0	0	2.5	12.5	15	27.5	22.5	16.25	2.5	1.3	
conductivity											37.72
IR = 25-cm (a)	0	0	5	21	17	23	7	4	3	0	4.38
(b)	0	0	6.25	26.25	21.25	28.75	8.75	5	3.8	0	
conductivity											31.77
IR = 20-cm (a)	4	18	20	20	12	6	0	0	0	0	2.45
(b)	5	22.5	25	25	15	7.5	0	0	0	0	
conductivity											17.77
IR = 15-cm (a)	19	37	19	5	0	0	0	0	0	0	1.13
(b)	23.75	46.25	23.75	6.25	0	0	0	0	0	0	
conductivity											8.20
IR = 10-cm (a)	59	19	2	0	0	0	0	0	0	0	0.29
(B)	73.75	23.75	2.5	0	0	0	0	0	0	0	
conductivity											2.10

†Conductivity is in 10^{-7} cm sec^{-1}. (a) = Number of Incidence
(b) = Percentage of Incidence

THE POCKET MODEL

A program was written to simulate a soil liner whose interlift flow was governed by the pocket model (Appendix C). Variables for this model are the same as in the channel-centered model. This program has the additional feature of counting through-going channels (flow paths) without the user having to draw tree diagrams. The program is similar to the channel-centered model, except in its way of determining a match-up of channels between lifts.

The results of these experiments are given in Tables 19 through 25, and Figure 13. Again, increasing the number of lifts and decreasing the interlift flow radius decrease the total conductivity of the liner.

The pocket model results indicate that if channel radius is 250 microns and conductivity of each lift is 10^{-5}cm sec^{-1}, the total conductivity would be 2.9 x 10^{-8} cm sec^{-1}, if the pockets of interlift flow were limited in radius to 10-cm. Similarly, 15-cm pockets resulted

TABLE 14. THE NUMBER OF THROUGH-GOING CHANNELS IN A SOIL LINER WITH FOUR LIFTS FOR THE CHANNEL-CENTERED MODEL [†]

	Number of Through-Going Channels								
IR	0	1	2	3	4	5	6	7	Avg.
IR = 30-cm (a)	1	1	4	17	24	16	6	1	3.99
(b)	1.4	1.4	5.7	24.3	34.3	22.9	8.6	1.4	
conductivity									28.94
IR = 25-cm (a)	2	11	16	20	15	5	1	0	2.77
(b)	2.86	15.71	22.86	28.57	21.43	7.14	1.43	0	
conductivity									20.09
IR = 20-cm (a)	14	31	14	7	4	0	0	0	1.37
(b)	20	44.29	20	10	5.71	0	0	0	
conductivity									9.94
IR = 15-cm (a)	42	26	2	0	0	0	0	0	0.43
(b)	60	37.14	2.86	0	0	0	0	0	
conductivity									3.12
IR = 10-cm (a)	68	2	0	0	0	0	0	0	0.029
(b)	97.14	2.86	0	0	0	0	0	0	
conductivity									0.21

[†] Conductivity is in 10^{-7} cm sec^{-1}. (a) = Number of Incidence
(b) = Percentage of Incidence

in a total conductivity of less than 1 x 10^{-7} cm sec^{-1} if there were at least five lifts. If there were seven lifts, 20-cm of interlift flow yields a conductivity of 4.4 x 10^{-8} cm sec^{-1}.

The program in Appendix C does not give useful results above IR = 40-cm. It shows, however, that number of lifts and interlift flow radius play a strong role in determining the hydraulic conductivity of a liner.

COMPARISON OF CHANNEL CENTERED AND POCKET MODELS

In both models, there was a substantial decrease in conductivity as the number of lifts increased and as IR decreased. As IR approaches 100 cm, the conductivity becomes that of individual lifts, and the number of lifts becomes unimportant. Except for two cases (IR = 10-cm with four lifts, and IR = 15-cm with eight lifts) the pocket model gives lower conductivities than the channel-centered model.

TABLE 15. THE NUMBER OF THROUGH-GOING CHANNELS IN A SOIL LINER WITH FIVE LIFTS FOR THE CHANNEL-CENTERED MODEL †

IR		Number of Through-Going Channels							
		0	1	2	3	4	5	6	Avg.
IR = 30-cm	(a)	1	4	11	21	13	8	2	3.22
	(b)	1.67	6.67	18.33	35	21.67	13.33	3.33	
conductivity									23.36
IR = 25-cm	(a)	5	16	24	9	6	0	0	1.92
	(b)	8.33	26.67	40	15	10	0	0	
conductivity									13.93
IR = 20-cm	(a)	29	21	10	0	0	0	0	0.68
	(b)	48.33	35	16.67	0	0	0	0	
conductivity									4.93
IR = 15-cm	(a)	51	9	0	0	0	0	0	0.15
	(b)	85	15	0	0	0	0	0	
conductivity									1.09
IR = 10-cm	(a)	60	0	0	0	0	0	0	0
	(b)	100	0	0	0	0	0	0	
conductivity									0

† Conductivity is in 10^{-7} cm sec^{-1}. (a) = Number of Incidence (b) = Percentage of Incidence.

PHYSICAL EXPLANATION OF THE CHANNEL-CENTERED MODEL

The channel-centered model assumed unlimited flow within a certain radius of the mouth of a channel (IR) in the plane between lifts, and zero flow beyond that radius. This was not based on physical principles, but rather the convenience for mathematical modeling. To examine the interlift plane in terms of physics, IR would actually be a function of time. In Appendix D, it is shown that:

$$IR = \quad tK_hH \qquad (4.9)$$

where t is time, K_h is the horizontal hydraulic conductivity and H is the head in that plane. Various values for the three variables were used to determine the resulting interlift flow radius. Let t = 30 years, the likely minimum time between construction of a soil liner and the end of the post-closure monitoring period; and let the interlift

TABLE 16. THE NUMBER OF THROUGH-GOING CHANNELS IN A SOIL LINER WITH SIX LIFTS FOR THE CHANNEL-CENTERED MODEL †

IR		Number of Through-Going Channels						
		0	1	2	3	4	5	Avg.
IR = 30-cm	(a)	2	5	10	16	4	3	2.60
	(b)	5	12.5	25	40	10	7.5	
conductivity								18.86
IR = 25-cm	(a)	9	14	15	1	1	0	1.28
	(b)	22.5	35	37.5	2.5	2.5	0	
conductivity								9.28
IR = 20-cm	(a)	27	12	1	0	0	0	0.35
	(b)	67.5	30	2.5	0	0	0	
conductivity								2.54
IR = 15-cm	(a)	37	3	0	0	0	0	0.075
	(b)	92.5	7.5	0	0	0	0	
conductivity								0.54
IR = 10-cm	(a)	40	0	0	0	0	0	0
	(b)	100	0	0	0	0	0	
conductivity								0

† Conductivity is in 10^{-7} cm $\sec^{-1}$. (a) = Number of Incidence (b) = Percentage of Incidence.

plane be under 45.7-cm of head. For the interlift flow radius to be 10-cm, the horizontal hydraulic conductivity in the interlift plane would be 2.3×10^{-9} cm $\sec^{-1}$. If interlift flow is limited to 20-cm, horizontal conductivity would be 9.2×10^{-9} cm $\sec^{-1}$. It is likely that, given current construction practice, this would be impossible to achieve. From Table 26, it can be seen that if the horizontal conductivity can be kept down to 10^{-8} cm $\sec^{-1}$, it could take 15 years for the IR to reach 20-cm. Consequently, it is critical that IR be kept to a minimum by decreasing the horizontal hydraulic conductivity.

THE UNIFYING MODEL

The unifying model is one that combines the channel-centered model, for which there is evidence in the field, to its physical basis. In this model, IR is not constant, but rather a function of time, as in equation (4.9). The program is given in Appendix E.

TABLE 17. THE NUMBER OF THROUGH-GOING CHANNELS IN A SOIL LINER WITH SEVEN LIFTS FOR THE CHANNEL-CENTERED MODEL†

		Number of Through-Going Channels						
IR		0	1	2	3	4	5	Avg.
IR = 30-cm	(a)	4	10	11	10	3	2	2.10
	(b)	10	25	27.5	25	7.5	5	
conductivity								15.23
IR = 25-cm	(a)	10	18	11	1	0	0	1.075
	(b)	25	45	27.5	2.5	0	0	
conductivity								7.80
IR = 20-cm	(a)	34	5	1	0	0	0	0.175
	(b)	85	12.5	2.5	0	0	0	
conductivity								1.27
IR = 15-cm	(a)	39	1	0	0	0	0	0.025
	(b)	97.5	2.5	0	0	0	0	
conductivity								0.18
IR = 10-cm	(a)	40	0	0	0	0	0	0
	(b)	100	0	0	0	0	0	
conductivity								0

†Conductivity is in 10^{-7} cm $\sec^{-1}$. (a) = Number of Incidence. (b) = Percentage of Incidence.

In this model, IR begins to grow from the time liquid reaches a particular through-going channel, and grows as a function of head, conductivity and time. In the program, notice that IR is an array, and that each channel has its own IR. The program gives an evolving picture of the flow in a liner, and marks the moment that liquid first reaches a channel in a new lift. Once the bottom lift has liquid in a channel, it is assumed that breakthrough has occurred.

To operate the program, it is necessary to supply the size (radius) of the channels and the actual vertical hydraulic conductivity. These imply the number of channels in a 2.3 m^2 area per lift. The number of lifts is supplied, as well as the horizontal conductivity at the bottom of a lift. It is assumed that there are 30-cm of liquid on the top of the first lift. The program could be adjusted to allow for a different starting head, as well as for different liquid properties (density, viscosity, etc.). The program generates the connections between channels in neighboring lifts, but it gives many models in sequence as a function of time, and it tells when a new lift has been has been penetrated. If the same parameters are used as in models presented above

TABLE 18. THE NUMBER OF THROUGH-GOING CHANNELS IN A SOIL LINER WITH EIGHT LIFTS FOR THE CHANNEL-CENTERED MODEL

		Number of Through-Going Channels					
IR		0	1	2	3	4	Avg.
IR = 30-cm	(a)	7	9	12	8	4	1.83
	(b)	17.5	22.5	30	20	10	
conductivity							13.24
IR = 25-cm	(a)	15	21	4	0	0	0.725
	(b)	37.5	52.5	10	0	0	
conductivity							5.26
IR = 20-cm	(a)	36	4	0	0	0	0.10
	(b)	90	10	0	0	0	
conductivity							0.73
IR = 15-cm	(a)	40	0	0	0	0	0
	(b)	100	0	0	0	0	
conductivity							0
IR = 10-cm	(a)	40	0	0	0	0	0
	(b)	100	0	0	0	0	
conductivity							0

Conductivity is in 10-7 cm sec-1. (a) = Number of Incidence (b) = Percentage of Incidence.

(i.e., a vertical hydraulic conductivity of 10-5 cm sec-1 caused by channels 250-microns in radius in an eight lift liner) with a horizontal hydraulic conductivity in the interlift plane of 10-5 cm sec-1, the result would be very rapid breakthrough (Table 27). Break through in a liner such as that described above would take slightly more than two weeks. During 50 runs of the model, the high value obtained was five weeks and the low was one week. If the conductivity between flaws is 10-8 cm sec-1, and increases to 10-5 cm sec-1 at the bottom of each lift due to density variation caused by improper compaction, then such a liner would be broken through in two weeks even though a 7.6-cm shelby tube taken at the surface would likely give a laboratory conductivity of 10-8 cm sec-1.

When the horizontal conductivity at the bottom of a lift was 10-6 cm sec-1, and given the same values for the other parameters as in the

TABLE 19. THE NUMBER OF THROUGH-GOING CHANNELS IN A SOIL LINER WITH TWO LIFTS FOR THE POCKET MODEL †

		Number of Through-Going Channels												
		0	1	2	3	4	5	6	7	8	9	10	11	Avg.
IR = 40-cm	(a)	0	0	0	0	0	5	8	10	14	10	2	1	7.52
	(b)	0	0	0	0	0	10	16	20	28	20	4	2	
conductivity														54.54
IR = 30-cm	(a)	0	0	4	4	10	12	9	7	1	3	0	0	51.6
	(b)	0	0	8	8	20	24	18	14	2	6	0	0	
conductivity														37.43
IR = 25-cm	(a)	0	2	1	5	7	15	9	9	0	2	0	0	5.14
	(b)	0	4	2	10	14	30	18	18	0	4	0	0	
conductivity														37.28
IR = 20-cm	(a)	0	1	5	13	12	10	5	2	1	1	0	0	4.18
	(b)	0	2	10	26	24	20	10	4	2	2	0	0	
conductivity														30.32
IR = 15-cm	(a)	3	8	11	20	5	2	1	0	0	0	0	0	2.52
	(b)	6	16	22	40	10	4	2	0	0	0	0	0	
conductivity														18.18
IR = 10-cm	(a)	11	24	6	8	1	0	0	0	0	0	0	0	1.28
	(b)	22	48	12	16	2	0	0	0	0	0	0	0	
conductivity KH														9.28

---

† Conductivity is in 10^{-7} cm sec^{-1}.

(a) = Number of Incidence

(b) = Percentage of Incidence

TABLE 20. THE NUMBER OF THROUGH-GOING CHANNELS IN A SOIL LINER WITH THREE LIFTS FOR THE POCKET MODEL†

IR		Number of Through-Going Channels										
		0	1	2	3	4	5	6	7	8	9	Avg.
IR = 40-cm	(a)	0	0	0	1	4	13	16	9	6	1	6.00
	(b)	0	0	0	2	8	26	32	18	12	2	
conductivity												43.52
IR = 30-cm	(a)	0	2	11	12	15	8	1	1	0	0	3.46
	(b)	0	4	22	24	30	16	2	2	0	0	
conductivity												25.10
IR = 25-cm	(a)	0	8	7	20	6	8	1	0	0	0	2.88
	(b)	0	16	14	30	12	16	2	0	0	0	
conductivity												20.89
IR = 20-cm	(a)	5	15	14	11	4	1	0	0	0	0	1.94
	(b)	10	30	28	22	8	2	0	0	0	0	
conductivity												14.07
IR = 15-cm	(a)	19	25	6	0	0	0	0	0	0	0	0.74
	(b)	38	50	12	0	0	0	0	0	0	0	
conductivity												5.37
IR = 10-cm	(a)	42	8	0	0	0	0	0	0	0	0	0.16
	(b)	84	16	0	0	0	0	0	0	0	0	
conductivity												1.16

† Conductivity is in 10^{-7} cm sec^{-1}. (a) = Number of Incidence (b) = Percentage of Incidence.

TABLE 21. THE NUMBER OF THROUGH-GOING CHANNELS IN A SOIL LINER WITH FOUR LIFTS FOR THE POCKET MODEL†

IR		Number of Through-Going Channels									
		0	1	2	3	4	5	6	7	8	Avg.
IR = 40-cm	(a)	0	0	0	6	8	16	14	3	3	5.18
	(b)	0	0	0	12	16	32	28	6	6	
conductivity											37.57
IR = 30-cm	(a)	4	6	19	10	9	1	1	0	0	2.42
	(b)	8	12	38	20	18	2	2	0	0	
conductivity											17.55
IR = 25-cm	(a)	7	17	13	11	2	0	0	0	0	1.68
	(b)	14	34	26	22	4	0	0	0	0	
conductivity											12.19
IR = 20-cm	(a)	18	21	8	3	0	0	0	0	0	0.92
	(b)	36	42	16	6	0	0	0	0	0	
conductivity											6.67
IR = 15-cm	(a)	42	8	0	0	0	0	0	0	0	0.16
	(b)	84	16	0	0	0	0	0	0	0	
conductivity											1.16
IR = 10-cm	(a)	48	2	0	0	0	0	0	0	0	0.04
	(b)	96	4	0	0	0	0	0	0	0	
conductivity											0.29

† Conductivity is in 10^{-7} cm sec^{-1}. (a) = Number of Incidence (b) = Percentage of Incidence.

TABLE 22. THE NUMBER OF THROUGH-GOING CHANNELS IN A SOIL LINER WITH FIVE LIFTS FOR THE POCKET MODEL†

IR		Number of Through-Going Channels									
		0	1	2	3	4	5	6	7	8	Avg.
IR = 40-cm	(a)	0	0	4	9	12	16	7	1	1	4.40
	(b)	0	0	8	18	24	32	8	2	2	
conductivity											31.91
IR = 30-cm	(a)	6	12	24	4	4	0	0	0	0	1.76
	(b)	12	24	48	8	8	0	0	0	0	
onductivity											12.77
IR = 25-cm	(a)	10	25	12	3	0	0	0	0	0	1.16
	(b)	20	50	24	6	0	0	0	0	0	
conductivity											8.41
IR = 20-cm	(a)	32	14	4	0	0	0	0	0	0	0.44
	(b)	64	28	8	0	0	0	0	0	0	
conductivity											3.19
IR = 15-cm	(a)	47	3	0	0	0	0	0	0	0	0.06
	(b)	94	6	0	0	0	0	0	0	0	
conductivity											0.44
IR = 10-cm	(a)	50	0	0	0	0	0	0	0	0	0.00
	(b)	100	0	0	0	0	0	0	0	0	
conductivity											0.00

† Conductivity is in 10^{-7} cm sec^{-1}. (a) = Number of Incidence (b) = Percentage of Incidence.

TABLE 23. THE NUMBER OF THROUGH-GOING CHANNELS IN A SOIL LINER WITH SIX LIFTS FOR THE POCKET MODEL [†]

		Number of Through-Going Channels								
IR		0	1	2	3	4	5	6	7	Avg.
IR = 40-cm	(a)	0	1	6	11	13	16	2	1	3.94
	(b)	0	2	12	22	26	32	4	2	
conductivity										28.58
IR = 30-cm	(a)	10	18	17	3	2	0	0	0	1.38
	(b)	20	36	34	6	4	0	0	0	
conductivity										10.01
IR = 25-cm	(a)	18	26	5	1	0	0	0	0	0.78
	(b)	36	52	10	2	0	0	0	0	
conductivity										5.66
IR = 20-cm	(a)	43	7	0	0	0	0	0	0	0.14
	(b)	86	14	0	0	0	0	0	0	
conductivity										1.02
IR = 15-cm	(a)	48	2	0	0	0	0	0	0	0.04
	(b)	96	4	0	0	0	0	0	0	
conductivity										0.29
IR = 10-cm	(a)	50	0	0	0	0	0	0	0	0.00
	(b)	100	0	0	0	0	0	0	0	
conductivity										0.00

[†] Conductivity is in 10^{-7} cm sec^{-1}. (a) = Number of Incidence
(b) = Percentage of Incidence.

TABLE 24. THE NUMBER OF THROUGH-GOING CHANNELS IN A SOIL LINER WITH SEVEN LIFTS FOR THE POCKET MODEL †

IR		Number of Through-Going Channels								
		0	1	2	3	4	5	6	7	Avg.
IR = 40-cm	(a)	0	1	11	13	11	12	1	1	3.58
	(b)	0	2	22	26	22	24	2	2	
conductivity										25.97
IR = 30-cm	(a)	14	24	11	1	0	0	0	0	0.98
	(b)	28	48	22	2	0	0	0	0	
conductivity										7.11
IR = 25-cm	(a)	30	20	0	0	0	0	0	0	0.40
	(b)	60	40	0	0	0	0	0	0	
conductivity										2.90
IR = 20-cm	(a)	47	3	0	0	0	0	0	0	0.06
	(b)	94	6	0	0	0	0	0	0	
conductivity										0.44
IR = 15-cm	(a)	49	1	0	0	0	0	0	0	0.02
	(b)	98	2	0	0	0	0	0	0	
conductivity										0.15
IR = 10-cm	(a)	50	0	0	0	0	0	0	0	0.00
	(b)	100	0	0	0	0	0	0	0	
conductivity										0.00

† Conductivity is in 10^{-7} cm sec^{-1}. (a) = Number of Incidence
(b) = Percentage of Incidence

TABLE 25. THE NUMBER OF THROUGH-GOING CHANNELS IN A SOIL LINER WITH EIGHT LIFTS FOR THE POCKET MODEL[†]

		Number of Through-Going Channels							
IR		0	1	2	3	4	5	6	Avg.
IR = 40-cm	(a)	0	2	14	12	13	8	1	3.28
	(b)	0	4	28	24	26	16	2	
conductivity									23.79
IR = 30-cm	(a)	20	22	7	1	0	0	0	0.78
	(b)	40	44	14	2	0	0	0	
conductivity									5.66
IR = 25-cm	(a)	36	14	0	0	0	0	0	0.28
	(b)	72	28	0	0	0	0	0	
conductivity									2.03
IR = 20-cm	(a)	49	1	0	0	0	0	0	0.02
	(b)	98	2	0	0	0	0	0	
conductivity									0.15
IR = 15-cm	(a)	49	1	0	0	0	0	0	0.02
	(b)	98	2	0	0	0	0	0	
conductivity									0.15
IR = 10-cm	(a)	50	0	0	0	0	0	0	0.00
	(b)	100	0	0	0	0	0	0	
conductivity									0.00

[†] Conductivity is in 10^{-7} cm sec^{-1}. (a) = Number of Incidence (b) = Percentage of Incidence.

TABLE 26. INTERLIFT FLOW RADIUS IN CENTIMETERS FOR SOIL LINER WITH VARIOUS HORIZONTAL HYDRAULIC CONDUCTIVITIES AND UNDER 30-CM OF WATER

Interlift Time	Number of Years						
	1	5	10	15	20	25	30
a) K = 10^{-5} cm sec^{-1}							
1-2	161	359	508	622	718	803	880
2-3	175	391	553	677	782	875	958
3-4	188	421	595	729	841	941	1031
4-5	201	448	634	777	897	1003	1098
5-6	212	474	671	822	949	1061	1162
6-7	223	499	706	865	998	1116	1223
7-8	234	523	739	905	1045	1169	1280
b) K = 10^{-6} cm sec^{-1}							
1-2	51	114	161	197	227	254	278
2-3	55	124	175	214	247	277	303
3-4	60	133	188	230	266	298	326
4-5	63	142	201	246	284	317	347
5-6	67	150	212	260	300	336	368
6-7	71	158	223	273	316	353	387
7-8	73	165	234	286	330	370	404

(CONTINUED)

TABLE 26 CONTINUED

Interlift Time	Number of Years						
	1	5	10	15	20	25	30
c) K = 10^{-7} cm $\sec^{-1}$							
1-2	16	36	51	62	72	80	88
2-3	17	39	55	68	78	87	96
3-4	19	42	60	73	84	94	103
4-5	20	45	63	78	90	100	110
5-6	21	47	67	82	95	106	116
6-7	22	50	71	86	100	112	122
7-8	23	52	74	91	104	117	128
d) K = 10^{-8} cm $\sec^{-1}$							
1-2	5	11	16	20	23	25	28
2-3	6	12	17	21	25	28	30
3-4	6	13	19	23	27	30	33
4-5	6	14	20	25	28	32	35
5-6	7	15	21	26	30	34	37
6-7	7	16	22	27	32	35	39
7-8	7	17	23	29	33	37	40

TABLE 27. AVERAGE BREAKTHROUGH TIME IN WEEKS WHEN THE HORIZONTAL HYDRAULIC CONDUCTIVITY IS 1 x 10^{-5} CM SEC^{-1}.

Breakthrough at Lift	Into Lift	Average Time
1	2	1.0
2	3	1.1
3	4	1.4
4	5	1.7
5	6	1.9
6	7	2.0
7	8	2.1

above example, the result of fifty runs of the model indicated that the liner would undergo breakthrough in a matter of months (Table 28). The fastest breakthrough in the 50 runs was one month, while the slowest was 12 months, and the average was in 6.8 months.

Using 10^{-7} cm sec^{-1} as the horizontal conductivity between lifts, breakthrough of the liner would be measured in years (Table 29). Fifty runs of the model yielded an average time to breakthrough of 4.7 years, with the shortest and longest times equal to one and eight years, respectively.

TABLE 28. AVERAGE BREAKTHROUGH TIME IN MONTHS WHEN THE HORIZONTAL HYDRAULIC CONDUCTIVITY IS 1 x 10^{-6} CM SEC^{-1}.

Breakthrough at Lift	Into Lift	Average Time
1	2	1.1
2	3	1.8
3	4	3.1
4	5	4.3
5	6	5.4
6	7	6.2
7	8	6.8

TABLE 29. AVERAGE BREAKTHROUGH TIME IN YEARS WHEN THE HORIZONTAL HYDRAULIC CONDUCTIVITY IS 1×10^{-7} CM SEC^{-1}.

Breakthrough at Lift	Into Lift	Average Time
1	2	1.1
2	3	1.7
3	4	2.4
4	5	3.1
5	6	3.7
6	7	4.1
7	8	4.7

When the horizontal conductivity between the lifts was modeled as 10^{-8} cm sec^{-1}, the breakthrough time of the liner was in decades (Table 30). Average time to breakthrough was 71 years, with a short and long time out of the 50 runs of 34 and 125 years, respectively. Assuming that a soil liner must prevent breakthrough during the active life and post-closure period of a disposal facility (approximately 40 years) then only 4% of 50 model runs indicated failure. The results of Tables 27 through 30 are presented in composite form as Figure 14.

TABLE 30. AVERAGE BREAKTHROUGH TIME IN YEARS WHEN THE HORIZONTAL HYDRAULIC CONDUCTIVITY IS 1×10^{-8} CM SEC^{-1}.

Breakthrough at Lift	Into Lift	Average Time
1	2	3.5 (100%)*
2	3	17.1 (96%)
3	4	30.3 (80%)
4	5	41.2 (54%)
5	6	52.5 (22%)
6	7	61.4 (10%)
7	8	70.7 (4%)

* Number in parentheses indicates the percentage of times out of fifty runs breakthrough did occur within 40 years.

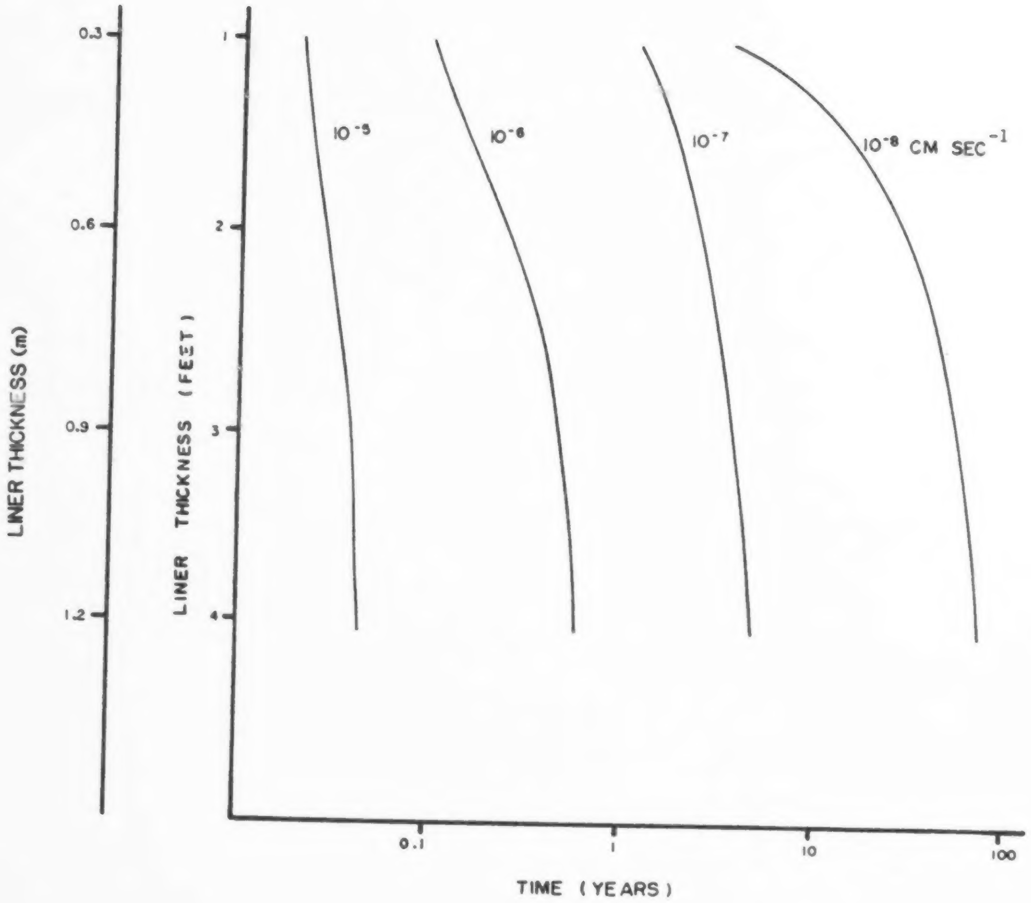

Figure 14. Liner thickness vs. breakthrough time for various interlift hydraulic conductivity values.

SECTION 5

LABORATORY STUDY

Recent data of Haxo (1988) show that organics can migrate by diffusion through synthetic liners and thus reach the underlying soil liners heretofore thought of as being protected. If flaws develop in the synthetic liner due to construction damage, poor seaming, or material defects, additional quantities of leachate may reach the underlying soil liner. It is, therefore, important that we learn how to construct soil liners to achieve the lowest possible hydraulic conductivity. Among the variables which may be involved in regulating the hydraulic conductivity of a compacted soil are the soil moisture content, compactive effort, type of compactor, and the size of the soil aggregates. This laboratory study was initiated to evaluate the effects of clod size on the hydraulic conductivity of compacted soils and the uniformity of conductivity with depth within a lift of compacted soil.

MATERIALS AND METHODS

The overall design of the laboratory study involved collecting two field soils suitable for use in constructing a clay liner, subjecting these soils to a detailed laboratory characterization and then compacting these soils under controlled conditions in 60-cm-diameter permeameters to evaluate the effects of initial clod size on hydraulic conductivity. The experiments were designed so that dyes could be used to evaluate flow paths and measurements could be taken sequentially to evaluate the uniformity of hydraulic conductivity with depth within a single lift.

Soils

Two soils were selected for this study. One soil, Beaumont clay, is classified as a fine, montmorillonitic, thermic entic pelludert and is a commonly occurring clay soil along the Gulf Coast. It is frequently used for constructing clay liners. The Beaumont soil was also used at the field site described later in Section 6.0. The second soil, a Kosse series, is a member of the fine-loamy, mixed, thermic family of Fluvaquentic Haplaquolls and is primarily a kaolinitic clay loam soil. Bulk soil samples were collected for use in the permeameters and subsamples were taken for laboratory characterization. Soil textures were measured by the pipette technique of Gee and Bauder (1986).

Mineralogy was determined using x-ray diffraction techniques as described by Whittig and Allardise (1986). Atterberg limits were measured using ASTM Procedures D-423-66 and D0424-59 for the liquid limit and plastic limit, respectively. The optimum moisture content was measured using ASTM method D698-70. Measurements of soil swelling were made by packing the soil at the optimum moisture content into a volume change apparatus (Soil Test C290) and exposing the soil to water. Compaction was achieved using a mechanical compactor and consisted of 25 blows with a 2.5-kg weight dropped from a 30-cm height. A 2-cm deep layer of free water was applied to the surface and allowed to infiltrate by gravity. Liquid additions were made as needed to maintain free liquid above the soil surface. Measurements of vertical swelling were made using a dial indicator accurate to 0.0025-cm and converted into a percentage of the original soil volume. Water retention was measured using a pressure chamber system as described by Klute (1986).

Containerized Test Sections

Sufficient volumes of these two clays were air-dried in the greenhouse and passed through a 2.5-, 5-, or 7.5-cm mesh screen to give soils with maximum clod sizes of <2.5, <5 and <7.5-cm, respectively. Each soil was brought to its optimum moisture content by adding water and allowing the moistened soil to equilibrate for 1 week in a closed 200-L drum. Permeameter bases (Fig 15) were prepared by unbolting and removing the straight-sided barrel, adding a small amount (0.5-cm) of concrete sand to the bottom of the permeameter and covering the sand with a 57-cm diameter circle of geotextile to prevent the sand from mixing with the soil during compaction. One hundred ten kg of soil were added in one lift on top of the geotextile and lightly tamped by hand. Using this amount of soil resulted in an average compacted lift thickness of 23-cm. The permeameter was then put on a MTS axial test system equipped with a specially designed compaction foot. The foot was designed with 18 individual pad feet which were spaced so that 100% coverage could be achieved using four strokes with a 90^{o} rotation of the permeameter between strokes. The pressure applied with each stroke of the compaction foot was sufficient to result in 1.38 MPa of contact area. The density and moisture content was checked following each set of four strokes using a Troxler model 3411B surface density meter. In addition, measurements of the compacted depth of soil were made. The permeameters were covered with plastic to prevent evaporation, transported to the greenhouse, and set on blocks to allow leachate collection. The head tank, an open-ended straight-sided drum, and a layer of Rubatex insulation tape (1/8 x 2") were set on the permeameter base and a flange was slipped over the tank and bolted in place. A 57-cm diameter circle of geotextile was placed on top of the soil to minimize soil disturbance due to adding water. Five g of dye (Brilliant Sulphaflavine) were dissolved in 20-L of water and poured on the soil surface. The head tank was lined with two 200-L plastic bags which were filled with water to provide about 1 meter of head without diluting the dye. Water levels were measured daily using a hook gauge. Effluent was

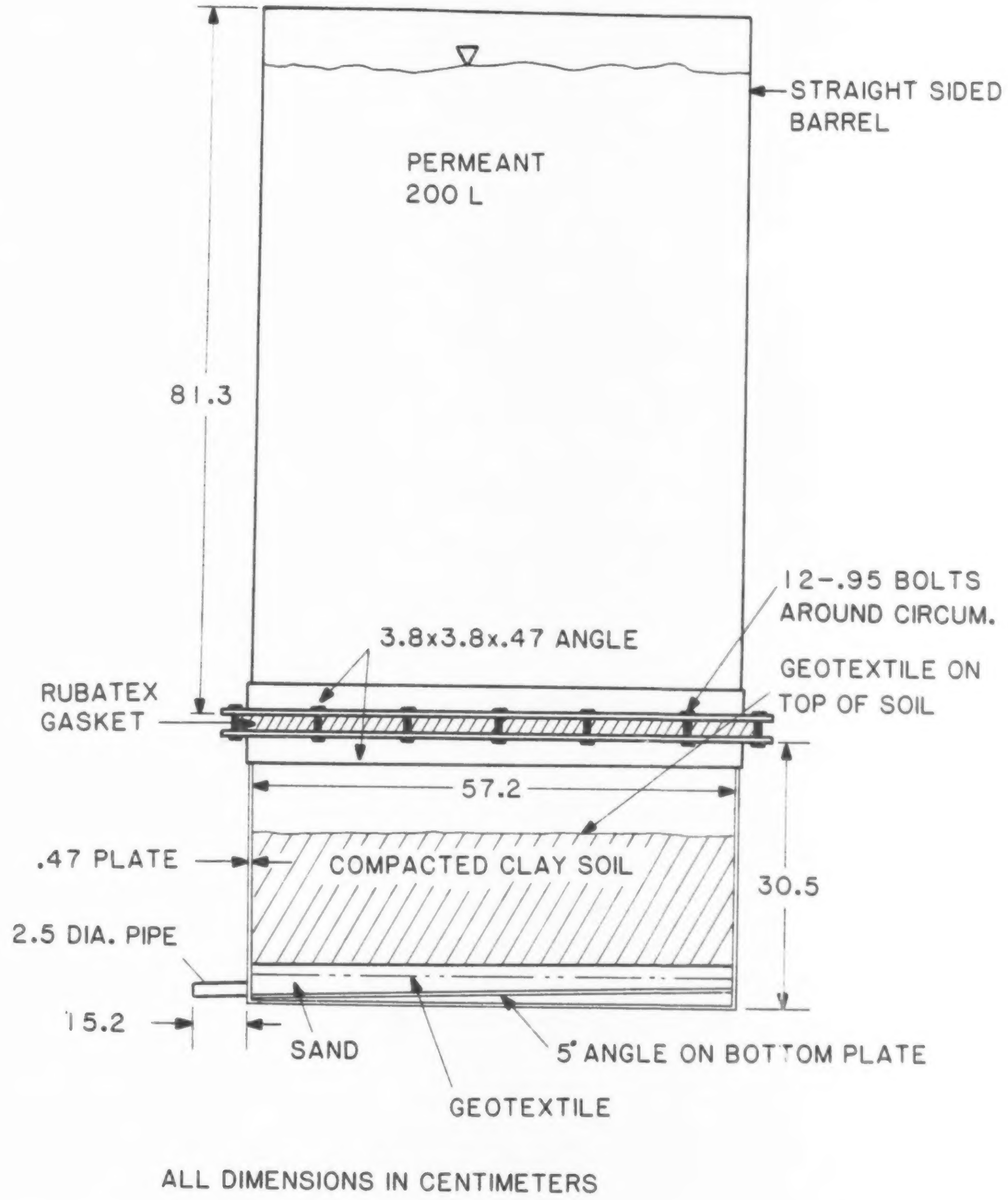
STRAIGHT SIDED BARREL
PERMEANT 200 L
81.3
12-.95 BOLTS AROUND CIRCUM.
3.8x3.8x.47 ANGLE
GEOTEXTILE ON TOP OF SOIL
RUBATEX GASKET
57.2
.47 PLATE
COMPACTED CLAY SOIL
30.5
2.5 DIA. PIPE
15.2
SAND
5° ANGLE ON BOTTOM PLATE
GEOTEXTILE
ALL DIMENSIONS IN CENTIMETERS

Figure 15. Schematic diagram of a permeameter for use in the containerized test section study.

caught and measured daily in a metal canister enclosed in a plastic bag sealed to the effluent spout to prevent evaporation. Measurements were continued until the effluent volume was within 95% of the inflow. When equilibrium was reached the liquid head was drained and the head tank was removed. A total of 7.5-cm of soil was removed in three increments of 2.5-cm. The soil surface was viewed under ultraviolet light after each 2.5-cm increment of soil was removed and schematic drawings were prepared showing the presence of dyed areas. The head tank and liquid were replaced and the conductivity measurements were repeated for the remaining soil (approximately 15-cm) until equilibrium was reached. Again, 7.5-cm of soil were removed in 2.5-cm increments with viewing of dyed areas between increments. The entire procedure was then repeated for the remaining 7.5-cm of soil.

RESULTS AND DISCUSSION

Soil Characterization

The Beaumont soil series contained 52.4% clay and had a USDA texture of clay (Table 31). It is classified as a fine montmorillonitic, thermic, Entic Pelludert. In the Unified Soil Classification System, this soil is classified as a highly plastic inorganic clay (CH). Because of its high clay content, it is able to retain 52% moisture at near saturation and 19% at the permanent wilting point (-16402 cm water, Figure 16). The predominant clay mineral in the Beaumont soil is smectite which is a highly expandable clay mineral, thus accounting for the 7% swelling upon wetting.

The Kosse soil series contained 63.8% sand and had a USDA texture of sandy clay loam. It is classified as a fine loamy, mixed, thermic, Fluvaquentic Haplaquoll. In the Unified Soil Classification System, this soil is classified as an SF. Due to its coarser texture, the Kosse soil retained only about half the amount of water that the Beaumont soil retained at any given potential. The predominant clay mineral in the Kosse soil was kaolinite, a nonexpandable clay mineral, and therefore this soil exhibits very little swelling.

Mineralogical Analysis

Because much of the behavior of soils is controlled by the clay fraction, a thorough understanding of the clay minerals in a soil is essential to an understanding of the mechanism controlling physical and chemical reactions in soils. Therefore, a detailed mineralogical analysis of the Beaumont and Kosse soils was conducted.

TABLE 31. PHYSICAL PROPERTIES OF THE TWO SOILS USED IN THIS STUDY

Soil	Texture				Engineering Properties						
	Sand	Silt (%)	Clay	USDA	Liquid Limit	Plastic Limit	Plastic Index	Unified Classification	Predominant Mineral	Optimum Swelling (%)	Moisture
Beaumont	16.2	31.4	52.4	clay	52	15	37	CH	Smectite	6.95	13.6
Kosse	63.8	12.7	23.5	sandy clay loam	18.6	13.4	5.2	SF	Kaolinite	0.0	12.0

Potential (cm H_2O)

	0.0	-2	-23	-49	-185	-646	-1047	-3420	-9771	-16402
	moisture retention (%)									
Beaumont	-	52.0	46.6	42.1	35.8	28.8	26.3	20.9	20.5	19.0
Kosse	30.3	25.6	20.2	16.2	13.0	12.8	11.9	10.5	10.2	9.7

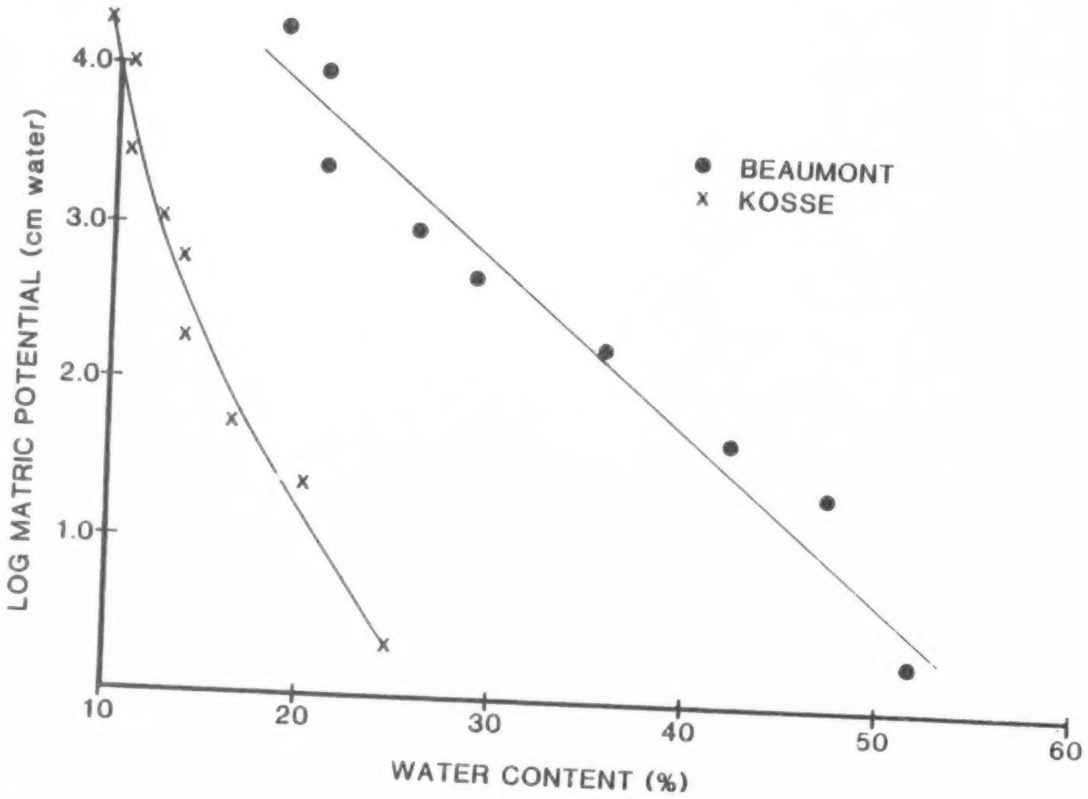

Figure 16. Water retention as a function of matric potential for the two soils used in this study.

Whole Sample - Beaumont Clay--

The X-ray diffraction (XRD) pattern of the whole sample (powder mount) indicates the presence of quartz, smectite, mica, calcite, and kaolinite. The intensity of quartz peaks (4.27 Å, 3.34 Å, and 2.45 Å), kaolinite (001 - 7.1 Å) and smectite (001-15.2 Å) indicate that they are the major minerals in the sample. In other words, mica (9.98 Å and 003 = 3.34 Å) and calcite (3.03 Å) are low in the sample as indicated by their intensity (Figure 17).

Coarse Clay Mineralogy, 2-0.2-um - Beaumont Clay--

The X-ray diffraction patterns for K and Mg - glycol saturation and various heat treatment of the oriented clay slides indicate the presence of smectite, mica, and kaolinite (Figure 18).

The 2-0.2-um clay comprise 25.9% of the sample. There is some smectite in this fraction. The 0.01 = 14.7 Å peak plus expansion after glycerol saturation and collapse of 001 peak to 10 A are indications of smectite presence. The two main peaks (001 = 10.0 Å, 002 = 4.8 Å) of mica remain unchanged upon ionic saturation, saturation with glycerol, and by heat treatment. The presence of 10 Å peak upon Mg saturation at 25°C indicates the presence of mica. The presence of 7.10 Å peak and its collapse upon K saturation plus 550°C heat is an indication of kaolinite presence since chlorite is not present in this fraction.

Fine Clay Mineralogy <0.2-um - Beaumont Clay--

Quantitative mineralogy of the less than 0.2-um size fraction was based on XRD analysis. The mineralogy of the fine clay fraction was similar to the coarse clay, but the relative abundance of the mineral types present differ.

XRD analysis of the fine clay fraction indicated the presence of smectite, mica, and kaolinite. Smectite 001 = 14.5 Å expands after glycerol saturation to 17.1 Å, and collapses to 10.0 Å upon K saturation and heat. Mica peaks (001 = 10, 002 = 5.0 and 003 = 3.3 Å) do not change upon heating and Mg glyceration. The presence of kaolinite is indicated by two peaks (001 = 7.10 Å and 002 = 3.6 Å) plus the collapse of 7.1 Å upon K-saturation and heating (Figure 19). The <0.2-um clay comprises 15.9%.

Whole Sample - Kosse Clay --

The presence of mica, kaolinite, and quartz are indicated by the X-ray diffraction pattern of the whole sample. The intensity of quartz peaks (4.46 Å, 3.05 Å, and 2.52 Å) and kaolinite (001 = 7.8 Å) indicate that these two are the major minerals in the sample. Examination of mica (001 = 11.2 Å) indicates that the presence of this mineral in the sample is low (Figure 20).

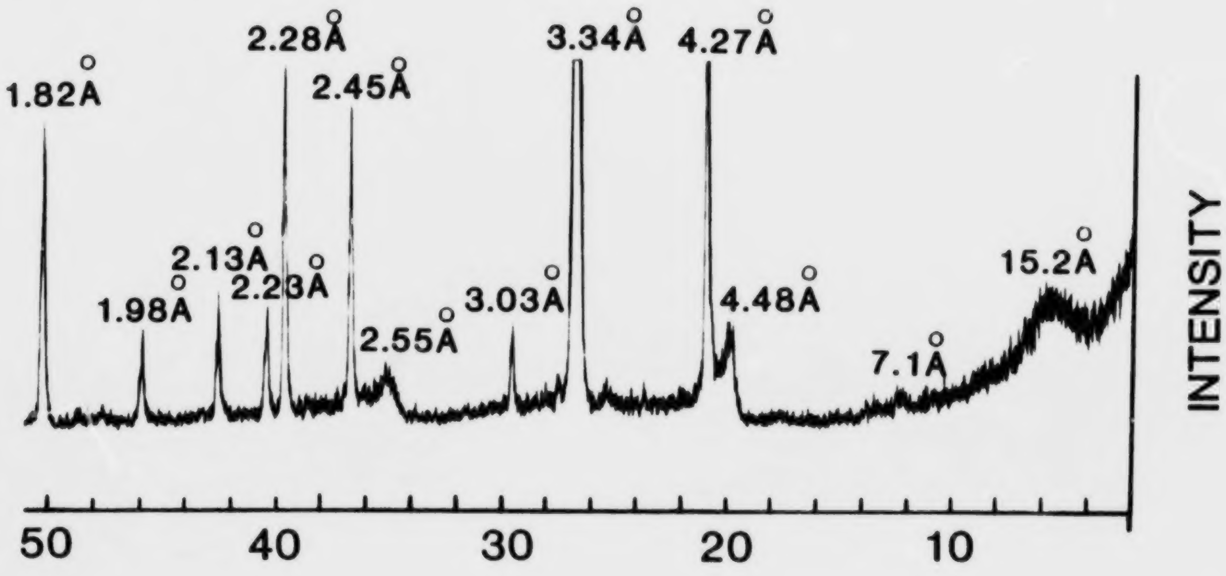

Figure 17. X-ray diffraction pattern of the clay fraction of Beaumont clay soil.

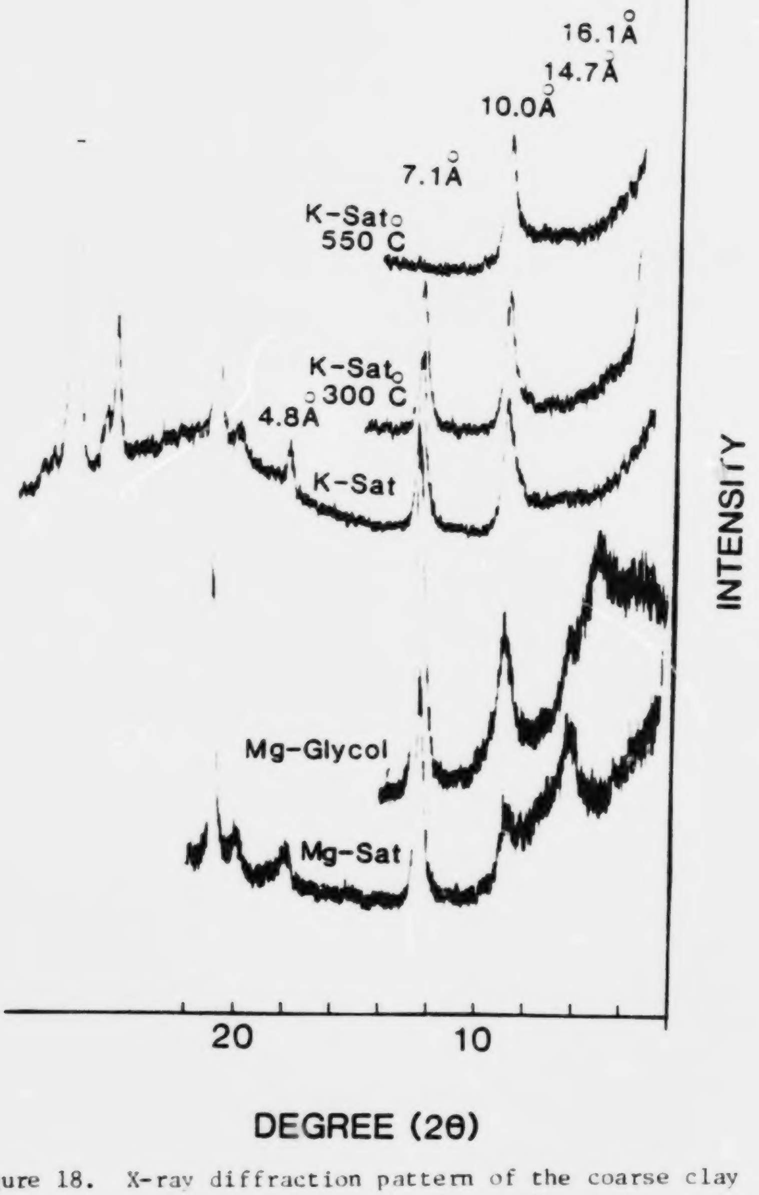

Figure 18. X-ray diffraction pattern of the coarse clay fraction of Beaumont clay soil.

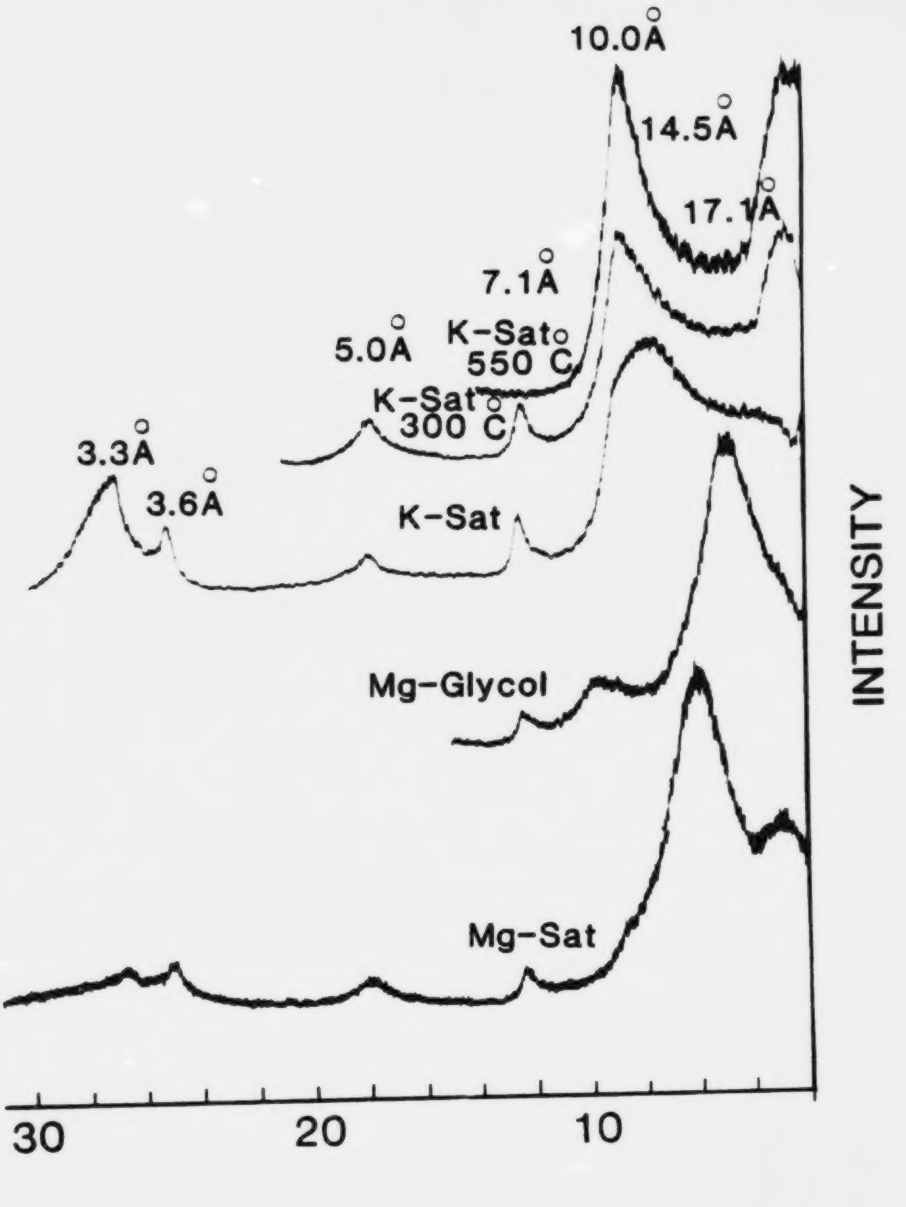

Figure 19. X-ray diffraction pattern of the fine clay fraction of Beaumont clay soil.

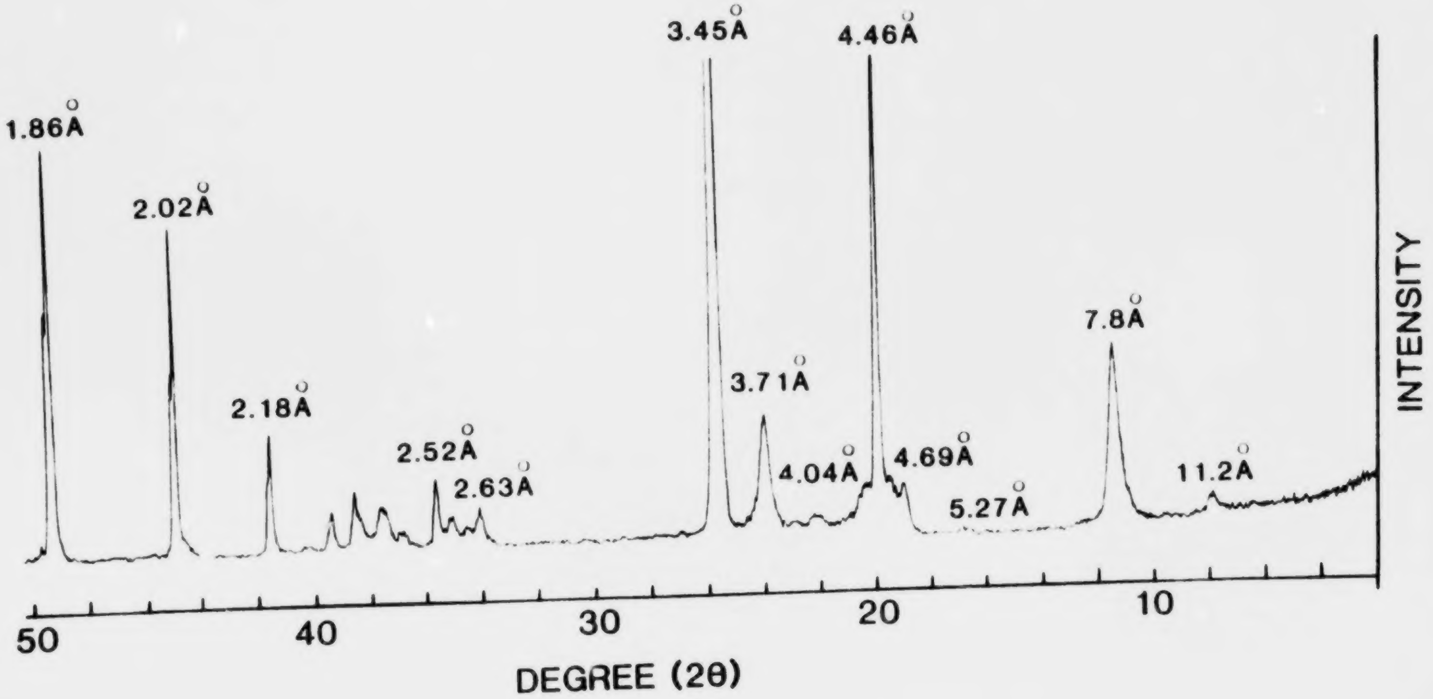

Figure 20. X-ray diffraction pattern of the clay fraction of Kosse soil.

Coarse Clay Mineralogy - Kosse Clay--

Qualitative mineral identification of 2-0.2-um and <0.2-um fractions were determined by XRD analysis. The analysis indicates the presence of kaolinite and mica in the coarse fraction (Figure 21). The 2-0.2-um clay comprises of 1.57% of the Kosse soil. There are some mica and kaolinite in this fraction. The three main peaks (001 = 10.0 Å, 002 = 4.98 Å, and 003 = 3.33 Å) of mica remain unchanged upon ionic saturation, saturation with glycerol, and by heat treatment. The presence of 7.1 Å peak and its collapse upon K saturation plus 550°C heat is an indication of kaolinite presence.

Fine Clay Mineralogy, <0.2-um - Kosse Clay--

The mineralogy of the fine clay fraction is similar to the coarse clay, but the relative abundance of mineral types present differ. It appears that fine clay contains less mica and more kaolinite than the coarse fraction (Figure 22).

The fine fraction of Kosse soil comprises 2.09% of the sample. It is important to mention that the indicated percentage of the fine and coarse clay are not an exact percentages in the sample. It is expected that some of the clay has been lost to the sand and silt fractions during the decantation process. Some of the sample loss can also be attributed to the amount of organic matter, iron oxide, carbonate, and oxide in the soil samples. In addition to the above factors, the loss of sample during the stirring, and inadvertent carelessness could have contributed to the observed loss of sample mass.

Hydraulic Conductivity

The results of measured steady state hydraulic conductivity for the entire 24-cm-thick-lift of Beaumont clay are presented in Table 32.

TABLE 32. HYDRAULIC CONDUCTIVITY (CM SEC^{-1}) OF BEAUMONT CLAY FOR COMPLETE LIFT

Clod Size (cm)	Rep 1	Rep 2	Rep 3	Average
2.5	6.89×10^{-7}	4.13×10^{-7}	0.41×10^{-7}	3.81×10^{-7}
5.0	8.60×10^{-7}	3.08×10^{-7}	3.36×10^{-7}	5.01×10^{-7}
7.5	7.83×10^{-8}	1.81×10^{-8}	2.19×10^{-8}	3.94×10^{-8}

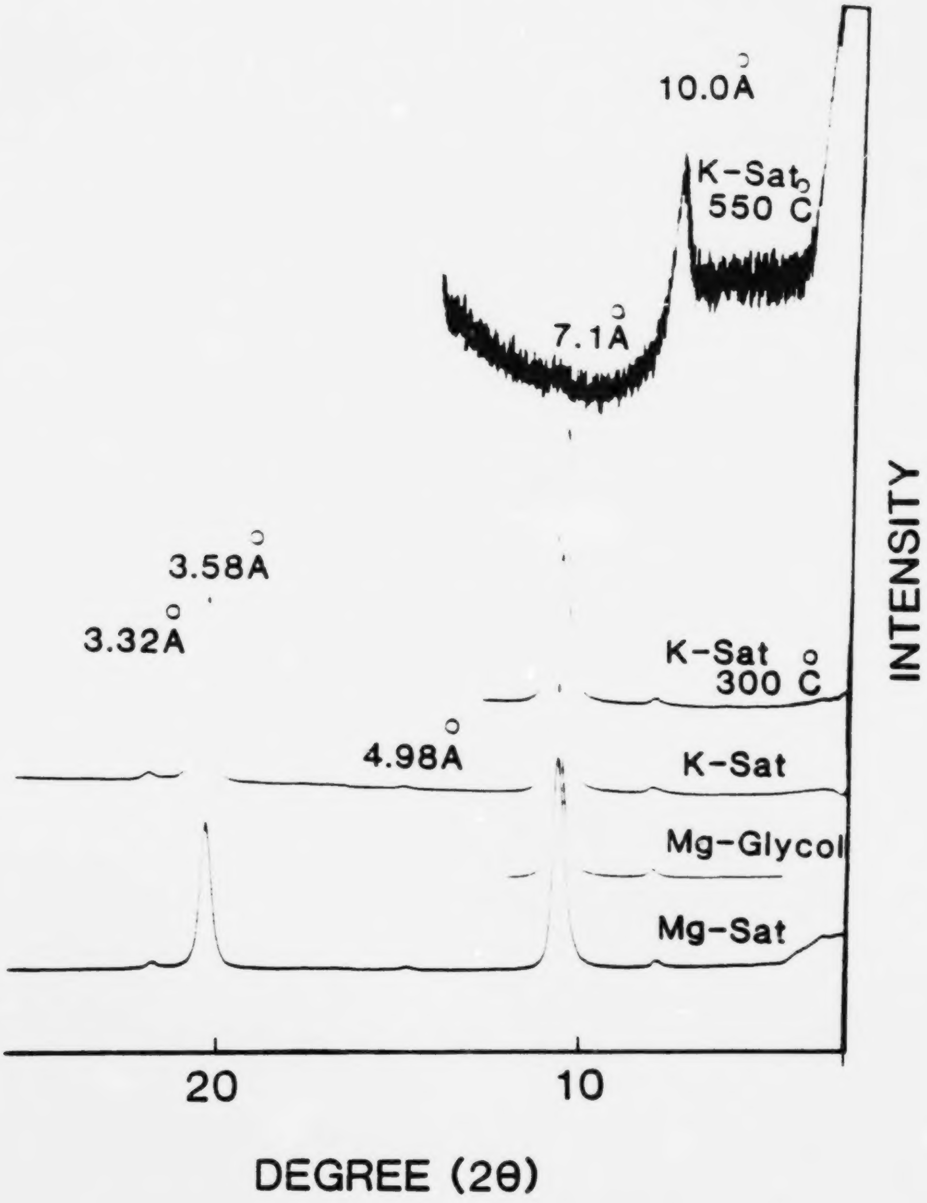

Figure 21. X-ray diffraction pattern of the coarse clay fraction of Kosse soil.

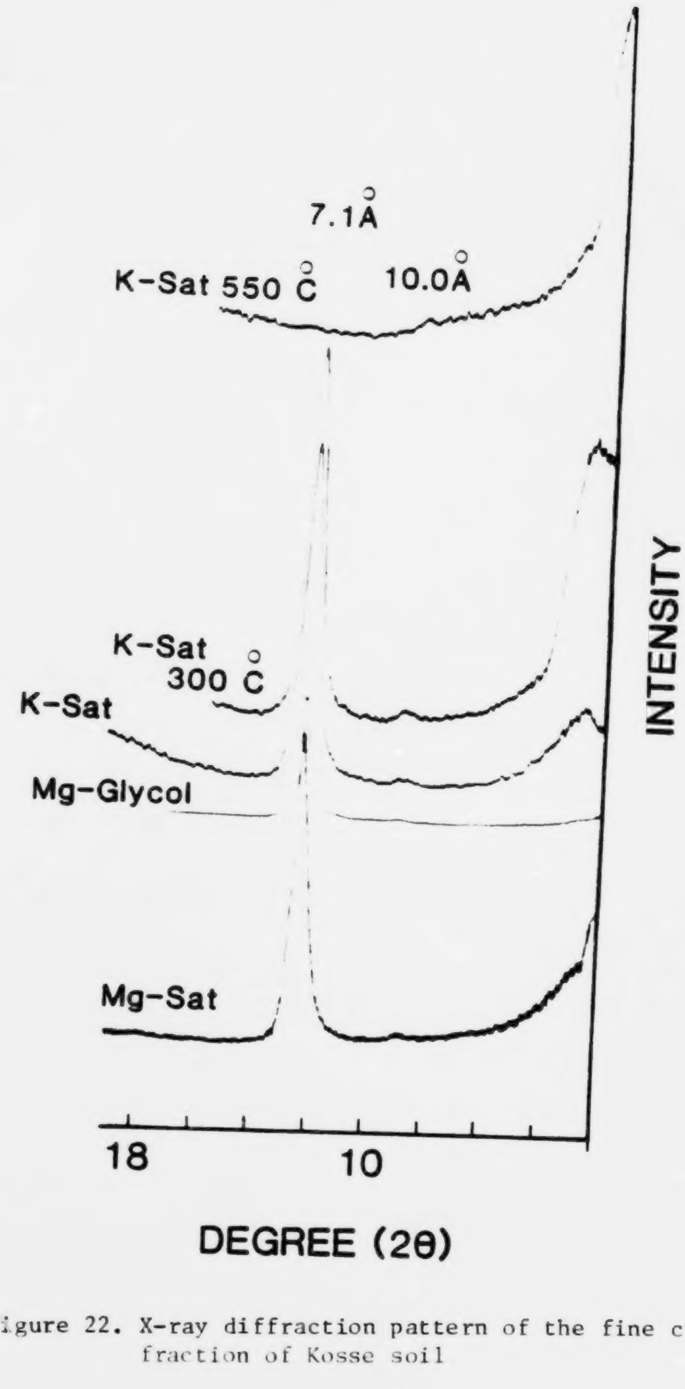

Figure 22. X-ray diffraction pattern of the fine clay fraction of Kosse soil

Examination of the data indicates that the clod size does not appear to have a significant effect on the hydraulic conductivity of the Beaumont clay. The results also indicate that the measured conductivity in the 60-cm permeameters is much greater than that measured in the laboratory (1.5 x 10^{-9} cm sec^{-1}) using small 10-cm-diameter permeameters compacted with soil having an an equivalent diameter of 2-mm or less.

Because of equipment limitations, it was necessary to pack the permeameters in two batches. The hydraulic conductivity of the permeameters in the second batch (Rep. 3 of 2.5-cm clod size and Reps 1 to 3 of the 7.5-cm clod size) were noticeably lower than those compacted first. Inspection of the data shows that the soil used in the second batch was wetter (about 6.6%) and this change in moisture content was responsible for the decreased conductivity.

To evaluate the uniformity of compaction with depth, 7.5-cm of the compacted soil was removed from each permeameter, and the conductivity was measured again after steady state flow was obtained. The results presented in Table 33, indicate that the hydraulic conductivity increased with depth.

TABLE 33. HYDRAULIC CONDUCTIVITY OF CM SEC^{-1} OF BEAUMONT CLAY AFTER 7.5-CM OF TOP SOIL WAS REMOVED

Clod Size (cm)	Rep 1	Rep 2	Rep 3	Average
2.5	15.63 x 10^{-7}	4.13 x 10^{-7}	1.51 x 10^{-7}	7.09 x 10^{-7}
5.0	21.08 x 10^{-7}	3.82 x 10^{-7}	2.92 x 10^{-7}	9.27 x 10^{-7}
7.5	1.30 x 10^{-7}	1.82 x 10^{-7}	6.01 x 10^{-7}	2.83 x 10^{-7}

Conductivities measured after removal of the upper 7.5-cm of soil ranged from 0.9 to 2.5 times that of the complete lift. The next 7.5-cm of soil was then removed and the hydraulic conductivity of the soil was measured again. The results (Table 34) show dramatic increases in hydraulic conductivity. Conductivities ranged from 3.19 x 10^{-7} to 99.66 x 10^{-7} cm sec^{-1} which is 0.9 to 11.6 times that of the entire lift.

The bulk density and moisture content values of the permeameters packed with Beaumont clay are reported in Tables 35 and 36, respectively. The densities of the permeameters compacted at moisture contents below optimum ranged from 1.58 to 1.74 g cm^{3} and in general were higher than the densities of the remaining permeameters compacted at near optimum moisture contents.

TABLE 34. HYDRAULIC CONDUCTIVITY (CM SEC^{-1}) OF BEAUMONT CLAY AFTER 15-CM OF THE TOP SOIL WAS REMOVED

Clod Size (cm)	Rep 1	Rep 2	Rep 3	Average
2.5	54.73×10^{-7}	3.50×10^{-7}	19.5×10^{-7}	25.91×10^{-7}
5.0	99.66×10^{-7}	5.49×10^{-7}	3.19×10^{-7}	36.11×10^{-7}
7.5	6.03×10^{-7}	18.28×10^{-7}	40.90×10^{-7}	21.74×10^{-7}

TABLE 35. MEASURED BULK DENSITY (G CM^{-3}) OF BEAUMONT CLAY AFTER COMPACTION

Clod Size (cm)	Rep. 1	Rep. 2	Rep. 3	Average
2.5	1.66	1.58	1.53	1.59
5.0	1.63	1.68	1.74	1.68
7.5	1.61	1.55	1.57	1.58

TABLE 36. MEASURED MOISTURE CONTENT (PERCENT BY WEIGHT) OF BEAUMONT CLAY AT THE TIME OF COMPACTION

Clod Size (cm)	Rep. 1	Rep. 2	Rep. 3
2.5	11.4*	11.1*	17.8
5.0	11.1*	11.3*	10.3*
7.5	19.0	19.3	14.6

* Calculated from volumetric moisture content measured with surface density meter.

The results of measured steady state hydraulic conductivity of the Kosse soil (Table 37) indicate that the clod size does not have a significant effect on the hydraulic conductivity. This is similar to that observed for the Beaumont clay.

TABLE 37. HYDRAULIC CONDUCTIVITY (CM SEC^{-1}) OF KOSSE SOIL FOR A COMPLETE LIFT

Clod Size (cm)	Rep 1	Rep 2	Rep 3	Rep 4	Average
2.5	3.55×10^{-7}	0.76×10^{-7}	2.60×10^{-7}	0.72×10^{-7}	1.91×10^{-7}
5.0	0.81×10^{-7}	1.30×10^{-7}	1.12×10^{-7}	NT	1.08×10^{-7}

NT - not tested.

The conductivity of the complete lifts of Kosse ranged from 0.72×10^{-7} to 3.55×10^{-7} cm sec^{-1}. Of these conductivities, three values (Reps 2 and 4 of the 2.5-cm clod size and rep 1 of the 5.0-cm clod size) closely approximated the conductivity measured in the laboratory (0.8×10^{-7} cm sec^{-1}). Plots representative of cumulative inflow and outflow for permeameters packed with 2.5 and 5-cm clods of Kosse soil are shown in Figures 23 and 24. During the initial 20 to 25 days, the flow rates changed, however after 25 days the inflow rates equaled the outflow rates and both remained relatively constant with time. Many of the fluctuations in the cumulative inflow curve on Figure 28 are due to temperature fluctuations causing expansion and contraction of the permeant water and creating an error in the inflow which was calculated as the difference in head measured daily.

After removal of the upper 7.5-cm of soil the conductivity approximately doubled and ranged from 0.94×10^{-7} to 6.15×10^{-7} cm sec^{-1} (Table 38), which is 1.2 to 1.7 times that of the complete lift. Again, the data show little influence of the clod size on the final conductivity of this layer.

TABLE 38. HYDRAULIC CONDUCTIVITY (CM SEC^{-1}) OF KOSSE SOIL AFTER 7.5-CM OF SOIL HAD BEEN REMOVED

Clod Size (cm)	Rep 1	Rep 2	Rep 3	Rep 4	Average
2.5	6.15×10^{-7}	0.94×10^{-7}	4.11×10^{-7}	1.05×10^{-7}	3.06×10^{-7}
5.0	1.20×10^{-7}	1.69×10^{-7}	1.32×10^{-7}	NT	1.40×10^{-7}

NT = Not tested.

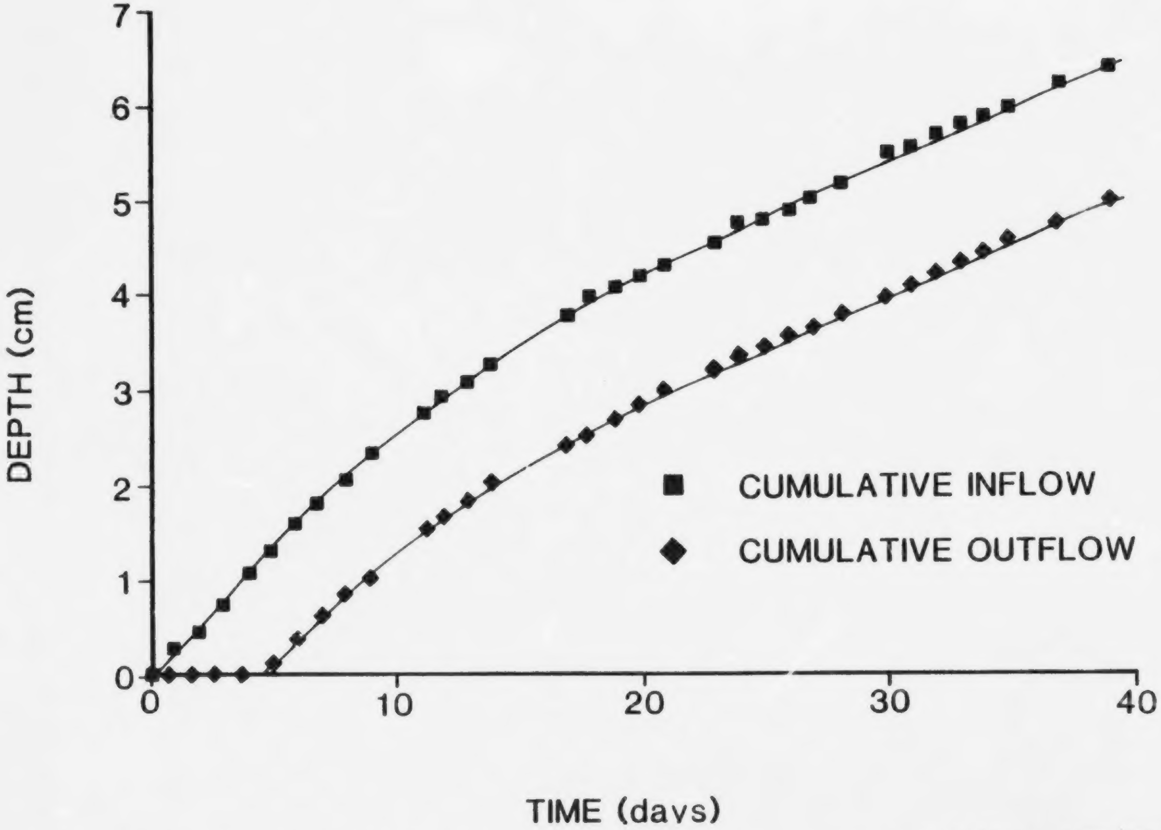

Figure 23. Cumulative water inflow and outflow from a permeameter containing a complete lift of Kosse soil compacted with 2.5 cm clods.

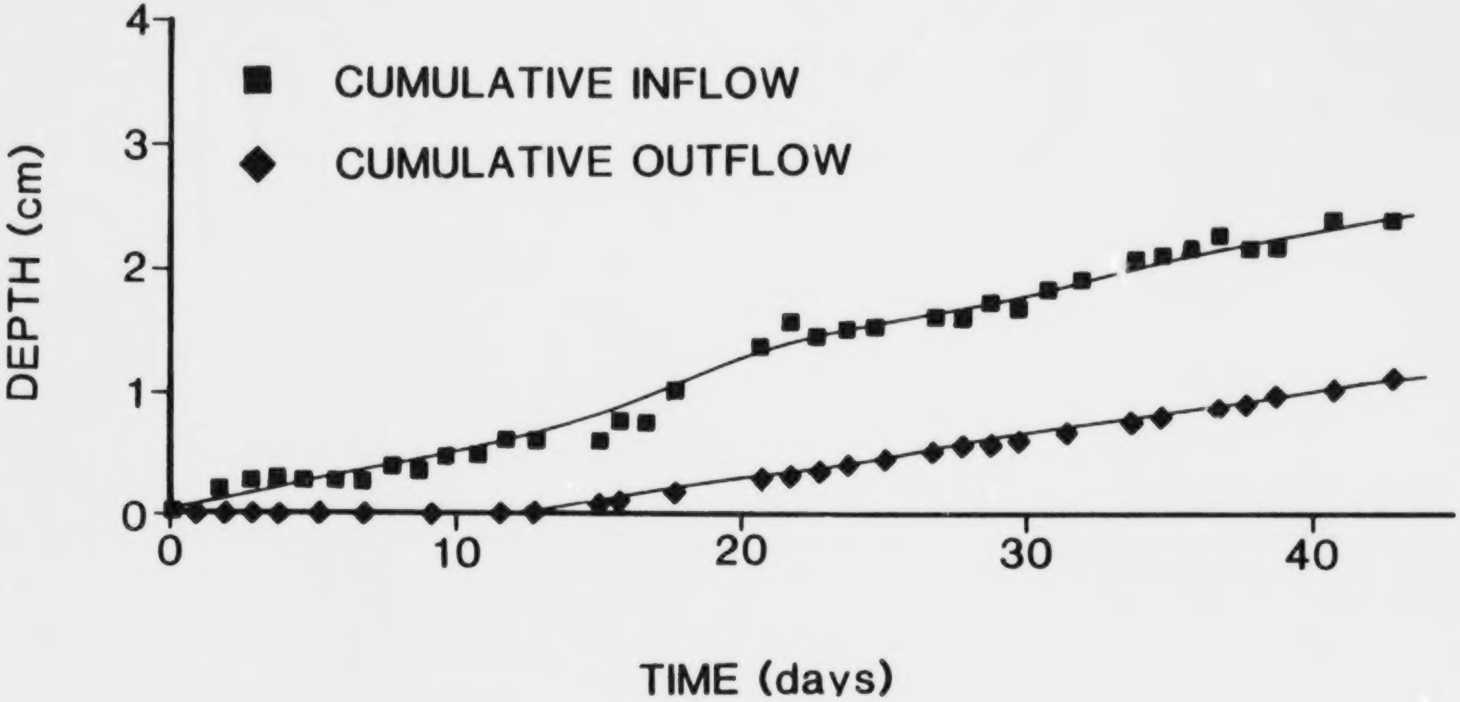

Figure 24. Cumulative water inflow and outflow from a permeameter containing a complete lift of Kosse soil compacted with 5.0 cm clods.

The hydraulic conductivity of the Kosse soil permeameters after removal of the upper 15-cm of compacted soil showed noticeable increases (Table 39) and ranged from 1.48×10^{-7} to 33.27×10^{-7} cm sec^{-1}. This represents an increase in hydraulic conductivity of 2 to 13 times that of the complete lift. Thus, it appears that the compactive effort was not sufficient to adequately remold the soil below 15-cm to achieve the desired hydraulic conductivity. The bulk density and moisture content values of the permeameters packed with Kosse clay are reported in Tables 40 and 41, respectively. The densities ranged from 1.66 to 1.80 g cm^{-3} and are typical for field values. The moisture contents averaged 11.5 and 12.0 percent for the permeameters packed with 2.5- and 5.0-cm clods, respectively. In both instances, moisture content remained within 0.6% of the average values. The above data for both soils indicates that clod sizes of 2.5- and 5.0-cm have a minimal influence on conductivity of the compacted soil. It is likely that the true impact of clod size under field conditions may be greater because the clods may not have sufficient time to come to equilibrium moisture content whereas in this study the clods were equilibrated for 1 week in a sealed container prior to compaction. Thus, under field conditions, the center of the clods may be drier or wetter than the outside thereby making it more difficult to achieve the minimum conductivity.

TABLE 39. HYDRAULIC CONDUCTIVITY (CM SEC^{-1}) OF KOSSE SOIL AFTER 15-CM OF SOIL HAD BEEN REMOVED

Clod Size (cm)	Rep 1	Rep 2	Rep 3	Rep 4	Average
2.5	8.01×10^{-7}	1.48×10^{-7}	33.27×10^{-7}	1.62×10^{-7}	11.10×10^{-7}
5.0	2.27×10^{-7}	3.45×10^{-7}	2.47×10^{-7}	NT	2.73×10^{-7}

NT = not tested.

TABLE 40. MEASURED BULK DENSITY (G CM^{-3}) OF KOSSE CLAY AFTER COMPACTION

Clod Size (cm)	Rep. 1	Rep. 2	Rep. 3	Rep. 4	Average
2.5	1.80	1.68	1.73	1.69	1.73
5.0	1.74	1.66	1.72	NT	1.71

NT = not tested.

TABLE 41. MEASURED MOISTURE CONTENT (PERCENT BY WEIGHT) OF KOSSE CLAY AT THE TIME OF COMPACTION

Clod Size (cm)	Rep. 1	Rep. 2	Rep. 3	Rep. 4	Average
2.5	11.0	12.0	11.0	12.1	11.5
5.0	12.6	11.9	11.4	NT	12.0

NT = not tested.

The data (Tables 37 to 39) show that conductivity of the Kosse soil is extremely sensitive to changes in soil moisture content. Laboratory data on the moisture-density relationship (Figure 25) show the optimum moisture to be 12 percent by weight. A plot of the conductivity-moisture content relationship (Figure 26) shows that the minimum conductivity of 0.8×10^{-7} cm sec^{-1} is achieved at moisture contents of 13 to 14 percent by weight. Since the gravimetric moisture content was measured on the soil which went into each permeameter of the time of compaction, the conductivity should be predictable by reading the curve in Figure 26. The conductivities and moisture contents measured using the large scale permeameters are also plotted on Figure 26 and show that a change in moisture content of 1% can change the conductivity by almost 1 order of magnitude. The measured vs. estimated values are plotted in Figure 27 and a linear regression showed an r^2 of 0.89 indicating that about 89% of the the variability was due to the moisture content.

Because both the soil bulk density and the hydraulic conductivity of a compacted soil are related to the soil moisture content at the time of compaction, people have assumed that there is a direct relationship between the soil bulk density and the hydraulic conductivity. Based on this assumption, workers have evolved the field practice of measuring the compacted bulk density and using this to estimate the hydraulic conductivity of the compacted soil. If the bulk density is a valid estimator of the hydraulic conductivity then there should be a direct relationship between these two parameters. A plot of these variables for the Kosse soil (Figure 28) shows very little relationship between bulk density and hydraulic conductivity. It, therefore, appears that the soil bulk density is a poor estimator of the hydraulic conductivity and that either direct measurements must be made or a new indicator needs to be developed for use in estimating the hydraulic conductivity of a compacted soil.

Breakthrough

For each of the experimental permeameters, the time interval between addition of the permeant and the first appearance of leachate

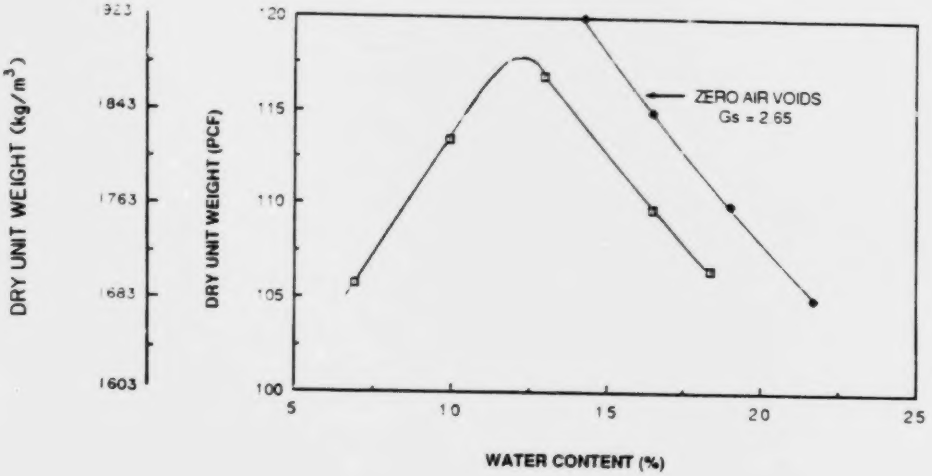

Figure 25. Laboratory measured moisture-density curve for Kosse soil.

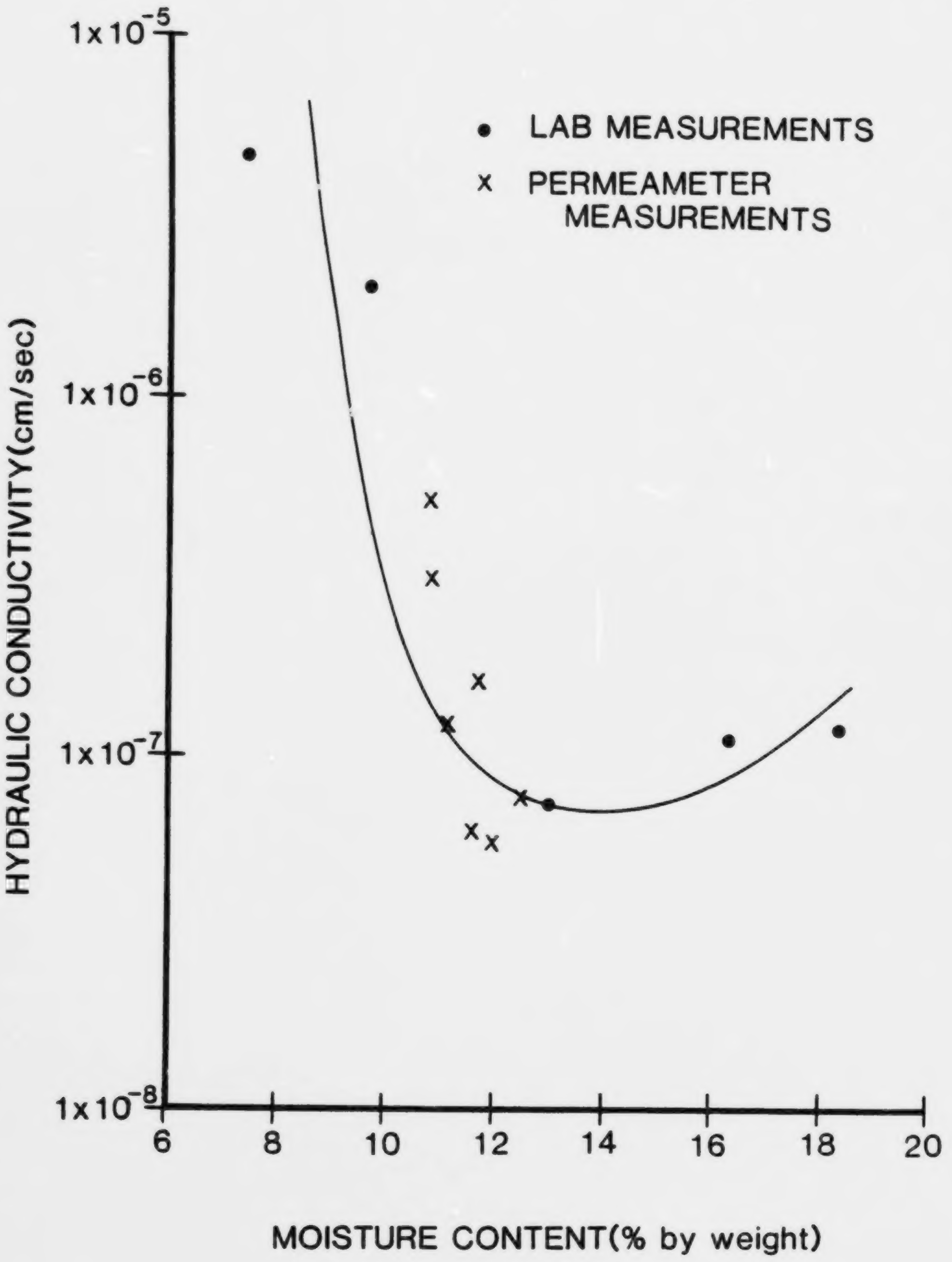

Figure 26. Hydraulic conductivity of Kosse soil measured in the laboratory and using large permeameters, as a function of moisture content.

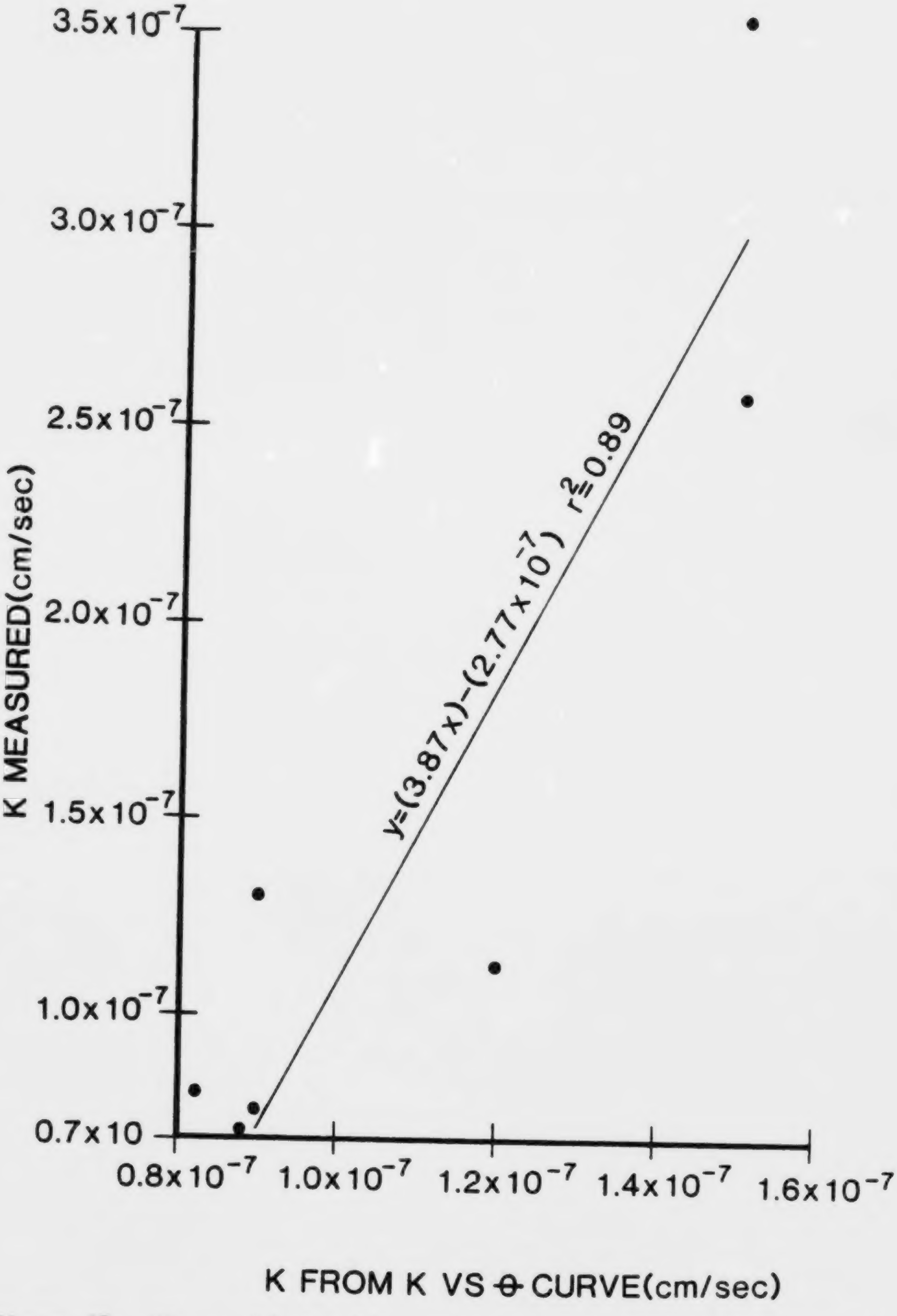

Figure 27. Measured hydraulic conductivity of compacted Kosse soil versus that predicted from the conductivity versus moisture content curve in Figure 26.

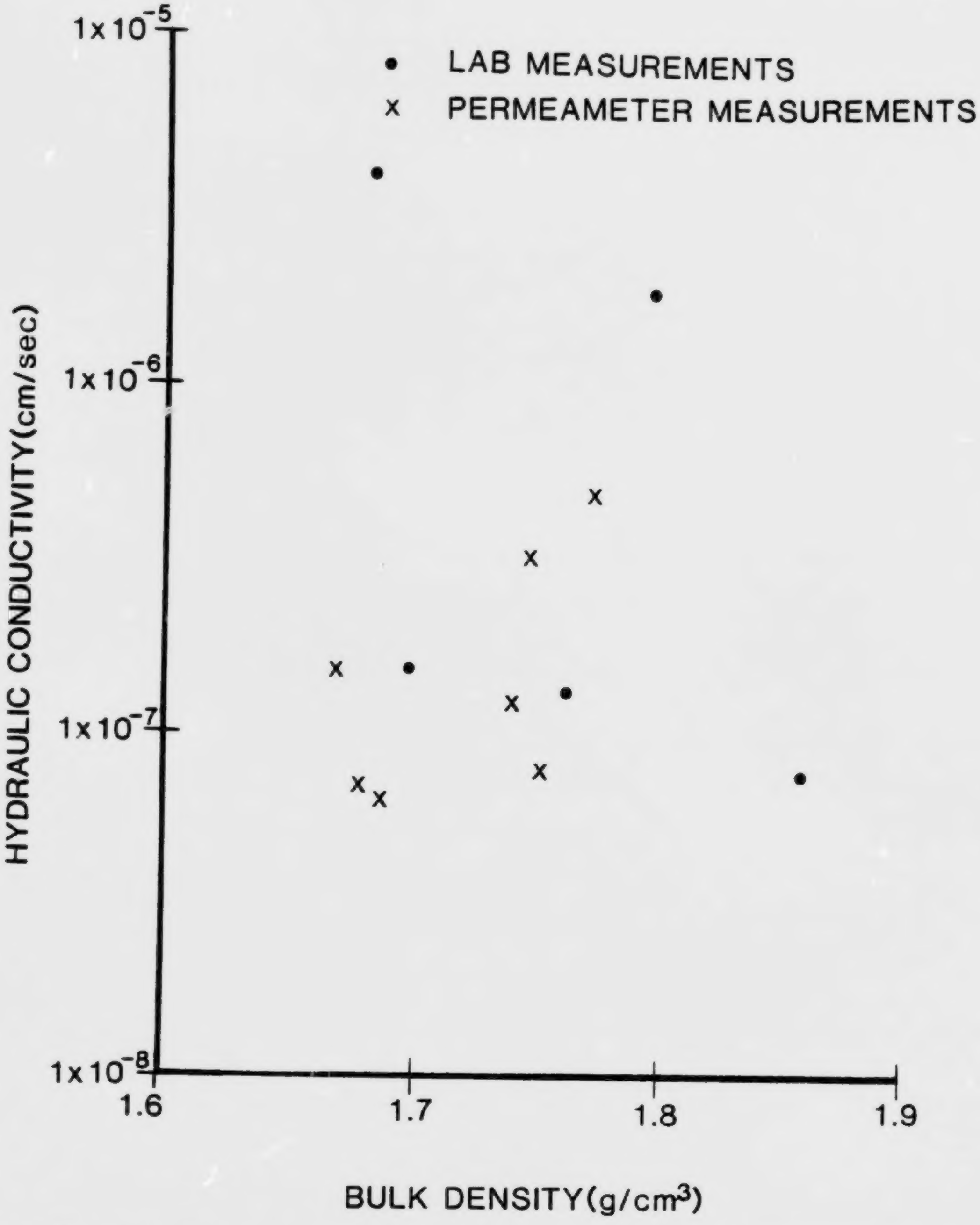

Figure 28. Hydraulic conductivity, as measured both in the laboratory and using large permeameters, of compacted Kosse soil as a function of the compacted soil bulk density.

was measured and called the breakthrough time. Breakthrough time was plotted as a function of hydraulic conductivity for a single lift of each soils. Data for the Beaumont soil (Figure 29) shows that at an effective conductivity of 1 x 10^{-7} cm sec^{-1}, breakthrough would occur in 400-hr (17 days). At an effective conductivity of 1 x 10^{-6} cm sec^{-1}, breakthrough would occur in 150 hr or about 6 days. Breakthrough for the Kosse soil was a little sooner (Figure 30) and an average conductivity of 1 x 10^{-7} cm sec^{-1} resulted in a breakthrough time of 186 hours (8 days). Thus, it appears that it will require 2 to 3 weeks for leachate to penetrate a lift of compacted clay with a conductivity of 1 x 10^{-7} cm sec^{-1}. Using this basis, flow through six lifts of a 90-cm thick liner would require only about 4 months. This assumes that the lifts are not well bonded and there is nearly unrestricted horizontal flow at all lift interfaces.

Effects of Desiccation

A small experiment was conducted to evaluate the effects of desiccation on the hydraulic conductivity of compacted soils. The soils were prepared and packed into permeameters as previously described, however, in this case, the soil was left uncovered for 1 to 2 days until noticeable soil cracks developed. Measurements were taken three times daily with the surface density meter during the drying period to measure changes in moisture content.

In the Beaumont soil, numerous small cracks 1- to 2-mm wide and 5- to 10-cm long, developed over the entire soil surface during the 24- to 48- hr drying period. Readings from the surface density meter indicated that the volumetric moisture content decreased an average of 5% over the drying period (Table 42). In the Kosse soil, fewer cracks were observed and the soil tended to dry and shrink as a unit resulting in cracking along the sidewall. Decreases in moisture content averaged 4.8% for the Kosse soil also (Table 42).

TABLE 42. CHANGES IN VOLUMETRIC MOISTURE CONTENT IN COMPACTED SOILS AS A RESULT OF DRYING

Soil	Clod Size (cm)	Rep. 1	Rep. 2	Rep. 3	Rep. 4	Average
Beaumont	2.5	-4.8	-5.3	-5.0	NT*	-5.0
Kosse	2.5	ND	-6.0	-3.7	-4.8	-4.8

*NT = not tested.
ND = no data due to instrument failure.

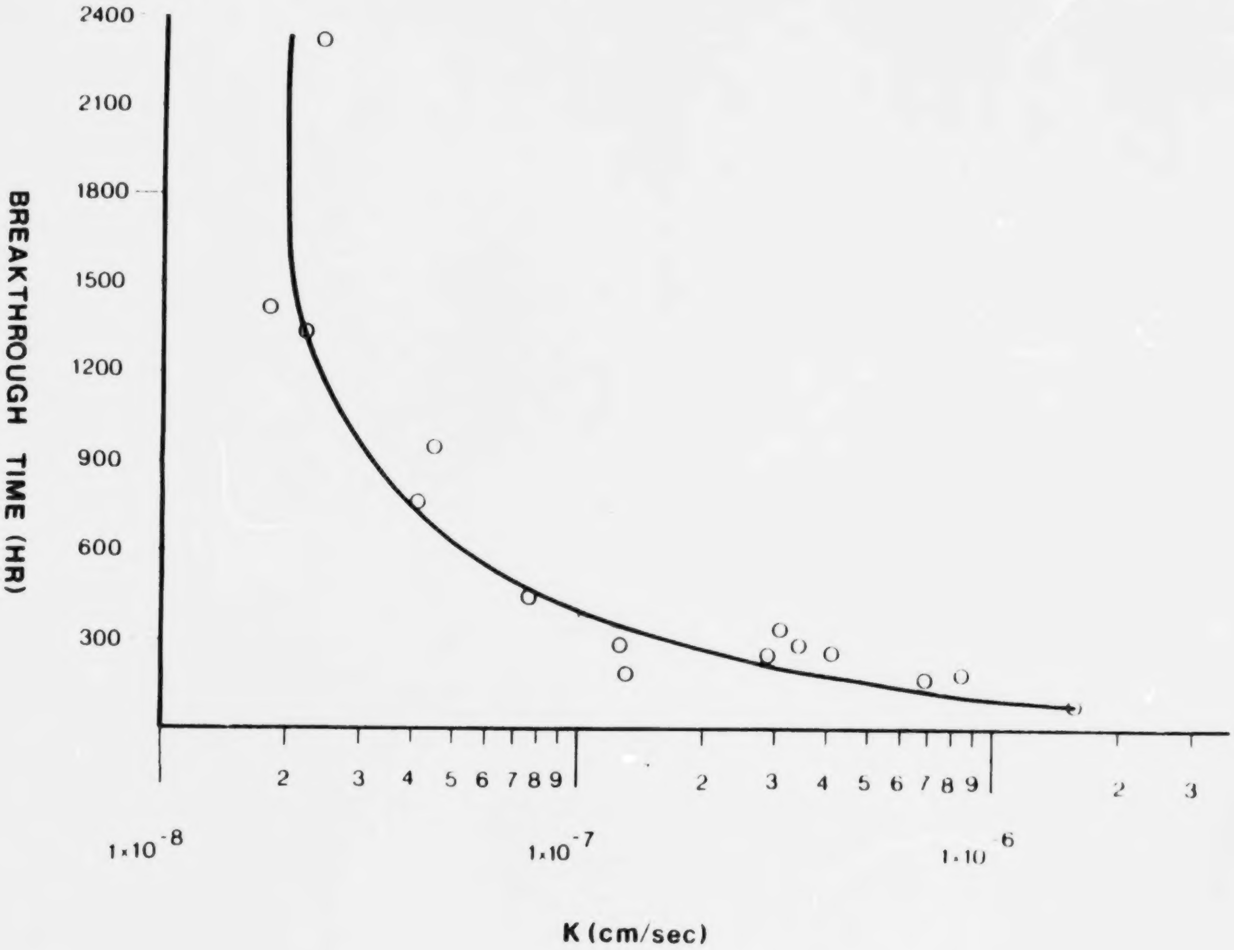

Figure 29. Breakthrough time as a function of saturated hydraulic conductivity for for a single lift of Beaumont clay soil.

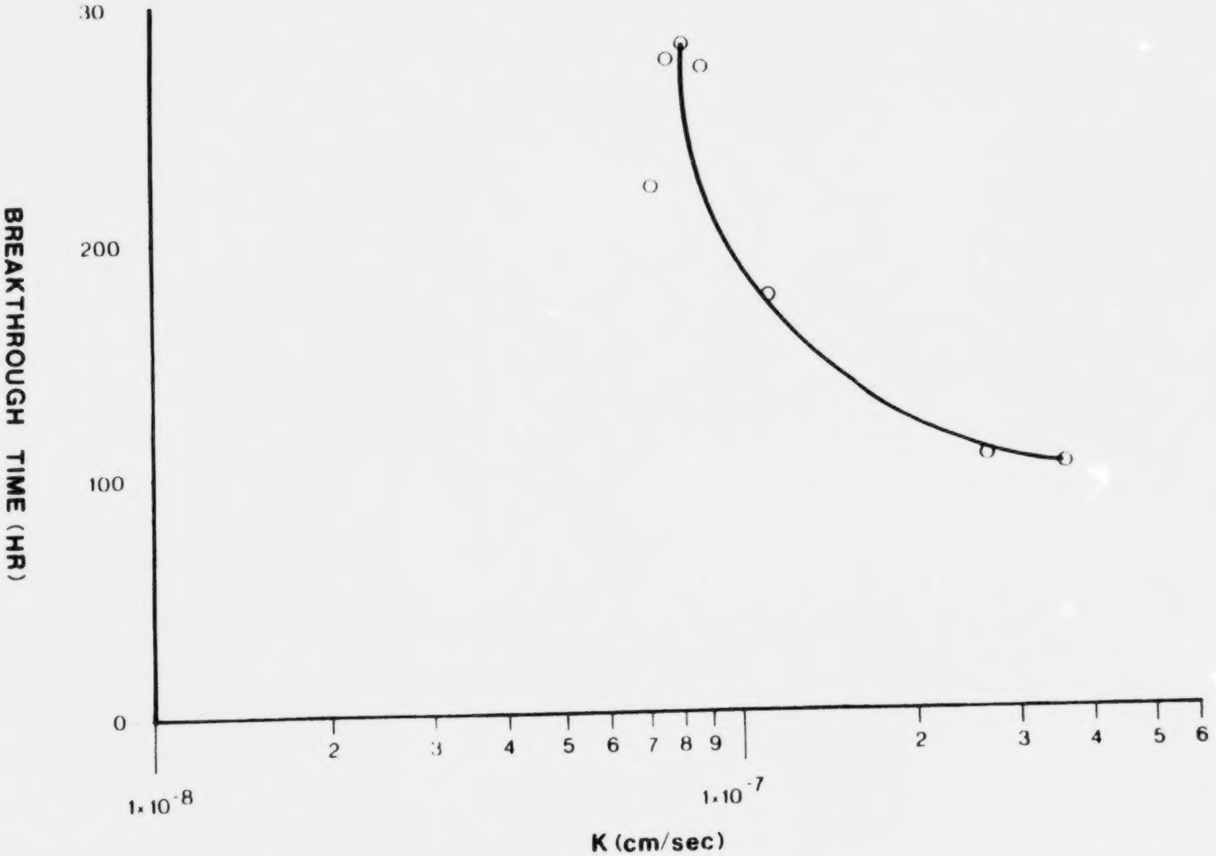

Figure 30. Breakthrough time as a function of saturated hydraulic conductivity for a single lift of Kosse soil.

Hydraulic conductivity measurements for the permeameters of Beaumont clay after drying are summarized in Table 43. Two of the three permeameters exhibited an initial high flow rate indicative of water bypass flow directly through large cracks either through the soil or along the sidewall. Calculated conductivities in the range of 5 x 10^{-2} cm sec^{-1} were likely influenced by the size of the outflow port and are not presented. In these instances, the outflow was plugged for 72-hr after which the conductivity was remeasured. The average conductivity of the complete lift in the absence of sidewall flow or crack flow was 5.06 x 10^{-8} cm sec^{-1} which is similar to the 4.9 x 10^{-8} cm sec^{-1} measured on the non-dried samples. Increases in conductivity with depth however were greater in the dried soils and averaged one and two orders of magnitude greater for the lower 2/3 and 1/3 of the lift.

TABLE 43. HYDRAULIC CONDUCTIVITY (CM SEC^{-1}) OF BEAUMONT CLAY AFTER DRYING

Clod Size (cm)	Depth	Rep. 1	Rep. 2	Rep. 3	Average
2.5	Full lift 23-cm	5.16 x 10^{-8}	2.18 x 10^{-8}	7.85 x 10^{-8}	5.06 x 10^{-8}
2.5	Bottom 2/3 of lift	1.58 x 10^{-6}	2.77 x 10^{-7}	1.04 x 10^{-6}	9.66 x 10^{-7}
2.5	Bottom 1/3 of lift	6.71 x 10^{-6}	8.50 x 10^{-6}	NT	7.61 x 10^{-6}

NT = not tested.

Conductivities of the Kosse soil after drying exhibited a similar trend. Two of the 4 replications exhibited crack flow and were stopped for 72-hr after which the conductivity was remeasured. The average conductivity for the complete lift was 1.5 x 10^{-7} cm sec^{-1} (Table 44). This rate increased to 3.09 x 10^{-7} and 1.01 x 10^{-6} cm sec^{-1} for the bottom 2/3 and 1/3 of the lift. These data clearly show the potential for the development of desiccation cracks and increased hydraulic conductivity of field compacted clay liners if not promptly covered to prevent evaporation. Drying periods in the order of 24- to 48-hr were sufficient to cause the observed phenomena in the laboratory. The presence of severe conditions (high temperature, wind, direct sunlight and low humidity) during certain field installations may substantially decrease the time required for desiccation cracks to develop.

TABLE 44. HYDRAULIC CONDUCTIVITY (CM SEC-1) OF KOSSE CLAY AFTER DRYING

Clod Size (CM)	Depth	Rep. 1	Rep. 2	Rep. 3	Rep. 4	Average
2.5	Full lift 23-cm	9.85 x 10-8	1.25 x 10-7	7.85 x 10-8	2.7 x 10-7	1.50 x 10-7
2.5	Bottom 2/3 of lift	7.83 x 10-8		3.73 x 10-7	4.76 x 10-7	3.09 x 10-7
2.5	Bottom 1/3 of lift	1.84 x 10-6		4.52 x 10-7	7.24 x 10-7	1.01 x 10-6

Dye Studies

After the permeameters reached an equilibrium flow rate and an accurate measurement of the hydraulic conductivity was made, the upper 7.5-cm of soil was removed in 2.5-cm increments. After each 2.5-cm increment was removed, the soil surface was viewed under ultraviolet light to observe dye patterns. Drawings were made of each permeameter showing the presence of dyed areas. Figures 31 through 37 are representative of the observations. In general, large dyed areas were observed at the 2.5-cm depth. The size of the dyed area decreased with each successive depth and by 5- to 7.5-cm below the soil surface only 6 to 10 small (1-2-mm diameter) spots of distinctly dyed areas were observed. In no case was any evidence seen which would indicate side wall flow below 2.5-cm depth. In some cases, such as that shown in Figure 32, a place of dark dye concentration was found at 2.5-cm depth (upper left quadrant of the permeameter) which decreased to a faint dye concentration at 5-cm depth and only 1 to 2 small spots remained by 7.5-cm depth. A similar trend exists for permeameter 19 (Figure 34) in which the large spot of faint concentration in the upper left quadrant of the permeameter at 2.5-cm depth decreased to several small spots of high concentration at 5-cm and was almost lost by 7.5-cm. These data indicate that the water is penetrating the upper 1-2-cm of soil and being rapidly funneled into a limited number of conductive channels.

It was also noted that a platy or scaly structure developed in the upper 5-cm of permeameters containing Beaumont clay packed at the higher moisture content. In these soils, the dye coatings were relatively uniform on the outside of all soil structural units (plates and clods). When individual units were removed and broken, no dye had penetrated into the soil unit. It is therefore quite clear from this that the water is not moving as a uniform wetting front but rather through a limited number of highly conductive pores or channels. In the absence of such channels the water is assuming a tortuous path between soil structural units and in no case was it found to be uniformly moving through the entire soil matrix. These observations are consistent with those reported by Brown et al., 1986 on the movement of xylene waste through recompacted soils. It is also in agreement with the "clod theory" developed by Olsen, 1962 and supported by Elsbury et al., 1988. The field observations of Elsbury et al., 1988 revealed that water seeping through a clay liner passed almost exclusively through interclod macropores.

It appears that the compactive effort applied during construction destroys the original clods present in the upper portion of a soil lift and results in a more platy structure. The amount of platy structure decreases and the number of highly conductive pores increases with depth within a single lift of compacted soil. Therefore, water flow through a lift of compacted clay is initially through a tortuous path between soil structural units and at deeper depths occurs through highly conductive interclod macropores.

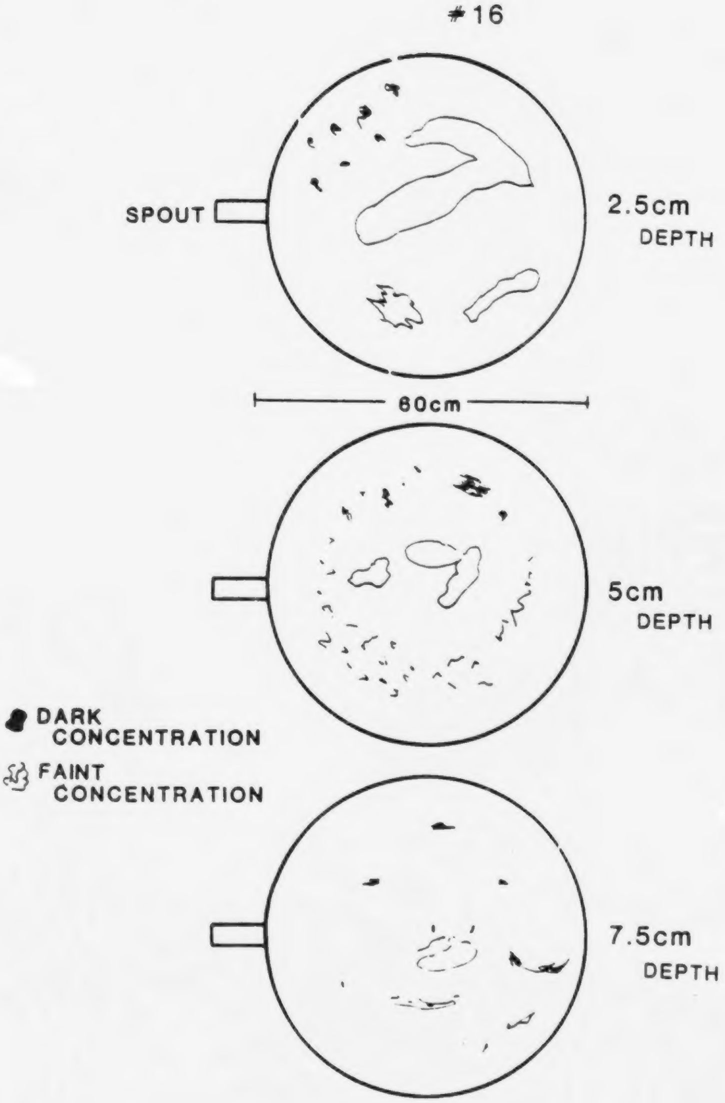
#16
SPOUT
2.5cm DEPTH
60cm
5cm DEPTH
DARK CONCENTRATION
FAINT CONCENTRATION
7.5cm DEPTH

Figure 31. Schematic diagram of dyed soil at three depths in a permeameter of compacted Kosse soil using a 2.5 cm clod size (Replication 1).

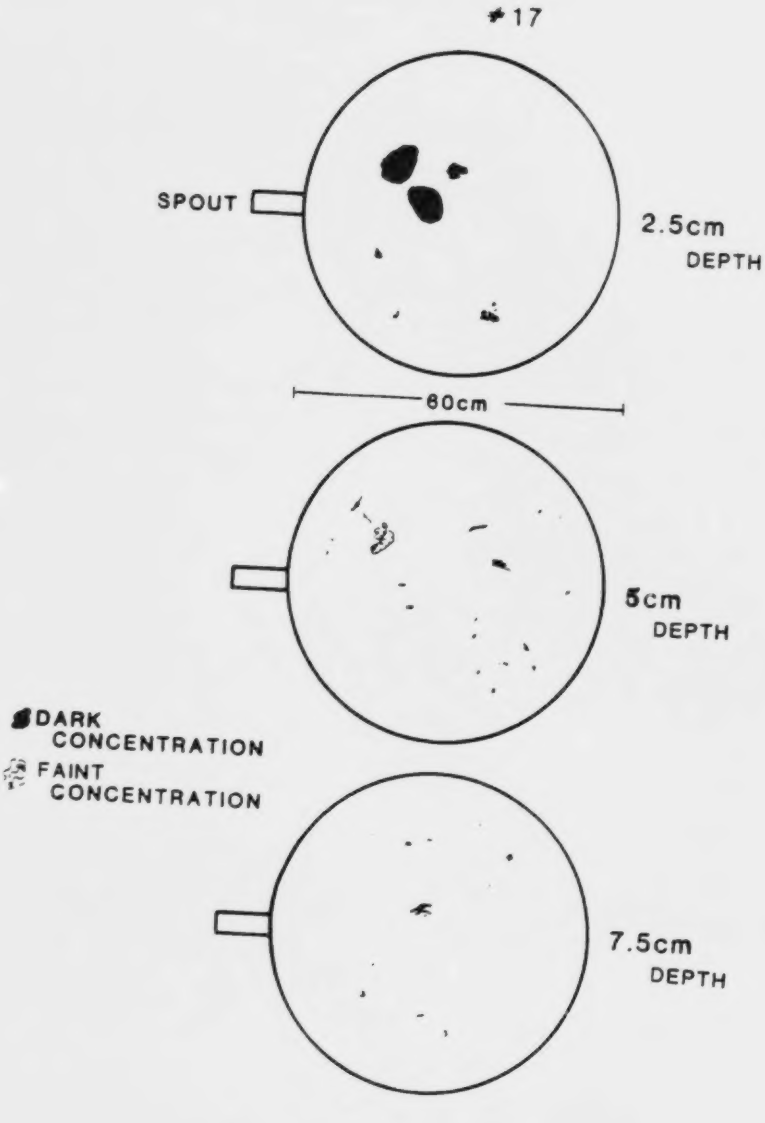
#17
SPOUT
2.5cm DEPTH
60cm
5cm DEPTH
DARK CONCENTRATION
FAINT CONCENTRATION
7.5cm DEPTH

Figure 32. Schematic diagram of dyed soil at three depths in a permeameter of compacted Kosse soil using 2.5 cm clod size (Replication 2).

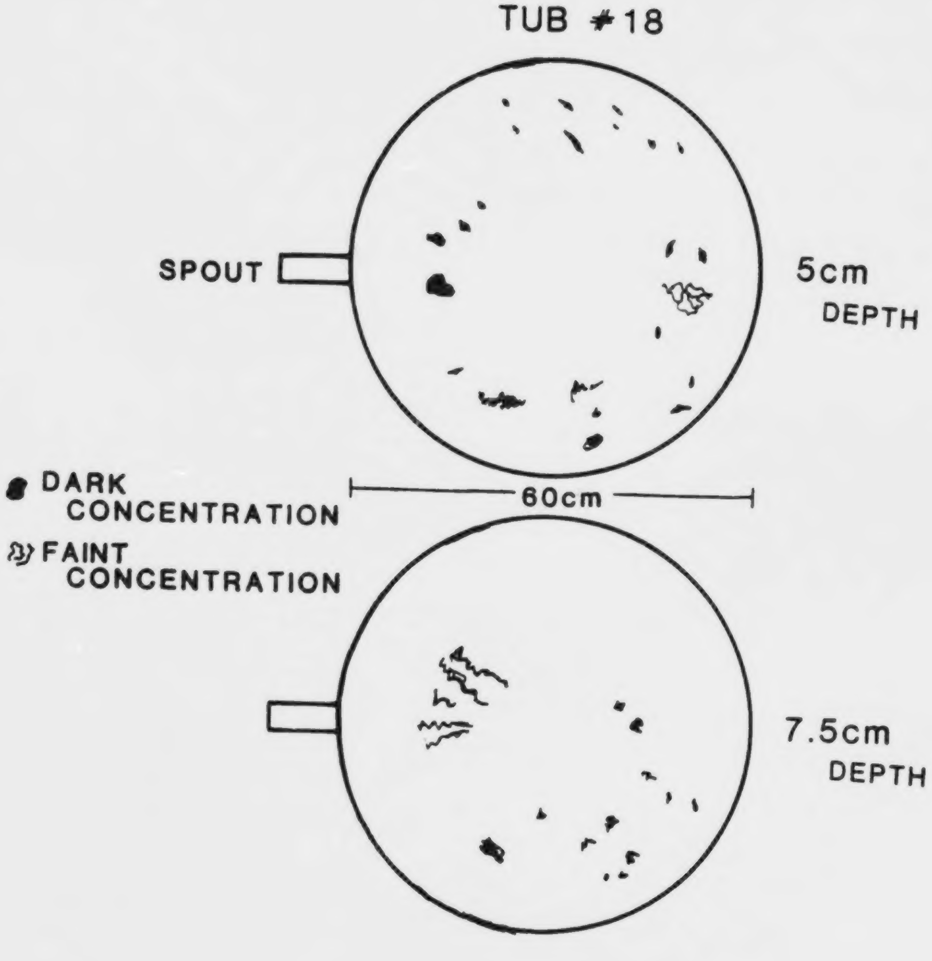
TUB #18
SPOUT
5cm
DEPTH
DARK
CONCENTRATION
FAINT
CONCENTRATION
60cm
7.5cm
DEPTH

Figure 33. Schematic diagram of dyed soil at two depths in a permeameter of compacted Kosse soil using 2.5 cm clode size (Replication 3).

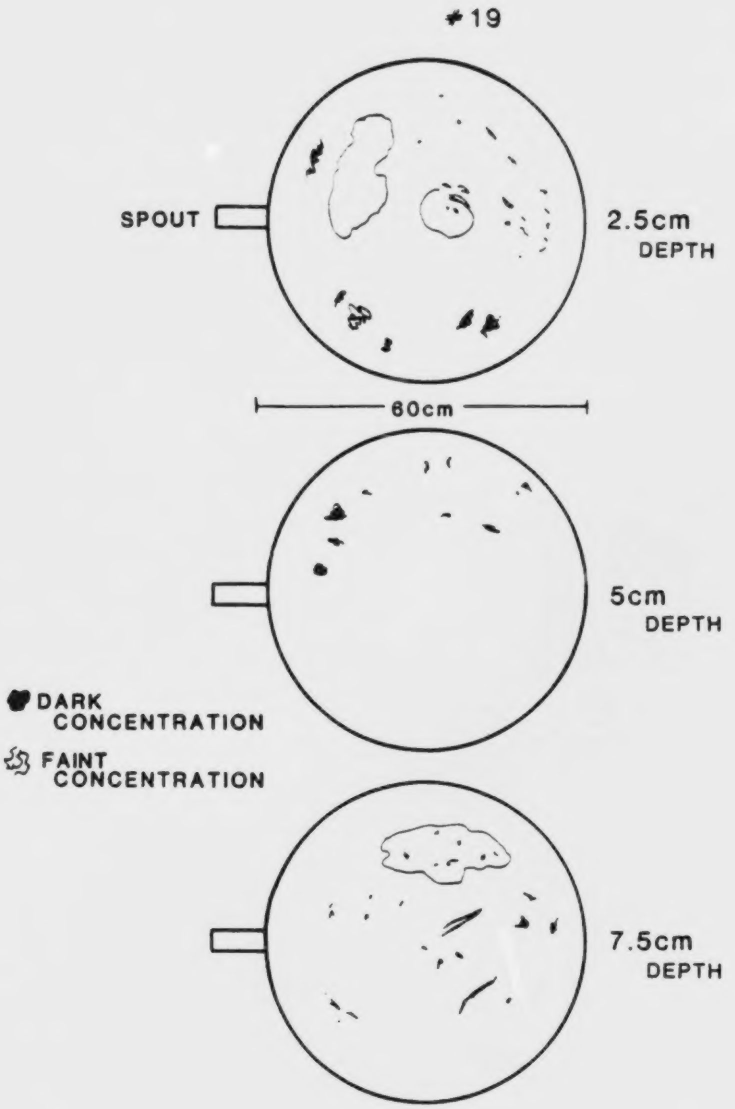
#19
SPOUT
2.5cm DEPTH
60cm
5cm DEPTH
DARK CONCENTRATION
FAINT CONCENTRATION
7.5cm DEPTH

Figure 34. Schematic diagram of dyed soil at three depths in a permeameter of compacted Kosse soil using 2.5 cm clod size (Replication 4).

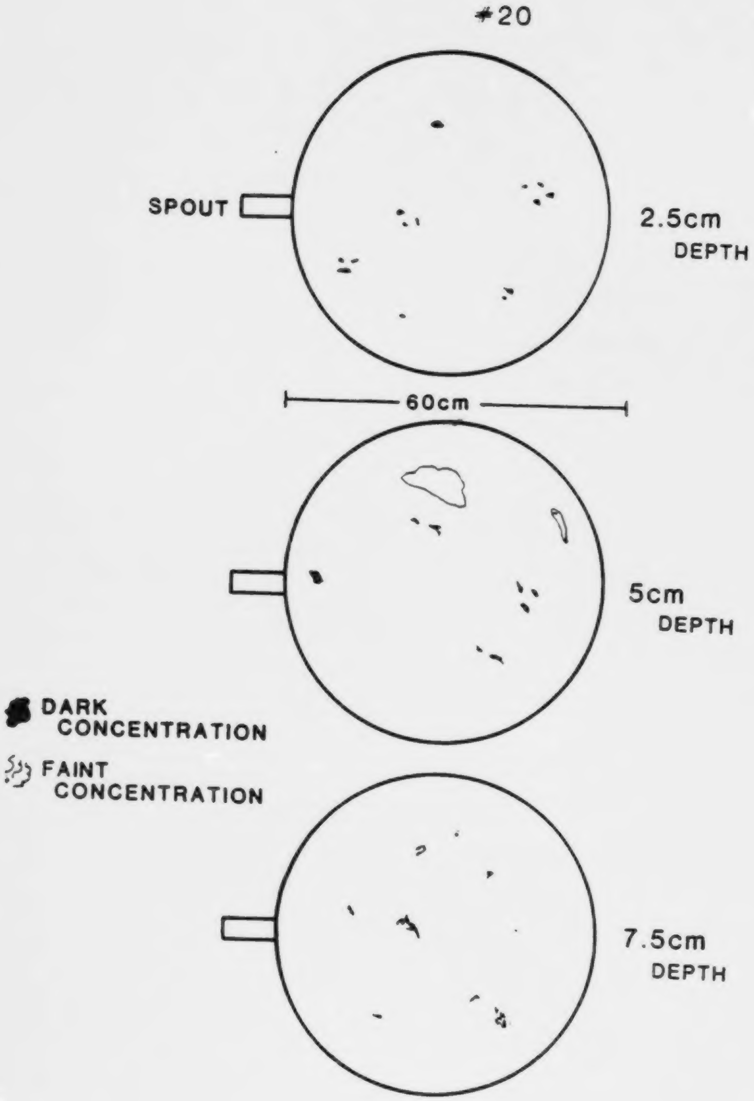
#20
SPOUT
2.5cm DEPTH
60cm
5cm DEPTH
DARK CONCENTRATION
FAINT CONCENTRATION
7.5cm DEPTH

Figure 35. Schematic diagram of dyed soil at three depths in a permeameter of compacted Kosse soil using a 5.0 cm clod size (Replication 1).

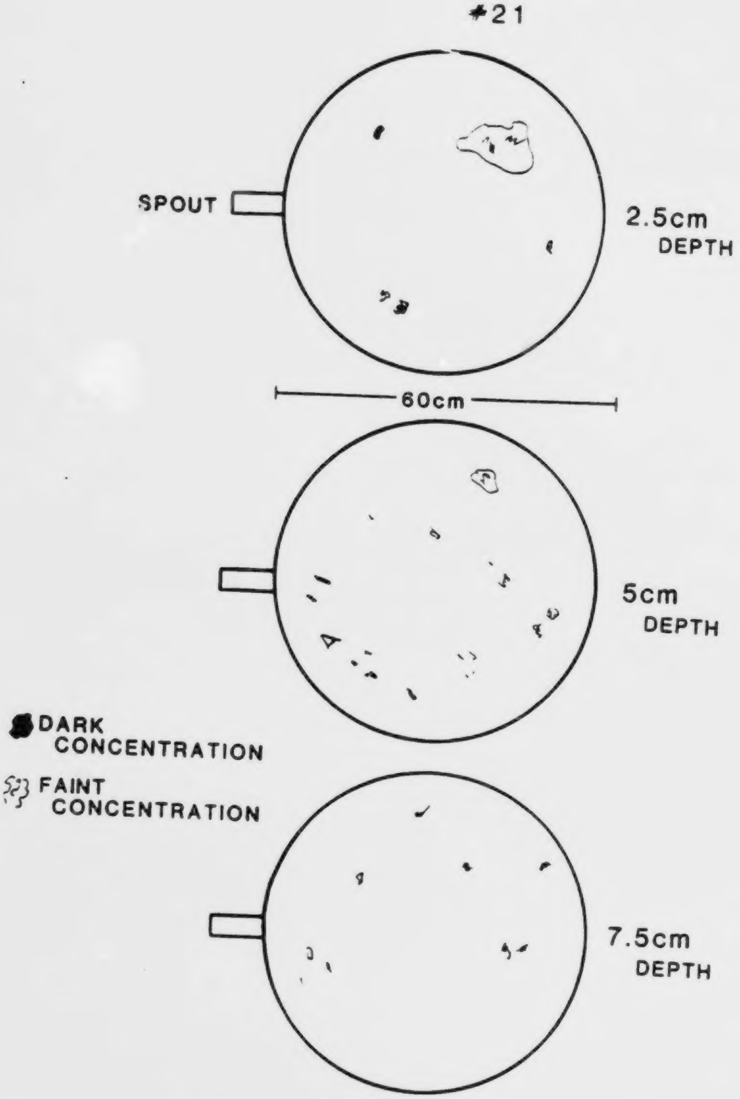
#21
SPOUT
2.5cm DEPTH
60cm
5cm DEPTH
DARK CONCENTRATION
FAINT CONCENTRATION
7.5cm DEPTH

Figure 36. Schematic diagram of dyed soil at three depths in a permeameter of compacted Kosse soil using a 5.0 cm clod size (Replication 2).

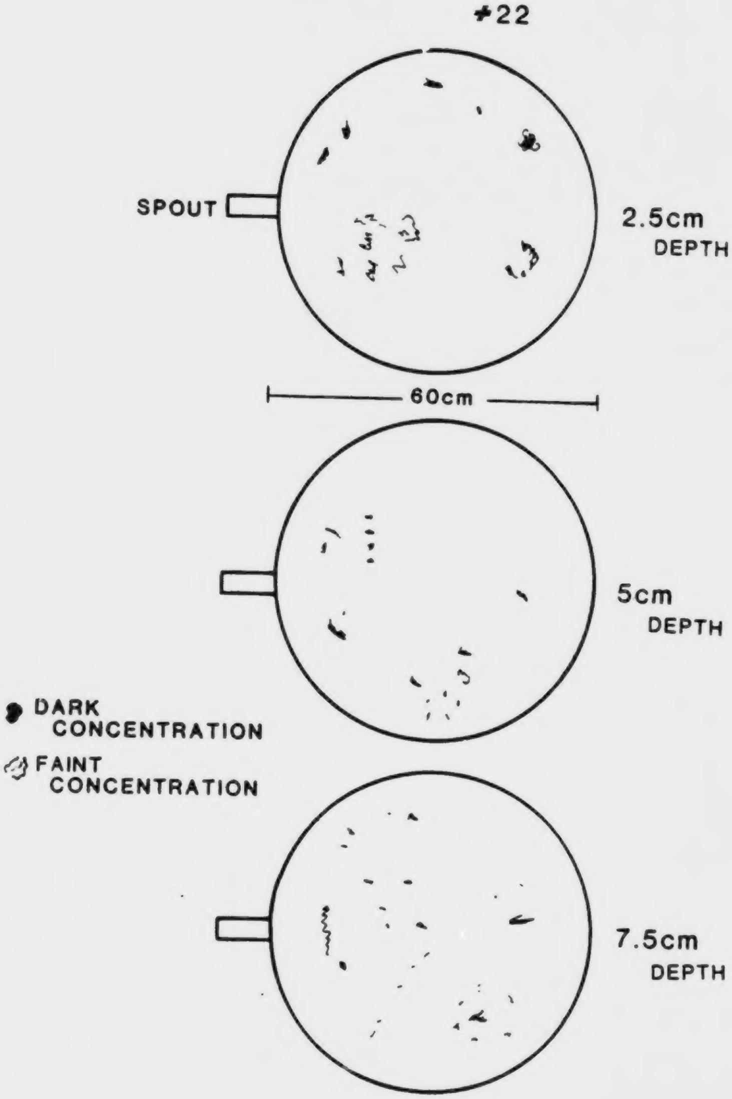

#22
SPOUT
2.5cm DEPTH
60cm
5cm DEPTH
DARK CONCENTRATION
FAINT CONCENTRATION
7.5cm DEPTH

Figure 37. Schematic diagram of dyed soil at three depths in a permeameter of compacted Kosse soil using a 5.0 cm clode size (Replication 3).

SECTION 6

FIELD STUDY

Sections 3 and 4 discussed some of the factors which influence the hydraulic conductivity of compacted soil liners, such as soil fabric, effective porosity, compaction water content, interlift flow, intralift channels, and density. To investigate some of these parameters in an experimental setting, a field study of a compacted soil liner was initiated. The investigation was designed to accomplish the following: (1) to examine the influence of the aforementioned factors on the integrity of the liner, (2) to measure the field hydraulic conductivity, and (3) to investigate the possible existence of zones of high horizontal hydraulic conductivity in interlift areas.

MATERIALS AND METHODS

The soil used to construct the liner was the Beaumont clay series, one of the two used in the laboratory study (Section 5). Physical properties of the soil which were measured included laboratory and field hydraulic conductivity, Atterberg limits, and moisture/density data. Physical features such as embedded debris, clod remnants, and fractures or cracks can greatly influence the hydraulic conductivity of a compacted soil. Measurements were made of these physical features. Accurate measurements were made of the width of cracks at the liner surface using the vernier calipers. Crack depths were gauged by placing a flexible wire into a crack opening, marking the extent of its penetration, and measuring this length.

Three double-ring, constant-head field infiltrometers, having inner ring diameters of 30-cm and outer ring diameters of 76-cm, were used to measure field hydraulic conductivity (Figure 38). Both the inner and outer rings were supplied with fluid via external reservoirs. Float valves connected to the fluid reservoirs were used to maintain a constant head in both the inner and outer rings. Two of the infiltrometers were operated using digital data recorders, and the third consisted of a float in the inner ring reservoir of the infiltrometer connected to an analog chart recorder. In the case of the digital recorders, a float connected to a pulse generator by a pulley system was placed on the water surface in the inner ring reservoir to measure the fluid level in the inner ring, thereby giving a record of water level versus time.

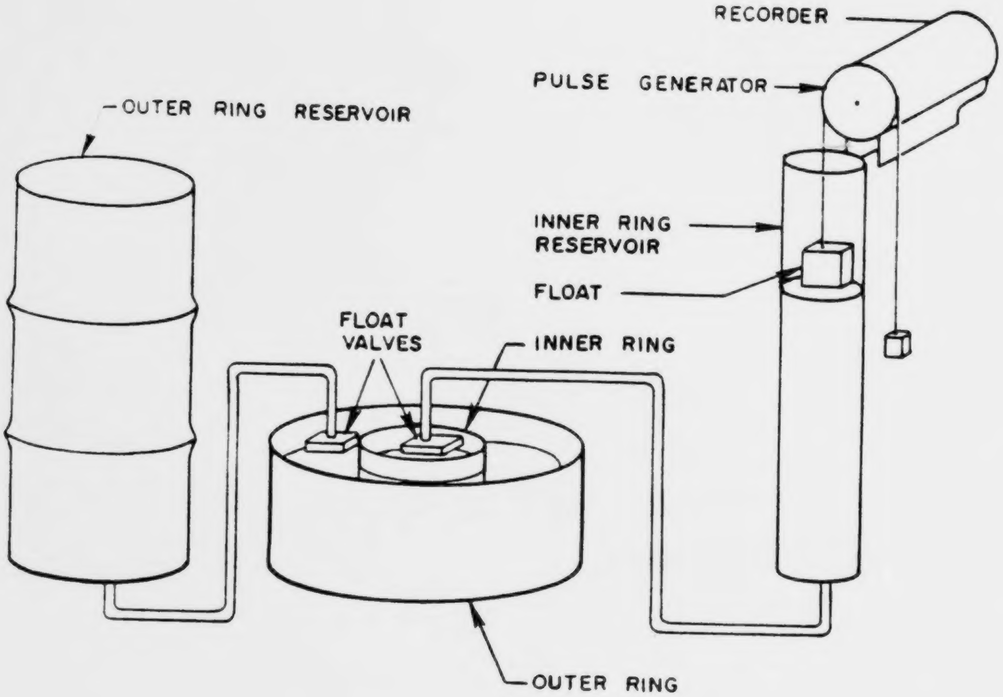
RECORDER
PULSE GENERATOR
OUTER RING RESERVOIR
INNER RING RESERVOIR
FLOAT
FLOAT VALVES
INNER RING
OUTER RING

Figure 38. Field infiltrometer configuration.

Investigation of interlift flow potential involved destructive testing of a section of the compacted soil. For this study, the test was run on a compacted soil liner consisting of three lifts each approximately 20-cm thick, giving a total liner thickness of about 60-cm. To accelerate the interlift infiltration process, four 7.5-cm diameter boreholes were augered vertically 50-cm into the liner, which allowed liquid to penetrate both lift interfaces. Next, a 7.5-cm I.D. length of Schedule 40 PVC pipe was hammered approximately 10-cm into each borehole in the uppermost lift. Finally, each borehole was filled with tracer solution and 15-liter bottles containing the same solution were inverted and placed into each of the 7.5-cm diameter PVC pipes (Figure 39). This solution was allowed to infiltrate for 10 days at which time excavations were made to expose a vertical surface extending outward from the borehole. This permitted direct observation of the infiltrated area (Figure 40).

It was expected that lateral infiltration of the tracer solution would be greater in the interlift zone than it would be within a lift (Figure 41). To locate the approximate edge of the wetting front in the interlift zone, multiple independent analyses were performed. For a visual determination of the wetting front, Rhodamine WT, a red colorimetric tracer which is moderately adsorbed to soil particles, was used. Since adsorption of the dye tracer onto the soil might limit the rate of dye migration, bromide was also added as a chemical tracer. Rhodamine WT was selected as the most suitable dye because of its resistance to adsorption by the soil, its photochemical stability, and its contrasting color. Bromide was selected as the chemical tracer because it is mobile in soil environments, it is not significantly sorbed by mineral or organic matter, and is generally the most suitable soil water tracer (see earlier discussion on tracers). Finally, gravimetric water content was measured in anticipation that the interlift wetting front would deviate significantly from the soil matrix wetting front. This would provide another line of evidence for the location of the wetting front.

The Rhodamine WT dye was prepared at a concentration of 1,000 mg L^{-1}. A potassium bromide solution (KBr) was also prepared at 1,000 mg L^{-1} (which yielded a bromide ion concentration of 671 mg L^{-1}). Both the dye and KBr were dissolved in the same 15-liter bottle. The tracers were infiltrated into the liner for a period of ten days. After ten days, an excavation was made so that the infiltrated zones could be examined and sampled (Figure 40). After excavation, it was noted that dye had accumulated at the lift #2/lift #3 interface for both boreholes #1 and #5, and that there was little, if any, dye detected at the lift #1/lift #2 interface for either borehole.

Soil samples were collected in the plane of the dye-stained lift interface at 5-cm intervals on either side of the borehole #1 so that moisture content and bromide concentration could be determined in the laboratory. Additionally, a sample of soil was taken near the excavated

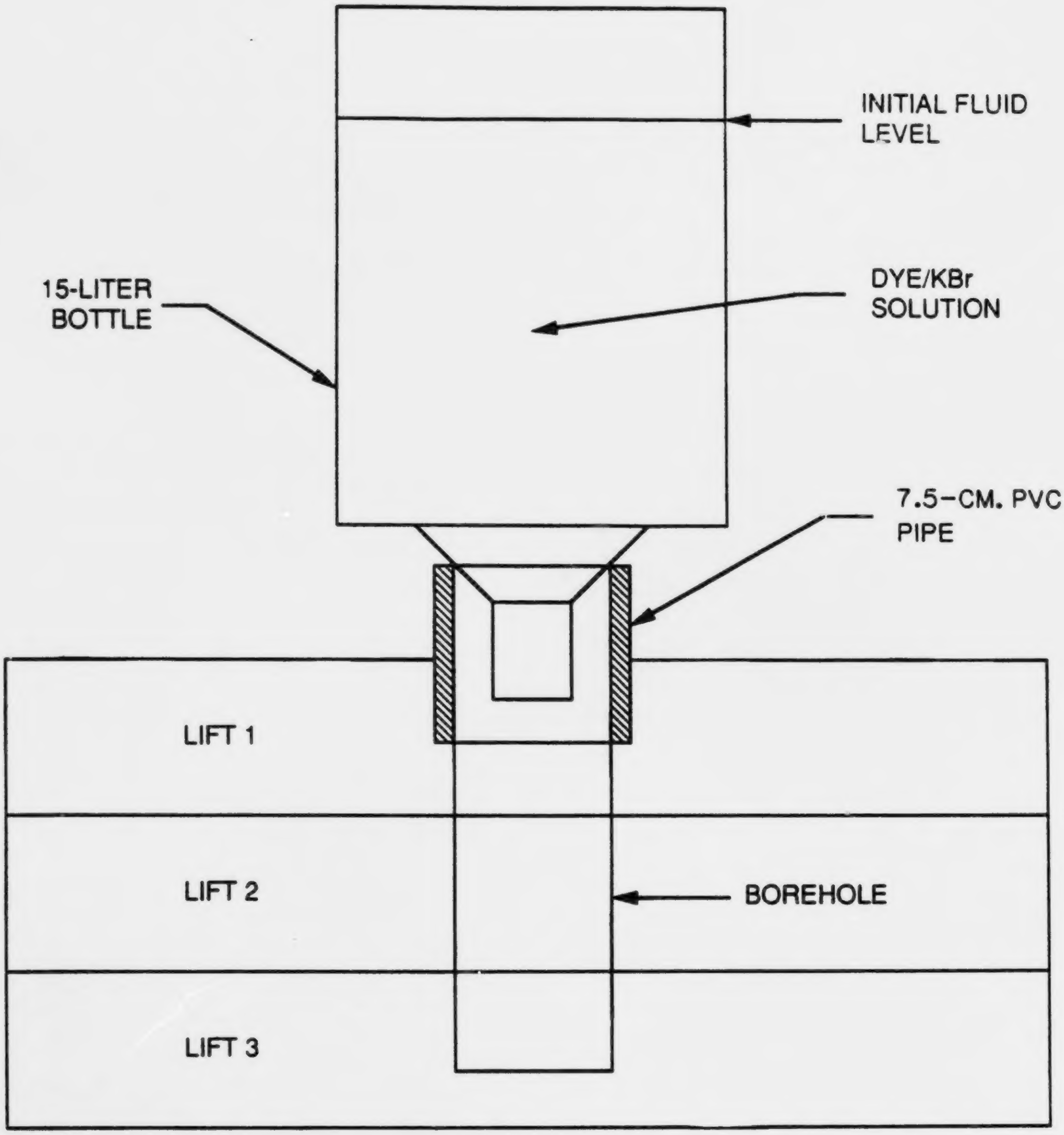
INITIAL FLUID LEVEL
15-LITER BOTTLE
DYE/KBr SOLUTION
7.5-CM. PVC PIPE
LIFT 1
LIFT 2
BOREHOLE
LIFT 3

Figure 39. Schematic of tracer infiltration apparatus.

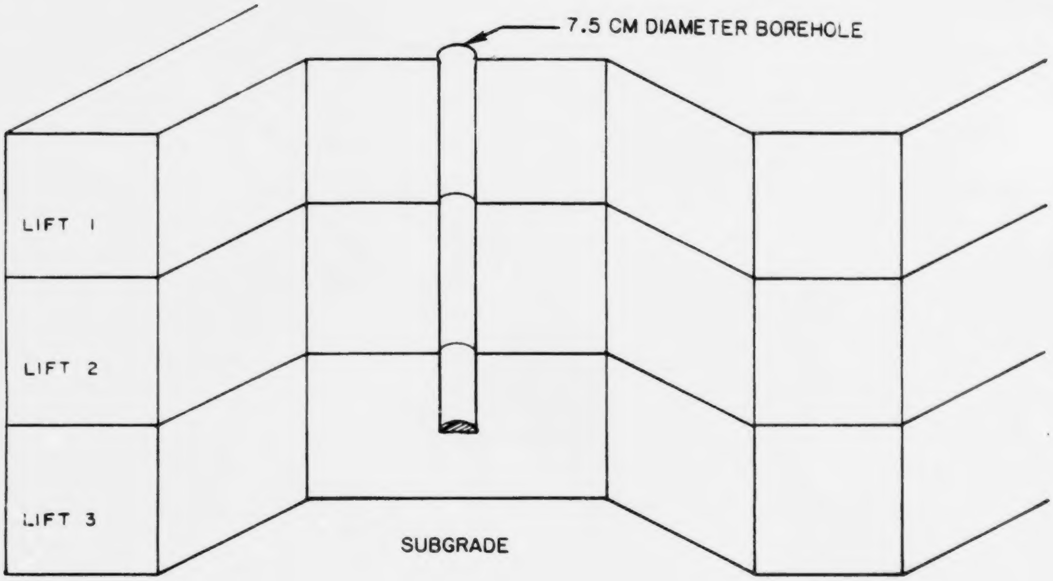
7.5 CM DIAMETER BOREHOLE
LIFT 1
LIFT 2
LIFT 3
SUBGRADE

Figure 40. Schematic of excavated borehole and infiltrated area.

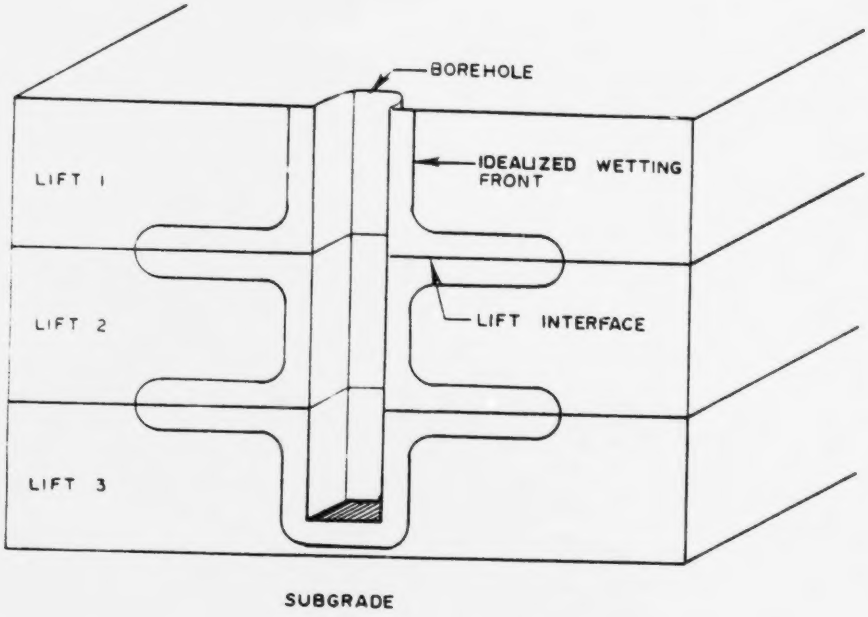
BOREHOLE
IDEALIZED WETTING FRONT
LIFT 1
LIFT 2
LIFT INTERFACE
LIFT 3
SUBGRADE

Figure 41. Schematic of idealized wetting front.

area in an undisturbed location to serve as an indicator of soil background conditions; this sample was subjected to the same moisture content and bromide concentration determinations.

With regard to the bromide analysis, 1:1 extracts of the dried soil samples were made so that interference from other ions adsorbed onto the clays would be minimized; bromide concentrations were determined using a specific ion electrode calibrated to the appropriate standards. For more detailed description of analytical procedures, see Adriano and Doner (1982).

RESULTS

Macrofeatures

Desiccation cracks were measured for a 0.37 m^2 area of the liner after approximately two days of drying had occurred. Figures 42 and 43 give the histograms for field-measured crack depths and widths. Mean values were 3 millimeters (0.116 inches) and 10 millimeters (0.386 inches) for width and depth, respectively. These values should be interpreted with caution, however, since crack formation and propagation are time-varying phenomena; (i.e., the cracks observed in the liner may or may not continue to grow in width and depth as time progresses). Nevertheless, the results of the experiment indicate that desiccation cracking begins very quickly in liners constructed of soils containing high percentages of expandable-lattice clay minerals.

Soil Index Properties

Atterberg limits, as determined by ASTM D-4318 methods, and laboratory hydraulic conductivity, measured using the U.S. Army Corps of Engineers Falling Head Test, are presented in Table 45. In addition to these measurements, a sieve analysis indicated that 94% of the sample was finer than the No. 200 sieve (0.075 mm). A moisture/density curve was also determined for a sample of the soil, according to ASTM D-698, and is given as Figure 44.

Tracer Study

One goal of the experiment was to define the wetting front in the interlift zone via three independent analyses: (1) by the use of a soil-staining dye, (2) by the construction of a horizontal moisture content profile, and (3) by the development of a bromide tracer breakthrough curve. It was anticipated at the outset that each of these analyses would produce a curve very similar to a "typical" breakthrough curve. Of these three methods, the dye gave the firmest evidence supporting the theory of preferential interlift liquid flow.

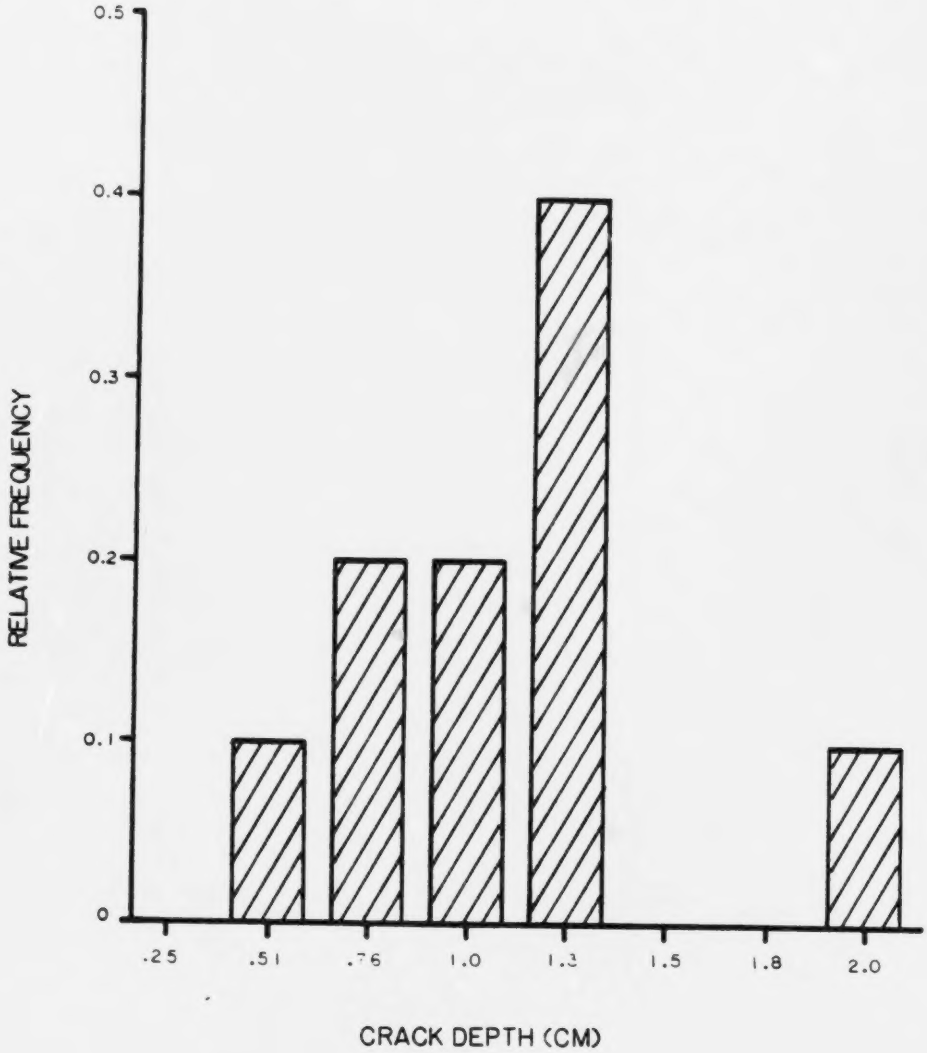

Figure 42. Histogram of crack depth determined from field study.

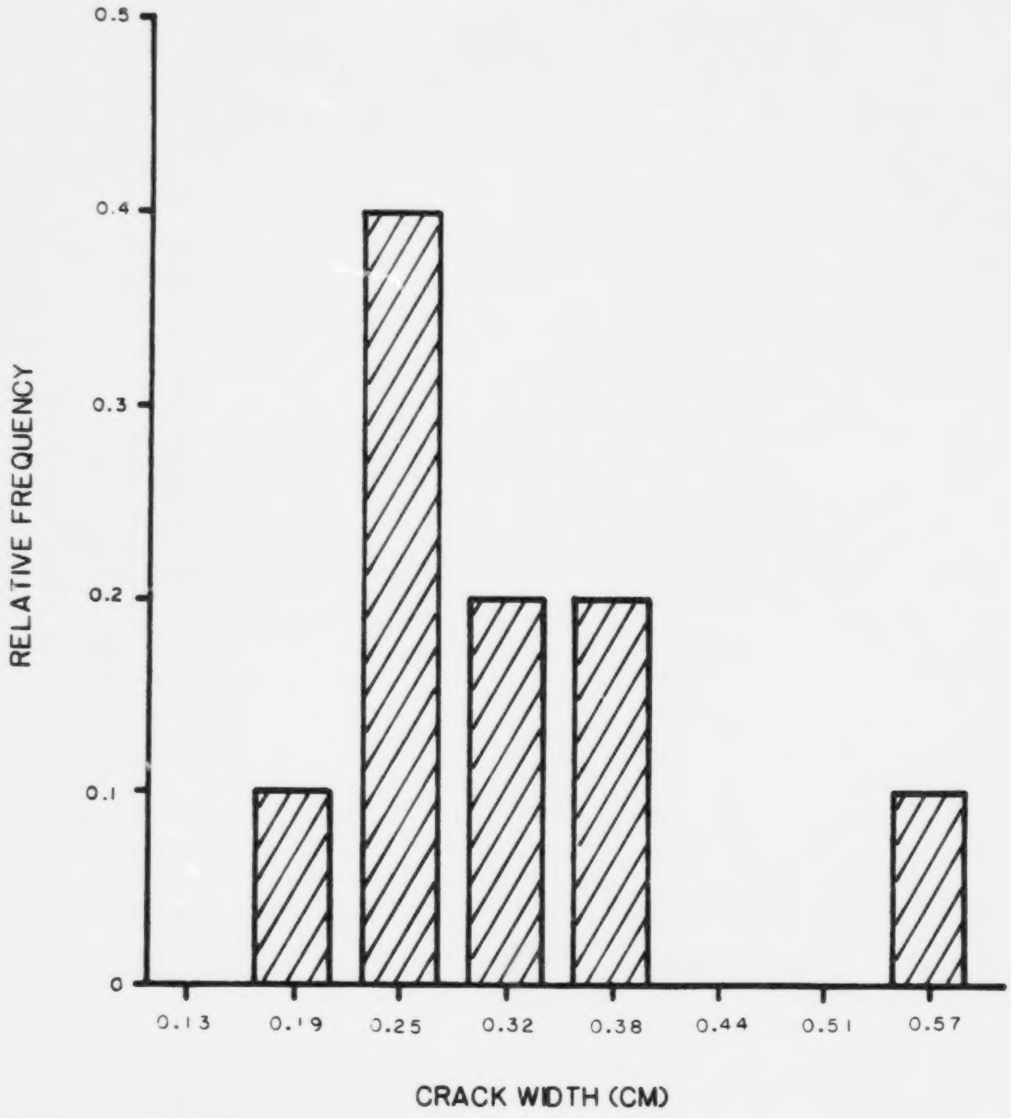

Figure 43. Histogram of crack width determined from field study.

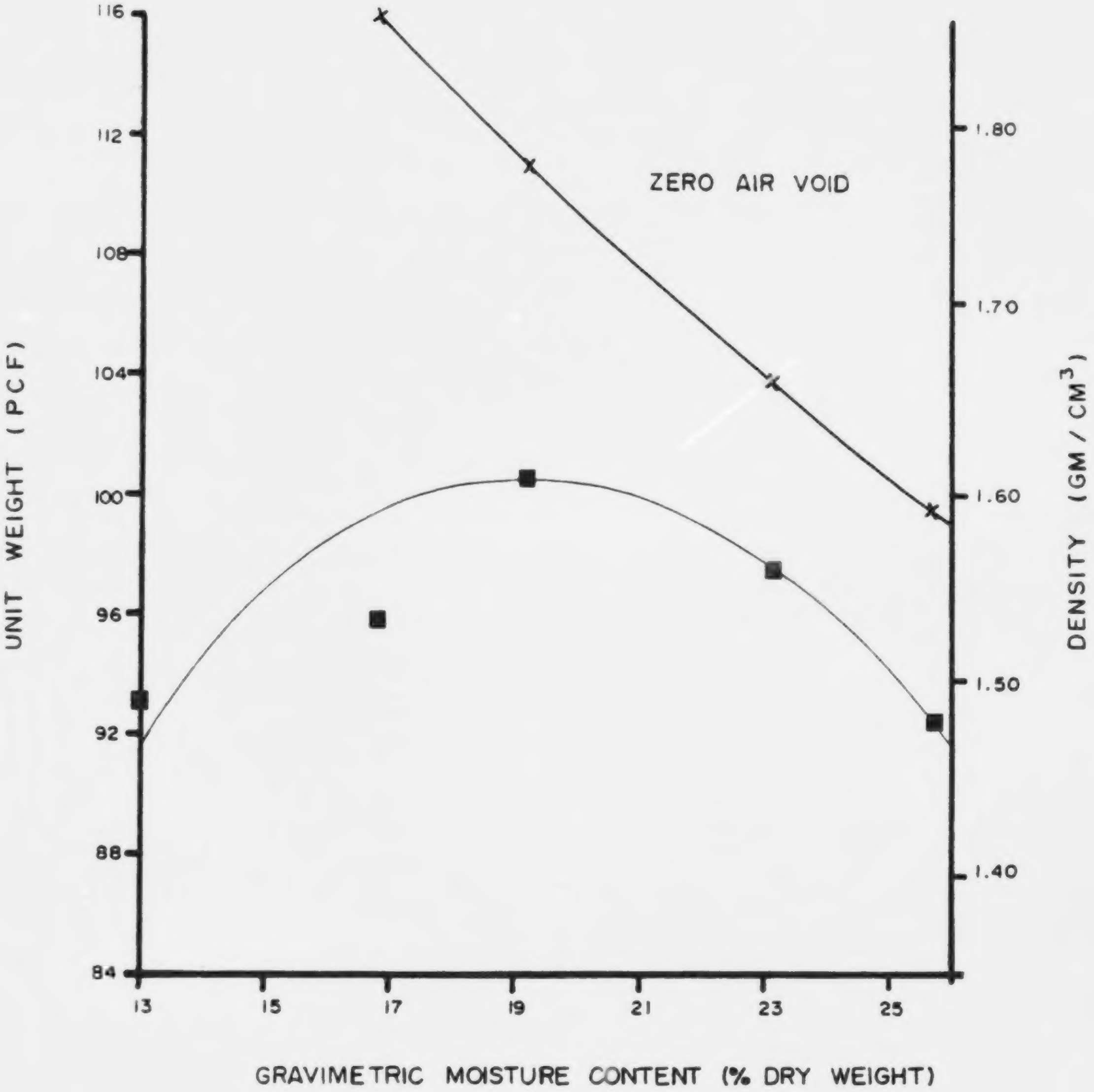

Figure 44. Moisture/density curve for borrow material used to construct the compacted soil cover.

TABLE 45. LABORATORY SOIL DATA

Parameter	Value
Liquid limit (LL)	54 %
Plastic limit (PL)	20 %
Plasticity index (PI)	34 %
Hydraulic conductivity #1	1.4×10^{-7} cm sec^{-1}
Hydraulic conductivity #2	7.4×10^{-8} cm sec^{-1}
Mean hydraulic conductivity	1.0 x 10-7 cm sec-1
Optimum moisture content	19.2 %
Maximum dry unit weight	100.5 PCF

Gravimetric moisture content was measured on samples taken from the plane of a lift interface at 5-cm intervals. These data are plotted in Figure 45. Note that moisture content for the background soil sample was 23.5%. Figure 46 is plot of bromide concentration, in parts per million, versus distance from the borehole (the source of bromide) after 10 days of infiltration. Note that bromide concentration for the background soil sample was 0.33 ppm. The data indicated that during the 10 days, bromide was transported at least 51-cm to the right of the borehole and as far as 41-cm to the left. The transport may have been a result of preferential flow through less well compacted lower layers of the lifts.

Initially, four auger boreholes were drilled for installation of the 15-liter bottles containing the tracer solutions (Figure 47). Each borehole was drilled to a depth of 50-cm and was 7.5-cm in diameter. Two of the auger boreholes remained full of liquid for several days after they were filled (#1 and #4). However, the remaining two completely drained the tracer solution within a matter of minutes (#2 and #3). Consequently, an additional borehole (#5), 30-cm deep, was drilled and filled with dye only. This auger borehole again drained completely within 10 minutes, indicating the existence of a high hydraulic conductivity zone in those three boreholes.

Although five boreholes were installed in the liner, due to time and budgetary constraints, only boreholes #1 and 5 were excavated.

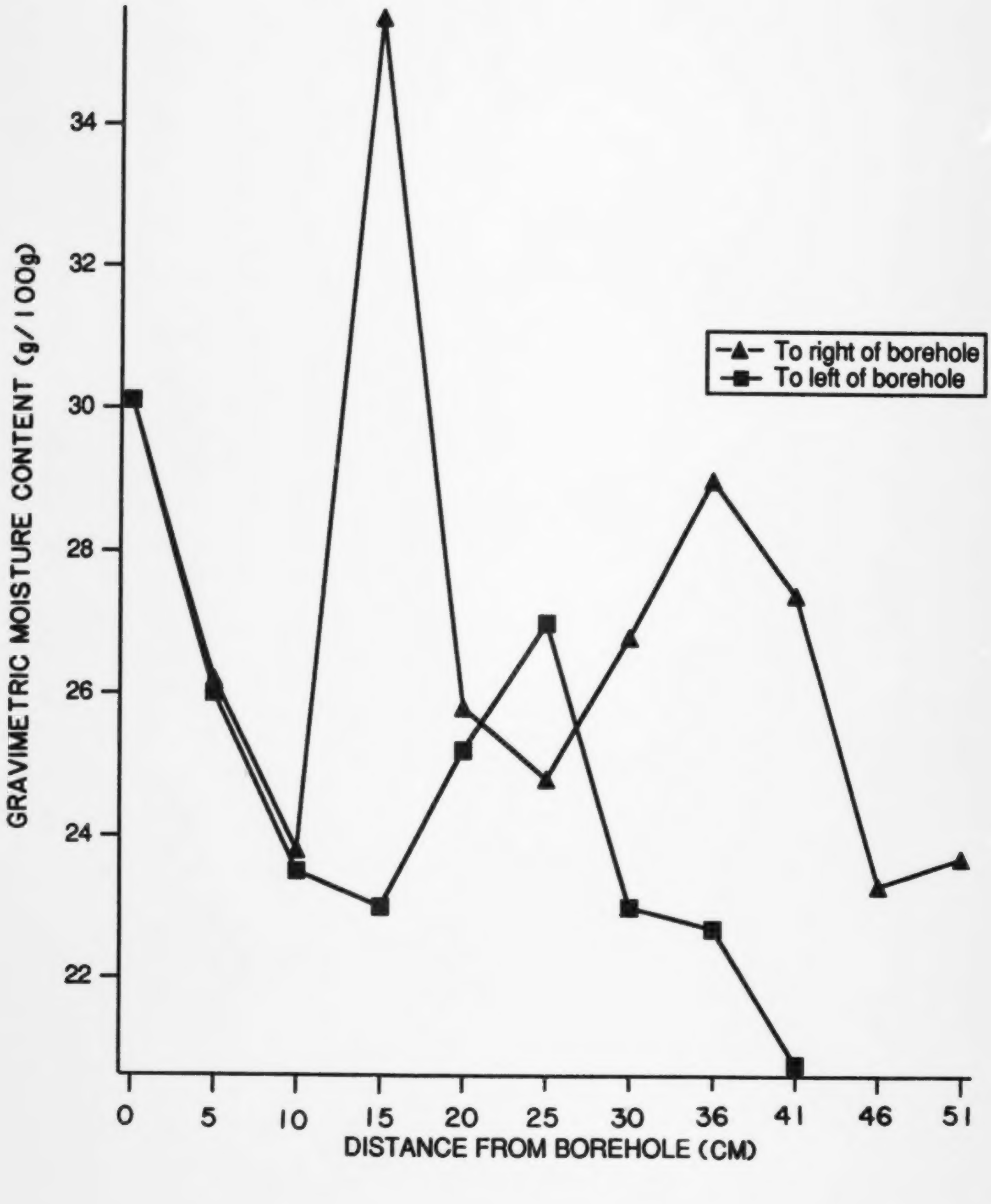

Figure 45. Moisture content profile in interlift zone at t = 10 days for borehore #1.

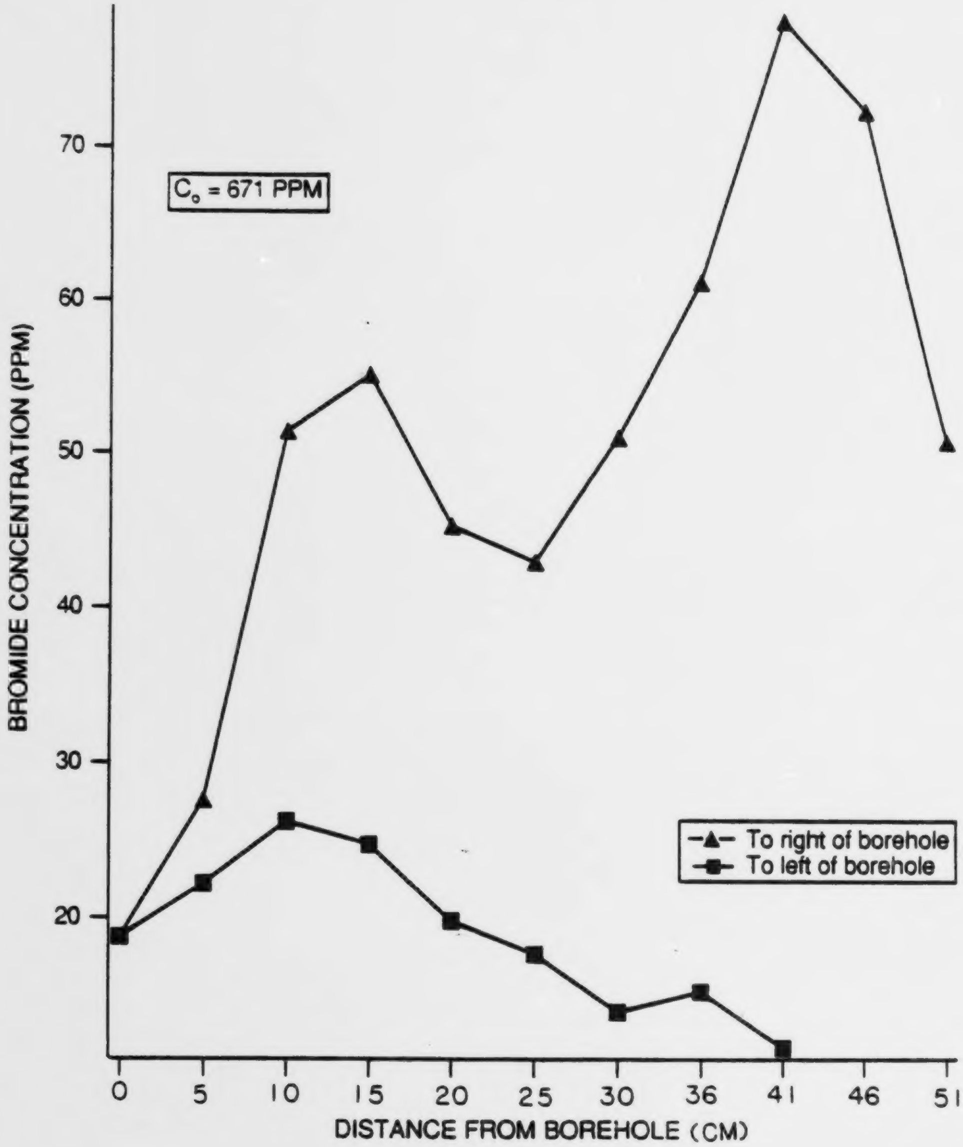

Figure 46. Bromide concentration gradient in interlift zone at t = 10 days for borehole #1.

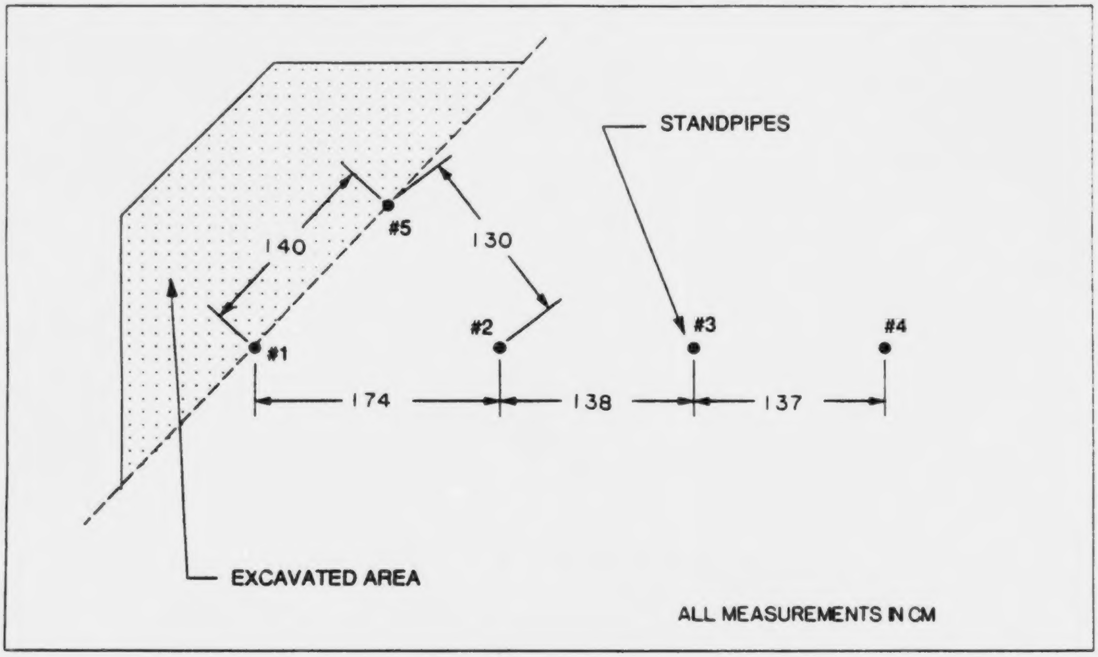
STANDPIPES
140
#5
130
#1
#2
#3
#4
174
138
137
EXCAVATED AREA
ALL MEASUREMENTS IN CM

Figure 47. Schematic showing the spatial relationship of infiltration standpipes.

Borehole #1 was drilled to 50-cm and remained filled with tracer for several days. Borehole #5 was drilled to 30-cm and dye in the borehole infiltrated very rapidly. Field observations revealed pockets of dye in the interlift zone near boreholes #1 and #5 (Figures 48 and 49, respectively). Additional, close-up observations indicated that these pockets were completely saturated with dye. Another interesting observation was the occurrence of debris-enveloping voids. A dye-stained root was unearthed in the infiltrated area, which suggested that fluids flow preferentially along such features.

DISCUSSION

The interpretation of the field data pertaining to desiccation crack width and depth should be exercised with caution. The development of cracks by any mechanism in a clayey soil is a time-dependent process. Since the time that elapsed between wetting of the soil and measurement of the cracks was very short (two days), it is unlikely that these dimensions had reached equilibrium. It is expected that the dimensions observed after two days drying would most likely have been exceeded had the cracks been measured after the soil had been allowed to further desiccate. It is also possible that application of a sealant to the soil surface may decrease evaporation and subsequent crack formation, however, this should be field-tested prior to use. It can be concluded that the characterization of soil cracks or fractures can be easily accomplished through physical measurements. Several factors determine the extent to which these fractures or cracks affect hydraulic conductivity, including the climate at the time of construction, the amount of time the liner is exposed prior to application of waste, and soil properties. Laboratory results, however, indicate greatly increased hydraulic conductivity as a result of desiccation cracks.

During the field study, it was noted that foreign debris was incorporated in the soil used for liner construction. However, with sufficient construction quality assurance (CQA), the occurrence of such features could be reduced. Elimination of voids associated with debris would shorten the list of factors which can increase the hydraulic conductivity.

The mean laboratory hydraulic conductivity of approximately 1×10^{-7} cm sec^{-1} (Table 45) meets the performance requirement for a compacted soil liner. These tests were conducted on recompacted laboratory samples of the soil using the Corps of Engineers' Falling Head Test. From an analysis of the Atterberg limits found in Table 45, it can be concluded that the soil has high water-retention capacity since it retains its plastic character at water contents as high as 20%. A mechanical analysis revealed that 94% of the soil is composed of particles smaller than 0.075 mm. Thus, the soil had properties generally considered to be ideal for use in constructing a compacted soil liner or cover. Laboratory data comparing the soil density after compaction to the hydraulic conductivity measured using large scale permeameters,

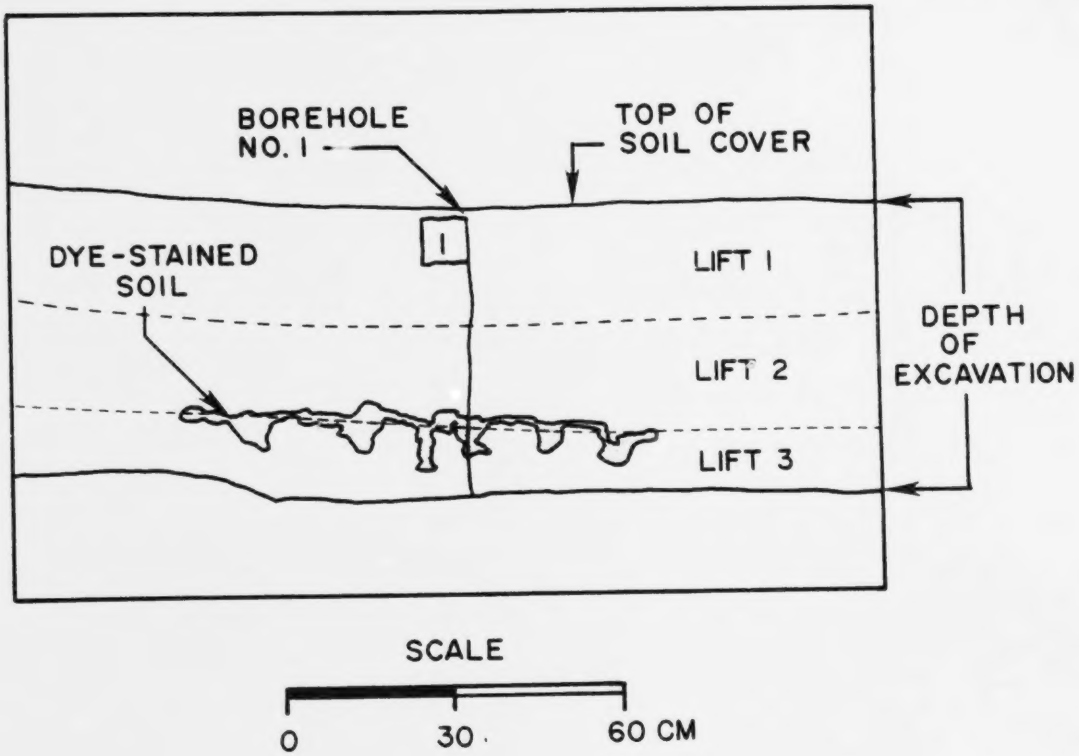
BOREHOLE NO. 1
TOP OF SOIL COVER
1
DYE-STAINED SOIL
LIFT 1
LIFT 2
LIFT 3
DEPTH OF EXCAVATION
SCALE
0
30
60 CM

Figure 48. Schematic diagram of the dye-stained soil in the area near borehole #1.

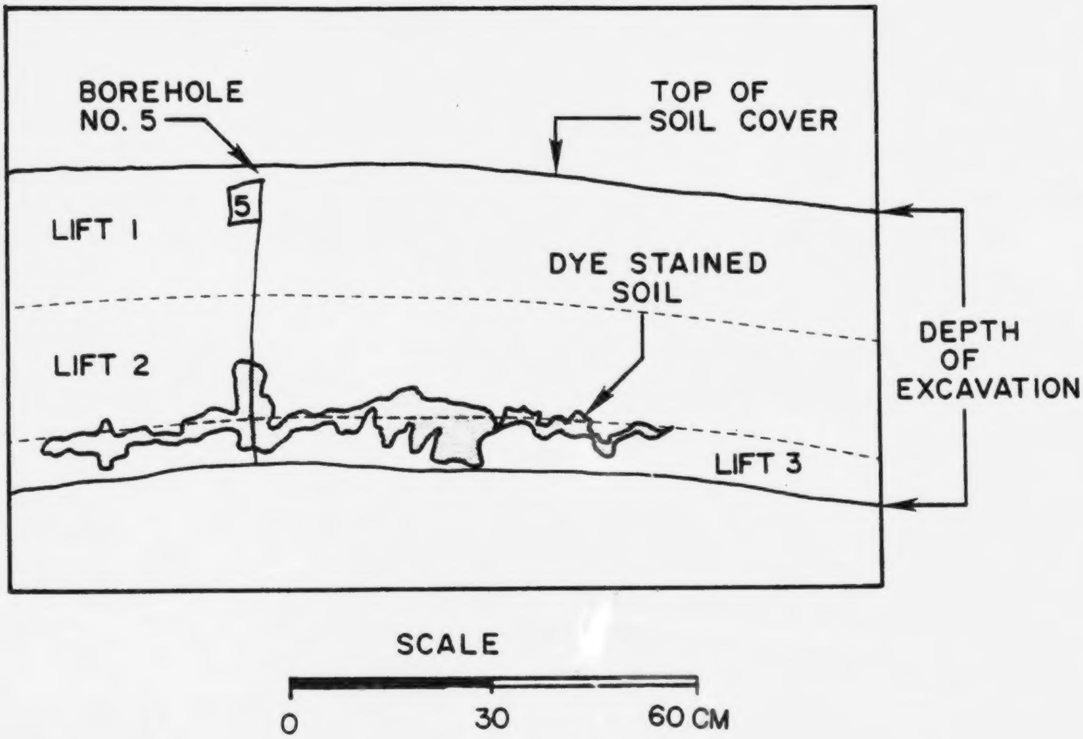
BOREHOLE
NO. 5
TOP OF
SOIL COVER
5
LIFT 1
DYE STAINED
SOIL
DEPTH
OF
EXCAVATION
LIFT 2
LIFT 3
SCALE
0
30
60 CM

Figure 49. Schematic diagram of the dye-stained soil in the area near borehole #5.

indicated that density is a poor predictor of the hydraulic conductivity. This indicates the need for field measurement of the conductivity of a clay liner prior to use.

A "channel-centered, interlift flow" model was proposed in Section 4 of this report to simulate the flow of liquids through a compacted soil. The concept of the model is embodied in the following text. Macrofeatures in a compacted soil are approximated by cylindrical channels oriented parallel to the direction of flow. Connected to the base of each channel are concentric disks defining the extent of a plume of liquid presumed to have leaked through the channel from above. The dimension defining the extent of these disks has been given the name "interlift flow radius" (IR), which is defined as the distance from the center of a channel to the edge of the disk.

As previously mentioned, the authors argue in favor of preferential interlift fluid flow because of the existence of high-permeability zones lying between liner lifts. Several causes have been cited for the development of such zones. Laboratory tests (Section 5) documented that the conductivity increases with depth within a lift. Field measurements suggest high rates of horizontal conductivity at the lift interfaces. Dye studies in both the laboratory and field studies showed water movement occurred between peds and through macropores rather than movement as a uniform wetting front. Attempting to compact a loose lift that is too thick for the compaction feet to penetrate may result in poor compaction at the base of the lift. Also, drying of a compacted lift may result in poor bonding of the lifts and an interlift zone with a high horizontal hydraulic conductivity. Dye patterns observed in the field portion of this study suggest that both phenomena can occur together. Pockets of dye 1 to 4-cm wide in the vertical dimension were found in the bottom portion of lift in some places. In other places only a thin horizontal band of dye, 1 to 5-mm thick was observed.

Several interesting observations concerning compaction technique were noted during construction. The liner was constructed by placing approximately 23-cm lifts with a bulldozer and compacting with a 5,450 kg (12,000 lb) sheepsfoot roller that was towed behind a bulldozer. Placing lifts with a heavy bulldozer resulted in significant compaction of the upper part of each lift. In most instances, the sheepsfoot roller feet did not extend into the soil their entire length because of prior compaction by the dozer. Also, the thickness of each lift after compaction was only slightly less than the initial thickness after placement. These facts indicate that the lifts were too thick to allow proper densification at the bottom of the lifts. Ideally, the compactor should make several passes over the soil by traversing first in one direction and then turning around to traverse back across the soil. In this instance, the compactor operator moved forward across the soil and then simply backed up across the same path (approximately 5 to 10 passes were made on each lift). This pattern of compaction resulted in the compaction feet entering the exact same depressions that were left on the forward pass. The result of this method was a "ridge and furrow" type structure on the surface of the lift. The efficiency of mixing of the loose lift with the underlying compacted lift has been questioned as a result of this compaction technique; this could be another mechanism responsible for the formation of the low bulk density, high hydraulic conductivity interlift zones.

Field observations revealed that interlift flow occurred in the compacted soil. The leading edge of the dye (IR), after 10 days of flow, was located at an average distance from the borehole of 36-cm. This indicated that the rate of horizontal flow at interlifts far exceeds that of vertical flow within a lift.

The second line of evidence aiding in the location of the wetting front came from the development of bromide concentration curves. From the data in Figure 46 it appears that the edge of the wetting front (IR) was located past the point at which the last soil sample was taken (41-cm from the borehole). Assuming that the bromide moved with the velocity of the infiltrating water, this indicates that the actual wetting front (IR) is even greater than that indicated by the dye. The rationale used during sampling was that samples were to be taken 10-cm past the point at which dye could no longer be visually detected. It is apparent that samples of the soil were not taken far enough from the source to define the maximum IR.

Examination of Figure 45 suggests that moisture content decreased with distance from the borehole. Logically, as the distance from the borehole exceeded IR, the moisture content should return to that characteristic of background levels.

In summary, the results of the laboratory and field studies indicated that the concept of the channel-centered interlift flow model was valid for compacted soil liners. Breaches will occur in a soil liner if the IR of a channel overlaps channels in underlying lifts. Consequently, the IR is a critical factor in the analysis of liner integrity.

SECTION 7

STOCHASTIC ANALYSIS

INTRODUCTION

Soil liners can be designed based on two criteria. One criterion is to maximize time required for liquid to travel from the surface to the base of the liner. This time of travel has been named the first-passage time (Benson, 1989). A second approach is to minimize the flux from the base of the liner without regard to first passage time.

The relationship between the number of lifts used to construct a soil liner and either the first-passage time or flux is not well established. The problem is difficult because properties of the soil are spatially variable. As more lifts are added to the liner, the chances of higher hydraulic conductivity zones in the various lifts forming a continuous pathway through the liner diminishes. However, the number of lifts needed to achieve a low overall hydraulic conductivity or long first passage time is ill defined.

Two models are presented in this chapter to simulate the flow of liquid through a soil liner. The first model, called the Convolution Model, is a model of one dimensional seepage. In this model, the liquid was assumed to be a continuum which extends throughout the confines of the soil liner. The second model, called the Macropore Model, simulates three-dimensional seepage in which the liquid is assumed to flow only through discrete channels within the lifts (macropores) and through thin horizontal zones between the lifts. Both models incorporate the spatial variability and uncertainty associated with the soil properties by treating them as random variables. The first-passage time and flux were quantified by probability distributions.

A quasi-analytic solution was obtained for the first-passage time from the convolution model and Monte Carlo simulation was used to estimate the distributions of the first-passage time and flux for the macropore model. In both models, the hydraulic conductivity was assumed to be the random variable which elicited the variations in first-passage time and flux.

The mathematical formulations of both models are complex and require voluminous documentation to describe them fully. In this section, only the key components of the model and findings are presented. The reader is directed to Benson (1989) for more detailed documentation.

VARIABILITY OF THE HYDRAULIC PROPERTIES OF SOIL

A practical way to quantify the uncertainty and variability in the magnitude of soil properties is to assume that they can be represented as random variables. Then, probability theory can be employed to assign the likelihood that a soil property, such as hydraulic conductivity, is a certain magnitude. Once probability distributions have been assigned to the soil properties, a probabilistic, or stochastic, model of flow can be formulated. The relationship between the hydraulic head and the properties of the soil is defined by a stochastic flow equation. The stochastic flow equation serves as a "translator" between the distributions of the hydraulic properties of the soil and the distributions of the properties of the flow field. Freeze (1975) and Benson (1989) have shown that the distribution of hydraulic conductivity of soil can be assumed to be log-normal. This means that when one plots a histogram of hydraulic conductivity measurements, the curve is skewed, but when one plots a histogram of the logarithm of hydraulic conductivity, the bell-shaped curve is symmetric and the logarithms are normally distributed. Freeze summarized the results of several authors who presented statistical data obtained from measurements performed on numerous natural soils. In each case, the hydraulic conductivity measurements were found to be log-normally distributed. Benson analyzed data presented by Rogowski (1989) who measured the spatial variability of the hydraulic conductivity of a pad of compacted clay. Benson concluded that the hydraulic conductivity measurements obtained by Rogowski were also normally distributed. He also found that the correlation structure of the hydraulic conductivity was non-existent at least for lags greater than 1,000 mm. In this study, hydraulic conductivity has been assumed to be log-normally distributed and uncorrelated.

Porosity has been found to be approximately normally distributed (Law, 1944; Benion and Griffiths, 1966; and Sinnock et al., 1986). However, since fluctuations in porosity are small in comparison to fluctuations in hydraulic conductivity, the effective porosity was assumed to be deterministic. Recent studies by Elsbury et al. (1988), Rogowski (1989) and Liao (1989) show that the effective porosity, which is defined as the volume of pores that actually conduct flow divided by the total volume of the soil, can be much smaller than the total porosity.

THE CONVOLUTION MODEL

A schematic diagram of the soil liner that was assumed in the analysis is presented in Figure 50. The soil liner was assumed to be

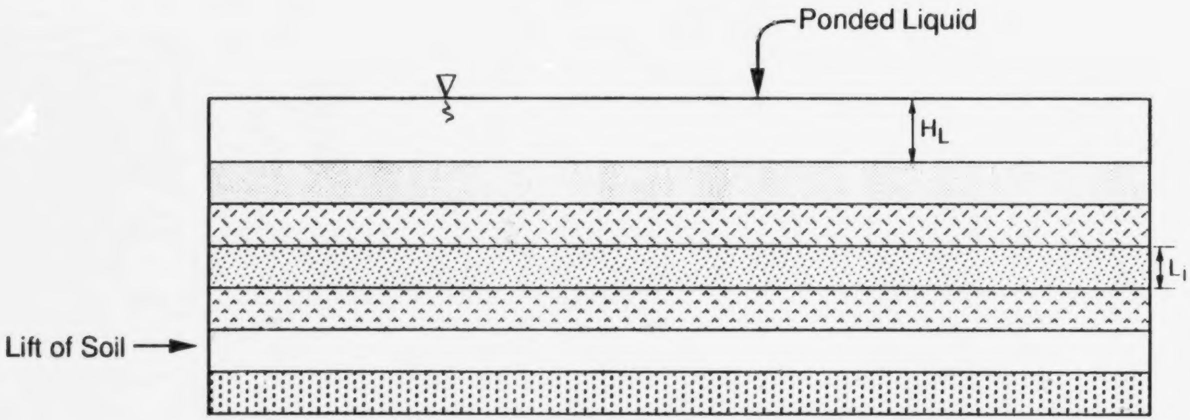
Ponded Liquid
H_L
L_i
Lift of Soil

Figure 50. Configuration of the soil liner which is modeled by the convolution model.

composed of N horizontal lifts of soil and the thickness of each lift is denoted by L_i. The liner was assumed to be covered with liquid to a depth H_L and the soil was assumed to be saturated with water. It was assumed that the liquid is ponded instantaneously and the depth does not change with time. Seepage was assumed to be steady and one-dimensional.

The First-Passage Time with the Convolution Model

Formulation --

A one-dimensional model is useful to visualize the probability distribution of first-passage time. One-dimensional seepage requires that a particle be constrained to flow along a vertical pathway even if the particle encounters zones of low hydraulic conductivity. The vertical lines in Figure 51a represent five different pathways through the soil liner. In any particular cross-section of soil, an infinite number of these pathways exist. A realization of the first-passage time along each of the five pathways is shown in Figure 51b. Along each pathway, the actual first-passage-time could be any value between zero and infinity with each value associated with a probability of occurrence. In reality, flow may be multi-dimensional (Fig. 52), but, for the Convolution Model, one-dimensional plug flow was assumed. The model discussed later simulated three-dimensional flow.

For mathematical convenience, the distribution of hydraulic conductivity was assumed to be homogeneous in the horizontal plane. Thus, the distributions of hydraulic conductivity and first-passage time are the same for every pathway through the liner such that the particular pathway to be used is both arbitrary and irrelevant.

The probability distribution of the first-passage time can be represented by a probability density function or a reliability function. A probability density function is shown in Figure 53a. The probability of first-passage occurring between the times t and t + dt is

$$P(t \le T \le t + dt) = \left\{ f_T(t + dt) - f_T(t) \right\} dt \tag{7.1}$$

where f_T is the probability density function of the first-passage time. A reliability function is shown in Figure 53b and it represents the probability that the first-passage time is greater than some time, t. The reliability function, RT(t), and the density function, f_T, are related by the integral equation:

$$R_T(t) \; = \; P_T(T > t) = \int_t^{\infty} f_T(t)\, dt \tag{7.2}$$

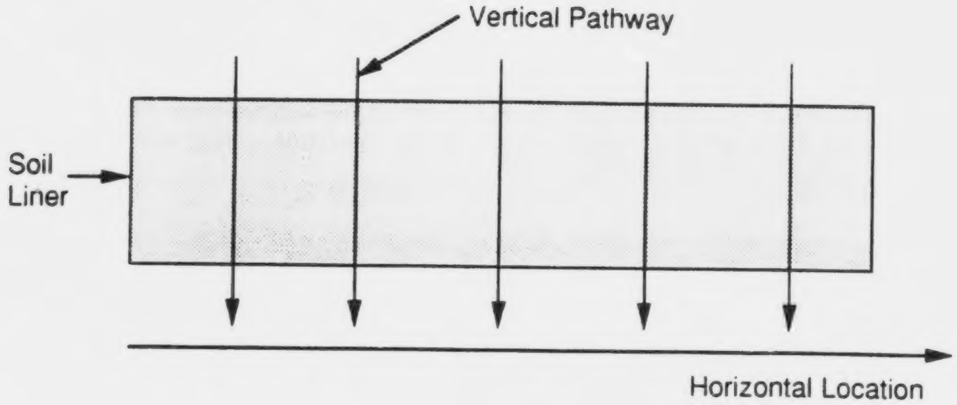
Vertical Pathway
Soil
Liner
Horizontal Location

Figure 51a. Vertical pathways through a soil liner.

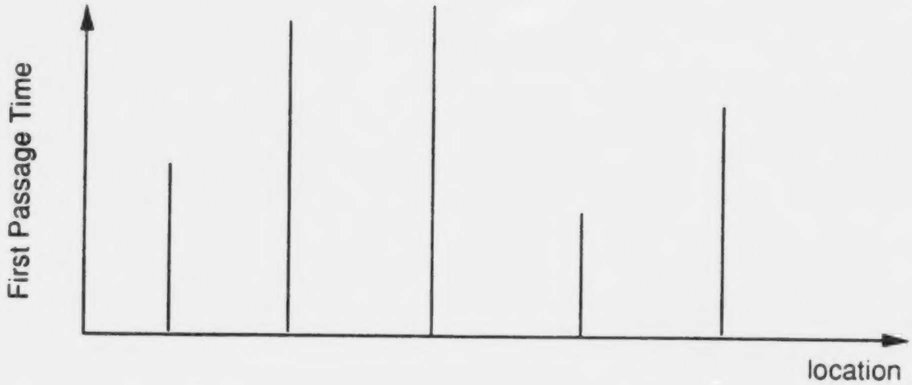

Figure 51b. Realizations of the first-passage times through a soil liner.

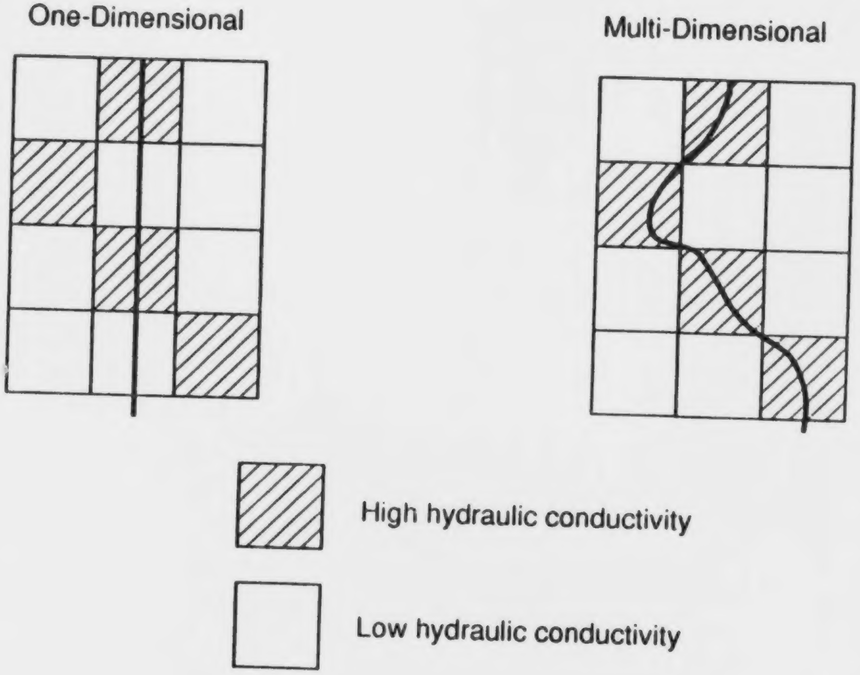
One-Dimensional
Multi-Dimensional
High hydraulic conductivity
Low hydraulic conductivity

Figure 52. Seepage in one-dimension and multi-dimensions.

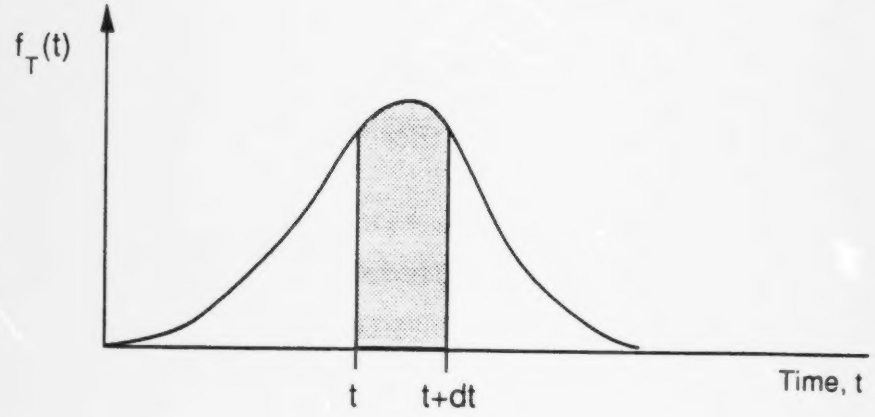

Figure 53a. A probability density function of the first-passage time.

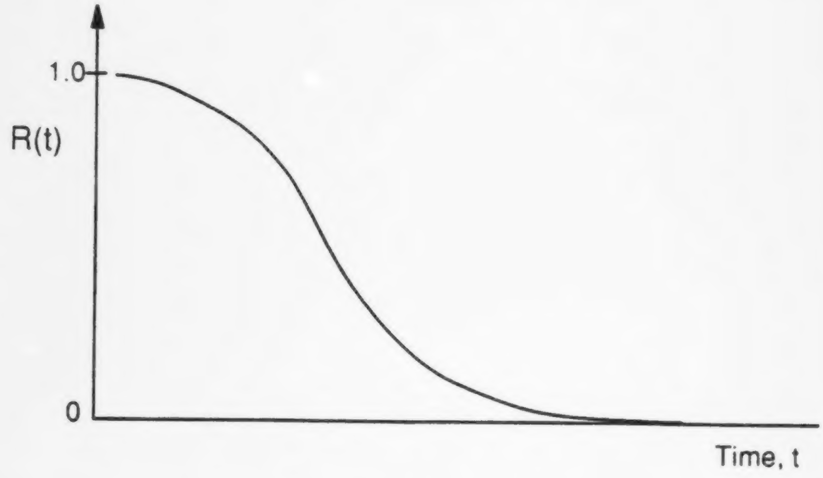

Figure 53b. A reliability function of the first-passage-time distribution.

The equations of fluid mechanics which are employed in the convolution model include the momentum equation (Darcy's Law) and the continuity equation. In a particular lift of soil, the average rate of flow along a vertical pathway is determined by Darcy's Law:

$$Q = K\frac{\Delta H}{L}A \tag{7.3}$$

where Q is the flow rate, K is the hydraulic conductivity, ΔH is the head loss across the lift, and A is the cross-sectional area of the pathway. In the convolution model, the hydraulic conductivity of a particular lift is assumed to be randomly distributed. However, the hydraulic conductivity is assumed to be constant over the full vertical extent of any one lift. If the soil is assumed to be saturated and the soil does not change volume, then no storage of liquid will occur in the soil. By continuity, the flux (q) along a particular vertical pathway must be the same in each lift.

$$q_1 = q_2 = \ldots = q_i = \ldots = q_n \tag{7.4}$$

Equation (7.4) can be combined with Eq. (7.3) and transformed to obtain the first-passage time, T, for plug flow along a vertical pathway:

$$T = \frac{\sum_{i=1}^{N} L_i}{v_s} = \sum_{i=1}^{N}\left(n_e\, L_i\right)\frac{\sum_{i=1}^{N}\frac{L_i}{K_i}}{\sum_{i=1}^{N}\Delta H_i} \tag{7.5}$$

All the independent variables of Equation 7.5 involve some type of uncertainty. Thus, the first-passage time, T, is inherently a random variable and its probability distribution is a function of the probability distributions of all the independent variables. The hydraulic conductivity is assumed to be the most significant random variable since it can vary widely. A constant depth of leachate (H_L) and thickness of lifts (L_i) was assumed; the values assumed were H_L = 300 mm and L_i = 150 mm. The effective porosity was assumed to be deterministic, although calculations were performed for more than one value of n_e. The assumptions described above permit Equation (7.5) to be simplified into the form:

$$T = \alpha \sum_{i=1}^{N}\frac{1}{K_i} \qquad \alpha = \frac{n_e\, NL^2}{H_L + NL} \tag{7.6}$$

where α is a deterministic coefficient. If the hydraulic resistivity, R_i, is defined as the reciprocal of the hydraulic conductivity, $(1/K_i)$, then Equation (7.6) can be rewritten as:

$$T = \alpha \sum_{i=1}^{N} R_i \tag{7.7}$$

The random variable T, the first-passage time, is now a simple linear function of the sum on the N random hydraulic resistivities. If the hydraulic conductivity is assumed to be log-normally distributed with parameters μ and σ^2, then the hydraulic resistivity is also log-normal but with parameters $-\mu$ and σ^2 (Benson, 1989). The probability distribution of the first-passage time can then be determined from the log-normal distributions of the hydraulic resistivities.

As indicated in Eq. (7.7), the first-passage time is a linear function of the summation of the random hydraulic resistivities and, hence, the distribution of the first-passage time can be computed by performing an N-fold convolution integral (Benson, 1989). The convolution integral was computed by assuming the hydraulic resistivities, R_i, were independent and identically distributed and by exploiting the Fourier convolution theorem (Churchill, 1972). The Fourier transformation integrals were performed numerically using the fast Fourier transform technique.

The mathematical formulation of the convolution model was translated into a computer program. The mathematical model was checked by comparison with a Monte Carlo simulation and by observing the convergence of the stochastic solution to a deterministic solution as the variability of the process converged upon zero. Details of the verification are given by Benson (1989).

Results--

A "typical" soil liner was assumed. The hydraulic conductivity was assumed to be log-normally distributed with a mean value 7×10^{-10} m sec^{-1} (7×10^{-8} cm sec^{-1}). The parameters of the distribution are the log-mean (μ) and the log-variance (σ^2), which have values of -17.0 and 1.0, respectively. A soil liner that can be described by these parameters would have 95 percent of the values of hydraulic conductivity between 5×10^{-11} and 3×10^{-9} m sec^{-1}. The liner was assumed to be 900 mm thick and to be composed of six lifts that are 150 mm thick. The effective porosity of the liner was assumed to be 0.40.

The mean value of hydraulic conductivity receives the most attention in design. Figure 54 depicts the 95th, 50th, and 5th percentile first-passage times as a function of the mean hydraulic conductivity. The largest sensitivity in first-passage time is associated with low reliability ($R = 0.05$) because the mean hydraulic

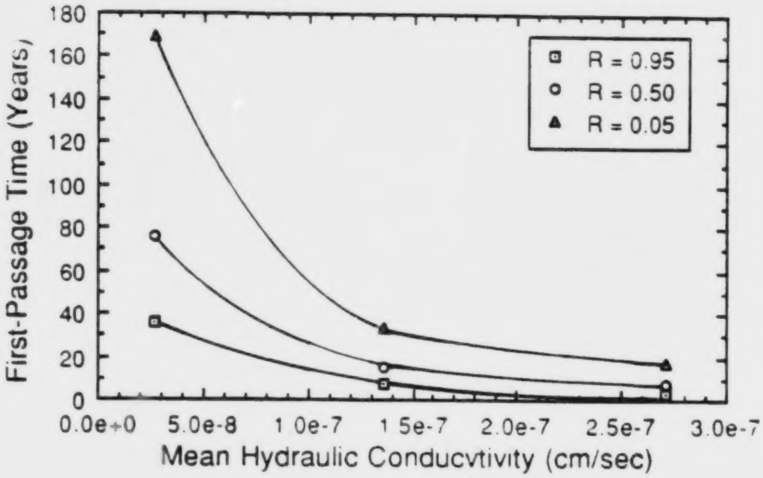

Figure 54. Effect of the mean hydraulic conductivity on the 95th, 50th, and 5th percentiles of first-passage-time.

conductivity has a greater effect on the upper tail than the lower tail of the first-passage-time distribution. The results shown in Figure 54 are consistent with the fundamental premise that a reduction in the mean hydraulic conductivity results in an increase in the first-passage time. Most importantly, the increase in first-passage time occurs not only at moderate values of reliability, but also near the important extreme values where the reliability is greater than 0.90.

The log-variance, σ^2, is a measure of the dispersion of the hydraulic conductivity distribution. As the log-variance increases, the variability of the hydraulic conductivity becomes greater. Intuitively, one would expect that a reduction in the log-variance would result in an increase in the reliability of a liner. As Figure 55 depicts, for high reliability (>0.90), the first-passage time does increase when the log-variance is reduced, but only slightly. The reason for the minimal increase in first-passage time with reduced variance in hydraulic conductivity is illustrated by Figure 56. The density function for the effective hydraulic conductivity is shown for values of the log-variance of 0.75 and 1.50. The probability density function has been converted

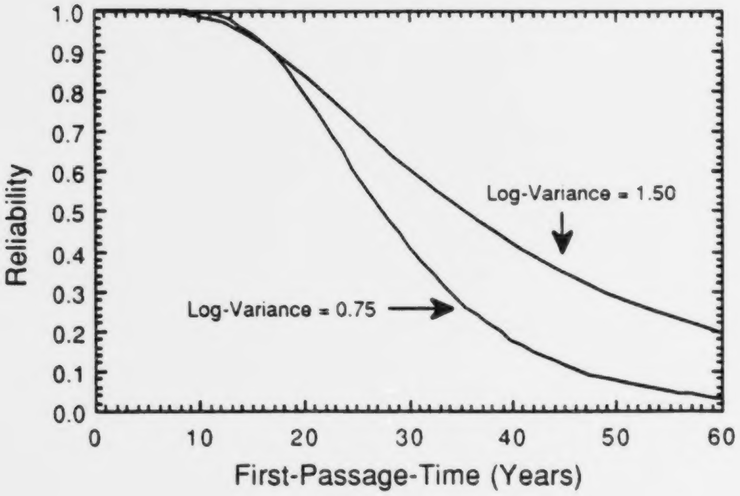

Figure 55a. The reliability function for log-variances of 0.75 and 1.50.

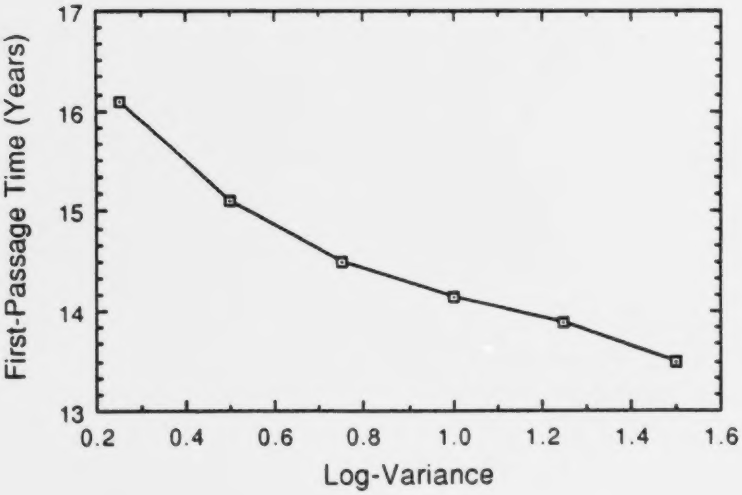

Figure 55b. The 95th percentile first-passage-time as a function of log-variance.

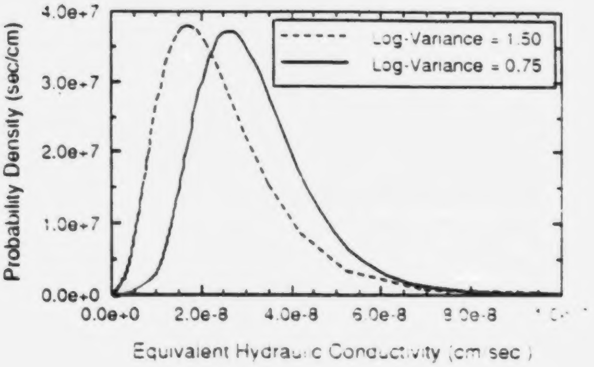

Figure 56. Density functions of the (a) equivalent conductivity, (b) Equivalent resistivity, (b) and first-passage-time log-variances of 0.75 and 1.50.

to a natural (rather than logarithmic) scale for K. Changing σ^2 does not change the mean K on a log-K distribution, but the mean K on a natural scale is lowered when σ^2 from the log K distribution is increased. Because of the fact that K is not normally distributed (the natural log of K is assumed to be normally distributed) different effects are seen at low and high reliabilities. Nevertheless it is clear that with the conditions assumed in this model, reducing the variability in hydraulic conductivity does not help significantly to increase time of travel through the liner; lowering the mean hydraulic conductivity has a much more significant effect.

The effective porosity was assumed to be a deterministic variable. It was recognized that a wide range of values have been reported for different soils (Rogowski, et al., 1988; Elsbury, et al., 1988; and Liao, 1989). Figure 57 depicts the reliability function of the typical soil liner for effective porosities of 0.05, 0.10, 0.20, 0.30, and 0.40. It is apparent that low effective porosity results in short first-passage times and also masks the influence of the variability of the hydraulic conductivity (the reliability function is shaped like a step function). If effective porosity is very small, the first-passage time will almost inevitably be small.

Flux with the Convolution Model

Although the first-passage time may be an important criterion in the design of soil liners, one is also concerned about the flux of liquid emanating from the base of a liner. In this section, the sensitivity of the distribution of the flux to the log-variance of hydraulic conductivity and the thickness of a soil liner is considered. The flux of liquid is defined as the flow rate per unit area.

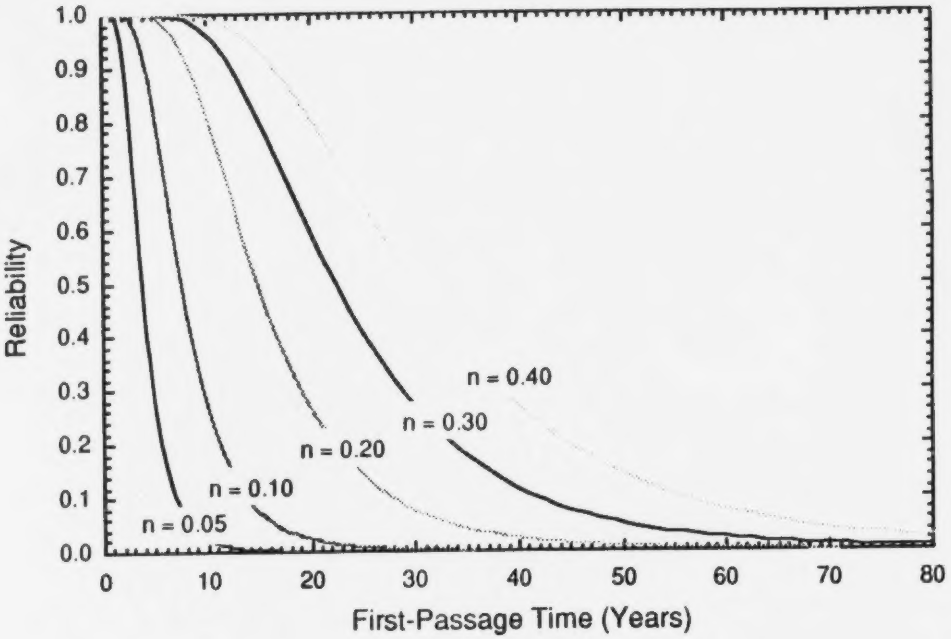

Figure 57. Reliability functions for several values of effective porosity.

Formulation

The equivalent hydraulic conductivity of a soil liner, K_e, is defined as the vertical flux, q, divided by the average hydraulic gradient, i, and is related to the hydraulic conductivities of the lifts and the geometry of the liner as follows:

$$K_e = \frac{q}{i} = \frac{\sum_{i=1}^{N} L_i}{\sum_{i=1}^{N} \frac{L_i}{K_i}} \qquad 7.8$$

The flux is computed by multiplying the equivalent hydraulic conductivity by the average hydraulic gradient. Hence, the flux emanating from the base of the liner, q, is:

$$q = \left(\frac{N}{\sum_{i=1}^{N} R_i}\right)\left(\frac{NL + H_L}{NL}\right) \qquad (7.9)$$

Equation (7.9) can be simplified as:

$$q = \left(\frac{\wp}{\sum_{i=1}^{N} R_i}\right) \qquad (7.10)$$

where ρ is a constant that equals the hydraulic gradient multiplied by the number of lifts, N. The distribution of the flux, q, can be determined from the distribution of the hydraulic resistivities, R_i, with Equation (7.10). A fast Fourier transform was used to compute the distribution of the sum of resistivities and a probability integral transform (Grimmett and Stirzaker, 1985) was used to transform the distribution of the sum of resistivities to the distribution of flux.

Results--

The sensitivity of the distribution of the flux to the log-variance of hydraulic conductivity, σ^2, and the thickness of a soil liner is described below. In contrast to the discussion of the distribution of first-passage time, the sensitivity of the flux to the mean hydraulic conductivity is not presented. A reduction in the mean hydraulic conductivity yields a similar reduction in mean flux because the flux and conductivity are linearly related by Darcy's Law. Furthermore, because the effective porosity and conductivity are assumed to be independent, the effective porosity has no effect on the distribution of flux.

A cumulative distribution function (cdf) and a probability density function (pdf) are used to describe the distribution of the flux. The cumulative distribution function of flux is the probability that the random flux is less than a particular magnitude.

Graphs of the cdf and pdf of flux are shown in Figure 58 for log-variances of hydraulic conductivity of 0.50, 1.00, and 1.50. The graphs display similar trends; the distribution of the flux becomes more dispersed and the probability mass associated with smaller flux becomes larger as the log-variance of hydraulic conductivity increases. In other words, as the variability in hydraulic conductivity increaes, the flux decreases.

An explanation for the greater increase in mass associated with small fluxes can be inferred from the log-normal pdf of hydraulic conductivity. Figure 59 depicts the probability density functions of hydraulic conductivity for log-variances of 0.50, 1.00, and 1.50. In each case, the log-mean, μ, was -17. The pdf with a log-variance of 1.50 has a greater skew toward small fluxes and only a slightly larger mass associated with large fluxes. Because hydraulic conductivity and flux are linearly related by Darcy's Law, the unequal shift in probability mass in the distribution of hydraulic conductivity is reflected in the distribution of the flux.

Figure 60 depicts the normalized 50th and 95th percentile fluxes as a function of the log-variance of hydraulic conductivity. The percentiles were normalized by dividing the flux by the 50th or 95th percentile flux of the assumed typical soil liner. An increase in the log-variance yields a decrease in the 50th percentile flux but an increase in the 95th percentile flux. Hence, an increase in log-variance may yield a larger probability of smaller fluxes, but it also yields a greater probability of a large flux. Because the probability of large fluxes increases with greater log-variance, greater variability of hydraulic conductivity is not beneficial. However, since the sensitivity of the 95th percentile flux to log-variance is not large, control of the log-variance of hydraulic conductivity appears to not be of great importance. As was found with first passage time, much more benefit is derived from lowering the mean K than from reducing the variability in K. The effect of number of "typical" soil liner lifts is shown in Figure 61. An increase in the number of lifts causes a decrease in flux. However, because the hydraulic gradient is smaller for a thicker liner, the flux from a thicker liner should be smaller than the flux from a thinner liner.

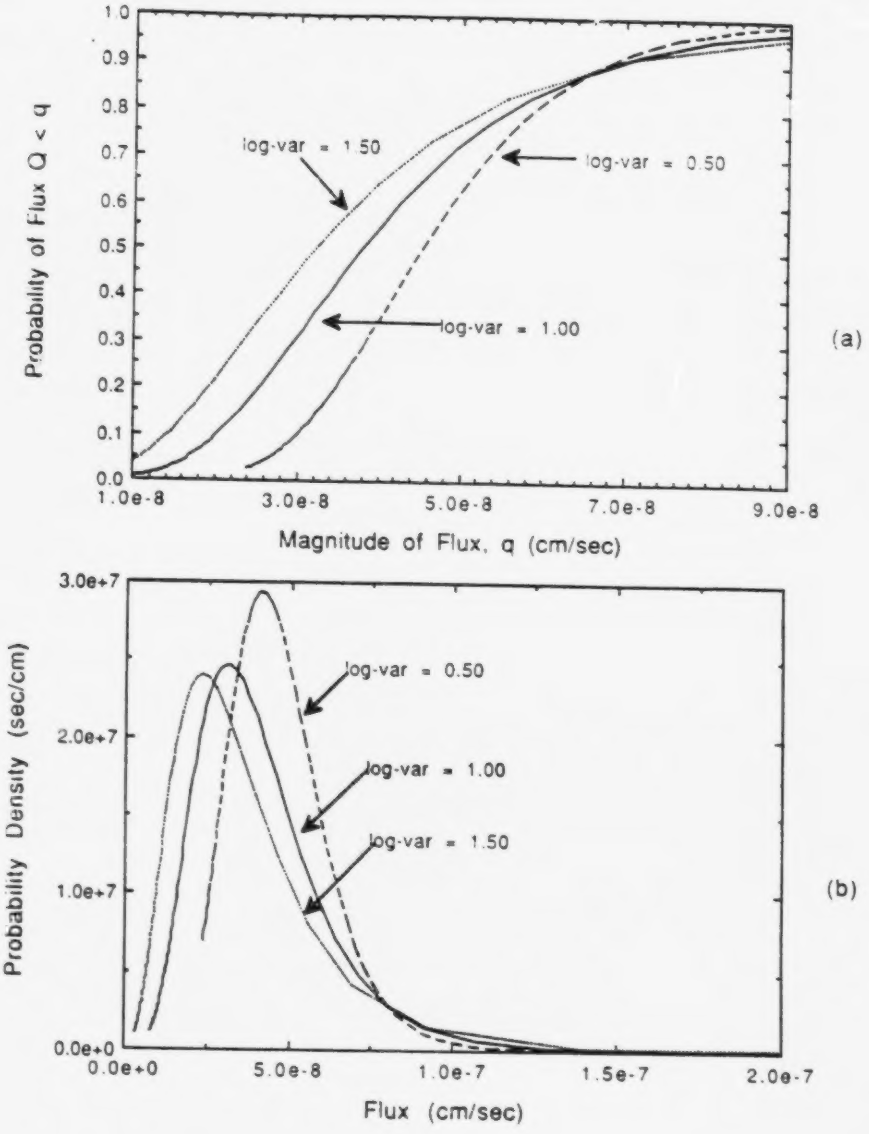

Figure 58. Influence of variance of hydraulic conductivity on flux presented (a) as a cumulative distribution function, and (b) a probability density function.

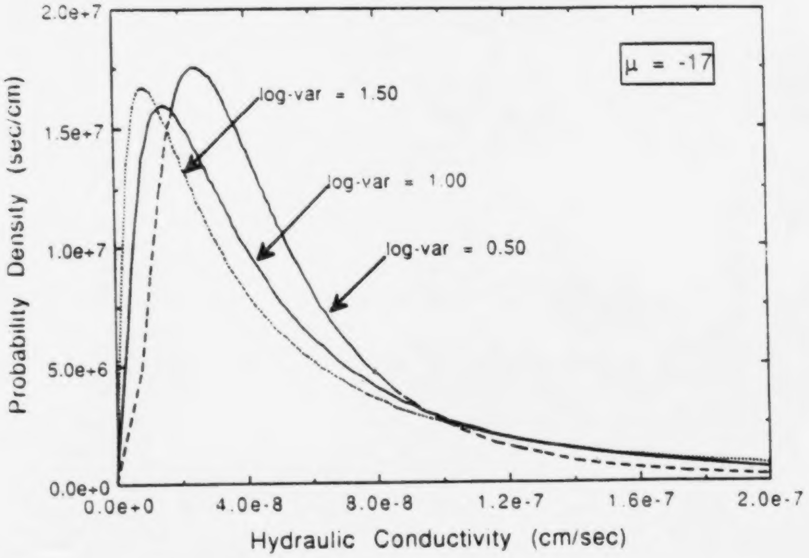

Figure 59. Probability density functions for hydraulic conductivity.

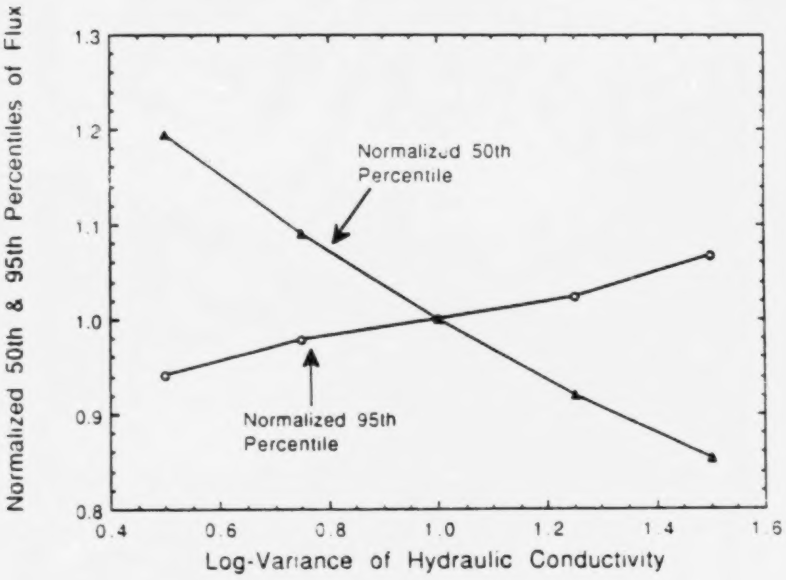

Figure 60. Normalized 50th and 95th percentile fluxes versus log variance of hydraulic conductivity.

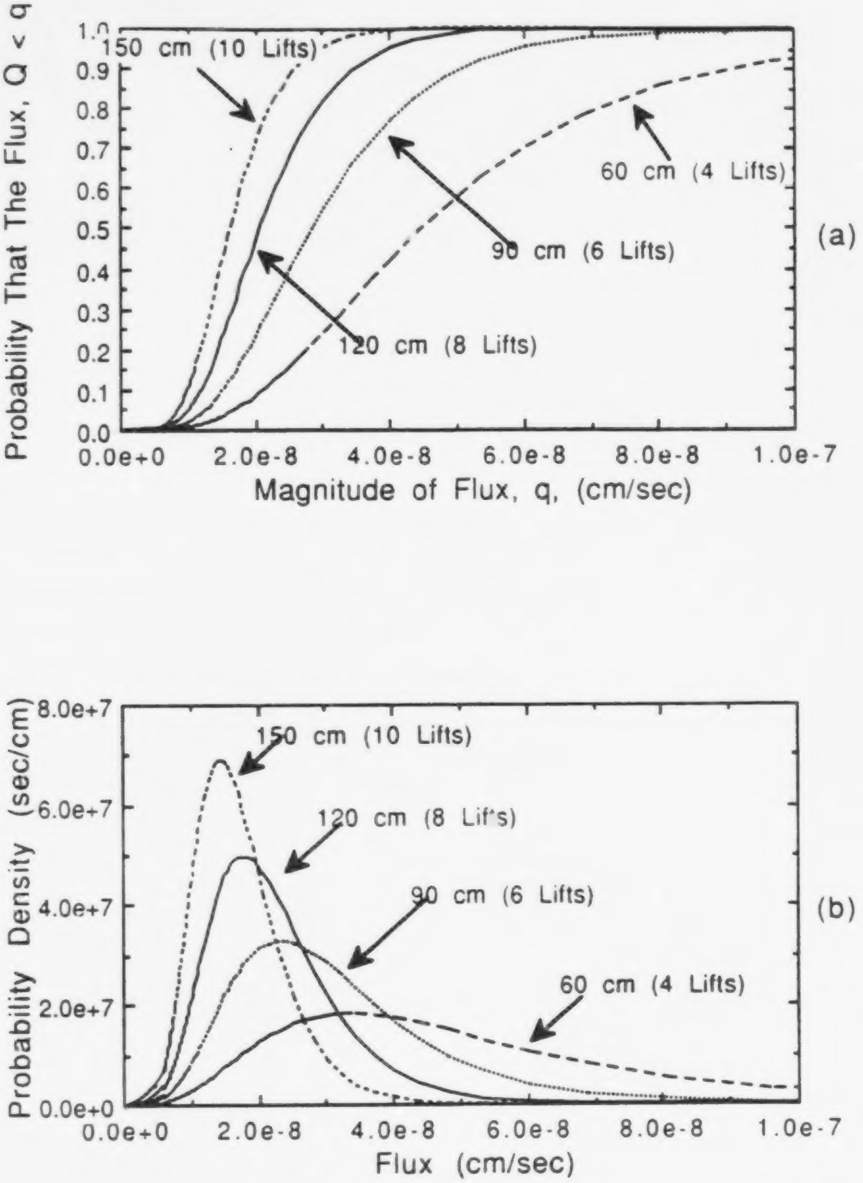

Figure 61. Effect of number of lifts on probability density function and cumulative density functions for flux.

Also, the shift in probability mass shifts towards smaller fluxes for thicker liners due to an increase in the proportion of lifts with low conductivity. Figure 62 depicts the shift in the distribution towards smaller fluxes in terms of the normalized 50th and 95th percentiles and the normalized hydraulic gradient. The figure illustrates that the normalized 50th and 95th percentile fluxes and the hydraulic gradient decrease as the thickness of the liner increases. Furthermore, the decrease in the 50th and 95th percentile fluxes is larger than the decrease in the hydraulic gradient. Hence, the decrease in flux is not only due to a decrease in hydraulic gradient, but is also due to an increase in the proportion of lifts with low conductivity. Figure 62 also shows that the benefits of a smaller and less variable flux diminish as the thickness increases. The greatest changes occur for liners that are thinner than 150 cm (4.9 ft).

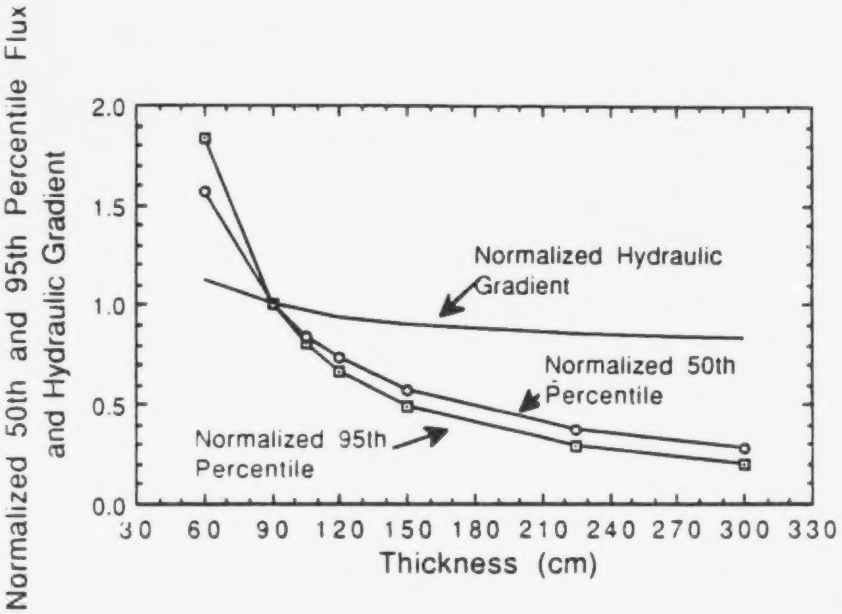

Figure 62. Normalized flux and hydraulic gradient versus thickness of liner.

THE MACROPORE MODEL

In the convolution model, it was assumed that seepage in soil liners can be modeled as a one-dimensional continuum with the domain of the continuum extended throughout the confines of a soil liner. Liquid does not necessarily flow through a soil liner as if the liner was a hydraulic continuum, but instead flows through a number of discrete channels called macropores. Hence, the type of model that is used to analyze seepage may make a significant impact on the determination of the first-passage time and flux.

Figure 63 depicts a soil liner that has extensive flow between the lifts and another soil liner with little flow between the lifts. If extensive flow between the lifts occurs, macropores in different lifts may become hydraulically interconnected resulting in a short first-passage time and large flux. However, if little flow between the lifts occurs, then it is unlikely that macropores would be interconnected throughout the entire depth of the liner. In this case, the first-passage time would be much longer and the flux much lower.

The seepage phenomenon depicted in Figure 63 was modeled with the macropore model. Macropores were modeled as vertical channels of circular cross-section and the spaces between the lifts were modeled as confined aquifers. The soil was assumed to be saturated. Monte Carlo simulation was used to incorporate the variability and uncertainty associated with the size, location, and the flow coefficient of the macropores.

Assumed Properties of the Macropores.

Hydraulic conductivity and porosity were obtained by spatial averaging as suggested in Figure 64. The upper part of Figure 64 depicts a lift of soil with many macropores. If the lift is divided into six blocks with equal volume, then a spatial average of the flux over each partition will yield six blocks each with a different hydraulic conductivity as shown in the center of the figure. A spatial average of the hydraulic conductivity of the six blocks of soil would yield a single value of the hydraulic conductivity as shown in the illustration at the bottom of the figure.

A lift of soil was divided into m square partitions of equal size and in each partition a number of channels, N_m, was specified. If the effective porosity of the soil in a partition is n_e, then the average squared-radius of the channels, $<r^2>$, can be determined by requiring the volume of the channels to equal the volume of the voids which carry the flow:

$$N_m \pi < r^2 > L = n_e S^2 L \qquad (7.11)$$

where L is the thickness of a lift and S is the length of the side of a partition. Equation 7.11 can be solved for $<r^2>$

$$< r^2 > = S^2 \frac{n_e}{N_m \pi} \qquad (7.12)$$

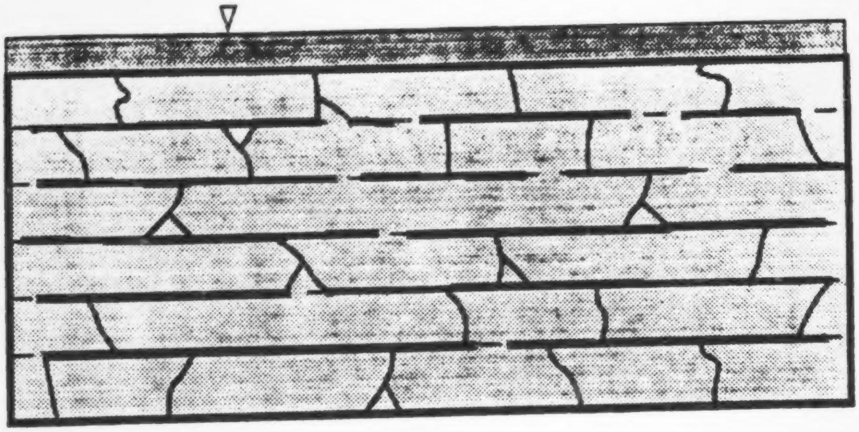

(a) Poor Interlift Bonding

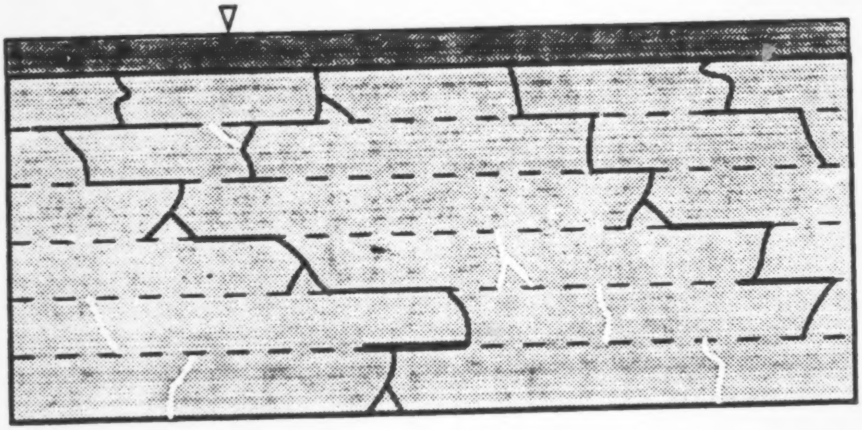

(b) Good Interlift Bonding

Figure 63. Seepage in macropores in liners with good and poor interlift bonding.

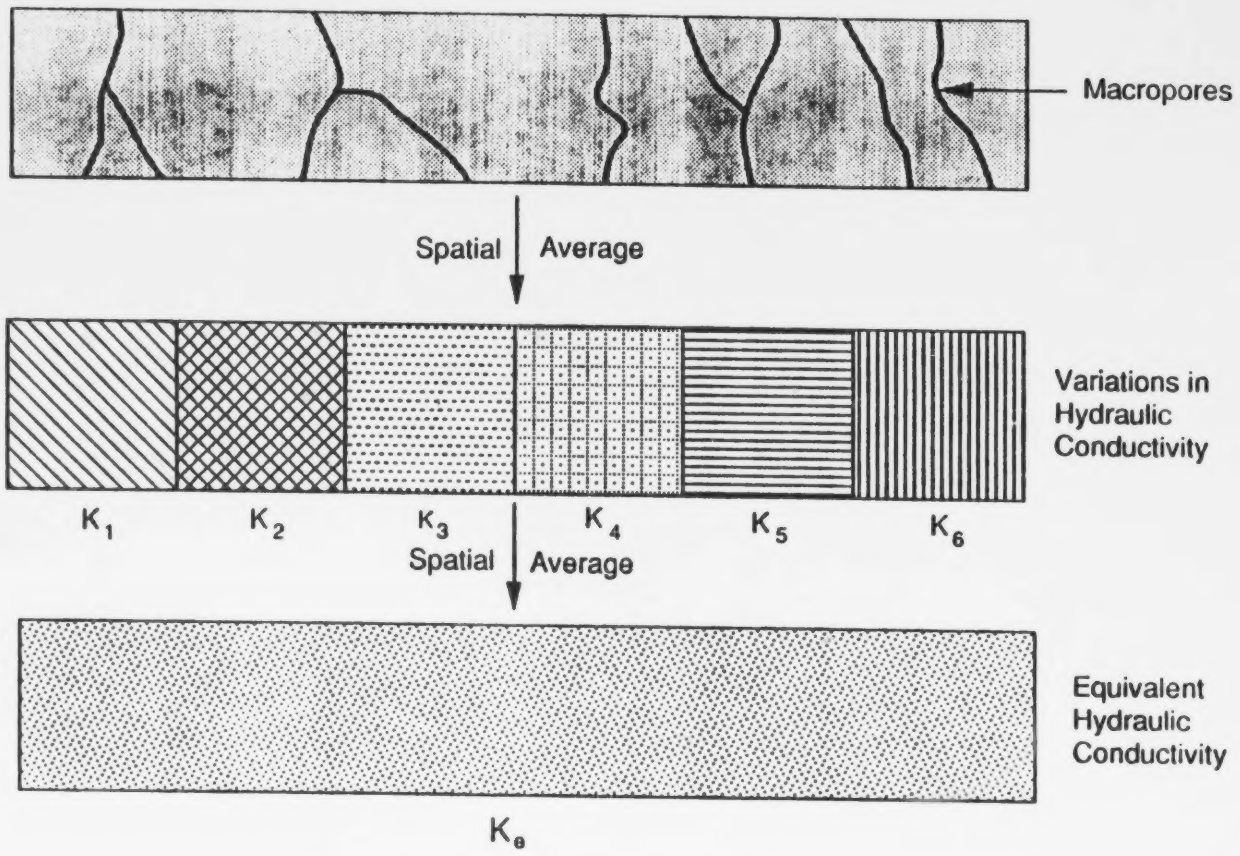
Macropores
Spatial Average
Variations in Hydraulic Conductivity
K_1
K_2
K_3
K_4
K_5
K_6
Spatial Average
Equivalent Hydraulic Conductivity
K_e

Figure 64. Macropores, spatial averaging, and hydraulic conductivity.

The radius of the channels can be distributed so that the average squared radius of the channels is $<r^2>$ because the effective porosity is also a spatial average.

The flow coefficient for the channels can be specified by ensuring continuity. The total flow rate through the channels in a partition must equal the flow rate through the partition, which is computed with the hydraulic conductivity, K_m.

$$\sum_{k=1}^{N_m} J_k \pi r_k^2 = K_m \; I \; S^2 \tag{7.13}$$

The variable J_k in Equation (7.13) is the flow coefficient for channel k and I is the hydraulic gradient. Equation (7.13) can be rearranged if the J_k are assumed to be equal. The J_k can then be denoted as J to yield:.

$$J = \frac{K_m S^2}{\sum_{k=1}^{N_m} \pi r_k^2} \tag{7.14}$$

Thus, the geometry and flow coefficient of the channels can be determined from the hydraulic conductivity and the effective porosity of a partition. The methods used to generate the random variates K_m, N_m, and r_k are discussed later.

Interlift Zone

The thin zone which exists between the lifts is called the interlift zone and was modeled as a confined aquifer. The Thiem equation was used to define the hydraulic head at any point in the interlift zone and the channels in the adjacent lifts were assumed to behave as recharge wells (upper lift) and discharge wells (lower lift) as shown in Figure 65. The Thiem equation can be written as:

$$h_{i,j} = \frac{1}{2\pi T} \sum_{k=1}^{TN_u + TN_l} Q_k \ln\left(\frac{r_{ki}}{r_k}\right) + W_j \tag{7.15}$$

where $h_{i,j}$ is the hydraulic head at some point i in interlift zone j, T is the transmissivity of the interlift zone, Q_k is the flow rate of channel k (positive for discharge), r_{ki} is the distance between point i and channel k, and W_j is an arbitrary constant. The variables TN_u and

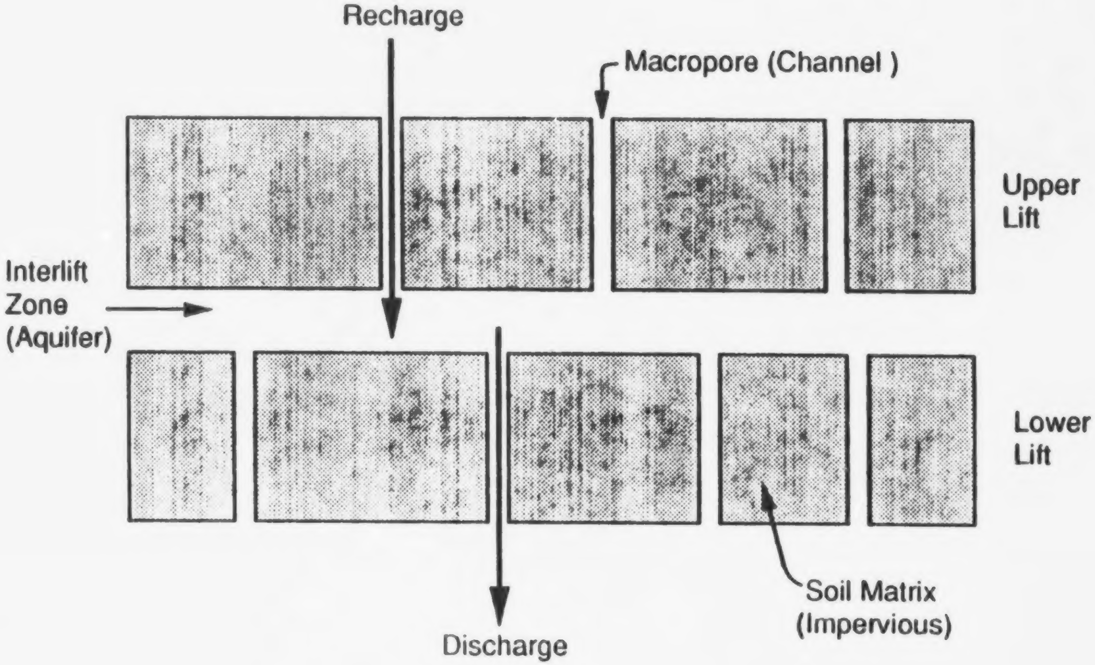
Recharge
Macropore (Channel)
Upper Lift
Interlift Zone (Aquifer)
Lower Lift
Soil Matrix (Impervious)
Discharge

Figure 65. A schematic of the hydraulic behavior of the interlift zone.

TN_l are the number of channels in the upper and lower lifts, respectively. Equation (7.15) is written for each interlift zone.

Equation (7.15) can be combined with the laminar flow equation for the channels to link the heads between adjacent interlift zones. If H_{tk} is the head at the top of channel k and H_{bk} is the head at the bottom of channel k then

$$h_{i,j} = \frac{\psi_k}{2TL} \sum_{k=1}^{TN_u + TN_l} \left(H_{tk} - H_{bk} \right) J_k \, r_k^2 \ln \left(\frac{r_{kl}}{r_k} \right) + W_j \qquad (7.16)$$

where L is the thickness of a lift and ψ_k is ± 1 if channel k is in the top or bottom lift, respectively.

Linear System of Equations

A linear system of equations can be defined to determine the hydraulic head at the end of each channel by combining Equation (7.16) and the continuity equation. Herein, the end of the channels will be referred to as nodes. For continuity, the flow into an interlift zone must equal the flow out of the interlift zone:

$$\sum_{k=1}^{N_u} Q_k = \sum_{k=1}^{N_l} Q_k \qquad (7.17)$$

Equations (7.16) and (7.17) can be combined and rewritten as:

$$\sum_{k=1}^{TN_u} J_k \left(H_{tk} - H_{bk} \right) r_k^2 = \sum_{k=1}^{TN_l} J_k \left(H_{tk} - H_{bk} \right) r_k^2 \qquad (7.18)$$

If Equation (7.16) is written to obtain the head of each node and Equation (7.18) is written for each interlift zone, a non-singular linear system of equations is obtained. The solution of the linear system of equations is a vector composed of the hydraulic head at each node in the soil liner and the parameters W_j in Equation (7.16). The hydraulic head at the nodes and the parameters W_j can be substituted in Equation (7.16) to define the hydraulic head anywhere within the soil liner.

The First-Passage Time

Liquid may take many different pathways when it travels from the top to the bottom of a soil liner. The pathway which requires the least time to traverse yields the first-passage time. To determine the first-passage time, the time to traverse each pathway must be computed and the minimum time selected. The time required for liquid to travel through a channel of length, L, which has hydraulic head H_i at the top node and H_j at the bottom node, is

$$t_{ij} = \frac{L^2}{J\left(H_i - H_j\right)} \qquad (7.19)$$

where J is the coefficient of flow assigned to the channel.

The calculation of the time for a liquid to travel in the interlift zone between two channels requires computing the gradient between the channels and the length of the pathway in the direction of the gradient. A contour map of the hydraulic head in the interlift zone is necessary to determine the pathway of flow between channels in the interlift zone. The time of travel along the pathway would have to be integrated to obtain the total time to travel from one channel to another. An analysis of this type would require a complex algorithm and an enormous amount of computer time to estimate the distribution of the first-passage time by Monte Carlo simulation. Hence, the time to travel between channels k and l has been approximated as:

$$t_{kl} = \frac{r_{kl}^2}{T/b\left(H_k - H_l\right)} \quad H_k > H_l \qquad (7.20)$$

which is a simple application of Darcy's Law between points k and l. Some error occurs when the time of travel between the channels is approximated by Equation 3.17, but if the algorithm is to be somewhat efficient, the approximation must be employed. Errors which occur due to the approximation will bias the first-passage time toward shorter times.

Monte Carlo Simulation

The discussion so far has dealt with the solution of a deterministic hydraulic model. The randomness of the hydraulic properties of the soil are incorporated by Monte Carlo simulation in the macropore model. For each simulation, realizations of the properties of each partition, such as the hydraulic conductivity, number and location of the channels, and flow coefficients are generated with random number generators. The hydraulic problem is solved with each set of realizations and the first-passage time, total vertical flux, and maximum interlift radius of the simulation are computed. The maximum interlift radius is defined to be the greatest horizontal distance which was traversed on the pathway of first-passage. Once a sufficient number of simulations are performed, statistics of the first-passage time, total vertical flux, and maximum interlift radius are computed.

Figure 66 is an illustration of a soil liner modeled by the macropore model. The liner is of cross-sectional area, A, and is divided into m partitions. Within a particular partition, a realization of N_m channels, each with radius r_k and flow coefficient J_k, is assigned by a random number generator. In this way, the spatially averaged quantities of hydraulic conductivity and effective porosity are "differentiated" so that an approximation of the actual phenomena can be analyzed.

The Number of Channels--

A truncated two-dimensional Poisson distribution was used to assign the number of channels, N_m, in each partition (Grimmett and Strizaker, 1985). The occurrence of an event in the macropore model corresponds to the occurrence of a macropore within a partition. The probability density function for a Poisson distribution with parameter λ is

$$f(n) = \frac{\lambda^n e^{-\lambda}}{n!} \quad n = 0, 1, 2, \ldots \tag{7.21}$$

The variable n is a realization of N_m and the parameter λ corresponds to the mean number of channels in a partition.

The distribution of the number of channels is not truly Poisson since two constraints have been applied to the simulation. First, the use of a Poisson distribution to distribute the number of channels implies that zero channels may exist in a partition. If no channels exist in a partition, then no liquid can pass through the partition. Since the soil in each partition has some non-zero hydraulic conductivity, at least one channel was assigned to each partition. Elimination of realizations of no channels results in a truncation of the Poisson distribution.

The channels in a particular lift cannot overlap with other channels within the lift or with channels in adjacent lifts. An algorithm was developed to ensure that the channels do not overlap (Benson, 1989). Because channels cannot overlap, the distribution of location is not uniform, and the distribution of the channels is not truly Poisson.

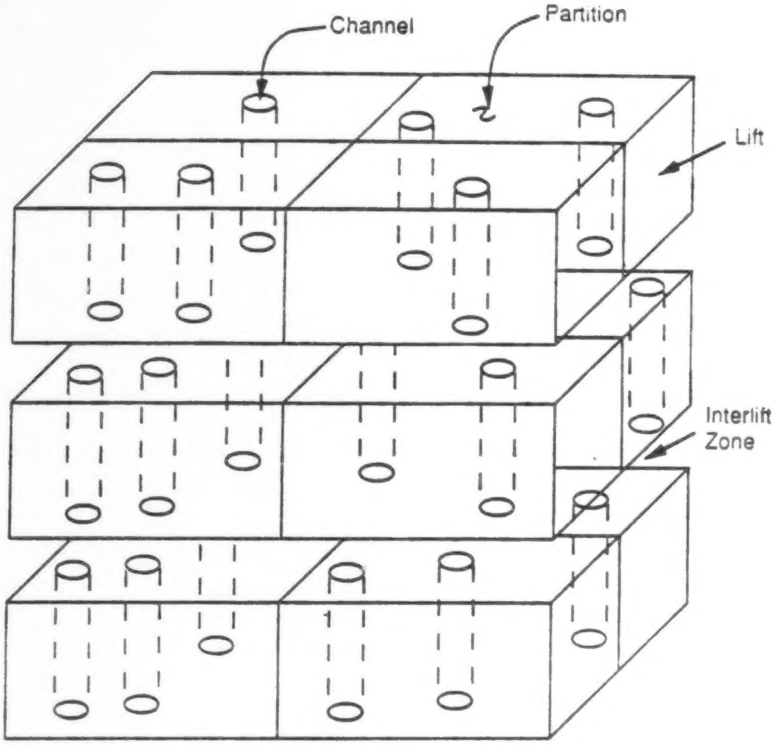
Channel
Partition
Lift
Interlift
Zone

Figure 66. A schematic of the liner approximated with the macropore model.

Size of the Channels--

The area of the channels was assumed to be normally distributed and have a small coefficient of variation. The mean area was determined by Equation 7.12. A small coefficient of variation was employed to minimize the probability of very large or very small channels.

Flow Coefficient--

The flow coefficient was assumed to be the same for each channel in a partition. The hydraulic conductivity was assumed to be log-normally distributed with parameters (μ, σ^2). Autocorrelation of hydraulic conductivity was not included in the macropore model for two reasons. First, as shown by Benson (1989), autocorrelation of hydraulic conductivity does not appear to exist in compacted soil at least for lags greater than about 1 meter. Second, proper representation of the autocorrelation function is difficult due to the effect of the boundaries unless a large number of partitions are employed (Smith and Freeze, 1979).

Number of Simulations--

The number of simulations used in the macropore model was determined by a compromise between expenditure of computer-time and precision of statistical estimators. An adequate precision of the estimators was selected by plotting the first four sample moments of the first-passage time as a function of the number of simulations and determining how many simulations are required to obtain stable estimates of the moments. It was determined that at least 800 simulations were needed to yield stable estimates of the moments.

The computer time required to perform the simulations was quite extensive and a practical limit of 1,000 simulations was selected. Most of the simulations were performed with 1,000 simulations, but some extremely long cases were estimated with only 800 simulations.

The Typical Soil Liner that was Assumed

A typical soil liner for the macropore model was defined by comparing the statistics of several analyses and selecting a set of parameters which yielded typical results. In each case, the soil liner was assumed to be composed of six lifts of soil and was covered with 300 mm of liquid. No suction was assumed to exist at the base of the liner. The lifts were assumed to be 150 mm thick. A typical soil liner was defined to have an equivalent hydraulic conductivity of 5 x 10^{-9} m sec^{-1} for a single lift of soil and an equivalent hydraulic conductivity of the entire liner of about 5 to 8 x 10^{-10} m sec^{-1} (5 to 8 x 10^{-8} cm sec^{-1}). As in the convolution model, the log-variance of hydraulic conductivity was 1.0.

Only a small section of an entire liner is analyzed by the macropore model because modeling an entire liner would be computationally impossible. It is unnecessary to model the hydraulics of the entire liner provided that, at some particular scale, the distribution of the first-passage time and flux become insensitive to any further increase in scale.

Number of Channels and Transmissivity of the Interlift Zone--

The equivalent hydraulic conductivity was computed for a soil liner with a mean number of channels of 4, 9, and 16 per square foot (about 900 cm^2). An area of 900 cm^2 was analyzed and the lifts were not divided into partitions. Equivalent hydraulic conductivity was computed by dividing the mean flow-rate from the base of the liner by the average hydraulic gradient and the cross-sectional area. The mean equivalent hydraulic conductivity of a single lift of soil was 5×10^{-9} m sec^{-1} and the transmissivity was varied between 3×10^{-6} cm^2 sec^{-1} and 3×10^{-8} cm^2 sec^{-1}.

It was found that the soil liner with 4 channels/900 cm^2 had an equivalent hydraulic conductivity that was too low and, conversely, the soil liner with 16 channels 900 cm^2 had an equivalent hydraulic conductivity that was too large. A soil liner with 9 channels per 900 cm^2 had an equivalent hydraulic conductivity of 6×10^{-10} m sec^{-1} when the transmissivity of the interlift zone was equal to 3×10^{-7} cm^2 sec^{-1}, which satisfied the single-lift and equivalent-conductivity criteria mentioned above. Hence, a "typical" soil liner was assumed to have a mean number of 9 channels/900 cm^2 and a transmissivity of the interlift zone of 3×10^{-7} cm^2 sec^{-1}.

Area of Analysis--

The areal extent of the section of the soil liner being analyzed was investigated to determine an appropriate cross-sectional area for use in the sensitivity analysis. A soil liner composed of six lifts was analyzed for mean values of 4, 9, and 16 channels per square foot. Each lift of the soil liner was divided into four partitions: the mean hydraulic conductivity of a partition was 5×10^{-9} m sec^{-1} and the transmissivity of the interlift zone was 3×10^{-7} cm sec^{-1}.

It was found that the results were insensitive to the area of analysis for areas greater than 1500 cm^2. An area of 1500 cm^2 was used for the main analyses reported later.

Number of Partitions--

A study of the effect of the number of partitions on the distribution of the first-passage time was also performed. The study was performed on an area of divided into 1, 4, 9, and 16 partitions. The results were the same for analyses with 4 or more partitions. Four partitions were used for the main analyses.

Summary--

A "typical" soil liner used for this study is summarized as follows. The area analyzed was 1500 cm^2 and was divided into four partitions. The mean equivalent hydraulic conductivity of a single lift within a partition was 5 x 10^{-9} m sec^{-1} and the log-variance was 1.0. The mean number of channels/900 cm^2 was 9, the mean transmissivity of the interlift zone was 3 x 10^{-7} cm^2 sec^{-1} and the effective porosity was assumed to be 0.05.

Results of Macropore Model with Regard to the First-Passage Time

A study of parameter sensitivity is presented below. In each case, the characteristics of the "typical" soil liner were used except for parameters which were varied to study the sensitivity.

Mean Number of Channels--

The influence of the mean number of channels on the distributions of the first-passage time and maximum interlift radius is shown in Figure 67. Figure 67(a) depicts the 95th percentile-first-passage time, t95, as a function of the mean number of channels for four transmissivities of the interlift zone. The magnitude of t95 decreases as the mean number of channels increases because the time to travel between channels in the interlift zone is reduced. The effect of the separation between the channels is magnified when the transmissivity is lowered since the time of travel within the interlift zone is inversely proportional to the transmissivity.

Figure 67(b) is a plot of the variance of the first-passage time as a function of the mean number of channels and the transmissivity of the interlift zone. The variance grows as the mean number of channels in the interlift zone is reduced. The influence of the mean number of channels on the variance is magnified when the transmissivity of the interlift zone is reduced because the large first-passage times become even larger, yet short first-passage times remain about the same.

Reliability functions for values of the mean number of channels of 4, 9 and 16 are shown in Figure 67(b). The transmissivity of the interlift zone is 3 x 10^{-7} cm^2 sec^{-1}. The reliability function is shifted toward larger times as the mean number of channels is decreased because the liquid must travel farther in the interlift zone to reach a highly conductive channel or flow down a closer, less conductive channel. The increase in the variance of the first-passage time, due to a decrease in the number of channels, results in a reliability function that is less steep.

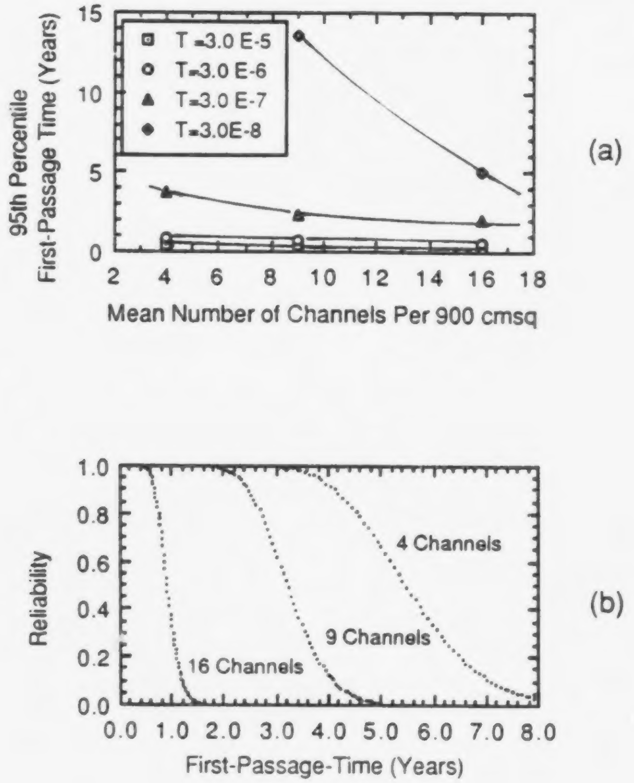

Figure 67. The effect of the number of channels on the 95th percentile and variance of the first-passage-time and the reliability function.

Mean Hydraulic Conductivity of a Partition--

Figure 68(a) shows the 95th percentile first-passage time, t_{95}, as a function of the mean hydraulic conductivity for three magnitudes of the mean number of channels. As expected, t_{95} increases as the mean hydraulic conductivity is decreased. When the mean number of channels is reduced, t_{95} increases because the liquid must flow farther in the interlift zone before it travels downward in another channel.

Figure 68(b) illustrates that the t_{95} increases if the transmissivity of the interlift zone is reduced.

Log-Variance of Hydraulic Conductivity--

The log-variance of the hydraulic conductivity has an interesting effect on the distribution of the first-passage time as shown in Figure 69(b). Figure 69(a) depicts the reliability function for log-variances of 0.25, 0.75, and 1.50 and a mean hydraulic conductivity of 5×10^{-9} m sec^{-1}. Figure 69(b) depicts the 95th percentile first-passage time as a function of the log-variance of hydraulic conductivity. In both graphs, the first-passage time increases when the log-variance of the hydraulic conductivity becomes larger. The result is counterintuitive; it was expected that greater variability in hydraulic conductivity would lead to shorter first passage times, but this was not the case.

The reason for this counter-intuitive result can be explained in light of the density function of hydraulic conductivity shown in Figure 69(c). An increase in the log-variance results in a slightly heavier upper tail, but a decrease in the mode. The mode of a log-normal distribution occurs at the peak of the density function. Hence, an increase in the log-variance will yield a greater increase in the number of zones with very low conductivity in comparison to the increase in the number of zones with very high hydraulic conductivity. The liquid will be forced to travel farther in the interlift zone to reach pervious channels or to proceed downward in less conductive channels in the lift below. Hence, the first-passage time is longer when the log-variance of hydraulic conductivity is increased.

Results of Macropore Model with Regard to the Flux

The flux was computed by summing the rates of flow in the tubes in the bottomlift. Since the rate of flow in each tube is a realization of a random variable, the distribution of the sum of the flow rates should be approximately log normal by virtue of the central limit theorem. Normality was checked, as described by Benson (1989).

Number of Channels of a Partition--

Figures 70(a) and (b) depict the mean and coefficient of variation of the flux, respectively, as a function of the mean number of channels

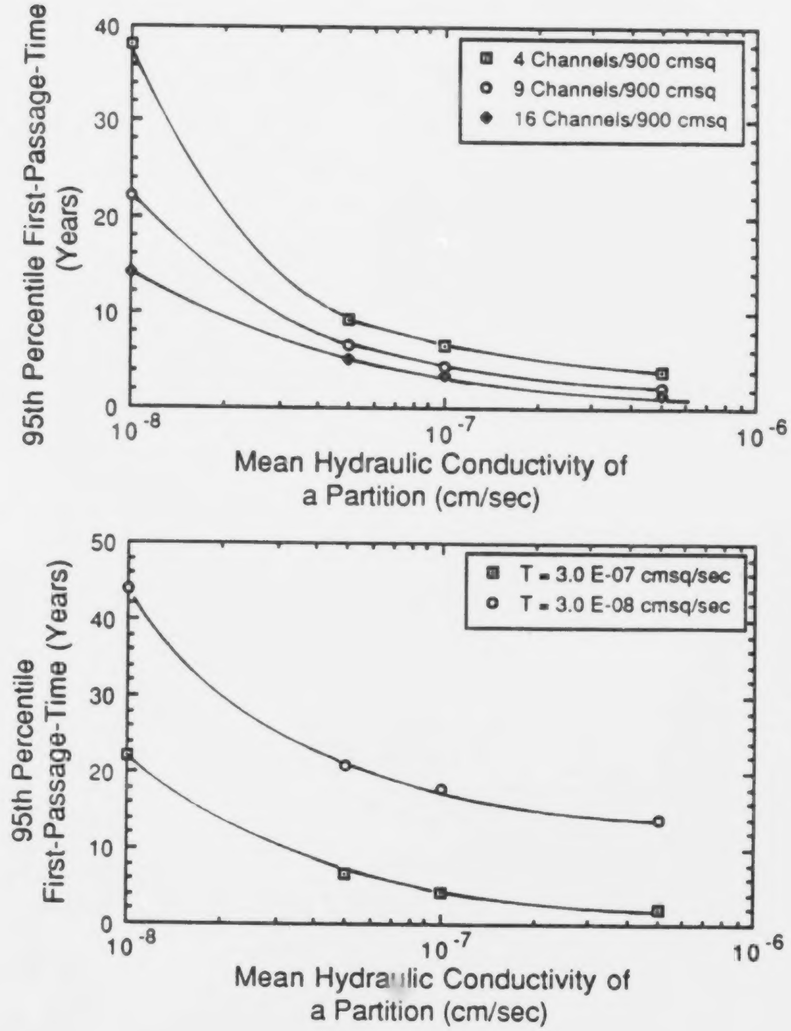

Figure 68. Effect of the mean hydraulic conductivity of a partition, (a) the mean number of channels, and (b) the transmissivity of the interlift zone on the 95th percentile first-passage-time.

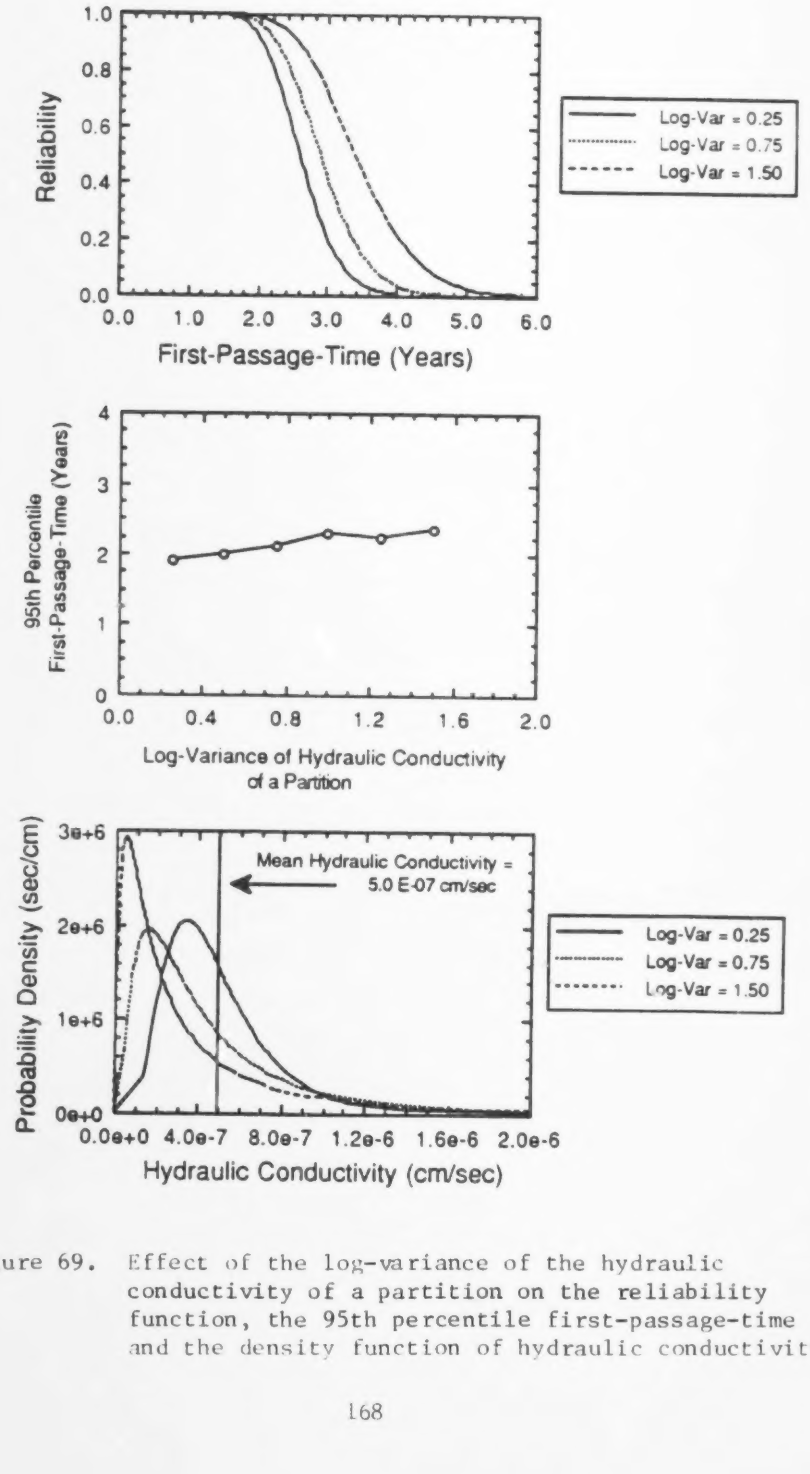

Figure 69. Effect of the log-variance of the hydraulic conductivity of a partition on the reliability function, the 95th percentile first-passage-time and the density function of hydraulic conductivity.

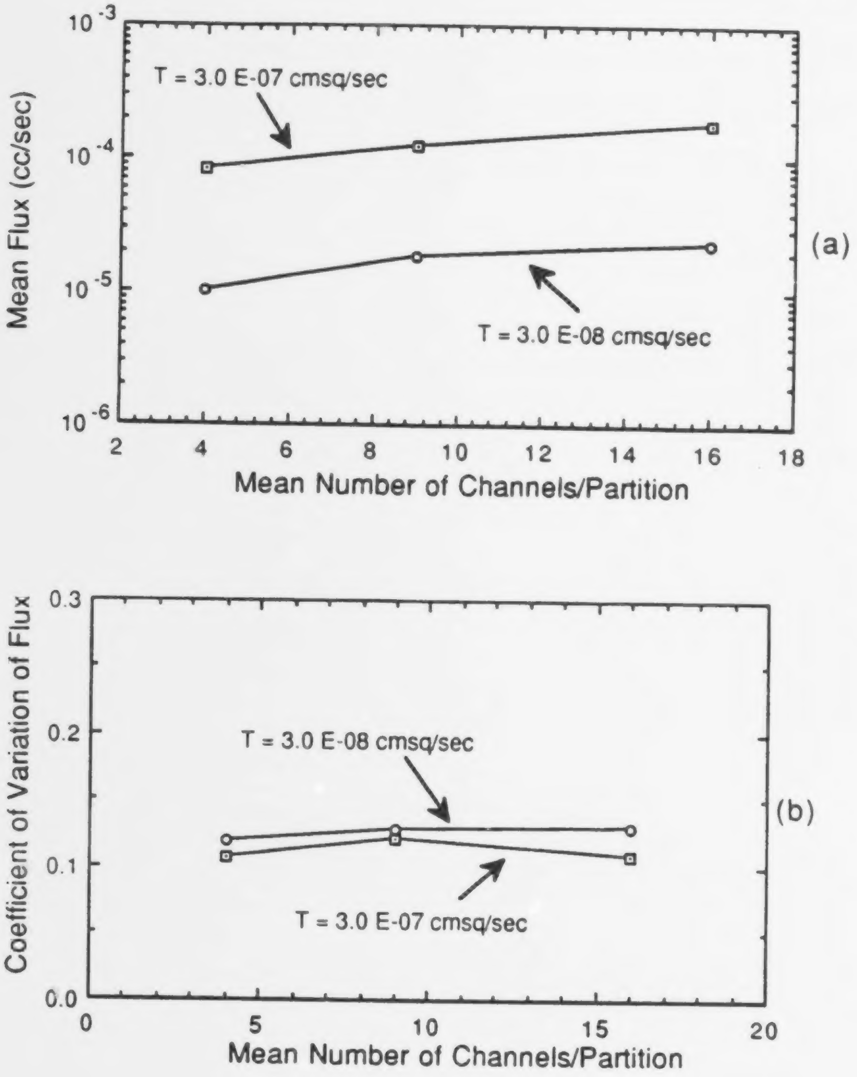

Figure 70. Effects of number of flow channels per partition on flux.

of a partition and the transmissivity of the interlift zone. The mean flux decreases slightly when the mean number of channels is reduced because liquid must dissipate more energy as the liquid travels between channels in the interlift zone. Furthermore, an order of magnitude change in the transmissivity of the interlift zone results in a corresponding change in the mean flux. The transmissivity of the interlift zone has a much more significant effect than the number of flow channels per partition.

The coefficient of variation of the flux is insensitive to the mean number of channels and the transmissivity of the interlift zone. Only a slight increase in the coefficient of variation occurs when the mean number of channels is increased or the transmissivity of the interlift zone is decreased.

Mean Hydraulic Conductivity of a Partition--

The sensitivity of the distribution of the flux to mean hydraulic conductivity of a partition and the transmissivity of the interlift zone are shown in Figures 71(a) and (b). Figure 71(a) shows that mean flux decreases as the mean hydraulic conductivity of a partition is reduced, but an order of magnitude decrease in the mean hydraulic conductivity of a partition does not result in an order of magnitude decrease in the mean flux. The results shown in Figure 71(a) also show that a decrease in the transmissivity of the interlift zone results in a decrease in the mean flux but the decrease in the mean flux becomes less significant as the mean hydraulic conductivity of a partition is reduced.

Figure 71(b) depicts the coefficient of variation of the flux as a function of the mean hydraulic conductivity of a partition. The figure shows that the coefficient of variation increases as the mean hydraulic conductivity is reduced and also shows that the increase in the coefficient of variation is damped when the transmissivity of the interlift zone is reduced. The damping effect due to a decrease in the transmissivity of the interlift may be an artifact of the formulation of the model. The transmissivity is assumed to be a deterministic variable and has more influence on the flux as the magnitude of the transmissivity is reduced. Hence, when the transmissivity is reduced, the fact that it is deterministic results in less dispersion of the flux.

Log-Variance of Hydraulic Conductivity of a Partition--

Figure 72 presents the mean flux as a function of the log-variance of hydraulic conductivity, the transmissivity of the interlift zone, and the number of lifts. Figure 72(a) shows that the mean flux decreases as the log-variance of hydraulic conductivity of a partition is reduced. A similar effect was shown earlier in terms of first-passage time.

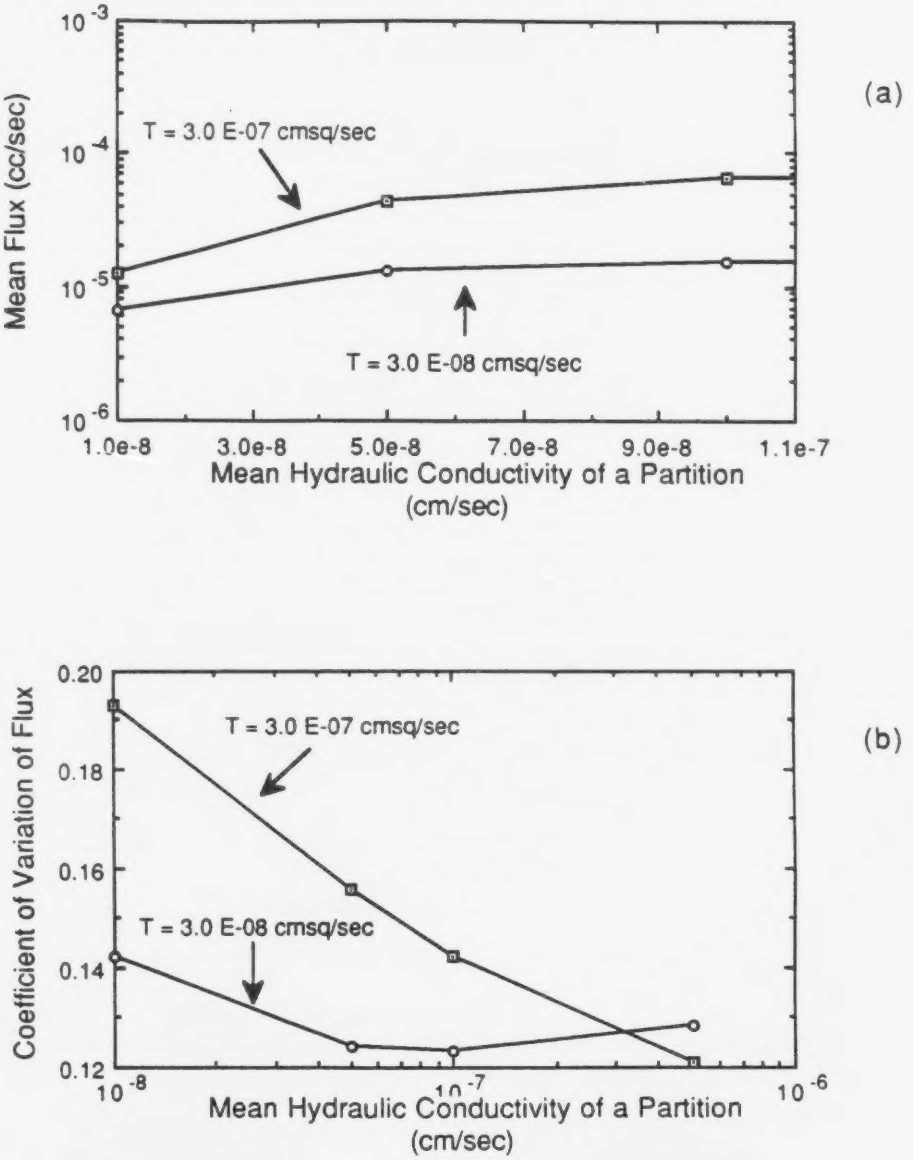

Figure 71. Effect of mean hydraulic conductivity upon flux.

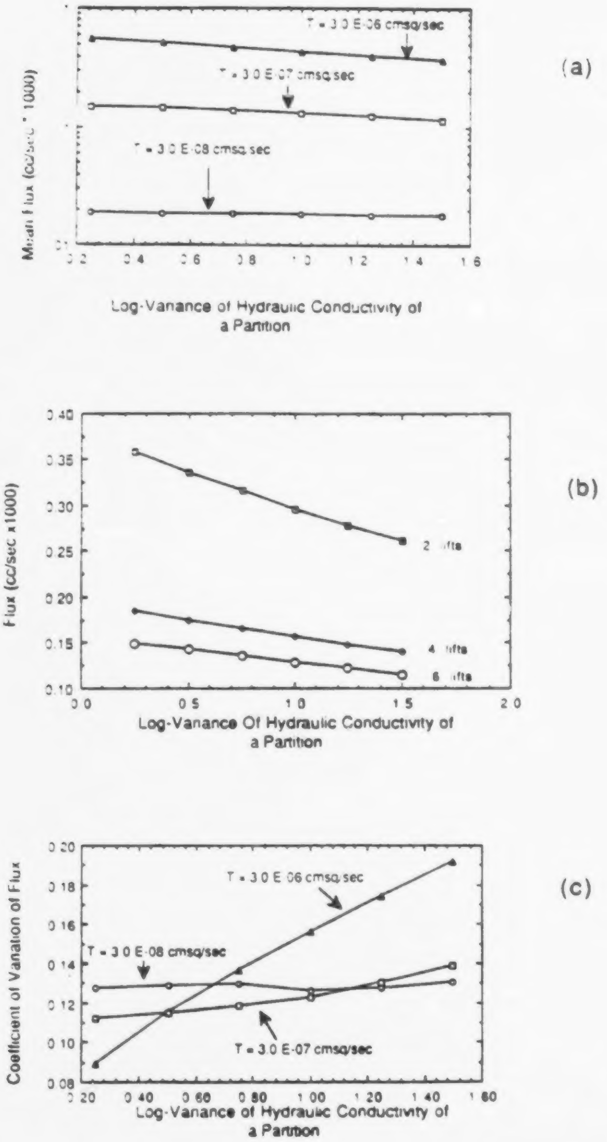

Figure 72. Effect of log-variance of hydraulic conductivity upon flux.

Figure 72(b) is similar to Figure 72(a) except that the number of lifts is varied and the transmissivity is assumed to be 3.0 x 10-7 cm2 sec-1. The trend shown in Figure 72(b) is similar to the trend shown in Figure 72(a); the mean flux decreases as the log-variance of the hydraulic conductivity of a partition is increased. This effect occurs even when the liners are thin.

Figure 72(c) depicts the coefficient of variation of the flux as a function of the log-variance of hydraulic conductivity of a partition and the transmissivity of the interlift zone. As expected, an increase in the log-variance results in an increase in the coefficient of variation of the flux. However, the increase in coefficient of variation is damped when the transmissivity of the interlift zone is increased.

Number of Lifts

An increase in the number of lifts should reduce flux and increase first passage time, but the cost of the liner also increases with increasing lifts. Thus, one must strive to minimize flux and maximize first passage time, but not to use so many lifts that the liner is too costly or too thick to be practical.

Figure 73 depicts the mean flux and mean first-passage time as a function of the number of lifts. When more lifts are added to a soil liner, the average first-passage time increases and the mean flux decreases. The first-passage time will be longer as the thickness of the liner is increased, no matter how thick the liner is. Thus, no "optimum" thickness can be defined based on first-passage time. In terms of flux, the flux levels out as the thickness of the liner beocomes large. Beyond 4 to 6 lifts, little reduction in flux is realized as more lifts are added.

The flux in the macropore model was computed by summing the flow rates in the channels in the bottom lift. Since continuity was enforced in the model, the flux is equal to the flow rate through each lift in the liner. Thus, an "equivalent" hydraulic conductivity can be defined as the mean flux divided by the hydraulic gradient and the cross-sectional area of the soil liner being analyzed.

Figure 74 summarizes the equivalent conductivity obtained from the macropore model as a function of the number of lifts and the transmissivity of the interlift zone. In each case, the equivalent hydraulic conductivity decreases as the thickness of the soil liner increases. The decrease in equivalent conductivity with increasing numbers of lifts is minimal for more than 4 to 6 lifts, i.e., for liners thicker than 600 to 900 mm (2 to 3 ft). Furthermore, the importance of bonding lifts together effectively is seen clearly in Figure 74; as a much lower equivalent hydraulic conductivity is achieved with a few well bonded lifts than with many poorly-bonded lifts.

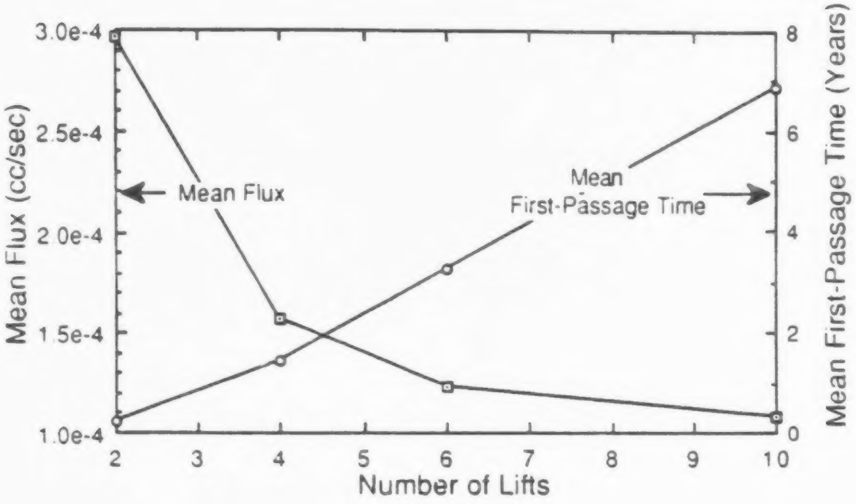

Figure 73. Effect of number of lifts on mean flux and mean first-passage time.

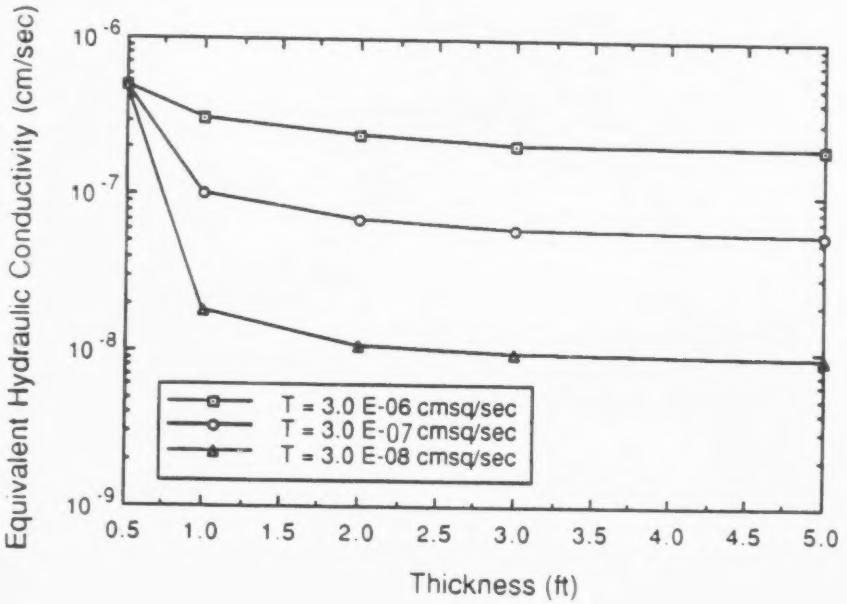

Figure 74. Effect of thickness on mean equivalent hydraulic conductivity.

CONCLUSIONS

The following conclusions are drawn from analyses presented in this section:

1. Decreasing the mean hydraulic conductivity within the lifts of a compacted soil liner increases the minimum time of travel (called "first-passage time" herein) and decreases the flux of water flowing through the liner.

2. Decreasing the dispersion (scatter) in hydraulic conductivity within the lifts of a soil liner neither lengthens the first-passage time nor reduces the flux. In fact, greater dispersion in hydraulic conductivity generally led to longer first-passage times and lower fluxes. Of far greater importance than the dispersion of hydraulic conductivity of a lift is the effectiveness of bonding adjacent lifts.

3. If the effective porosity of the soil is low (on the order of 0.05 or less), the first-passage time will almost inevitably be short, and the influence of variance in hydraulic conductivity is negligible in terms of predicting first-passage time.

4. Thicker liners lead to proportionally longer first-passage time. No ideal thickness of a soil liner can be determined from examination of first-passage time.

5. As the number of lifts increases, the benefits in terms of reduced flux through the liner diminish. The calculations presented suggest that building a liner with more than 4 to 6 lifts does little to reduce the flux or overall hydraulic conductivity of the liner.

6. The Macropore Model showed that the most important variables controlling first-passage time and flux were mean hydraulic conductivity of a lift and transmissivity of the interlift zone. The results suggested that much more benefit can be derived by bonding lifts together well than by adding more poorly-bonded lifts. In other words, the calculations indicated that better results would be achieved using a few well-bonded lifts than many poorly-bonded lifts.

7. Based on the preceding conclusions, it is concluded that attention should be focused on building each lift of soil so it has a low mean hydraulic conductivity and on bonding lifts effectively. Adding more lifts (beyond a critical minimum of lifts) and reducing the scatter in hydraulic conductivity within a given lift will not be very effective in lengthening first-passage time or lowering flux.

REFERENCES

Adriano, D. C. and H. E. Doner. 1982. Bromine, Chlorine, and Fluorine Methods of Soil Analysis. Second Ed. Chemical and Microbiological Properties, Agronomy Monograph. pp. 449-455.

Aisenstein, B., E. Diamant and L. Saidoff. 1961. Fat Clay as a Blanketing Material for Leaky Reservoirs. Proceedings of the Fifth International Conference of Soil Mechanics and Foundation Engineering, Paris, France. 2:523-529.

Ali, E. M., C. A. Moore and I. L. Lee. 1982. Statistical Analysis of Uncertainties in Flow of Liquids Through Landfills. In: Land Disposal of Hazardous Waste. Proceedings of the Eighth Annual Research Symposium at Ft. Mitchell, KY. March 8-10. pp. 26-52.

Alkire, B. D. and J. Jashimuddin. 1984. Changes in Strength of Silt Due to Freeze-Thaw. Jour. of Tech. Topics in Civil Engineering 100:48-53.

Alkire, B. D. 1980. A Mechanism for Predicting the Effect of Cyclic Freeze-Thaw on Soil Behavior. Proc. Second Int. Conf. on Ground Freezing, Trondheim, Norway. pp. 285-296.

Anderson, D. C., J. O. Sai, and A. Gill. 1984. Surface Impoundment Soil Liners: Permeability and Morphology of a Soil Liner Permeated by Acid and Field Permeability Testing for Soil Liners. Report to U.S. Environmental Protection Agency, by K. W. Brown and Associates, Inc., College Station, Texas. EPA Contract #68-03-2943.

Anderson, D. C. 1986. Soil Liners for Hazardous Waste Disposal Facilities. In: Proceedings of the National Conference on Hazardous Wastes and Hazardous Materials in Atlanta, Georgia. March 4-6, 1986. pp. 206-209.

Anderson, D. C. and J. A. Rehage. 1986. Weathering Effects on Exposed Soil Liners. Proc. Twelfth Annual Research Symposium. Land Disposal, Remedial Action, Incineration and Treatment of Hazardous Waste. U.S. EPA. Cincinnati, OH.

Anderson, D. C., K. W. Brown and J. A. Rehage. 1986. Minimum Compacted Soil Thickness. Under Subcontract to GCA Corp. for U. S. Environmental Protection Agency, Office of Disposal Branch, Washington, D.C. EPA Contract No. 68-01-6871.

Barst, J. F. 1965. Subaqueously Formed Shrinkage Cracks in Clay. Journal of Sedimentary Petrology 35:348-353.

Baver, L. D., W. H. Gardner and W. R. Gardner. 1972. Soil Physics. John Wiley and Sons, Inc. New York, N.Y. 498 p.

Bennion, D. W. and J. C. Griffiths. 1966. A Stochastic Model for Predicting Variations in Reservoir Rock Properties. Trans, AIME 237 Part 2, 9-16.

Benson, C. H. 1989. A Stochastic Analysis of Water and Chemical Flow Through Compacted Soil Liners. Ph.D. Dissertation, Univ. of Texas, Austin, Texas, 246 p.

Bogardi, I. and W. E. Kelly. 1986. Study of Clay Liners: Principles for Predicting Performance of Clay Liners. Univ. Nebraska Engineering Research Center. Lincoln, NE. 44 p.

Boutwell, G. C. and V. R. Donald. 1982. Compacted Clay Liners for Industrial Waste Disposal. Presented at the ASCE National Meeting in Las Vegas. April 26, 1982.

Bowman, R. S. 1984. Evaluation of Some New Tracers for Soil Water Studies. Soil Science Society of American Journal 48:987-993.

Boynton, S. S. 1983. An Investigation of Selected Factors Affecting the Hydraulic Conductivity of Compacted Clay. M.S. Thesis. Civil Engineering Department, University of Texas, Austin, Texas. 79 p.

Boynton, S. S. and D. E. Daniel. 1985. Questions Concerning Hydraulic Conductivity of Compacted Clay. J. of Geotechnical Eng. 111:1-31.

Brewer, R. 1976. Fabric and Mineral Analysis of Soils. Robert Krieger Publ. Co. Huntington, NY. 482 p.

Broms, B. B. 1963. The Bearing Capacity of Flexible Pavements Subjected to Frost Action. Highway Research Board Record 39. Washington, D.C. pp. 166-177.

Broms, B. B. and L. Y. C. Yao. 1964. Shear Strength of a Soil after Freezing and Thawing. Soil Mechanics and Foundation Division, Proc. of the ASCE. 90:1-26.

Brown, K. W. 1986. Use of Soils to Retain Wastes in Landfills and Surface Impoundment. Proceedings of the Workshop entitled Utilization, Treatment and Disposal of Waste on Land. Soil Science Society of America. Madison, Wisconsin. pp. 279-300.

Brown, K. W., J. C. Thomas and J. W. Green. 1986. Field Cell Verification of the Effects of Concentrated Orgranic Solvents on the Conductivity of Compacted Soils. Haz. Waste & Haz. Matls. 3:1-19.

Churchill, R. V. 1972. Operational Mathematics. McGraw-Hill Book Company, New York, 481 p.

Currie, J. B. 1974. Study Examines Fracture Porosity and Permeability in Stratigraphic Traps. Soil and Gas Journal, June 24. pp. 178-181.

Daniel, D. E. 1984. Predicting Hydraulic Conductivity of Clay Liners. J. of Geotech. Eng. 110:285-300.

Day, S. R., D. E. Daniel and S. S. Boynton. 1985. Field Permeability Test for Clay Liners. In: Hydraulic Barriers in Soil and Rock. ASTM STP 874.

Day, S. R. 1984. A Field Permeability Test for Compacted Clay Liners. M.S. Thesis, University of Texas, Austin, Texas. 105 p.

Dubose, L. A. 1956. Discussion. In: W. G. Holtz and H. G. Gibbs (eds.) Engineering Properties of Expansive Clays. Transactions of ASCE 121:641-677.

Duguid, J. O. and P. C. Y. Lee. 1977. Flow in Fractured Porous Media. Water Resources Research 13:558-566.

Elsbury, B. R., D. E. Daniels, G. A. Sraders and D. C. Anderson. 1988. Lessons Learned from a Compacted Clay Liner. Paper presented at the October 6-8, 1988 ASCE Texas Section Fall Meeting. College Station, Texas 77843, 29 pp.

Elsbury, B. R., G. A. Sraders, D. C. Anderson, J. A. Rehage, J. O. Sai and D. E. Daniel. 1988. Field and Laboratory Testing of a Compacted Soil Liner. McClelland Engineers, Inc., 142 p.

EPA. 1984. Soil Properties Classification and Hydraulic Conductivity Testing. U. S. Environmental Protection Agency, Washington, D. C. SW-925.

EPA. 1986. SOILINER Model - Documentation and User's Guide (Version 1). EPA-530/SW-86-006.

Fickies, R. H., R. H. Fakundiny and E. T. Mosley. 1979. Geotechnical Analysis of Soil Samples from Test Trench at Western New York Nuclear Service Center. West Valley, N.Y. Report to U.S. Nuclear Regulatory Commission.

Folkes, D. J. 1982. Fifth Canadian Geotechnical Colloquium: Control of Contaminant Migration by the Use of Liners. Canadian Geotechnical Journal 19:320-344.

Garcia-Bengochea, I. 1978. The Relation Between Permeability and Pore Size Distribution of Compacted Clayey Silts. Report to the Indiana Dept. of Hwys., Purdue Univ., Lafayette, IN. pp. 1-179.

Gardner, W. R. 1958. Some Steady-State Solutions of the Unsaturated Moisture Flow Equation With Application to Evaporation From a Water Table. Soil Science 8:228-232.

Gee, G. W. and J. W. Bauder, 1986. Particle Size Analysis. Chapter 15. In: A. Klute (ed.). Methods of Soil Analysis, Part 1. Physical and Mineralogical Methods. Second Edition. Agronomyy 9:383-412. American Society of Agronomy, Madison, WI.

Gordon, M. E. and P. M. Huebner. 1983. An Evaluation of the Performance of Zone of Saturation Landfills in Wisconsin. Presented at the Sixth Annual Madison Waste Conference. September 14-15, 1983. University of Wisconsin.

Green, J. W., K. W. Brown and J. C. Thomas. 1985. Effective Porosity of Compacted Clay Soils Permeated With Organic Liquids. Proc. 11th Annual Research Symposium. Land Disposal of Hazardous Waste. EPA 600/9-85-013. Cincinnati, OH.

Griffin, R. A., B. L. Herzog, T. M. Johnson, W. J. Morse, R. E. Hughes, S. F. J. Cou and L. R. Follmer. 1985. Mechanisms of Contaminant Migration Through a Clay Barrier. Case Study, Wilsonville, Illinois. In: Land Disposal of Hazardous Waste: Proceedings of the Eleventh Annual Research Symposium. pp. 27-37.

Griffin, R. A., R. E. Hughes, L. R. Follmer, C. J. Stohr, W. J. Morse, T. M. Johnson, J. K. Bartz, J. D. Steele, K. Cartwright, M. M. Killey and P. B. DuMontelle. 1984. Migration of Indusrrial Chemicals and Soil-Waste Interactions at Wilsonville, Illinois. In: Proceedings of the Tenth Annual Research Symposium on Land Disposal of Hazardous Waste. EPA-600/9-84-007.

Grimmett, G. R. and D. R. Stirzaker. 1982. Probability and Random Processes. Claredon Press, Oxford, England, 354 p.

Haxo, H. E., Jr., T. P. Lahey and M. L. Rosenberg. 1988. Factors in Assessing the Compatibility of FMLs and Waste Liquids. Project Summary, EPA/600/S2-88/017.

Harrop-Williams, K. 1985. Clay Liner Permeability: Evaluation and Variation. Journal of Geotechnical Engineering 111:1211-1225.

Herzog, B. L. and W. J. Morse. 1984. A Comparison of Laboratory and Field Determined Values of Hydraulic Conductivity at a Disposal Site. pp. 30-52. In: Proceedings of the Seventh Annual Madison Waste Conference, University of Wisconsin-Extension, Madison, Wisconsin.

Hilf, J. F. 1975. Compacted Fill. In: H. F. Winterkorn and H. Fang (eds) Foundation Engineering Handbook. pp. 244-311.

Hillel, D. 1971. Soil and Water: Physical Principle and Processes. Academic Press. New York. 288 pp.

Holtz, W. G. and H. J. Gibbs. 1956. Engineering Properties of Expansive Clays. American Society of Civil Engineers Transactions 121: 641-677.

Holtz, R. D. and W. D. Kovacs. 1981. An Introduction to Geotechnical Engineering. Prentice-Hall, Inc. Englewood Cliffs, NJ. 733 p.

Horton, R. and M. L. Thompson. 1986. Determination of Effective Porosity of Soil Material. U.S. EPA Hazardous Waste Engineering Research Laboratory Grant No. CR-811093-01-0. Cincinnati, OH.

Horton, R., M. L. Thompson and J. F. McBride. 1985. Estimating Transit Times of Noninteracting Pollutants Through Compacted Soil Materials. Proc. 11th Annual Research Symposium Land Disposal of Hazardous Waste. pp. 275-282. EPA/600/9-85/013. Cincinnati, OH.

Hubbert, M. K. 1940. The Theory of Ground Water Motion. J. Geol. 48:785-944.

Jessberger, H. L. and D. L. Carbee. 1970. Influence of Frost Action on the Bearing Capacity of Soils. Highway Research Board Record 304, Washington, D.C. pp. 14-26.

Klute, A. 1986. Water Retention: Laboratory Methods. Chapter 26. In: A. Klute (ed.). Methods of Soil Analysis, Part 1. Physical and Mineralogical Methods. Second Edition. Agronomyy 9:635-662. American Society of Agronomy, Madison, Wisconsin.

Krauskopf, K. B. 1979. Introduction to Geochemistry. Second Edition. McCraw-Hill Book Co., NY. pp. 140-164.

Law, J. 1944. A Statistical Approach to the Interstitial Heterogeneity of Sand Reservoirs, Trans. AIME 155:202-222.

Liao, Wing Ping. 1989. Transport of Inorganic Compounds Through Compacted Clay. Ph.D. Dissertation. The University of Texas at Austin, 198 p.

McCarthy, D. F. 1982. Essentials of Soil Mechanics and Foundations: Basic Geotechnics Second Edition. Reston Publ. Co., Reston, VA. pp. 31-101.

McDowell, Chester. 1946. Progress Report on Development and Use of Strength Tests for Subgrade Soils and Flexible Base Materials. Proc. Highway Research Board 26:484-511.

Mitchell, J. K., D. R. Hooper and R. G. Campanella. 1965. Permeability of Compacted Clay. Journal of Soil Mechanics and Foundations. ASCE 91 (SM 4):41-65.

Mitchell, J. K. 1976. Fundamentals of Soil Behavior. John Wiley and Sons, Inc., New York, NY. 422 p.

Moore, C. A. and E. M. Ali. 1982. Permeability of Cracked Clay Liners. In: Land Disposal of Hazardous Waste, Proceedings of the Eighth Annual Research Symposium at Ft. Mitchell, KY. pp. 174-190.

Murphy, W. L. and P. A. Gilbert. 1985. Settlement and Cover Subsidence of Hazardous Waste Landfills. Report to U.S. EPA, U.S. Army Engineers Waterways Experiment Station, Vicksburg, MS. (EPA Contract # AD-96-F-2-A079). pp. 1-110.

Nielson, D. R., J. W. Biggar and K. T. Erh. 1973. Spatial Varaibility of Field-Measured Soil Water Properties. Hilgardia 42:215-259.

Olson, R. E. and D. E. Daniel. 1981. Field and Laboratory Measurement of the Permeability of Saturated and Partially Saturated Fine-Grained Soils. In: Permeability and Groundwater Contaminant Transport, ASTM STP 746.

Omoti, U. and A. Wild. 1979a. Use of Fluorescent Dyes to Mark the Pathways of Solute Movement Through Soils Under Leaching Conditions: 1. Laboratory Experiments. Soil Science 128:28-33.

Omoti, U. and A. Wild. 1979b. Use of Fluorescent Dyes to Mark the Pathways of Solute Movement Through Soils Under Leaching Conditions: 2. Field Experiments. Soil Science ?:98-104.

Parsons, R. W. 1966. Permeability of Idealized Fractured Rock. Soc. Pet. Eng. J. 6:126-136.

Patrick, D. M. 1975. Scanning Electron Microscope Evaluation of Fabric in Impact-Compacted Kaolinite. U.S. Army Engineers Waterways Exp. Sta., Vicksburg, MS. pp. 1-34.

Peyton, G. R., J. P. Gibb, M. H. LeFaiure, J. D. Ritchey, S. L. Burch and M. J. Barcelona. 1986. Effective Porosity of Geologic Materials. Proc. 12th Annual Research Symposium Land Disposal of

Hazardous Waste. U.S. EPA Hazardous Waste Engineering Laboratory. Cincinnati, OH.

Puckett, W. E., J. H. Dane and B. F. Hajek. 1985. Physical and Mineralogical Data to Determine Soil Hydraulic Properties. Soil Science Society of America Journal 49:831-836.

Rehage, J.A., R. L. Shiver, D. C. Anderson, W. W. Crawley, M. Unger and C. Cocke. 1986. Weathering on Exposed Soil Liners and Their Prevention. U.S. Environmental Protection Agency Hazardous Waste Eng. Research Lab. Contract No. 68031816.

Reynolds, E. R. C. 1966. The Percolation of Rainwater Through Soil Demonstrated by Fluorescent Dyes. J. of Soil Science 17:127-132.

Ritchie, J. T., D. E. Kissel and E. Burnett. 1972. Water Movement in Undisturbed Swelling Clay Soil. Soil Science Society of America Proceedings 36:874-879.

Rogowski, A. S. 1986. Hydraulic Conductivity of Compacted Clay Soils. Proc. 12th Annual Research Symposium on Land Disposal, Remedial Action, Incineration and Treatment of Hazardous Waste. U.S. EPA. Cincinnati, OH.

Rogowski, A. S. 1989. Relationship of Laboratory and Field Determined Hydraulic Conductivity in Compacted Clay Layer (Draft Final Report) EPA, 247 p.

Russo, D. and E. Bressler. 1981a. Effect of Field Variability in Soil Hydraulic on Solutions of Unsaturated Water and Salt Flows. Soil Science Society of America Journal 45:675-681.

Russo, D. and E. Bressler. 1981b. Soil Hydraulic Properties as Stochastic Processes. In: An Analysis of the Field Spatial Variability. Soil Sci. Soc. Am. J. 45:682-687.

Rutter, A. J. 1964. Studies in the Water Relations of Pinus sylvestris in plantation conditions. II. The Annual Cycle of Soil Moisture Change and Derived Estimates of Evaporation. J. Appl. Ecol. 1, 29-44.

Seed, H. B. and C. K. Chan. 1959. Structure and Strength Characteristics of Compacted Clays. J. Soil Mechanics and Foundation Division 85:87-128.

Shiver, R. and D. C. Anderson. 1985. White Paper No. 8: Lift Thickness Considerations. U.S. EPA. Washington, D.C.

Sinnock, S., Y. T. Lin and M. S. Tierney. 1986. Preliminary Estimates of Groundwater Travel Time and Radionuclide Transport at the Yucca

Mountain Repository Site. Sandia National Laboratories, Albuquerque, New Mexico. 73 p.

Skempton, A. W., R. L. Schuster and D. J. Petley. 1969. Joints and Fissures in the London Clay at Wraysbury and Edgeware. Geotechnique 19:205-217.

Smart, P. L. and I. M. S. Laidlaw. 1977. An Evaluation of Some Fluorescent Dyes for Water Tracing. Water Resources Research 13:15-33.

Smettem, K. R. J. and S. T. Trudgill. 1983. An Evaluation of Some Fluorescent and Non-Fluorescent Dyes in the Identification of Water Transmission Routes in Soils. J. of Soil Science 34:45-56.

Smith, S. J. and R. J. Davis. 1974. Relative Movement of Bromide and Nitrate Through Soils. Journal of Environmental Quality 5:152-155.

Smith, L. and R. A. Freeze. 1979. Stochastic Analysis of Steady State Groundwater Flow in a Bounded Domain 1. One-Dimensional Simulations. Water Resources Research 15:521-528.

Spangler, M. G. and R. L. Handy. 1982. Soil Engineering. 4th Ed. Harper and Row, New York, NY pp. 819.

Speake, R. C. 1986. An Analysis of Selected Factors Controlling or Affecting the Hydraulic Conductivity of Compacted Soil Liners. M.S. Thesis, Texas A&M Univ., College Station, TX. 115 p.

Specht, R. L. 1957. Dark Island Heath (Ninety-Mile Plain, South Australia). IV. Soil moisture patterns produced by rainfall interception and stemflow. Aust. J. Bot. 5, 137-50.

Tamm, C. O., and T. Troedsson. 1957. A New Method for the Study of Water Movement in Soil. Geol. For Stockh. Forh. 79, 581-7.

Todd, D. K. 1959. Ground Water Hydrology. John Wiley and Sons, Inc., New York, NY. pp. 44-61.

Trudgill, S. T., A. M. Pickles, K. R. J. Smettem, and R. W. Crabtree. 1983. Soil Water Residence Time and Solute Uptake. I. Dye Tracing and Rainfall Events. J. of Hydrology 60:257-279.

Turcotte, D. L. and G. Schubert. 1982. Geodynamics: Applications of Continuum Physics to Geological Problems. John Wiley and Sons, NY. pp. 231-238.

Turnbull, Willard J. and Charles R. Foster. 1958. Stabilization of Materials by Compaction. Journal of the Soil Mechanics and Foundations Division Transactions. ASCE 123:1.

U.S. Bureau of Reclamation. 1974. Design of Small Dams. United States Printing Office. Washington, D.C. 816 p.

Voigt, G. K. 1960. Distribution of Rainfall Under Forest Stands. Forest Sci. 9:2-10.

Wang, M. C. and C. C. Huang. 1984. Soil Compaction and Permeability Prediction Models. Journal of Environmental Engineering 110:1063-1083.

White, W. A. 1964. Origin of Fissure Fillings in a Pennsylvanian Shale in Vermilion County, Illinois. Transactions: Illinois Academy of Science 57:208-215.

Whittig, L. D. and W. R. Allardice. 1986. X-ray Diffraction Techniques. Chapter 12. In: A. Klute (ed.). Methods of Soil Analysis, Part 1. Physical and Mineralogical Methods. Second Edition. Agronomyy 9:331-362. American Society of Agronomy, Madison, WI.

Wood, L. E., A. G. Altschaeffl and C. W. Lovell. 1983. Effects of Pore Size Distribution on Permeability and Frost Susceptibility of Selected Subgrade Materials. Report to Indiana Dept. of Hwys., Purdue Univ., Lafayette, IN.

Wood, J. L. 1976. Influence of Repetitious Freeze-Thaw on Shear Strength of Leda (Messena) Clay. Ph.D. Dissertation, Clarkson College of Technology. p. 152.

Yao, L. Y. and B. B. Broms. 1965. Excess Pore Pressure which Develop During Thawing of Frozen Fine-grained Subgrade Soils. Highway Research Record 101. Washington, D.C. pp. 39-57.

Yoder, E. J. and K. B. Woods. 1946. Compaction and Strength Characteristics of Soil Aggregate Mixtures. Proc of Highway Research Board 26:511-520.

APPENDIX A

A relation is derived that relates permeability to channel radius and channel density. Basic physics and mathematics are used to develop this mathematical expression. This method is similar to that used by Turcotte and Schubert (1982).

Let there be an impermeable slab with thickness ℓ, with a planar fracture of thickness h, perpendicular to the slab. Let the fracture be full of a fluid with density ρ and viscosity μ. Let the pressure on one side be maintained at P_2 and on the other at P_1 so that there is a pressure gradient in the fracture of $(P_2 - P_1)/\ell$. Let the z axis denote vertical distance and the x axis denote the horizontal. Then according to Newton's law, the shear stress exerted by the fluid on the walls of the fracture is τ such that

$$\tau = \mu \frac{dv}{dx} \qquad \text{(A.1)}$$

where dv/dx is the velocity gradient in the channel perpendicular to the direction of flow. A fluid in which (A.1) holds is said to be Newtonian.

The net pressure on a vertical layer of fluid must be zero. Let a layer have thickness dx. Then

$$P_2\,dx - P_1\,dx + \tau(x)\,\ell - \tau(x + dx)\,\ell = 0 \qquad \text{(A.2)}$$

Notice that

$$\tau(x + dx)\,\ell = \left(\tau(x) + \frac{d\tau}{dx}\,dx\right)\ell \qquad \text{(A.3)}$$

Thus

$$\frac{d\tau}{dx} = -\left(\frac{P_2 - P_1}{\ell}\right) = \frac{dP}{dz} \qquad \text{(A.4)}$$

as dx goes to zero. Equation (A.4) is the equation of motion. Differentiating (A.1) by x,

$$\frac{d\tau}{dx} = \frac{d}{dx}\left(\mu \frac{dv}{dx}\right) = \mu \frac{d^2v}{dx^2} \qquad \text{(A.5)}$$

Thus

$$\frac{dP}{dz} = \mu \frac{d^2v}{dx^2} \qquad \text{(A.6)}$$

This can be rewritten as

$$\frac{d^2v}{dx^2} = \frac{1}{\mu}\frac{dP}{dz} \tag{A.7}$$

It is possible to solve for v by integration. Integrating (A.7),

$$\frac{dv}{dx} = \frac{1}{\mu}\frac{dP}{dz}x + C_1 \tag{A.8}$$

where C_1 is a constant. Integrating again,

$$v = \frac{1}{2\mu}\frac{dP}{dz}x^2 + C_1x + C_2 \tag{A.9}$$

where C_2 is a constant. A coordinate system is defined so that $x = 0$ is in the center of the fracture. Then the faces are at $x = \underline{+}h/2$. If the boundary conditions are imposed so that the velocity is zero at the walls (the "no-slip" condition) then

$$v = \frac{1}{2\mu}\frac{dP}{dz}\left(x^2 - \frac{h^2}{4}\right) \tag{A.10}$$

Integrating all such layers in the fracture and dividing by the thickness h will give the average velocity.

$$v = \frac{1}{h}\int_{-h/2}^{h/2}\frac{1}{2\mu}\frac{dP}{dz}\left(x^2 - \frac{h^2}{4}\right)dx$$

$$= \frac{1}{2\mu h}\frac{dP}{dz}\left[\frac{x^3}{3} - \frac{h^2x}{4}\right]_{-h/2}^{h/2}$$

$$= \frac{1}{2\mu}\frac{dP}{dZ}\left[\frac{h^2}{12} - \frac{h^2}{4}\right]$$

$$= \frac{-h^2}{12\mu}\frac{dP}{dz} \tag{A.11}$$

Darcy's law defines the Darcy velocity, the average velocity to be

$$v = \frac{-k}{\mu}\frac{dP}{dz} \tag{A.12}$$

From (A.11) and (A.12) we can derive

$$k = \frac{h^2}{12} \tag{A.13}$$

known as the Muskat relation (Muskat, 1949). Thus, the permeability of a fissure with smooth parallel walls is a function of aperture, h. If the aperture is in centimeters, the permeability will be in square centimeters.

The permeability of the entire slab with this fracture is given by the cubic law.

$$\overline{v} = \frac{h^3}{12D}\frac{dP}{dx} \tag{A.14}$$

where D is fracture spacing. This law comes from the following reasoning. Let the slab have width w and length L. Then the volumetric flow in the slab is

$$Q = \int_{-h/2}^{h/2} w\ v(x)\ dx$$

Substituting v from equation (A.10),

$$Q = \frac{w}{2\mu}\ \frac{dP}{dz}\ \int_{-h/2}^{h/2}\left(x^2 - \frac{h^2}{4}\right)dx$$

$$= \frac{w}{2\mu}\ \frac{dP}{dz}\ \left[\frac{x^3}{3} - \frac{h^2x}{4}\right]_{-h/2}^{h/2}$$

$$= -\frac{wh^3}{12\mu}\ \frac{dP}{dz} \tag{A.15}$$

Darcy velocity is volumetric flow divided by area.

$$v = Q/A$$

Since

$$A = wL \tag{A.16}$$

then

$$v = -\frac{h^3}{12\mu L}\ \frac{dP}{dz} \tag{A.17}$$

Now if the slab is infinitely long, and if there are an infinite number of fractures evenly spaced with a spacing D, then (A.17) becomes

$$\bar{v} = -\frac{h^3}{12\mu D}\frac{dP}{dz} \tag{A.18}$$

which is the "cubic law." Separating the permeability out of this statement of Darcy's law,

$$k = \frac{h^3}{12D}$$

This is the permeability of a slab with an infinite number of fractures with spacing D and aperture h. So far it has been assumed that the fracture is parallel to the pressure gradient and perpendicular to the slab. If the parallel faces are at an angle α from the z axis, then

$$k = \frac{h^3 \cos^2\alpha}{12D} \tag{A.19}$$

Let this permeability be known as k_f where the subscript f denotes fracture. If the slab itself has a permeability k_r, where r denotes the soil or rock, then the total permeability is given by

$$k = k_r + k_f \tag{A.20}$$

(Parsons, 1966). This equation is known in the oil industry as Parsons' Equation. In general, the permeability of a soil liner or any slab is the permeability of the slab matrix plus the permeability of the defects in that slab.

With this in view, let us consider cylindrical channels instead of planar fractures. In this case, consider a channel with radius R. Equation (A.9) becomes

$$v(r) = \frac{-1}{4\mu}\frac{dP}{dz}(R^2 - r^2) \tag{A.21}$$

where r is the distance from the center of the channel, assuming the no-slip condition.

Now consider a cylindrical shell of fluid of radius r and thickness dr. The amount of fluid flowing across a plane intersecting this cylinder is $2\pi r dr\ v(r)$. Thus, the sum of the flow of all such cylinders, from $r = 0$ to $r = R$ would be the total flow in the pipe. Therefore

$$Q = \int_0^R 2\pi r\ v(r)\ dr$$

$$= -2\pi \frac{1}{4\mu} \frac{dP}{dz} \int_0^R (R^2 r - r^3)\, dr$$

$$= \frac{-\pi}{2\mu} \frac{dP}{dZ} \left[R^2 \frac{r^2}{2} - \frac{r^4}{4} \right]_0^R$$

$$= -\frac{\pi R^4}{8\mu} \frac{dP}{dz} \tag{A.22}$$

Since the area of the channel is πR^2, the Darcy velocity is

$$v = -\frac{R^2}{8\mu} \frac{dP}{dz} \tag{A.23}$$

From Darcy's law, the permeability of a cylindrical channel is

$$k = \frac{R^2}{8} \tag{A.24}$$

which is a function only of channel radius. Suppose that the average spacing between channels is D. Then there is one conducting channel per D^2 area. Thus, the flow of fluid through the slab per unit area is

$$\bar{v} = \frac{Q}{D^2} = \frac{\pi R^4}{8D^2} \left(\frac{-1}{\mu}\right) \frac{dP}{dz} \tag{A.25}$$

Thus

$$k = \frac{\pi R^4}{8D^2} \tag{A.26}$$

If the slab has an intrinsic permeability k_r, then the total permeability of a slab of channels with spacing D is

$$k = k_r + \frac{\pi R^4}{8D^2} \tag{A.27}$$

Equations (A.26) and (A.27) can be used to obtain many interesting results because permeability has been quantified in terms of channel radius R and spacing D. It is now possible to evaluate the permeability of compacted soil lifts with defects if the distance between defects is known as well as the size of the defect, whether the defects be planar or cylindrical.

APPENDIX B

To run the program for the channel-centered model, it is only necessary to have a system that supports the language BASIC. The program should be loaded into the system and run in BASIC. No other files are needed to run this program.

The program is interactive. After giving the RUN command, the user is prompted as to whether the results should go to a printer. The user may answer in the affirmative by typing any one of the following responses: Y, YES, PRINTER, or P. Any other answer is interpreted as a negative answer. The results will be displayed on the terminal whether or not they are also printed.

Next, a menu appears. The first option allows the user to read the controlling parameters. The second option allows the user to edit the parameters. The third actually runs the program. The fourth helps the user to select controlling parameters by telling the user how many macropores would result for the given hydraulic conductivity and channel radius.

The fifth option terminates the program.

If the edit option is chosen, the user is given a menu with five options. Any one of four parameters may be edited. The fifth choice is to return to the main menu.

Once the option to run the program is selected, a computation is made as to how many macropores would be necessary in an area of 25 square feet of the given channel radius to give the selected conductivity. The user is prompted as to whether or not the number is acceptable. Low numbers may not give interesting results. High numbers may require unacceptably long run times for the program, and the resulting tree diagram will be complicated. An affirmative response (YES, Y, YY) will allow the computation to begin. A negative response will send the user into edit mode in the channel option automatically. After editing the channel radius, the user must exit the edit mode and select option 3 of the menu as before. When prompted as to whether or not the number of channels is acceptable, the user may also answer affirmatively with a B. In this case, the user can run the program a multiple number of times.

At this time, a list will be given on the screen of which macropores are interconnected. At the end of this, the user is asked whether the the experiment should be repeated with another set of randomly located macropores. A negative response will return the user to the main menu.

The source code for the channel-centered model follows.

```
7 PRINT"THIS PROGRAM DEALS WITH THE CHANNEL-CENTERED MODEL OF INTERLIFT FLOW"
8 INPUT"SHALL THE RESULTS GO TO THE PRINTER ";PL$
10 RANDOMIZE TIMER
12 PI=3.1415926
20 MU=.008924
30 GRAV=980
40 TR=.025
50 HC=.00001
60 IR=25
65 N=8
66 PL=0
68 IF PL$="YES" OR PL$="Y" OR PL$="PRINTER" OR PL$="P" THEN PL=1
70 PRINT"OPTIONS":PRINT"1. SHOW THE PARAMETERS"
80 PRINT"2. EDIT THE PARAMETERS"
90 PRINT"3. RUN THE PROGRAM"
100 PRINT"4. CHECK PORE NUMBERS":PRINT"5. EXIT"
110 INPUT Q
120 IF Q=1 THEN 170
130 IF Q=2 THEN 260
140 IF Q=3 THEN 600
150 IF Q=4 THEN 2000
152 IF Q=5 THEN END
160 PRINT"INVALID RESPONSE!":GOTO 70
170 SR=TR*10000:PRINT"CHANNEL RADIUS,";SR;"MICRONS
180 SR=HC:PRINT"HYDRAULIC CONDUCTIVITY,";SR;"CM/SEC"
190 SR=IR:PRINT"INTERLIFT FLOW RADIUS,";SR;"CM"
200 SR=N:PRINT"NUMBER OF LIFTS,";SR
210 K=HC*MU/GRAV
220 SR=K/9.869699E-12:PRINT"PERMEABILITY,";SR;"MILLIDARCY"
230 DS=PI*(TR^4)/(8*K)
240 SR=SQR(DS):PRINT"AVERAGE SPACING BETWEEN MACROPORES,";SR;"CM"
250 PRINT:IF LL=0 THEN 70
255 END
260 PRINT"WHICH PARAMETER SHOULD BE EDITED?"
270 PRINT"C CHANNEL RADIUS":PRINT"H HYDRAULIC CONDUCTIVITY"
280 PRINT"I INTERLIFT FLOW RADIUS":PRINT"N NUMBER OF LIFTS"
290 PRINT"R RETURN TO MAIN MENU"
300 INPUT Q$
310 IF Q$="C" THEN 360
320 IF Q$="H" THEN 410
330 IF Q$="I" THEN 460
340 IF Q$="N" THEN 510
345 IF Q$="R" THEN 70
350 PRINT"INVALID RESPONSE!!":PRINT:GOTO 260
360 SR=TR*10000:PRINT"CHANNEL RADIUS,";SR;"MICRONS
370 PRINT"GIVE THE NEW CHANNEL RADIUS (HIT RETURN TO RETAIN OLD ONE)"
380 INPUT SR
390 IF SR = 0 THEN 260
400 TR=SR*.0001:GOTO 260
410 SR=HC:PRINT"HYDRAULIC CONDUCTIVITY,";SR;"CM/SEC"
420 PRINT"GIVE THE NEW HYDRAULIC CONDUCTIVITY (HIT RETURN TO RETAIN OLD ONE)"
430 INPUT SR
440 IF SR = 0 THEN 260
450 HC=SR:GOTO 260
460 SR=IR:PRINT"INTERLIFT FLOW RADIUS,";SR;"CM"
```

```
470 PRINT"GIVE THE NEW INTERLIFT FLOW RADIUS (HIT RETURN TO RETAIN OLD ONE)"
480 INPUT SR
490 IF SR = 0 THEN 260
500 IR=SR:GOTO 260
510 SR=N:PRINT"NUMBER OF LIFTS,";SR
520 PRINT"GIVE THE NEW NUMBER OF LIFTS (HIT RETURN TO RETAIN OLD ONE)"
530 INPUT SR
540 IF SR = 0 THEN 260
545 IF SR>10 THEN PRINT"SORRY! MORE THAN 9 LIFTS WILL NOT BE ACCEPTED."
550 IF SR>10 THEN 510
560 IF SR < 2 THEN PRINT"SORRY! LESS THEN 2 LIFTS WILL NOT BE ACCEPTED."
570 IF SR<2  THEN 510
580 N=SR:GOTO 260
600 K=HC*MU/GRAV:DS=PI*(TR^4)/(8*K):REP=0
610 NP=INT(23225.76/DS)
620 PRINT"IN THIS MODEL, EACH LIFT HAS";NP;"THROUGH-GOING MACROPORES"
625 PRINT"THE AREA OF THE LIFT IS 25 SQ FEET, OR 2.32 SQ METERS."
630 INPUT"IS THIS AN ACCEPTABLE NUMBER OF CHANNELS";Q$
635 IF  Q$="B" THEN 645
640 IF Q$="Y" OR Q$="YY" OR Q$="YES" OR Q$="JA" THEN 660
642 GOTO 650
645 INPUT"HOW MANY TIMES SHOULD THIS BE REPEATED?";NR
646 IF NR<1 OR NR>100 THEN 645
647 GOTO 660
650 PRINT"THEN YOU MUST ADJUST THE CHANNEL RADIUS.":GOTO 360
660 IF NP>99 THEN PRINT"YOU MUST ADJUST THE CHANNEL RADIUS.":PRINT"IF NOT, THE P
ROGRAM WILL TAKE AN UNACCEPTABLE AMOUNT OF TIME":GOTO 360
670 DIM XP(N,NP):DIM YP(N,NP):DIM EP(N,NP):DIM TU(N):DIM UP(N,NP),GP(N,NP)
673 REP=REP+1
675 FOR I=1 TO N:FOR J=1 TO NP
680 XP(I,J)=RND(1)*152.4
690 YP(I,J)=RND(1)*152.4:NEXT
700 NEXT
702 FOR J=1 TO NP:EP(1,J)=1:NEXT
710 FOR I=2 TO N
720 IB=I-1
730 FOR J=1 TO NP
740 IF EP(IB,J)=0 THEN 790
750 FOR K=1 TO NP
760 DI=SQR(((XP(I,K)-XP(IB,J))^2)+((YP(I,K)-YP(IB,J))^2))
770 IF DI>IR THEN 780
771 IF EP(I,K)=0 THEN TU(I)=TU(I)+1
772 EP(I,K)=1:GP(IB,J)=GP(IB,J)+1:PRINT"CHANNEL(";IB;",";J;") WITH (";I;",";K;")
"

774 IF PL=1 THEN LPRINT"CHANNEL(";IB;",";J;") WITH (";I;",";K;")"
780 NEXT
790 NEXT
800 PRINT"LIFT #";IB;"DONE.":NEXT
1750 FOR I=1 TO N:FOR J=1 TO NP:UP(I,J)=0
1760 NEXT:NEXT
1870 PRINT:PRINT"SO FAR THIS EXPERIMENT HAS BEEN PERFORMED ";REP;"TIMES."
1871 IF NR=0 THEN 1880
1873 IF REP<NR THEN Q$="Y":GOTO 1900
1880 INPUT"SHALL THE EXPERIMENT BE REPEATED";Q$
1900 ERASE XP,YP,EP,TU,GP,UP
```

```
1950 IF Q$="Y" OR Q$="YES" OR Q$="JA" OR Q$= "YY" THEN 670
1960 GOTO 70
2000 INPUT"WHAT IS THE CHANNEL RADIUS";TT
2001 IF TT=0 THEN 70
2005 TT=TT/10000:K=HC*MU/GRAV:DS=PI*(TT^4)/(8*K)
2010 NP=INT(23225.76/DS)
2020 PRINT"IN THIS MODEL, EACH LIFT HAS";NP;"THROUGH-GOING MACROPORES"
2025 PRINT"THE AREA OF THE LIFT IS 25 SQ FEET, OR 2.32 SQ METERS."
2030 GOTO 2000
```

APPENDIX C

To run the pocket model program, the same instructions apply as in Appendix B. The results will be different in that the number of throughgoing paths in each lift is given in this program. Option 4 is different in this program in that the user can examine the number of flaws in any one of five settings (3 inch shelby tube, 6 inch shelby tube, 5 x 5 square foot infiltrometer, 16 x 16 foot square foot infiltrometer or an one-acre test fill). The source code for the pocket model follows.

```
7 PRINT:PRINT"THIS PROGRAM DEALS WITH THE POCKET MODEL.":PRINT
8 INPUT"PLEASE TYPE 'P' OR 'PRINTER' TO GET A HARD COPY OF RESULTS";P$
10 RANDOMIZE TIMER
12 PI=3.1415926
20 MU=.008924
30 GRAV=980
40 TR=.025
50 HC=.00001
60 IR=25
65 N=8
66 PL=0
68 IF P$="P" OR P$="PRINTER" THEN PL=1
70 PRINT"OPTIONS":PRINT"1. SHOW THE PARAMETERS"
80 PRINT"2. EDIT THE PARAMETERS"
90 PRINT"3. RUN THE PROGRAM"
100 PRINT"4. CHECK PORE NUMBERS":PRINT"5. EXIT"
110 INPUT Q
120 IF Q=1 THEN 170
130 IF Q=2 THEN 260
140 IF Q=3 THEN 600
150 IF Q=4 THEN 2000
152 IF Q=5 THEN END
160 PRINT"INVALID RESPONSE!":GOTO 70
170 SR=TR*10000:PRINT"CHANNEL RADIUS,";SR;"MICRONS
180 SR=HC:PRINT"HYDRAULIC CONDUCTIVITY,";SR;"CM/SEC"
190 SR=IR:PRINT"INTERLIFT FLOW RADIUS,";SR;"CM"
200 SR=N:PRINT"NUMBER OF LIFTS,";SR
210 K=HC*MU/GRAV
220 SR=K/9.869699E-12:PRINT"PERMEABILITY,";SR;"MILLIDARCY"
230 DS=PI*(TR^4)/(8*K)
240 SR=SQR(DS):PRINT"AVERAGE SPACING BETWEEN MACROPORES,";SR;"CM"
250 PRINT:IF LL=0 THEN 70
255 END
260 PRINT"WHICH PARAMETER SHOULD BE EDITED?"
270 PRINT"C CHANNEL RADIUS":PRINT"H HYDRAULIC CONDUCTIVITY"
280 PRINT"I INTERLIFT FLOW RADIUS":PRINT"N NUMBER OF LIFTS"
290 PRINT"R RETURN TO MAIN MENU"
300 INPUT Q$
310 IF Q$="C" THEN 360
320 IF Q$="H" THEN 410
330 IF Q$="I" THEN 460
340 IF Q$="N" THEN 510
345 IF Q$="R" THEN 70
350 PRINT"INVALID RESPONSE!!":PRINT:GOTO 260
360 SR=TR*10000:PRINT"CHANNEL RADIUS,";SR;"MICRONS
370 PRINT"GIVE THE NEW CHANNEL RADIUS (HIT RETURN TO RETAIN OLD ONE)"
380 INPUT SR
390 IF SR = 0 THEN 260
400 TR=SR*.0001:GOTO 260
410 SR=HC:PRINT"HYDRAULIC CONDUCTIVITY,";SR;"CM/SEC"
420 PRINT"GIVE THE NEW HYDRAULIC CONDUCTIVITY (HIT RETURN TO RETAIN OLD ONE)"
430 INPUT SR
440 IF SR = 0 THEN 260
450 HC=SR:GOTO 260
460 SR=IR:PRINT"INTERLIFT FLOW RADIUS,";SR;"CM"
```

```
470 PRINT"GIVE THE NEW INTERLIFT FLOW RADIUS (HIT RETURN TO RETAIN OLD ONE)"
480 INPUT SR
490 IF SR = 0 THEN 260
500 IR=SR:GOTO 260
510 SR=N:PRINT"NUMBER OF LIFTS,";SR
520 PRINT"GIVE THE NEW NUMBER OF LIFTS (HIT RETURN TO RETAIN OLD ONE)"
530 INPUT SR
540 IF SR = 0 THEN 260
545 IF SR>10 THEN PRINT"SORRY! MORE THAN 9 LIFTS WILL NOT BE ACCEPTED."
550 IF SR>10 THEN 510
560 IF SR < 2 THEN PRINT"SORRY! LESS THEN 2 LIFTS WILL NOT BE ACCEPTED."
570 IF SR<2  THEN 510
580 N=SR:GOTO 260
600 K=HC*MU/GRAV:DS=PI*(TR^4)/(8*K):REP=0
610 NP=INT(23225.76/DS)
620 PRINT"IN THIS MODEL, EACH LIFT HAS";NP;"THROUGH-GOING MACROPORES"
625 PRINT"THE AREA OF THE LIFT IS 25 SQ FEET, OR 2.32 SQ METERS."
630 INPUT"IS THIS AN ACCEPTABLE NUMBER OF CHANNELS";Q$
640 IF Q$="Y" OR Q$="YY" OR Q$="YES" OR Q$="JA" OR Q$="B" OR Q$="BATCH" THEN 660
650 PRINT"THEN YOU MUST ADJUST THE CHANNEL RADIUS.":GOTO 360
660 IF NP>99 THEN PRINT"YOU MUST ADJUST THE CHANNEL RADIUS.":PRINT"IF NOT, THE P
ROGRAM WILL TAKE AN UNACCEPTABLE AMOUNT OF TIME":GOTO 360
662 IF Q$="Y" OR Q$="YY" OR Q$="YES" OR Q$="JA" THEN 670
663 INPUT"HOW MANY TIMES SHOULD IT BE REPEATED";RRP
664 IF RRP>80 OR RRP<1 THEN 663
665 RFL=1
670 REP=REP+1
671 IF REP>RRP AND RFL=1 THEN 70
672 DIM XP(N,NP):DIM YP(N,NP):DIM EP(N,NP):DIM TU(N):DIM UP(N,NP),GP(N,NP)
673 IF PL=1 THEN LPRINT:LPRINT"MODEL # ";REP
675 FOR I=1 TO N:FOR J=1 TO NP
680 XP(I,J)=RND(1)*152.4
690 YP(I,J)=RND(1)*152.4:NEXT
700 NEXT
710 ER=INT(152.4/(IR*2))+1
802 FOR J=1 TO NP:EP(1,J)=1:NEXT
810 FOR I=2 TO N
820 IB=I-1
830 FOR J=1 TO NP
840 IF EP(IB,J)=0 THEN 990
850 FOR KX= 1 TO ER:FOR KY=1 TO ER
860 XK=(KX-.5)*2*IR:YK=(KY-.5)*2*IR
870 DI=SQR(((XK-XP(IB,J))^2)+((YK-YP(IB,J))^2))
880 IF DI>IR THEN 930
890 FOR K=1 TO NP
900 DI=SQR(((XP(I,K)-XK)^2)+((YP(I,K)-YK)^2))
910 IF DI>IR THEN 920
911 IF EP(I,K)=0 THEN TU(I)=TU(I)+1
912 EP(I,K)=1:GP(IB,J)=GP(IB,J)+1:PRINT"CHANNEL(";IB;",";J;") WITH (";I;",";K;")
"

920 NEXT
930 NEXT
940 NEXT
990 NEXT
1000 PRINT"LIFT #";IB;"DONE.":NEXT
```

```
1005 NPATH=NP
1010 FOR I = 2 TO N:IB=I-1
1020 PRINT I;" LIFT CASE"
1021 IF PL=1 THEN LPRINT I;" LIFT CASE"
1030 IF TU(I)<2 THEN NPATH=TU(I)
1040 IF NPATH < 2 THEN 1680
1050 FOR J=1 TO NP:M=1
1060 IF EP(IB,J)=0 THEN 1570
1065 IF UP(IB,J)=0 AND IB>1 THEN 1570
1066 FOR KX= 1 TO ER:FOR KY=1 TO ER
1067 XK=(KX-.5)*2*IR:YK=(KY-.5)*2*IR
1068 DI=SQR(((XK-XP(IB,J))^2)+((YK-YP(IB,J))^2))
1069 IF DI>IR THEN 1260
1070 FOR K = 1 TO NP
1080 IF EP(I,K)=0 THEN 1250
1090 DI=SQR(((XP(I,K)-XK)^2)+((YP(I,K)-YK)^2))
1100 IF DI>IR THEN 1250
1110 IF UP(I,K)=0 THEN 1240
1120 IF GP(IB,UP(I,K))=1 THEN 1250
1125 DI=SQR(((XK-XP(IB,UP(I,K)))^2)+((YK-YP(IB,UP(I,K)))^2))
1126 IF DI>IR THEN 1250
1130 FOR KK=K TO NP
1140 IF EP(I,KK)=0 THEN 1220
1150 DI=SQR(((XP(I,KK)-XK)^2)+((YP(I,KK)-YK)^2))
1160 IF DI>IR THEN 1220
1170 IF UP(I,KK)=0 THEN 1210
1180 GP(IB,UP(I,K))=GP(IB,UP(I,K))-1
1190 IF GP(IB,UP(I,K))=1 THEN KK=NP:GOTO 1220
1200 UP(I,KK)=UP(I,K)
1210 KK=NP:UP(I,K)=J
1220 NEXT
1230 GOTO 1250
1240 UP(I,K)=J:K=NP:M=0
1250 NEXT
1260 NEXT
1270 NEXT
1560 NPATH=NPATH-M
1570 NEXT
1680 PRINT"THERE ARE ";NPATH;" THROUGHGOING PATHS."
1690 IF PL=1 THEN LPRINT"THERE ARE ";NPATH;" THROUGHGOING PATHS."
1700 DK=PI*(TR^4)*NPATH/(8*23225.76)
1710 HH=DK*GRAV/MU
1720 PRINT"THUS, THE EFFECTIVE HYDRAULIC CONDUCTIVITY IS";HH;"CM/SEC."
1725 IF PL=0 THEN 1740
1730 LPRINT"THUS, THE EFFECTIVE HYDRAULIC CONDUCTIVITY IS";HH;"CM/SEC."
1740 NEXT
1750 FOR I=1 TO N:FOR J=1 TO NP:UP(I,J)=0
1760 NEXT:NEXT
1870 PRINT:PRINT"SO FAR THIS CALCULATION HAS BEEN PERFORMED ";REP;"TIMES."
1900 ERASE XP,YP,EP,TU,GP,UP
1910 IF RFL=1 THEN 670
1920 INPUT"SHALL THE CALCULATION BE REPEATED";Q$
1950 IF Q$="Y" OR Q$="YES" OR Q$="JA" OR Q$= "YY" THEN 670
1960 GOTO 70
```

```
2000 PRINT"SET THE AREA":PRINT"1.  3 IN DIAM CORE BARREL   4. 16x16 FT INFILTROM
ETER"
2010 PRINT"2.  6 IN DIAM CORE BARREL   5. ONE ACRE (4047 SQ METERS)"
2020 PRINT"3.  5x5 FT INFILTROMETER    6. EXIT TO MAIN MENU"
2030 INPUT SZ:IF SZ=0 OR SZ=6 THEN 70
2040 IF SZ=1 THEN AR=45.60367:A$="(3 INCH CORE BARREL)"
2050 IF SZ=2 THEN AR=182.4147:A$="(6 INCH CORE BARREL)"
2060 IF SZ=3 THEN AR=23225.76:A$="(5x5 SQ FT INFLTR.) "
2070 IF SZ=4 THEN AR=237831.8:A$="(16x16 SQ FT INFLTR)"
2080 IF SZ=5 THEN AR=4.047E+07:A$="(ACRE)              "
2090 IF SZ>6 OR SZ<0 THEN 2000
2091 IF PL=0 THEN 2100
2095 LPRINT:LPRINT"THE AREA IS",AR,A$
2096 LPRINT"THE CONDUCTIVITY IS",HC
2100 INPUT"WHAT IS THE CHANNEL RADIUS";TD
2101 IF TD=0 THEN 2000
2105 TT=TD/10000:K=HC*MU/GRAV:DS=PI*(TT^4)/(8*K)
2110 NP=INT(AR/DS)
2120 PRINT"IN THIS MODEL, EACH LIFT HAS";NP;"THROUGH-GOING MACROPORES"
2122 IF PL=0 THEN 2130
2125 LPRINT"IF R= ",TD", EACH LIFT HAS";NP;"THROUGH-GOING MACROPORES"
2130 IF NP>0 THEN 2100
2140 PB=(AR*100)/DS
2150 PRINT" THE PROBABILITY OF THERE BEING A MACROPORE IS ",PB," %."
2155 IF PL=0 THEN 2100
2160 LPRINT" THE PROBABILITY OF THERE BEING A MACROPORE IS ",PB," %."
2170 GOTO 2100
```

APPENDIX D

A relation is derived for interflift flow radius in terms of time, conductivity and head.

If t is time and v is the Darcy velocity of fluid in the plane between lifts, then

$$IR = tv \tag{D.1}$$

According to Darcy's law,

$$v = K_h \nabla H \tag{D.2}$$

where K_h is the horizontal hydraulic conductivity and the latter expression is hydraulic gradient. This is actually the change in potential over distance. In this case, it is

$$\nabla H = \frac{H}{IR} \tag{D.3}$$

Thus, by combining these three relations, interlift flow radius can be expressed in terms of head, time, and horizontal hydraulic conductivity.

$$IR = \sqrt{tK_h H} \tag{D.4}$$

which is Equation (4.9) in the text.

If interlift flow is not taking place in an "interlift plane" but in the lower part of a porous lift, then (D.2) should be modified to include the affect of effective porosity (Horton et al., 1985). In that case

$$IR = \sqrt{tK_h H/\varphi} \tag{D.5}$$

where φ is effective porosity. If this is the case, effective porosities are likely to be higher in this portion of the lift. That coupled with the fact that it is inside the square-root sign decrease the size of the error introduced if (D.4) is used where (D.5) is more appropriate.

APPENDIX E

This program is a breakthrough model for the channel-centered model. It is run similarly to the programs given in Appendix B and Appendix C. It gives successive lists of macropore interconnection for the same set of macropore locations as a function of time. Interlift flow radius grows with time as a function of horizontal hydraulic conductivity and depth (head). In this program when asked if the number of channels is acceptable, the user may not respond with B. Only one model is conducted at a time due to the length of time necessary to run one model. The source code for the breakthrough model follows.

```
7 PRINT"THIS PROGRAM DEALS WITH THE BREAKTHROUGH MODEL FOR INTERLIFT FLOW"
8 INPUT"SHALL THE RESULTS GO TO THE PRINTER ";PL$
10 RANDOMIZE TIMER
12 PI=3.1415926
15 KN=3600*24*365.24
20 MU=.008924
30 GRAV=980
40 TR=.025
50 HC=.00001
60 HZ=1E-08
65 N=8
66 PL=0
68 IF PL$="YES" OR PL$="Y" OR PL$="PRINTER" OR PL$="P" THEN PL=1
70 PRINT"OPTIONS":PRINT"1. SHOW THE PARAMETERS"
80 PRINT"2. EDIT THE PARAMETERS"
90 PRINT"3. RUN THE PROGRAM"
100 PRINT"4. EXIT"
110 INPUT Q
120 IF Q=1 THEN 170
130 IF Q=2 THEN 260
140 IF Q=3 THEN 600
150 IF Q=4 THEN END
160 PRINT"INVALID RESPONSE!":GOTO 70
170 SR=TR*10000:PRINT"CHANNEL RADIUS,";SR;"MICRONS
180 SR=HC:PRINT"HYDRAULIC CONDUCTIVITY,";SR;"CM/SEC"
190 SR=HZ:PRINT"HORIZONTAL HYDRAULIC CONDUCTIVITY,";SR;"CM/SEC"
200 SR=N:PRINT"NUMBER OF LIFTS,";SR
210 K=HC*MU/GRAV
220 SR=K/9.869699E-12:PRINT"PERMEABILITY,";SR;"MILLIDARCY"
230 DS=PI*(TR^4)/(8*K)
240 SR=SQR(DS):PRINT"AVERAGE SPACING BETWEEN MACROPORES,";SR;"CM"
250 PRINT:IF LL=0 THEN 70
255 END
260 PRINT"WHICH PARAMETER SHOULD BE EDITED?"
270 PRINT"C CHANNEL RADIUS":PRINT"H HYDRAULIC CONDUCTIVITY"
280 PRINT"Z HORIZONTAL HYDRAULIC CONDUCTIVITY":PRINT"N NUMBER OF LIFTS"
290 PRINT"R RETURN TO MAIN MENU"
300 INPUT Q$
310 IF Q$="C" THEN 360
320 IF Q$="H" THEN 410
330 IF Q$="Z" THEN 460
340 IF Q$="N" THEN 510
345 IF Q$="R" THEN 70
350 PRINT"INVALID RESPONSE!!":PRINT:GOTO 260
360 SR=TR*10000:PRINT"CHANNEL RADIUS,";SR;"MICRONS
370 PRINT"GIVE THE NEW CHANNEL RADIUS (HIT RETURN TO RETAIN OLD ONE)"
380 INPUT SR
390 IF SR = 0 THEN 260
400 TR=SR*.0001:GOTO 260
410 SR=HC:PRINT"HYDRAULIC CONDUCTIVITY,";SR;"CM/SEC"
420 PRINT"GIVE THE NEW HYDRAULIC CONDUCTIVITY (HIT RETURN TO RETAIN OLD ONE)"
430 INPUT SR
440 IF SR = 0 THEN 260
450 HC=SR:GOTO 260
460 SR=HZ:PRINT"HORIZONTAL HYDRAULIC CONDUCTIVITY,";SR;"CM/SEC"
470 PRINT"GIVE THE NEW HORIZONTAL HYD. CON. (HIT RETURN TO RETAIN OLD ONE)"
```

```
480 INPUT SR
490 IF SR = 0 THEN 260
500 HZ=SR:GOTO 260
510 SR=N:PRINT"NUMBER OF LIFTS,";SR
520 PRINT"GIVE THE NEW NUMBER OF LIFTS (HIT RETURN TO RETAIN OLD ONE)"
530 INPUT SR
540 IF SR = 0 THEN 260
545 IF SR>10 THEN PRINT"SORRY! MORE THAN 9 LIFTS WILL NOT BE ACCEPTED."
550 IF SR>10 THEN 510
560 IF SR < 2 THEN PRINT"SORRY! LESS THEN 2 LIFTS WILL NOT BE ACCEPTED."
570 IF SR<2  THEN 510
580 N=SR:GOTO 260
600 K=HC*MU/GRAV:DS=PI*(TR^4)/(8*K):REP=0
610 NP=INT(23225.76/DS)
620 PRINT"IN THIS MODEL, EACH LIFT HAS";NP;"THROUGH-GOING MACROPORES"
625 PRINT"THE AREA OF THE LIFT IS 25 SQ FEET, OR 2.32 SQ METERS."
630 INPUT"IS THIS AN ACCEPTABLE NUMBER OF CHANNELS";Q$
640 IF Q$="Y" OR Q$="YY" OR Q$="YES" OR Q$="JA" THEN 660
650 PRINT"THEN YOU MUST ADJUST THE CHANNEL RADIUS.":GOTO 360
660 IF NP>99 THEN PRINT"YOU MUST ADJUST THE CHANNEL RADIUS.":PRINT"IF NOT, THE P
ROGRAM WILL TAKE AN UNACCEPTABLE AMOUNT OF TIME":GOTO 360
670 DIM XP(N,NP):DIM YP(N,NP):DIM EP(N,NP):DIM TU(N):DIM UP(N,NP),GP(N,NP)
671 DIM IR(N,NP),TB(N,NP),FL(N)
675 FOR I=1 TO N:FOR J=1 TO NP
680 XP(I,J)=RND(1)*152.4
690 YP(I,J)=RND(1)*152.4:NEXT
700 NEXT
710 TY=0
720 TY=TY+1
730 PRINT:PRINT"THE SITUATION AFTER ";TY;"YEARS."
740 IF PL=1 THEN LPRINT:LPRINT"THE SITUATION AFTER ";TY;"YEARS."
750 FOR I=1 TO N
760 HD(I)=(2+I)*15.24
770 FOR J=1 TO NP
775 IF EP(I,J)=0 THEN TB(I,J)=0
780 TB(I,J)=TB(I,J)+KN
790 IR(I,J)=SQR(TB(I,J)*HZ*HD(I))
800 NEXT:NEXT
902 FOR J=1 TO NP:EP(1,J)=1:NEXT
910 FOR I=2 TO N
920 IB=I-1
930 FOR J=1 TO NP
940 IF EP(IB,J)=0 THEN 990
950 FOR K=1 TO NP
960 DI=SQR(((XP(I,K)-XP(IB,J))^2)+((YP(I,K)-YP(IB,J))^2))
970 IF DI>IR(IB,J) THEN 980
971 IF EP(I,K)=0 THEN TU(I)=TU(I)+1
972 EP(I,K)=1:GP(IB,J)=GP(IB,J)+1:PRINT"CHANNEL(";IB;",";J;") WITH (";I;",";K;")
"
974 IF PL=1 THEN LPRINT"CHANNEL(";IB;",";J;") WITH (";I;",";K;")"
980 NEXT
990 NEXT
1000 PRINT"LIFT #";IB;"DONE."
1010 IF TU(I)=0 THEN I=N:GOTO 1040
1020 IF FL(I)=1 THEN 1040
```

```
1030 FL(I)=1:PRINT"BREAKTHROUGH AT LIFT";IB;"****************************"
1035 IF PL=1 THEN LPRINT"BREAKTHROUGH AT LIFT";IB;"*****************************
****************"
1040 NEXT
1745 IF FL(2)=0 THEN PRINT"FLUID CONTAINED BY THE FIRST LIFT"
1746 IF FL(2)=0 AND PL=1 THEN LPRINT"FLUID CONTAINED BY THE FIRST LIFT"
1750 FOR I=1 TO N:FOR J=1 TO NP:UP(I,J)=0
1760 NEXT:NEXT
1780 IF TY<30 THEN 720
1880 INPUT"SHALL THE CALCULATION BE REPEATED";Q$
1900 ERASE XP,YP,EP,TU,GP,UP
1950 IF Q$="Y" OR Q$="YES" OR Q$="JA" OR Q$= "YY" THEN 670
1960 GOTO 70
```

APPENDIX F

QUALITY ASSURANCE

This report resulted from a research study conducted with the primary objective of documenting the necessary thickness of compacted clay liner required to retain leachate for 30 years. The approach to the study involved laboratory studies of many of the variables, a limited number of large scale containerized tests, field measurements on a test section, and mathematical modeling of the results.

The laboratory study involved selecting and obtaining samples of two soils of diverse mineralogy which would be suitable for use as a clay liner construction material. Bulk samples of these two soils were collected, checked for uniformity, and transported to the laboratory for analysis. A subsample of each soil was collected, dried, ground and homogenized prior to analysis. Analyses included the following parameters and utilized well documented ASTM procedures when available:

1. Atterberg limits by ASTM DA318 procedure

2. Grain size distribution by ASTM D422 procedure

3. Laboratory compaction by ASTM D698 procedure

4. Laboratory conductivity as measured with a triaxial permeameter.

Large scale containerized tests of the hydraulic conductivity of 60 cm diameter samples were conducted using specially constructed permeameters. A specially constructed compactor designed to simulate field equipment was made and utilized in conjunction with a computer controlled MTS axial test system to compact the large samples. The compacted permeameters were transported to the greenhouse and fitted with a straight sided barrel to contain a 1 meter head of water. Fluorescent dye was added to the permeant to allow evaluation of flow paths through the compacted soils. Treatments included two soils and three initial clod sizes.

Data from the laboratory tests were used to calibrate the mathematical model to help gain a better understanding of liner performance. In addition, field data from a test pad near Houston, TX were collected and compared to the laboratory and modeled data.

All laboratory experiments were replicated three times and periodic checks were made to compare the replications for variability and consistency. Efforts were made to prevent any bias from the study. Whenever possible, measurements of both inflow and outflow were utilized to assure that the results were consistent. Whenever possible, the results are expressed as a mean ± the standard deviation. All data analysis and interpretation were done within the context of the experimental design and particular care was taken not to extrapolate the data beyond reasonable limits. Comparison of data within and/or between treatments provided further quality assurance. Data from the laboratory, the large permeameters and the field test pad were internally consistent and all confirmed and supported each other thereby providing further assurance as to the quality of the data. The mathematical models are based on the field and laboratory data and therefore have been calibrated.

While this study did not use a large number of sophisticated instrumentation, the few that were utilized were calibrated routinely and checked daily to be sure of proper performance. On one occasion, the surface moisture density meter malfunctioned and required corrective action (return to factory for repair). The daily calibration check was sufficient to catch the malfunction and prevent the collection of erroneous data.